INVESTIGATIONS OF COOLANT MIXING IN NUCLEAR REACTOR FUEL PIN BUNDLES

By

A MOORTHI

(Enrollment Number: ENGG02201204015)

Indira Gandhi Centre for Atomic Research, Kalpakkam

A thesis submitted to the Board of Studies in Engineering Sciences

In partial fulfillment of requirements

for the Degree of

DOCTOR OF PHILOSOPHY

of

HOMI BHABHA NATIONAL INSTITUTE

August, 2018

Homi Bhabha National Institute

Recommendations of the Viva Voce Committee

As members of the Viva Voce Committee, we certify that we have read the dissertation prepared by **Mr. A. MOORTHI** entitled **"Investigations of Coolant Mixing in Nuclear Reactor Fuel Pin Bundles"** and recommend that it may be accepted as fulfilling the thesis requirement for the award of Degree of Doctor of Philosophy.

Chairman – **Dr. K. Velusamy**	**Date: 15.02.2019**
Guide / Convener – **Dr. Anil Kumar Sharma**	**Date: 15.02.2019**
Examiner –**Dr. B.V.S.S.S. Prasad**	**Date: 15.02.2019**
Member 1- **Dr. S. Murugan**	**Date: 15.02.2019**
Member 2- **Dr. Anish Kumar**	**Date: 15.02.2019**

Final approval and acceptance of this thesis is contingent upon the candidate's submission of the final copies of the thesis to HBNI.

I hereby certify that I have read this thesis prepared under my direction and recommend that it may be accepted as fulfilling the thesis requirement.

Date: 15/02/19

Place: Indira Gandhi Centre for Atomic Research
Kalpakkam

Dr. Anil Kumar Sharma
(Guide)

STATEMENT BY AUTHOR

This dissertation has been submitted in partial fulfillment of requirements for an advanced degree at Homi Bhabha National Institute (HBNI) and is deposited in the Library to be made available to borrowers under rules of the HBNI.

Brief quotations from this dissertation are allowable without special permission, provided that accurate acknowledgement of source is made. Requests for permission for extended quotation from or reproduction of this manuscript in whole or in part may be granted by the Competent Authority of HBNI when in his or her judgment the proposed use of the material is in the interests of scholarship. In all other instances, however, permission must be obtained from the author.

Kalpakkam
August, 2018

A. Moorthi

DECLARATION

I, hereby declare that the investigation presented in the thesis has been carried out by me. The work is original and has not been submitted earlier as a whole or in part for a degree / diploma at this or any other Institution / University.

Kalpakkam

August, 2018

A. Moorthi

List of Publications Arising from the Thesis

Journal

1. "Laminar fluid flow and heat transfer in non-circular sub-channel geometries of nuclear fuel bundle", **Moorthi, A.**, Anil Kumar Sharma, *Progress in Nuclear Energy*, **2018**, *Vol. 103*, 243-253.
2. "Investigation of cross flow mixing on rod bundle safety margins using sub-channel analysis framework", **Moorthi, A.**, Anil Kumar Sharma, *Nuclear Engineering and Design*, **2018**, *Vol. 335*, 30-43.
3. "A review of sub-channel thermal hydraulic codes for nuclear reactor core and future directions", **Moorthi, A.**, Anil Kumar Sharma, Velusamy, K., *Nuclear Engineering and Design*, **2018**, *Vol. 332*, 329-344.
4. "CFD investigations of flow between adjacent sub-channels of nuclear fuel bundle", **Moorthi, A.**, Anil Kumar Sharma, *Nuclear Engineering and Technology*, **2018**, (Submitted).

Conferences

1. "Development of thermal hydraulic analysis framework (pre & postprocessors)", **Moorthi, A.,** Premsai, K., Ravi, K. V., *New Horizons in Nuclear Reactor Thermal Hydraulics and Safety*, January 13-15, **2014**, Mumbai, India.
2. "CFD simulation of turbulent velocity and temperature profiles in non-circular and rod bundle sub-channel geometries", **Moorthi, A.**, Anil Kumar Sharma, *Proceedings of the 23rd National Heat and Mass Transfer Conference and 1st*

International ISHMT-ASTFE Heat and Mass Transfer Conference, 17-20, December, **2015**, Thiruvananthapuram, India, (IHMTC-2015-591).

3. "Study on the effect of cross flow mixing between rod bundle sub-channels on coolant enthalpy rise in a fuel bundle", **Moorthi, A.,** Anil Kumar Sharma, *Proceedings of CANSAS-2015 (CANDU Safety Association for Sustainability and NRTHS-2015 (New Horizons in Nuclear Reactor Thermal Hydraulics and Safety)*, 8-11, December, **2015**, Anushaktinagar, Mumbai, India, (CANSAS-2015-B-10).
4. "Flow characteristics in a compound triangular sub-channel of nuclear fuel bundle", **Moorthi, A.,** Anil Kumar Sharma, *Proceedings of the 6th International and 43rd National Conference on Fluid Mechanics and Fluid Power*, December 15-17, **2016**, MNNITA, Allahabad, U.P., India (FMFP-2016-285).
5. Advanced sub-channel thermal hydraulic analysis systems framework (ASTHYANS), **Moorthi, A.,** Anil Kumar Sharma, Proceedings of the 7th International and 45th National Conference on Fluid Mechanics and Fluid Power, (FMFP-**2018**-359).

Kalpakkam
August, 2018

A. Moorthi

*Dedicated to my beloved **family members**, very supportive **guide***
for all those scientific discussions, encouragement and
*to my dear grandmother Late **M. Selsammal**,*
without her dedication and sacrifice,
I would have not reached this stage.

ACKNOWLEDGEMENTS

The scientific research is a collective effort of motivated individuals and research organizations towards an improved understanding, enhancing the safety and the progress of society. Without constant guidance and involvement of supervisors, colleagues and the support of family, significant progress in any field of research is difficult. Therefore, with humbleness and gratitude, I am extremely grateful to my research guide **Dr. Anil Kumar Sharma** for his valuable guidance, constant support, encouragement, motivation and sincere interest throughout my Ph. D. I am highly obliged to him for his constructive criticism, valuable suggestions and sharing his abundance of knowledge with me. He was a great support even before he took over the responsibility for supervising me. His foresight and keen scientific intuition was absolutely vital for the progress of this work and led to the timely completion of thesis.

I wish to thank the honourable members of my doctoral advisory committee **Dr. K. Velusamy**, **Dr. S. Murugan**, **Dr. Anish Kumar, Dr. M. Saibaba**, **Dr. K. Nagarajan** and **Dr. P.M. Sathya Sai**, for their scientific discussions and helpful suggestions at different time throughout my research, which helps me in redirecting my thinking and keeps me motivated and focused.

The work here has been collaborative throughout and there is a huge array of people to acknowledge. I like to thank my immediate superior **Mr. K. Premsai** for his suggestions, continuous support since the beginning of my doctoral program and introducing me into the field of core thermal hydraulics. My heartiest thanks to **Mr. K. V. Ravi**, **Mr. K. C. Krishnamurthy**, **Mr. N. Rathinasamy**, **Mr. E. K. Murali** and **Mr. G. Babulal** for their continuous encouragement and constant support in pursuing my research work.

I would also like to thank my colleagues especially **Mr. Abdul Mohideen Razak**, **Mr. Ajay Kumar Mishra**, **Mr. Niraj Uttam**, **Mr. Partha Baksi**, **Mr. Ibungohal**, **Mr. S. R. Vashishtha**, **Mr. B. Srinivasan**, **Mr. Padam S.R. Rao**, **Mr. Bharath Kumar**, **Mr. Alok Chaurey** and **Mr. Praveen R Menon**, **Mr. Rajan Kumar Singh, Mrs. Manju Bhargavi Rajan** and all other colleagues of PRPD for the discussions and suggestions during my research work for fruitful scientific discussions and for creating scientific atmosphere. I wish to thank all other members of PRPD, BARC. I have been benefited one way or the other from their association and timely help.

I would also like to thank **Dr. R. Ananthanarayanan**, EIG, IGCAR for his friendly support, suggestions and guidance during the preparation of the manuscript.

I am thankful to my wife **Mrs. M. Kavitha** for the support and care she had taken during this work. I thank my sons **Mr. M. Lokesh** and **Mr. M. Jeevesh** for providing cheerful atmosphere at home.

I would like to express my sincere gratitude to my parents **Mr. M. Annamalai** and **Mrs. A. Janaki** and to my uncle **Mr. M. Vedachalam** and aunty **Mrs. K.C. Usha Rani** and my brother **Mr. A. Yuvaraj** and sister **Mrs. V. Devaki** and all my relatives for their encouragements and never-ending love, and affection to me.

There are many people that I wish to thank who have helped me to complete this thesis. Although I do not mention you all by name, you are not forgotten - thank you all!. Last but not the least, I thank the almighty for protecting all of us from harm and blessing with health and happiness, and for allowing me to reach this far.

Kalpakkam
August, 2018

A. Moorthi

SYNOPSIS

Many countries are constructing advanced nuclear reactors with enhanced safety features to fulfil their ever growing energy demand. The safety of nuclear reactor core is ensured based on the accurate estimation of the local conditions of the coolant in the fuel assemblies. These predictions are in general performed using sub-channel analysis codes. The large increase in the applications of sub-channel analysis codes on reactor safety requires continued development of software and its improvements on sub-channel analysis from the angle of user convenience features as well as the options available for analysis. These types of development of sub-channel analysis utility software help in, fuel assembly design optimization, fuel cycle design and optimization studies and core power level uprating studies. These improvements are also aimed at cost reduction, improvise the quality, repeatability of analysis for both vendor as well as regulator which ultimately results in overall improvement of the safety of nuclear reactor core. The gap in this area gives motivation to develop an advanced, general purpose, automated sub-channel analysis framework for performing the sensitivity studies at different stages of design and analysis of nuclear reactor core for the estimation of thermal-hydraulic safety margins.

In the present study, general purpose automated sub-channel analysis framework is developed to perform the thermal hydraulic analysis of nuclear reactor core. The framework involves the preprocessor to generate the sub-channel layout of the fuel assemblies of different sizes and shapes such as square and triangular pitched pin bundle. Even today, the application of CFD for thermal hydraulics analysis of full bundle is a challenge due to limitations of computational resources and large number

of design calculations has to be performed for different operating regimes of a nuclear reactor. However, CFD can be applied to the sub-channel level geometries to get more insight to the flow and temperature distribution within the rod bundle.

Keeping this in mind, simulations of fully developed laminar and turbulent fluid flow and heat transfer in non-circular sub-channel geometries of a typical nuclear fuel bundle are also carried out. The governing equations of fluid flow and heat transfer are reduced in the form of Poisson's equation and implemented in COMSOL multi physics code as classical PDEs. The fully developed flow equations are solved on the non-circular sub-channel and fuel bundle geometries in a two dimensional domain cut in the longitudinal cross section. The domain is solved for the flow velocities in the out of plane direction by applying the pressure gradient as the boundary condition. The study is focused on the detailed analysis of the Poiseuille number (fRe) and average Nusselt number (Nu) in square and triangular pitched sub-channel geometries of rod bundle. These investigations are carried out for two distinct boundary conditions as axially uniform wall heat flux with uniform wall temperature in the periphery (H1 Boundary condition) and uniform wall heat flux in both axial and circumferential directions (H2 boundary condition) for different p/d ratios varying from 1 to 2. It is found that the fRe increases significantly from 6.5 to 24 for p/d ratio of 1–1.15 for the sub-channel shaped geometry. In case of the sub-channel shaped tube of the same p/d ratio, the fRe increases sharply up to p/d ratio ~1.15 and then starts decreasing slightly till the p/d ratio of 1.5. Analyses are also carried out for square pitched bundles of different sizes varying from 2 × 2 to 10 × 10 to find the variation of fRe with p/d and W/d in the laminar flow regime. The effect of bundle size on the variation of bundle friction factor (fRe) reveals that for an equal p/d and W/d ratios, the change in bundle friction factor (fRe) is within 5% and

the effect of bundle sizes vanishes. Correlations are developed to predict the flow and heat transfer characteristics as a function of p/d ratio for non-circular sub-channels by least square regression analysis. The investigations of turbulent quantities in non-circular geometries reveals that an average developed length and the secondary velocity is reduced by 5% on considering the secondary velocities.

Subsequently, investigation on effect of cross-flow mixing on rod bundle thermal hydraulic safety margins are carried out using developed sub-channel analysis framework. The study is carried out for different simulated rod bundles of square pitched array of typical nuclear fuel assembly. The parameters considered are the size of the bundle, p/d ratio, intensity of turbulent mixing, mass flux, uniform and non-uniform axial power distribution. It is found that the coolant local conditions are significantly affected due to the inter-channel mixing between sub-channels. The sub-channel layouts are generated for fuel bundles of different sizes varying from 2 × 2 to 17 × 17 and different p/d and w/d ratios. The intensity of turbulent mixing parameter (c) is varied from 0 (no mixing) to 0.1 (high mixing). It is seen that hot channel temperature decreased by 26% in smaller bundle due to strong interaction between wall and corner channel. In case of large sized assembly above 5 × 5, hot channel temperature is less affected. The estimation of coolant temperature, fuel pin surface temperature and local quality are also carried out without considering the inter-channel mixing. The results are compared with a change in the local conditions for different degree of mixing among the fuel bundle sub-channels. The developed framework is also used for performing the sensitivity-studies during the design and analysis phase of nuclear reactor core for estimation of thermal hydraulic safety margins in an efficient way with minimum human intervention.

Table of Contents

Chapter No.	Title	Page No.
ACKNOWLEDGEMENTS		**i**
SYNOPSIS		**iii**
LIST OF FIGURES		**x**
LIST OF TABLES		**xviii**
NOMENCLATURE		**xix**
CHAPTER 1	**INTRODUCTION**	**2-10**
1.1	Background	2
1.2	Problem Statement	5
1.3	Organization of the Thesis	8
1.4	Closure	10
CHAPTER 2	**REVIEW OF LITERATURE**	**12-53**
2.1	Literature on Inter Sub-Channel Mixing	13
2.2	Inter Sub-Channel Mixing in Rod Bundles	15
2.3	Inter Channel Mixing Models	18
2.4	Development of Sub-Channel Analysis Codes	18
2.5	Fluid Flow and Heat Transfer Characteristics in Sub-Channel Geometries	47
2.6	Summary and Future Directions of Research	50

2.7	Motivation	52
2.8	Objective and Scope of the Present Work	53
2.9	Closure	53
CHAPTER 3	**MATHEMATICAL FORMULATION AND METHOD OF SOLUTION**	**55-71**
3.1	Introduction	55
3.2	Governing Equations of Fluid Flow	55
3.3	Boundary Conditions	59
3.4	Hydrodynamic Model of Non-Circular Geometry	59
3.5	Sub-Channel Analysis	62
3.6	Closure	71
CHAPTER 4	**DEVELOPMENT OF FRAMEWORK FOR SUB-CHANNEL ANALYSIS**	**73-90**
4.1	Introduction	73
4.2	Sub-channel Thermal Hydraulic Analysis	74
4.3	Architecture of Sub-Channel Analysis Framework	78
4.4	Fuel Assembly Layout Generator Module	82
4.5	Core Layout Generator Module	82
4.6	Power Profile Module	87
4.7	Analysis Module	88
4.8	Post Processing and Report Generation Module	88
4.9	Summary	89
4.10	Closure	90

CHAPTER 5	**FLUID FLOW AND HEAT TRANSFER CHARACTERISTICS IN SUB-CHANNEL GEOMETRIES**	**92-125**
5.1	Introduction	92
5.2	Laminar Flow and Heat Transfer in Sub-Channel Geometry	92
5.3	Numerical Simulation	93
5.4	Grid Independence Study and Validation	94
5.5	Results and Discussion	98
5.6	Analysis of Fuel Bundle	113
5.7	Turbulent Flow and Heat Transfer in Sub-Channel Geometries	118
5.8	Summary	124
5.9	Closure	125
CHAPTER 6	**INVESTIGATIONS OF FLOW BETWEEN ADJACENT SUB-CHANNELS OF NUCLEAR FUEL BUNDLE**	**127-137**
6.1	Introduction	127
6.2	Computational Geometry of Triangular Sub-channel	127
6.3	Results and Discussion	129
6.4	Summary	137
6.5	Closure	137

CHAPTER 7	**INVESTIGATION OF CROSS-FLOW MIXING IN FUEL PIN BUNDLES**	**139-171**
7.1	Introduction	139
7.2	Core Thermal Hydraulic Analysis	141
7.3	Geometrical Details and Boundary Conditions	143
7.4	Comparison and Validation of Sub-channel Analysis with CFD	146
7.5	Result and Discussion	152
7.6	Summary	170
7.7	Closure	171
CHAPTER 8	**CONCLUSIONS AND SCOPE FOR FUTURE WORK**	**173-176**
8.1	Introduction	173
8.2	Highlights of the Present Study	173
8.3	Broad Conclusions of the Present Study	174
8.4	Suggestions for Future Work	176
REFERENCES		**177-199**

LIST OF FIGURES

Figure No.	Title of Figure	Page No.
1.1	Schematic of a typical pressurized water reactor (PWR) plant	3
1.2	Schematic of a typical nuclear reactor core cross section and a hexagonal nuclear fuel assembly	4
1.3	Schematic of a typical square and triangular pitched nuclear reactor fuel assembly of different shapes	4
2.1	Research articles published in turbulent inter sub-channel mixing	13
2.2	Thermal Hydraulic Modeling of approaches of Nuclear Reactor systems and components	22
2.3	Cross section of test section	29
2.4	Cross section of test section used by Eiffler and Nijsing for velocity field measurement (1967)	29
2.5	Cross section of test section used by Kejellstrom, 1972, (p/d=1.217)	29
2.6	Cross section of test section used by Trupp and Azad (1973)	29
2.7	Cross section of test section used by Carajilescov	29
2.8	Cross Section of the test channel used by Rehme	29
2.9	Cross section of test Section used by Tapucu	31
2.10	Test section used in mixing experiments	31
2.11	Cross section of Seale's facility (Seale, 1979)	33
2.12	Cross section of Five rod sector of 37 rod bundle test section	33

2.13	GE-9 rod and ISPRA-16 rod two phase flow distribution test bundles	33
2.14	Test section used in CHF and mixing experiment	34
2.15	Rod bundle with mixing vanes	34
3.1	Schematic of fuel assembly and sub-channel connectivity	62
3.2	Control volumes with neighboring sub-channel connectivity for mass balance	63
3.3	Control volumes with neighboring sub-channel connectivity for energy balance	64
3.4	Control volumes with neighboring sub-channel connectivity for equation of axial momentum	66
4.1	Definition of fuel assembly sub-channels	76
4.2	Architecture of advanced sub-channel analysis framework	79
4.3	Schematic flow chart of sub-channel analysis framework	79
4.4	Screen shot of ASTHYANS workbench showing various features	81
4.5	Schematic of the layout generator	83
4.6	Layout of the fuel pin and sub-channel arrangements in different sizes of hexagonal fuel assembly generated using fuel bundle layout generator	83
4.7	Typical sub-channel layout of square pitched fuel bundle generated using fuel bundle layout generator	84
4.8	Typical core layout of square pitched fuel assembly	85

4.9	Typical core layout of hexagonal fuel assembly, the Contours of fuel pin and Sub-channel temperatures and HS-MCPR values of the fuel assembly at different power	86
4.10	The three dimensional fuel assembly peaking factors and power profile viewer	89
5.1	Four pin bundle with three different sub-channels of square assembly and (b) Triangular pitched sub-channel geometry	93
5.2	Grid independence study of circular, square and triangular tube fRe with various sizes of mesh	95
5.3	The contours of non-dimensional velocity and shear stress profiles in regular non-circular geometries	97
5.4	Effect of p/d on fRe in square and triangular sub-channel shaped tube	100
5.5	Effect of p/d on fRe in square and triangular sub-channel	101
5.6	Average Nusselt number for H1 and H2 boundary conditions of square pitched sub-channel	103
5.7	Average Nusselt number for H1 and H2 boundary conditions of triangular pitched sub-channel	103
5.8	Average Nusselt number for H1 and H2 boundary conditions of Square pitched sub-channel shaped tube	104
5.9	Average Nusselt number for H1 and H2 boundary conditions of triangular pitched sub-channel shaped tube	104
5.10	Non-dimensional velocity and shear stress in interior square pitched sub-channel	105

5.11	Non-dimensional velocity and shear stress in interior triangular sub-channel	105
5.12	Non-dimensional velocity and shear stress in a) Square pitched 4 pin bundle b) triangular pitched 7 pin bundle	106
5.13	Effect of p/d and W/d ratio on non-dimensional velocity and shear stress in hexagonal and square bundle	107
5.14	Effect of p/d and W/d ratio on non-dimensional velocity in hexagonal and square bundle	108
5.15	Comparison of $\overline{Nu}_{\mathrm{H1}}$ with p/d for triangular pitched sub-channel	111
5.16	Comparison of $\overline{Nu}_{\mathrm{H2}}$ with p/d for triangular pitched sub-channel	111
5.17	Parity plot showing comparison of Poiseuille number (data) with Poiseuille number (predicted)	112
5.18	Parity plot showing comparison of average Nusselt number (data) with average Nusselt number (predicted)	112
5.19	Variation of fRe of triangular pitched 7 pin bundles for different p/d and W/d ratio	115
5.20	Variation of fRe of square pitched 4 pin bundles for different p/d and W/d ratio	115
5.21	The effect of different size of fuel bundle on fRe at different p/d ratios and W/d ratio of 1.05	116
5.22	Effect of different size of fuel bundle on fRe at different p/d ratios and W/d ratio of 1.15	116
5.23	Effect of different size of fuel bundle on fRe at different p/d ratios and W/d ratio of 1.3	117

5.24	Effect of bundle size on fRe for an equal p/d and W/d ratios of 1.15 and 1.30 (ratio with reference to 4 pin bundle)	117
5.25	The non-dimensionalised velocity in different non-circular channels with secondary velocity vectors	118
5.26	Friction factor of square and triangular sub-channel at different Reynolds number with Blasius correlation for p/d =1.25	119
5.27	the variation of velocity ratio Uavg/Umax for square and triangular pitched sub-channel having p/d ratio of 1.25 for different Reynolds number	120
5.28	Turbulent geometry (G) factor for square and triangular pitched sub-channel for p/d ratio of 1.25 for different Reynolds number	121
5.29	The contours of velocity (m/s) in a triangular pitched non-circular sub-channel with p/d ratio of 1.25 at Re = $5x10^4$ with k-ε and RSM turbulent model	122
5.30	The contours of temperature (K) distribution in triangular sub-channel for an input heat flux of 0.5 MW/m^2 for a p/d ratio of 1.25 at Re = $5x10^4$ with k-ε model	123
6.1	Schematic of geometry and mesh of compound triangular sub-channel	128
6.2	Contours of velocity across the sub-channel along the length and at the outlet of sub-channel for an inlet mass flux of channel-1 at 600 kg/m^2s and channel-2 at zero mass flux	130

6.3	Contours of the variation of coolant velocity along the flow direction in compound triangular sub-channel at isothermal condition	131
6.4	Effect of change in the inlet mass flux of channel-1 on the flow development and the velocity at the centre of sub-channels. (Ch-1-channel-1, Ch-2- channel-2, G- inlet mass flux of respective channels)	131
6.5	Effect of change in the coolant mass flux along the sub-channels for p/d =1.05 (Ch-1-channel-1, Ch-2- Channel-2)	132
6.6	Effect of change in the coolant mass flux along the sub-channels for p/d =1.10 (Ch-1-channel-1, Ch-2-channel-2)	133
6.7	Comparison of change in coolant mass flux along the channel for p/d ratio 1.05 and 1.10. (Ch-1-channel-1, G1- mass flux of Channel-1, G2-mass flux of channel-2)	134
6.8	Contours of the variation of coolant velocity in a compound triangular sub-channel with heating of one sub-channel	135
6.9	Contours of coolant temperature variation along a compound triangular sub-channel with heating of one sub-channel	135
6.10	Variation of coolant velocity along the centre line of the triangular sub-channel with heating of one sub-channel	136
7.1	Typical sub-channel layout of square pitched fuel bundle generated using ASTHYAN Framework	146
7.2	Comparison of the outlet temperature of 2x2 pin bundle by CFD and sub-channel analysis	148

7.3	Comparison of the outlet temperature of 3x3 pin bundle by CFD and sub-channel analysis	149
7.4	The contours of velocity at the outlet of 3x3 GE nine pin Bundle	151
7.5	The contours of mass flux (Mlb/hrft^2) at the outlet of 3x3 GE nine pin bundle from sub-channel analysis	151
7.6	Effect of change in the sub-channel outlet temperature with the parameter (c) in the mixing correlation for different size of the bundle	153
7.7	Effect of bundle size on the center sub-channel outlet temperature with parameter (c) in the mixing correlation	154
7.8	Effect of bundle size on the wall sub-channel outlet temperature with parameter (c) in the mixing correlation	154
7.9	Effect of bundle size on the corner sub-channel outlet temperature with parameter (c) in the mixing correlation	155
7.10	Contours of sub-channel temperature (ºC) at the outlet of 3x3 square pitched fuel assembly for mixing parameter (a) c = 0.00 and (b) c=0.0	157
7.11	Contours of sub-channel temperature (ºC) at the outlet of 3x3 square pitched fuel assembly for mixing parameter (a) c=0.05 and (b) c=0.10	158
7.12	Contours of sub-channel temperature (ºC) at the outlet of 10x10 square pitched fuel assembly for mixing parameter c=0.00	159
7.13	Contours of sub-channel temperature (ºC) at the outlet of 10x10 square pitched fuel assembly for mixing parameter c=0.10	160

7.14	Contours of sub-channel temperature (ºC) at the outlet of 17x17 square pitched fuel assembly for mixing parameter c=0.10	161
7.15	Variation of Non-Uniform Axial Power Profile for 3X3 bundle	162
7.16	Variation of critical heat flux ratio with uniform axial power profile for 3x3 bundle	163
7.17	Variation of critical heat flux ratio with non-uniform axial power profile for 3x3 bundle	164
7.18	Variation of minimum critical heat flux ratio with mass flux with uniform axial and radial power distribution for different size of bundle	165
7.19	Non-dimensional temperature of the center sub-channel for different p/d ratio of 1.05	167
7.20	Non-dimensional temperature of the center sub-channel for different p/d ratio of 1.10	168
7.21	Non-dimensional temperature of the center sub-channel for different p/d ratio of 1.20	168
7.22	Non-dimensional temperature of the center sub-channel for different p/d ratio of 1.30	169
7.23	Variation of non-dimensional temperature with parameter (c) for 2x2 pin bundle at different p/d ratios	169

LIST OF TABLES

Table No.	Title of Table	Page No.
2.1	Different mixing phenomena in rod bundles	16
2.2	Comprehensive list of sub-channel analysis codes	20
2.3	List of experimental studies of nuclear fuel bundle sub-channels	23
3.1	Empirical constants used in the turbulence model	59
5.1	Comparison of the friction factor (fRe) and average Nusselt number ($\overline{Nu}$)	98
5.2	The effect of p/d ratio on Poiseuille Number (fRe) and average Nusselt number (Nu)	99
5.3	Coefficients of least square fit of fRe, $\overline{Nu}_{\mathrm{H1}}$ and $\overline{Nu}_{\mathrm{H2}}$ data of Square and triangular pitched sub-channel shaped tube	110
7.1	Comparison of coolant temperature at the outlet of assembly	150
7.2	Comparison of GE nine pin bundle test – Isothermal test cases	150

NOMENCLATURE

English Symbols (in alphabetical order)

Symbol	Description	Unit
A	area of sub-channel	m^2
C	loss coefficient for transverse momentum,	
c	coefficient in mixing correlation	
d	fuel rod diameter	m
d_h	hydraulic diameter	m
f	friction factor	-
f_T	correction factors of turbulent momentum	
f_D	correction factors of diversion momentum	
g_c	gravitational constant	kg-m/(N-s^2)
$\overline{G_{ij}}$	average of mass flux through sub-channel i and j	kg/(m^2s)
h	heat transfer coefficient	w/m^2-K
	enthalpy of Sub-channel	J/kg
k	thermal conductivity	w/m-K
L	length	m
m	mass flow rate	kg/s
N	number of sub-channel	
$\overline{Nu}$	Average Nusselt Number	
p	pitch	m
P	pressure	Pa

q''	heat flux	W/m^2
q_w	wall heat flux	W/m^2
Re	Reynolds number ($\rho v d_h/\mu$)	-
s	gap between pins	m
S	perimeter	m
T	temperature	K
T_b	bulk temperature	K
T_w	wall temperature	K
T^*	non-dimensional temperature	
u	velocity in x direction	m/s
v	velocity in y direction	m/s
	effective velocity	m/s
V’	effective specific volume	m^3/kg
w	velocity in z direction	m/s
	diversion cross-flow between adjacent sub-channels	kg/(m-s)
w_a	average velocity	m/s
W	wall distance (W=wall gap + pin dia.)	m
w’	turbulent cross-flow	kg/(m-s)
x, y, z	spatial coordinates	m
x	quality of coolant in sub-channel	
z	axial distance along the pin	m

Greek Symbols

Symbol	Description	Unit
α	thermal diffusivity,	m^2/s
β	mixing coefficient or mixing Stanton number	
ϕ	two phase friction multiplier	
Δ	difference	
Γ	domain boundary	
μ	viscosity	kg/(m-s)
ρ	density of fluid	kg/m^3
τ_w	wall shear stress	Pa
Ψ	pitch to diameter ratio	p/d
θ	two phase mixing multiplier	

Subscripts

Symbol	Description
a	air,
o	outlet
t	turbulent
l	Laminar
avgo	average outlet
fmax	fuel maximum
fmin	fuel minimum

in	average inlet
i , j	Sub-channel identification number
smax	sub-channel maximum
smin	sub-channel minimum
SP	single phase
TP	two phase
subo	sub-channel outlet

Superscripts

Symbol	Description
a	air
o	outlet
t	turbulent

ACRONYMS

Acronym	Expansion
ANL	Argonne National Laboratory
ASTHYANS	Advanced Sub-channel Thermal Hydraulic Analysis System
BWR	Boiling Water Reactor
CANDU	Canadian Deuterium Uranium
CASL	Consortium of Advanced Simulations of Light Water Reactor
CHF	Critical Heat Flux
CHFR	Critical Heat Flux Ratio
CPR	Critical Power Ratio
CFD	Computational Fluid Dynamics
COBRA	Coolant Boiling in Rod Array
DNB	Departure from Nucleate Boiling
DNS	Direct Numerical Simulations
EM	Equal Mass
EVVD	Equal Volume Exchange with Void Drift
FBR	Fast Breeder Reactor
GE	General Electric
GUI	Graphical User Interface
IAEA	International Atomic Energy Agency
IAPWS	International Association for Properties of Water and Steam
KAERI	Korean Atomic Energy Research Institute
LDA	Laser Doppler Anemometry
LES	Large Eddy Simulations
LHF	Local Heat Flux
LMFBR	Liquid Metal Fast Breeder Reactor

LOCA	Loss of Coolant Accident
LWR	Light Water Reactor
MATPRO	Material Properties
PIV	Particle Image Velocimetry
PWR	Pressurized Water Reactor
RANS	Reynolds Averaged Navier Stokes
SCWR	Super Critical Water Reactor
VVER	Water Cooled Water Moderated Energy Reactor
URANS	Unsteady Reynolds Averaged Navier Stokes Equation
LRGR	Low Resolution Geometry Resolving
VB .Net	Visual Basic .Net

CHAPTER-1

INTRODUCTION

CHAPTER-1

1 INTRODUCTION

1.1 Background

The contribution of global energy requirement from nuclear power is going to be increased in future keeping in view on the effect of greenhouse gases on the environment. Today about 440 nuclear power plants are operating around the world and 120 nuclear reactors are under construction (IAEA-RDS-2/36). The capacity of nuclear power plants is also increasing to reduce the capital cost with enhanced safety features. Following the nuclear emergencies caused by Three Mile Island (TMI) in the year 1979 in the US, Chernobyl in the year 1986 in Russia and Fukushima in the year 2011 in Japan, more importance has been attached to passive core cooling features to ensure the safety of reactor core under all these kinds of situations. The lessons learned from the previous experiences of analysis, experiments and accidents of nuclear systems are to be considered in the new design of reactors and to have enhanced safety features.

The nuclear reactor is a system/device in which the sustained fission chain reaction has been initiated, controlled and maintained at different power levels during steady operating conditions. In the case of any anticipated operational occurrences such as the tripping of primary pumps, loss of power supply etc., the reactor power is to be reduced and kept at different power levels or the reactor is to be tripped depending upon the events occurred. The safety of reactor core has to be ensured during both steady state as well as transient operating conditions by keeping the primary system pressure and temperature of the fuel within limits. In case of emergencies, the reactor has to be

shutdown and the residual heat has to be removed to keep the fuel temperatures within safety limits. The detailed thermal hydraulic analysis of reactor core is performed to estimate the maximum operating power of the reactor core and the available thermal margins of the reactor core. The schematic loops of a typical nuclear reactor of pressurized water reactor (PWR) type are shown in Fig.1.1. The nuclear reactor consists of a primary coolant system where the heat generated from the fission chain reaction in the fuel is transferred to the primary coolant. The primary system transfers the heat to the secondary system using the steam generator. The steam generated in the steam generator is used to run the turbine and electrical generators to produce electrical energy. The schematic layout and the cross-section of a typical nuclear reactor core are shown in Fig. 1.2. The nuclear reactor core consists of a large number of fuel assemblies in square, hexagonal and circular in shape. The fuel pins are arranged in square or triangular pitched arrays within a fuel assembly. Figure 1.3 depicts the schematic of a typical square and triangular pitched nuclear reactor fuel assemblies of square, hexagonal and circular shapes.

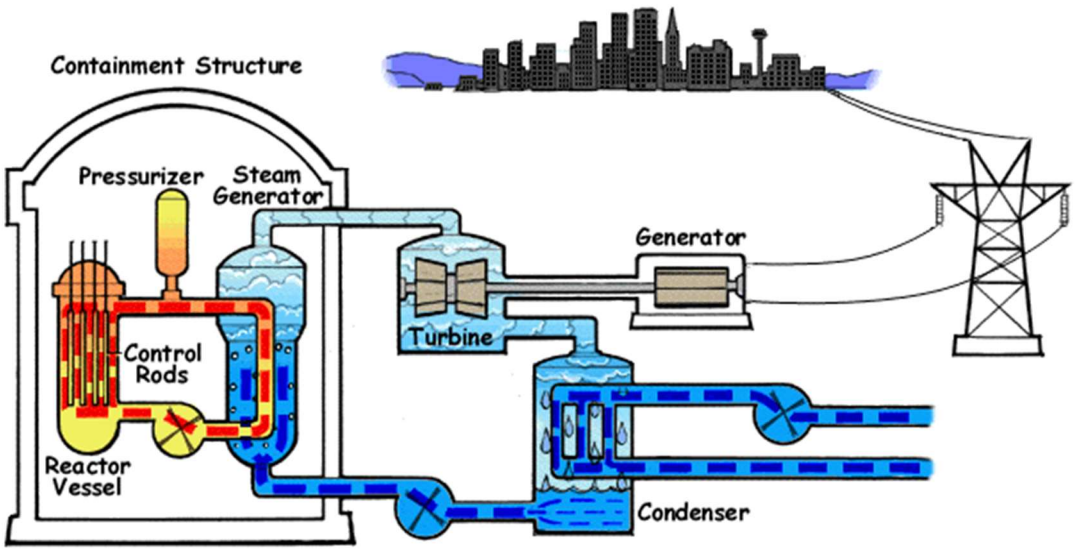

Fig. 1.1 Schematic of a typical pressurized water reactor (PWR) plant (U.S. NRC)

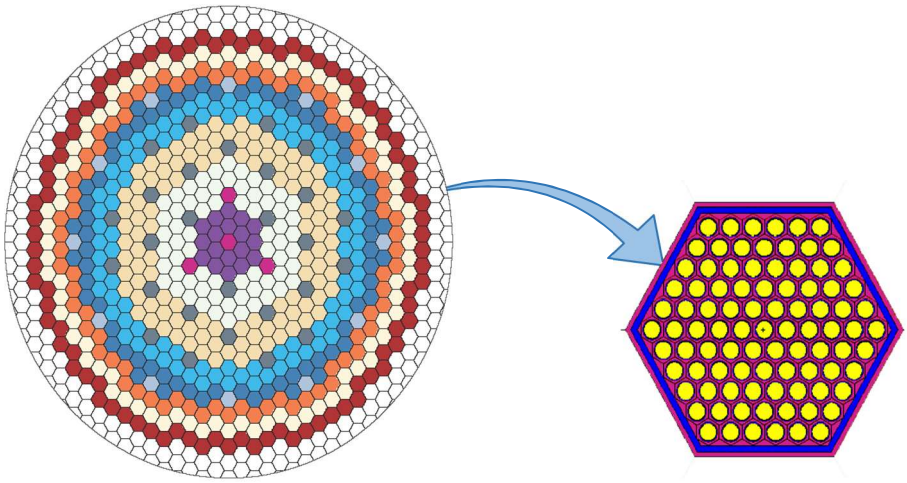

Fig. 1.2 Schematic of a typical nuclear reactor core cross section and a hexagonal nuclear fuel assembly (Touran)

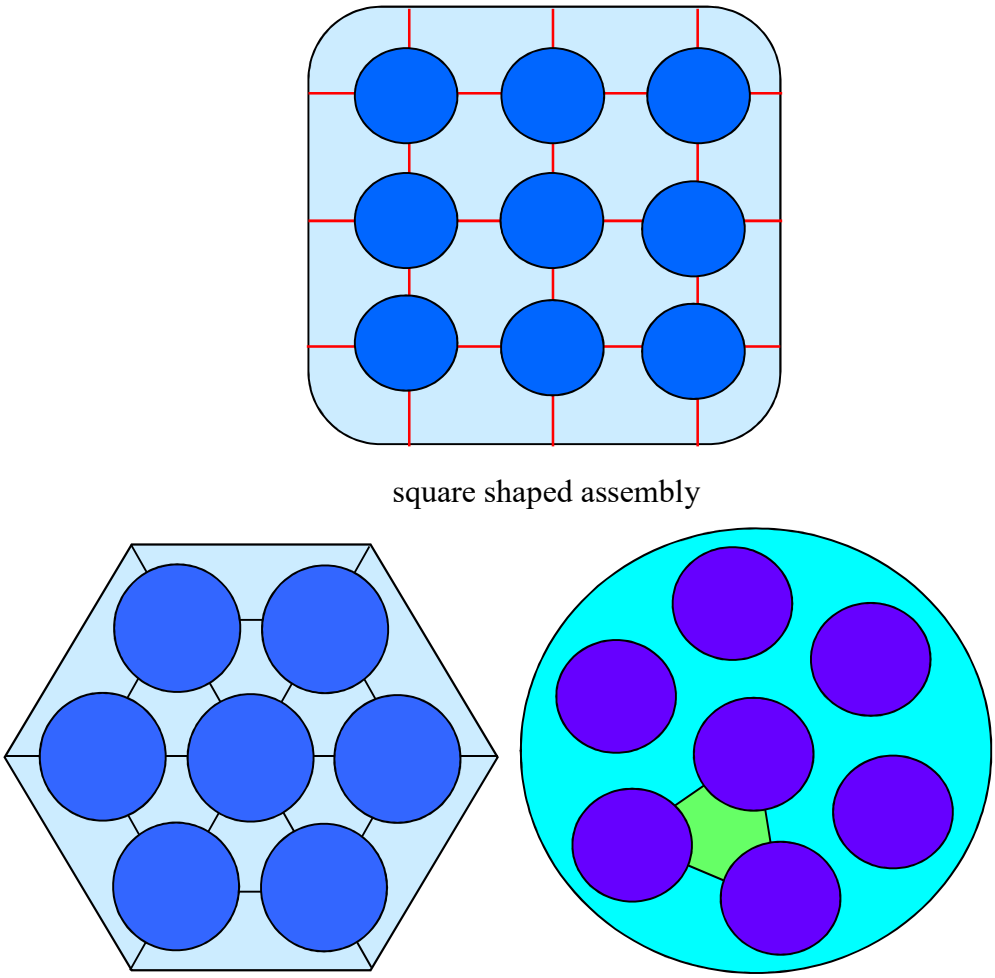

Fig. 1.3 Schematic of a typical square and triangular pitched nuclear reactor fuel assembly of different shapes.

The safety of the nuclear reactor system under all operating conditions of the core is ensured mainly by the detailed thermal hydraulic analysis of reactor core (Sha, 1980). The experiments and numerical simulations of the nuclear reactor core is required to ensure reactor safety (Yadigaroglu, 2003). This is ensured based on the accurate estimation of local conditions of the coolant in the fuel assembly using sub-channel analysis codes (Cheng and Muller, 1998). They are used to estimate different thermal-hydraulic safety margins and operating power limits of nuclear reactor core under different operating conditions. Considering the complexity of rod bundle geometry, different turbulent scales and limitations of computational resources, performing the full-scale computational fluid dynamic (CFD) analysis for nuclear reactor core is a cumbersome and time-consuming task. In sub-channel analysis codes, the governing equations of mass, momentum, and energy are solved in control volumes which are connected in both radial and axial directions. The flow distributions in the rod bundle geometry are estimated by considering lateral momentum balance and the inter-channel mixing models to account for the cross-flow between adjacent sub-channels (Rowe, 1967). The accurate estimations of local conditions of sub-channels are required to predict fuel temperature, critical heat flux ratio (CHFR) and critical power ratio (CPR) (Cheng and Muller, 2003).

1.2 Problem Statement

Extensive numerical simulations are required to estimate the thermal hydraulics safety margins as well as the safe limiting power of operation, under different conditions of the nuclear reactor core. Traditionally, the safety margins are estimated by sub-channel analysis codes, which are applied at the bundle level as well as the partial symmetry of

the core, demanding a very large computational time. In the sub-channel analysis, the key input parameters like sub-channel loss coefficients and inter-channel loss coefficients are required to calculate the flow distribution within the fuel bundle. These are obtained experimentally on simple geometries. Even today, the application of CFD for thermal hydraulics analysis of full bundle is a challenge due to limitations of computational resources and a large number of design calculations for different nuclear reactor operating regimes. However, CFD can be applied to the sub-channel level geometries to get more insight into the flow and temperature distribution within the rod bundle.

In a fuel bundle, during the normal operation forced convective heat transfer takes place. In the case of operation under decay heat removal during shutdown conditions natural convection heat transfer takes place. The flow through the fuel assemblies are in turbulent flow regimes under normal operating conditions and in laminar flow regimes in low flow and off-normal operating conditions.

Performing thermal hydraulic analyses to estimate the available thermal margins of reactor core for geometrical parameters and operating conditions such as pressure coolant inlet temperature, coolant flow and reactor power is an important element of reactor safety. The temperature distributions within the core must be predicted during normal operating conditions and during transients and accidents such as a loss of coolant accident (LOCA). Several thermal hydraulic analysis codes have been developed by the nuclear industry since its inception to predict core temperatures. As the detailed simulations of the core similar to the CFD analysis are not feasible even today to analyse

the wide variety of events to qualify the reactor core. Hence, the sub-channel analysis codes a number of simplifying assumptions are made to predict the coolant flow distribution within the fuel bundle. The complex three-dimensional problem of fluid flow and heat transfer in fuel bundle is simplified to a one-dimensional problem and the turbulent inter-channel mixing is considered to account for the cross-flow between the adjacent sub-channels. Sub-channels are subsections of the bundle flow area formed by imaginary boundary connecting the centroids of adjacent rods. The square sub-channel is formed by connecting four fuel/non-fuel rods, the triangular sub-channels are formed by three rods, and the wall sub-channel is formed by two rods and the wall. The Sub-channels are divided axially and are connected laterally by narrow gaps between the pins. The interchange of mass, momentum, and energy between sub-channels is solved using empirical correlations derived from the experimental results. However, the detailed velocity and temperature distributions are required to understand the complexities of the flow and heat transfer phenomena in a fuel bundle. The Computational Fluid Dynamics (CFD) approaches to solve the conservation equations of mass, momentum, and energy on very fine grids and can predict detailed velocity and temperature distributions within the fuel bundle. However, due to its high computational cost, simplified geometries are commonly used and even today the sub-channel analysis approach is used for the analysis of reactor core.

The large increase in the applications of sub-channel analysis codes on reactor safety requires continued development of software and its improvements on sub-channel analysis from the angle of user convenience features as well as the options available for analysis. These types of development of sub-channel analysis utility software help in,

fuel assembly design optimization, fuel cycle design, and core power level uprating studies. These improvements are also aimed at cost reduction, improvise the quality, repeatability of analysis for both vendor as well as a regulator which ultimately results into the overall improvement of the safety of nuclear reactor core (Swindlehust, 1995).

This thesis is focused on the thermal hydraulic analysis and safety-related issues of a nuclear reactor. The development of an advanced, general purpose, automated sub-channel analysis framework for performing the sensitivity-studies at different stages of design and analysis of nuclear reactor core for the estimation of thermal-hydraulic safety margins is carried out. The detailed understanding of fluid flow and heat transfer characteristics of non-circular sub-channel geometry are performed. The investigations of coolant mixing in nuclear fuel pin bundle are carried out using the developed sub-channel analysis framework.

1.3 Organization of the Thesis

The thesis is divided into eight chapters, inclusive of the present chapter. The essential features of each chapter are described below.

Chapter 1 gives a general introduction to the problem taken up in the present study and an outline of the organization of the thesis.

Chapter 2 reviews the literature pertaining to the problems considered in the present work along with the aim and scope of the study.

Chapter 3 gives the mathematical formulation of the problems and the method of solution along with the boundary conditions.

Chapter 4 discusses about the development of an advanced sub-channel analysis frame work and its requirement in the sub-channel thermal hydraulic analysis of nuclear reactor core.

Chapter 5 deals with the laminar fluid and heat transfer in non-circular sub-channel geometries of square and triangular pitched nuclear fuel bundle for different p/d and w/d ratio. The correlations are developed to predict the heat transfer and pressure drop in sub-channel as well as in a sub-channel shaped tubes are highlighted in this chapter. The effect of bundle size on the pressure drop and flow distribution is also studied in detail by solving the fully developed flow through the assembly using an out of plane flow problem rather than a conventional CFD methodology. This chapter also includes the vital results of turbulent flow and heat transfer characteristics in a triangular sub-channel.

Chapter 6 discusses the results of CFD investigations carried out on the flow characteristics in a compound triangular sub-channel due to pressure gradient alone caused by the differences in the mass flux among channels. The effect of heat addition to adjacent sub-channel on the flow exchange is also presented.

Chapter 7 includes the results of the investigations on the effect of cross-flow mixing on the coolant enthalpy rise in a typical nuclear reactor fuel pin bundle using the

developed sub-channel analysis framework. The parametric studies are presented by varying the coolant mixing parameter for different size of the fuel assembly. The effect of coolant inlet mass flux, uniform and non-uniform axial power profile on critical heat flux is also studied for different size of the bundle.

Chapter 8 gives broad conclusions derived from these studies. The limitations of the present study and the future directions of the research are also presented.

1.4 Closure

In this chapter, a brief background of the problems considered in the present study has been given. Broad outlines of the thesis and salient features of the respective chapters have also been highlighted.

CHAPTER-2

REVIEW OF LITERATURE

CHAPTER-2

2 REVIEW OF LITERATURE

The evaluation of the thermal-hydraulic safety margins of nuclear reactor core involves the accurate estimation of the local conditions of coolant within a fuel pin bundle. The prediction of local pressure gradient and turbulent inter-channel mixing receives a considerable amount of attention among the scientists and engineers in the field of core thermal hydraulic analysis. The cross-flow mixing under single phase and two-phase conditions play a vital role in the sub-channel analysis for the design and safety analysis of nuclear reactor core. The turbulent forced convection heat transfer takes place during the normal operating regimes. The flow through the assembly is in the laminar regime during the decay heat removal and low flow conditions. The coolant flow distribution within the fuel assembly is mainly affected due to many factors such as local pressure gradient, turbulent inter-channel mixing and spacer geometries. A lot of development has taken place in the methodology of sub-channel analysis codes resulting in improvement in the prediction of cross-flow mixing within a fuel bundle. In this chapter, a detailed literature survey related to sub-channel analysis methods, codes used for sub-channel analysis and coolant inter sub-channel mixing is carried out. A comprehensive review of sub-channel thermal-hydraulic codes for nuclear reactor core is also presented on various aspects of experimental, analytical and computational studies related to the rod bundle sub-channel analysis. Further perspectives for future directions are derived from the earlier research. The various experimental and analytical works conducted by researchers on different geometries of the sub-channels are identified. The application

of CFD technique to rod bundle flow distributions and heat transfer is also brought out from open literature and briefly discussed in different subsections with major findings and the gap areas. For the convenience and better presentation, important and relevant literature specific to the geometries considered in the present study is discussed in the following paragraphs.

2.1 Literature on Inter Sub-Channel Mixing

The literature review carried out on the topic of turbulent inter sub-channel mixing is shown in Fig. 2.1. It indicates that a vast amount of literature is available in the form of laboratory reports and journal articles.

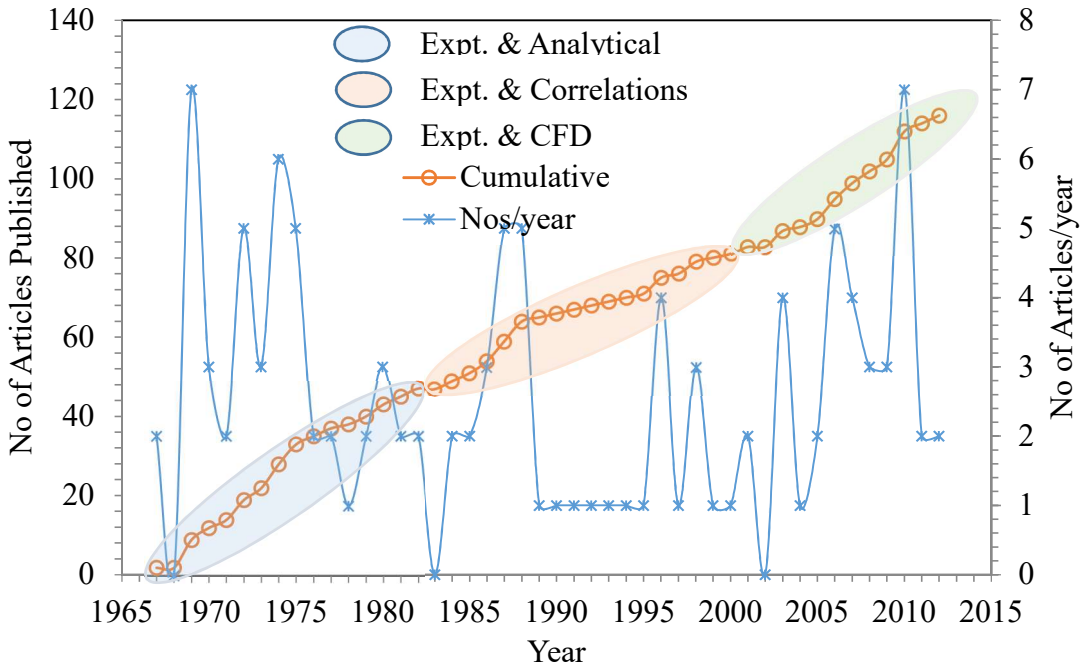

Fig. 2.1 Research articles published in turbulent inter sub-channel mixing

A recent review on critical heat flux (Cheng and Muller, 2003) in a water-cooled reactor shows that the empirical models describing inter-channel mixing affect the sub-channel conditions and a strong effect of the turbulent mixing coefficients on the calculated sub-

channel conditions is observed. The accuracy of the CHF prediction method in the rod bundle geometry is coupled with the accuracy of determining sub-channel flow conditions. Also, the use of a constant mixing factor assigned without regard to differences in power distributions is improper as the effect of mixing on enthalpy rise depends on the radial thermal gradient between the channels as well as flow conditions (Chelemer et al., 1972, 1977).

Study on CHF and turbulent mixing (Cheng and Muller, 2003) suggest that despite the large amount of theoretical and experimental studies on CHF and turbulent mixing, the knowledge of the precise nature of these phenomena is incomplete and that for each specific design, experimental investigations should be performed and validated prediction methods must be derived. Further, in their conclusion, a detailed literature survey has indicated that the experimental and theoretical works on CHF and turbulent mixing in tight hexagonal rod bundles under high pressure and high mass fluxes are very limited.

During the initial period (1960s and 1970s) of reactor design, the reactor core conditions are predicted based on the sub-channel analysis with suitable inter-channel mixing models derived from the experimental data of their respective geometries or simulated tests. The survey further shows that recent research is towards the phenomenological understanding of the turbulent flow structure in the rod bundles with the help of computational fluid dynamic techniques (Biemüller et al., 1996; Chang and Tavoularis, 2008; Tsutomu et al., 2010; Yan et al., 2012).

The topic of research articles in the early stages of sub-channel thermal hydraulic analysis was concentrated mainly on experimental and analytical works devoted to the

development of sub-channel analysis codes. Further, experimental and research works were oriented towards the development of various correlations of mixing models and verification/validation of sub-channel analysis codes with experiments. In the recent past, due to increased computational resources with advancement in CFD techniques and measuring instrumentations, the current research is devoted to simulation of experiments of rod bundle geometry using CFD techniques. These efforts were oriented towards gaining confidence in CFD predictions and also deriving the models from CFD for new fuel geometries and thereby, reducing the time required for design and optimization of fuel assembly (Hu and Fanning, 2011). Further, these efforts are aimed towards the improvement of safety and conducting the minimal number of experiments to save the resources and time. Also, CFD techniques help to get the detailed flow and temperature distributions within assembly as in experiments.

2.2 Inter Sub-Channel Mixing in Rod Bundles

In order to improve thermal-hydraulic characteristics of the nuclear reactor core, a considerable amount of research has been carried out to obtain an improved understanding of coolant flow and enthalpy distributions in rod bundle geometries. One form of fundamental research has been the study of the mixing process between complex geometries of sub-channels.

In analyzing the effect of mixing on rod bundle temperature and pressure gradient, it has generally been assumed that the mixing process is the result of several components as shown in Table 2.1. Further, the natural mixing describes turbulence in bundles of smooth bare rods (without protuberances) which include both turbulent and diversion cross-flow mixing.

Turbulent mixing results from the oscillatory component of flow in a transverse direction between two sub-channels and it can be characterized by the eddy diffusivity of momentum. On the other hand, the diversion cross-flow mixing is the rate of mass flow in a transverse direction through the gap between two sub-channels caused by radial pressure gradients. This flow contributes to the variation of the sub-channel flow rate in an axial direction. In the case of forced mixing, the sub-channel mass exchange is induced by the presence of spacers in the rod bundle. The flow scattering due to the non-directional mixing effect is generally described in literature associated with grid spacers which break up streamlines; the turbulence intensity increases immediately downstream from the device and the flow sweeping is referred as directed cross-flow effect associated with wire wrap spacers or grid spacers with mixing vanes which give a net cross-flow in a preferred direction.

Table 2.1 Different mixing phenomena in rod bundles

Phase	Natural Mixing	Diversion Cross-flow
Single Phase	Molecular Diffusion	Pressure Difference
	Turbulent Mixing	Forced Diversion
Two Phase	Void Drift	Pressure Difference
		Forced Diversion

2.2.1 Mixing under single-phase flow conditions

Much research has been devoted to the study of turbulent flow processes and improved understanding of mixing phenomena. Most of the experimental works have been

focused on quantifying the mechanism1s individually and their dependency. First, the relative importance of these processes in rod bundle performance varies significantly with bundle geometrical characteristics, particularly, gap spacing and flow parameters. Secondly, though turbulence interchange is present in all situations, major emphasis has been laid on determining turbulent cross-flow (diversion and sweeping) because of its most inherent property of momentum and energy transfer. It improves the thermal hydraulic performance of rod bundles and serves as an important mechanism for equalizing temperatures throughout the bundle. An excellent review of the related aspects of turbulent mixing and diversion cross-flow is given by Rogers and Rosehart (1972); the reviewers describe the circumstances in which crossflow mixing is developing, particularly, in the entrance region of bundles, region of beginning and development of boiling crisis in the various sub-channels and region of physical distortion of the bundle elements.

2.2.2 Mixing under two-phase flow conditions

Experimental data available in the literature about the mixing rate under boiling flow conditions are limited. Some investigations have been made with air-water mixtures to explain mechanisms of mixing in two-phase flow and to indicate the effect of various parameters, such as quality and mass flux on turbulent interchange rates. However, the principal information has been developed by Rowe (1967) through the use of thermal hydraulic code COBRA which constitutes a significant contribution to the knowledge of boiling flow behavior in rod bundles. It has been observed that boiling turbulent interchange appears to be a function of the channel geometry, quality and flow regime, with a maximum at low qualities in the transition region from bubbly to annular flow.

2.3 Inter Channel Mixing Models

2.3.1 Equal mass exchange turbulent mixing model (EM)

In the EM model (Hwang et al., 2000), it is assumed that the fluctuating mass flow rates between the interacting sub-channels are identical (i.e. $\rho v'_{ij} = \rho v'_{ji}$). Hence, there is no net transfer of mass due to the turbulent mixing and the diversion cross-flow is the only mechanism transferring mass between the sub-channels.

2.3.2 Equal volume exchange with void drift (EVVD)

In two-phase flow conditions, a substantial amount of net mass transfer has been experimentally observed in addition to the energy and momentum transfer. In order to explain this behavior, a model is devised by considering the equal-volume exchange of two-phase mixture between sub-channels ($v'_{ij} = v'_{ji}$), and assuming that two-phase turbulent mixing is proportional to the non-equilibrium void fraction gradient. The EVVD models (Hwang et al., 2000) consider the transverse mixing attributed to fluctuating flow at the interface and void drift between neighboring sub-channels. The void drift phenomenon is characterized by a strong trend towards the equilibrium void distribution, i.e., the vapor has a strong affinity for the sub-channel with the larger cross-sectional area and higher velocity (Sadatomi et al., 1994; Kawahara et al., 1997). Further, the effect of buoyancy on horizontal bundle under two-phase turbulent conditions and buoyancy drift is studied by Carlucci and Rowe in 2004.

2.4 Development of Sub-Channel Analysis Codes

An extensive literature review on the development and use of the sub-channel analysis codes applied to the nuclear reactor core design has been carried out from the existing literature which includes journals, books, laboratory reports of different research

organizations and thesis of other investigators on the similar research topics. Table 2.2 gives the comprehensive list of sub-channel analysis codes like HECTIC, ENERGY, SUPERENERGY, COBRA (I, II, IIIC, IV), CANAL, HAMBO, FLICA, THINC, VIPRE and COBRA-FLX developed at different times. These codes are still under development and undergoing improvements. They are used for design calculations and thermal-hydraulic analysis of different reactors since 1960. Among all these codes, COBRA type of sub-channel codes were applied largely to many types of reactors. It has been modified continuously (COBRA-WC (George et al., 1980), COBRASC, COBRA-LM, COBRA-EN (Basile et al., 1999), COBRA-TF (Gluck, 2007), COBRAFLX (AREVA NP Inc, 2010) and many more (DOE/ET-0009, 1977)) to improve the predictions of local conditions under single phase as well as two-phase and hence, the thermal hydraulic margins of core. Traditionally sub-channel analysis was applied in addition to modeling the local effects from the experimental data to account the local flow variations. Recently, with a significant increase in the computing power and the numerical techniques, CFD kind of approach is also made possible but still applying CFD to the whole core is a cumbersome task. To some extent, CFD analysis of sub-channel can be used for deriving the modeling parameters instead of experimental setup. The typical approach used in the analysis from sub-channel analysis to CFD for obtaining the modeling parameters, followed by other researchers is systematically depicted in Fig. 2.2 (Hu and Fanning, 2011). Further, the experimental, analytical and computational works carried out for the development of sub-channel codes to predict the thermal margins are discussed in this section.

Table 2.2 Comprehensive list of sub-channel analysis codes

Sub-Channel Code	Version /Year	Organization / Country	Application	Reference
HECTIC	I/1961, II/1962	Aerojet Nucleonics/ USA	GAS COOLED, PWR	Reynolds and Kattchee,1961 & Reynolds and Kattchee, 1962
SCEPTIC	1971	EIR/ Switzerland	GAS / PWR	Eriksson, 1971
COBRA	I/1967, II/1970, III/1971, IIIC/1973, IV-I/1976, IV/1977,	BNWL, USA	PWR, LMFBR	Rowe, 1967, 1970, 1971, 1973 Wheeler, et al., 1976 Stewart et al., 1977
VIPRE	1/1993, 2/1994	PNL/ EPRI/ USA	PWR	Stewart et al., 1993, VIPRE-02,1994
SCRIMP	1977	EIR/ Switzerland	GAS / PWR	Huggenberger, 1977
MATTEO	1973	MIT/USA	BWR	Forti and Gonzalez-Santalo, 1973
WOSUB	1978	MIT/USA	BWR	Wolf L. et al., 1978
CANAL	1979	MIT/USA	BWR/PWR	Faya et al., 1979
ASSERT	4/1984	AECL/CA, USA	CANDU	Tye et al, 1994
ENERGY	I, II, IV/1975	MIT/USA	LMFBR	Chen & Todreas, 1975
SUPERENERGY	I, II/1980	MIT/USA	LMFBR	Basehore & Todreas, 1980
MISTRAL	II/1972	KFK/ Germany	PWR	Baumann, 1972

DIANA	1974	Hitachi/ Japan	PWR	Hirao & Nakao, 1974
THERMIT	II/1981	MIT/US	LMFBR	Kelly etal., 1981
MATRA	1999	KAERI/S. Korea	PWR	Yoo et al., (1999)
MATRA-LMR	2002	KAERI/S. Korea	LMFBR	Kim et al., 2002
HAMBO	1967	AEEW/UK	PWR	Bowring, 1967
FLICA	III, IV/2000	CEA/France	LMFBR	Toumi et al., 2000
THINC	I/1968 ,II/1972 ,IV/1973	USA	PWR	Chu et. Al., 1973
SASS	I/1966	Sweden	CANDU	Pierre, 1966
SABRE	4,1992	France	LMFBR	Macdougall and Lillington, 1984; Dobson and O'Neill, 1992
SACoS	2012	Jiaotong University, China	SCWR	Khurrum et al., 2012
LYNXT	1 & 2/1976	B & W/US	PWR	BAW-10156-A
TORC	1975	CE/USA	PWR	CENPD-206-NP
SABENA	1985	Japan	LMFBR	Ninokata and Okano, 1985
NASCA	2001	Japan	PWR/LMFBR	Ninokata et al., 2001
MONA	2003	KOREA	LMFBR	Nordsveen, et al., 2003
SUBCHANFLOW	2010	KIT/Germany	PWR	Imke et al., 2010
ATHAS/OE	2016	Jiaotong University, China	PWR	Pan Wu et al., 2016

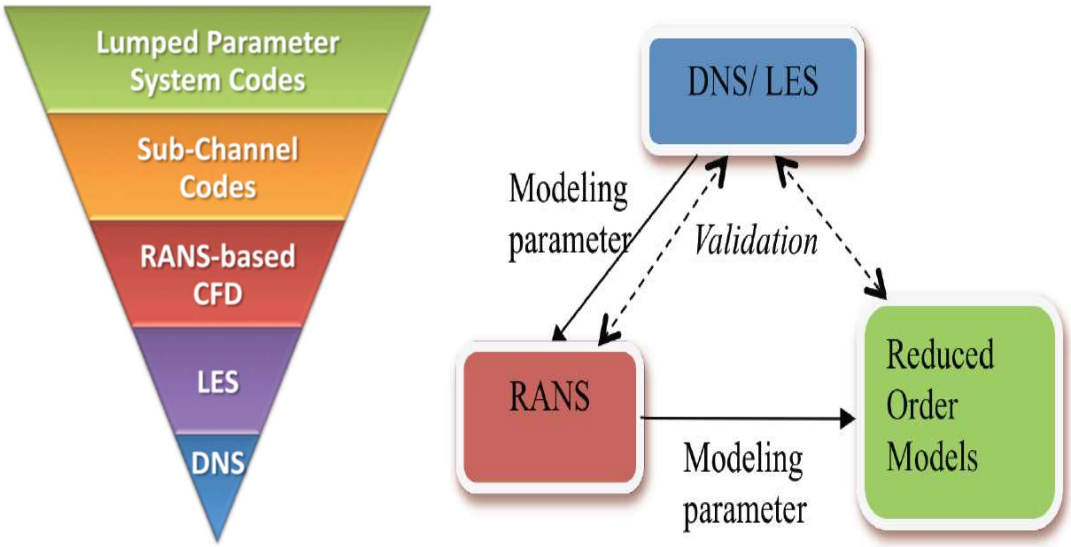

Fig. 2.2 Thermal Hydraulic Modeling of approaches of Nuclear Reactor systems and components (Hu and Fanning, 2011, ANL/NE-11/35)

2.4.1 Experimental works of rod bundles

The detailed literature survey indicates that a vast amount of research works was taken upon flow and heat transfer characteristics of rod bundle geometries in the form of experimental and analytical estimations. These studies were oriented towards the improved understanding of the coolant mixing inside the fuel assembly sub-channel and hence, the safety of nuclear reactor core under the different operating conditions. This section describes the experimental investigations carried out by different researchers from simple sub-channel geometries to rod bundle geometries. The list of different experimental studies of nuclear fuel bundle sub-channels is given in Table 2.3. The extensive experimental works of rod bundle sub-channels were aimed at the measurement of pressure drop across the rod bundle as well as in sub-channels (Novendstern, 1972; Maubach and Rehme, 1973; Rehme, 1980a, 1989; Grover and Venkat Raj, 1980; Hudina and Huggenberger, 1986).

Table 2.3 List of experimental studies of nuclear fuel bundle sub-channels

Investigator	Geometry	P/D	Re	Measured Data	Methodology
Walton (1969)	Triangular array, T-T	1.052	1900-90000	Concentration	Water, Air tests, Dye injection
Tachibana et al. (1969)	7 Pin bundle	1.125	8000-45000	Heat Transfer Factors	Naphthalene sublimation
Skinner et al. (1969)	6 equally spaced rod	1.420	20000-80000	Velocity (V), Pressure	Nitrous oxide tracer, Pitot static probe
Van Der Ros & Bogaardt (1970)	Compound rectangular channel	1.050	5000-30000	Pressure, velocity, Temperature (T)	Pitot tubes, thermocouple, thermal tracer
Rowe et al. (1974)	Square array 3x3	1.125 1.250	50000-200000	Turbulent Intensity (TI) auto correlation functions	Laser Doppler Velocimetry
Trupp & Azad (1975)	Triangular array	1.200 To 1.500	12000-84000	Axial velocity, wall shear stress, Reynolds stress, eddy diffusivity	Pitot static probe, Hot Wire Anemometry (HWA)
Carajilescov and Todreas (1976)	Square Channel	1.120	27000	Axial velocity, Turbulent kinetic energy, Reynolds stress	Laser Doppler Anemometry (LDA)
Rehme (1978)	Four Parallel rods	1.120	87000	V, τ_w, k	Pitot tubes, Preston tubes, HWA
Seale (1979)	Row of 3, 4, 5 rods	1.833 1.375 1.100	34369-299603	T and Velocity distributions	Pitot temperature probe, manometer

Hooper (1980)	Square array	1.150	48000-156000	τ_w, V, K	Pitot tube, Preston tube, HWA
Renksizbulut (1986)	Square array	1.150	500000	τ_w, V, TI	Preston Tube, LDA
Aly, Trupp & Gerrard (1978)	Equilateral triangular array	1.200 - 1.500	53000-107000	V, τ_w, secondary flow, friction factor	Pitot tube, X-wire probe, HWA
Vonka (1988)	Triangular Array	1.300	60000 175000	Secondary flow vortices	LDA
Hooper & Rehme (1984)	Four parallel Rods, 6 square array	1.026-1.118 1.107	54600-105000 22600-207600	V, τ_w, Reynolds stress, TI	Pitot tube, Preston tube, HWA
Rehme (1987)	Four par. rods	1.036-1.400	76000-119000	Reynolds Stress, TI, τ_w	HWA, Preston tubes
Moller (1991)	Four Par.	1.036-1.148	85000	V, τ_w, TI, pressure fluctuations	Pitot tube, HWA, microphone
Moller(1992)	Four Parallel rod	1.036-1.223	60880-148100	V, τ_w, TI	Pitot tube, HWA, microphone
Wu Trupp (1994)	Single Rod Trapezoidal	1.039-1.240	21300-52700	Fluctuating V, PSD	X-Wire probe
Meyer & Rehme (1994)	Compound rectangular channel	1.06-1.25	250000	V, τ_w, Reynolds Stress, TI, TKE	Pitot tube, preston tube, HWA
Wu (1995)	Asymmetric rod in trapezoidal duct	1.220, 1.039-1.079	26300	V, V', Energy spectra	Pitot tube, preston tube, HWA
Krauss and Meyer (1996)	Wall Sub-channel in	1.120	65000	V, T, τ_w, Turbulent velocity,	Pitot tube, preston tube,

	37 rod bundle			heat flux	HWA, Sheathed thermocouple
Krauss and Meyer (1998)	Triangular sub-channel in 37 rod bundle	1.12	65000	V, T, τ_w, Turbulent velocity, heat flux	Pitot tube, Preston tube, HWA, Sheathed thermocouple
Guellouz & Tavoularis (1992)	Rectangular channel	1.025-1.350	108000	V, τ_w, Reynolds stress, flow visualization	2-D PIV, Acetic acid tracer
Gosset & Tavoularis (2006)	Rectangular Channel With rods	g/d =0.025-0.7	388-2223	Flow visualization	Dye injection
Baratto et al. (2006)	5 rods	1.149	42000	V, V', PSD, Turbulent stress	HWA, Preston tube
Nicolas Silin & Juanico (2006)	Three rods in circular channel	1.20, 1.12	1400, 130000	Temperature	Thermocouple

The major studies in rod bundles includes: measurement of flow velocity and its distribution (Ibragimov et al., 1967; Chieng and Lin, 1979; Neti et al., 1983), secondary flow vortices inside the sub-channel (Vonka, 1988), measurement of wall shear stress (Eichhorn et al., 1980) and turbulence quantities, the structure of turbulence and its implications on natural mixing. The pressure drop and flow distributions were measured on bare rod bundles, bundles with grid spacers, wire wrap spacers and mixing vanes (Collingam et al., 1971). Experiments were also conducted for determination of turbulent exchange coefficients in triangular, square pitched and asymmetric rod bundles by measurement of sub-channel cross-flow due to pressure gradient and diversion cross-flow (Roidt et al., 1974; Yue et al., 1991). The enhancements in mixing in the rod bundles are also investigated in detail. The increase in turbulent mixing is

attributed to the large scale periodic flow pulsation between the sub-channels (Meyer, 2010). The measurement of frequencies and special correlations of coherent structures are carried out in recent times (Baratto et al., 2006). The averaged characteristics of the transport of momentum and energy in a heated rod bundles (Meyer, 1994) are also carried out to measure the turbulent mixing coefficient and also the cross-flow mixing during boiling conditions. In single phase coolant mixing experiments, either temperature (Silin et al., 2004), dye concentration, conductivity or the radioactive tracers (Carelli et al., 1969; Castellani et al., 1975) are used to measure the coolant mixing between sub-channels. The single-phase convective heat transfer characteristics of rod bundles of PWR (Holloway et al., 2008; Hochreiter et al., 2010), LMFBR (Chiu et al., 1980; Dwyer et al., 1972; Engle et al., 1980) and GCR (Hudina and Markbczy, 1977; Dalle Donne et al., 1977, 1979) are carried out to measure the temperature distribution (Nijsing et al., 1966). For the cases of two-phase flow conditions in rod bundle, investigations on cross-flow mixing during boiling, void distribution and two-phase model for light water reactor sub-channel analysis were carried out by many researchers (Beus, 1970; Kelly, 1980; Anklam and White, 1981; Wolf et al., 1987). The core coolability (Grandjean, 2007) under LOCA conditions such as reflooding and rewetting experiments (Ihle and Rust, 1987; Duffey and Porthouse, 1973; Thompson, 1974; Muto et al., 1990; Tuzla et al., 1991; Abdul-Razzak et al., 1992; Sahu et al., 2010) were conducted.

The measurement of flow and enthalpy, in case of the cross-flow mixing between parallel channels during boiling, is carried out by Rowe (1967, 1970). The geometry of the interconnected square and triangular channel considered for the study is shown in Fig. 2.3. The electrically heated test section is made up of SS-321 material is used in

these experiments. The amount of natural mixing occurring between two interconnected parallel channels during boiling as well as under the single-phase conditions is ~~are~~ investigated. The findings from the experimental works are used to validate the COBRA code. The results of the calculations (Rowe, 1967) showed that turbulent mixing during non-boiling conditions is nearly independent of rod spacing. In the case of two-phase flow, boiling can cause an increase in mixing only for certain conditions. The experiments indicated insignificant mixing in tightly packed rods with incremental influence on mixing at very high quality in two-phase flow.

Figure 2.4 shows the geometry considered (Eifler and Nijsing, 1973) to study the effect of secondary flow in rod bundle geometry (Eifler and Nijsing, 1967). Turbulent diffusion of momentum around the rod periphery is neglected in the model of Deisler and Taylor (Carajilescov, 1975). Their finding indicates that the secondary flow must transport turbulent rich fluid away from regions where turbulence production exceeds dissipation. The experimental works revealed that lateral variation of wall shear stress must be considered the prime cause for the existence of secondary flow. Local wall shear stress gradient will induce circular motion tending to transport of high momentum fluid through main flow in the direction of decreasing wall shear stress. Nijsing et al. (1967) conducted the experiment for various p/d ratios (1.05, 1.1, 1.15) and for a range of Reynolds number from 15,000 to 50,000. The pitot tube is used for the measurement of flow velocities in the sub-channel and also observed the fluid mixing between sub-channels in a bundle of finned tube.

The measurement of turbulent intensities and wall shear stress in rod bundle geometry (Fig. 2.5) was carried out by Kjellstrom (1972) for a p/d ratio of 1.217 using air at a fixed Reynolds number of 2.74×10^5. The measurement of flow velocity and turbulence

intensity distribution in axial, tangential and radial directions were performed by using hot wire anemometer, while the Reynolds stress distributions were obtained using Preston tube. Many experiments on rod bundle hydrodynamics were carried out by Trupp and Azad (1975) using the hot wire anemometer for different p/d ratios varied from 1.20 to 1.50 and Reynolds number in the range of 1.2×10^4 to 8.4×10^4. The cross-section of the test section used in their study is shown in Fig. 2.6. The measurements were carried out for axial velocity, turbulent intensity, shear stress and power spectra of axial turbulence. Wall shear stress distribution was presented and discussed in detail.

Experimental and analytical study of axial turbulent flow in an interior sub-channel of a bare rod bundle is investigated by many other researchers. Experimental measurement of the distribution of the axial velocity, turbulent kinetic energy, and Reynolds stress were performed using Laser Doppler Anemometer (LDA) by Carajilescov (1975) for p/d ratio of 1.123 and L/d_{hy} of 77 for the geometry depicted in Fig. 2.7. The comparison of HYBBAC code predictions with experimental data at the symmetry locations was ~~were~~ made in his dissertation, work.

Experimental investigations on the structure of turbulent flow in rod bundles (Rehme, 1978, 1979, 1980a, 1981, 1987a, b) wall sub-channels and the fluid flow through an asymmetric rod bundles were studied extensively by (Rehme, 1976, 1980, 1981, 1986, 1987, 1992) and Hooper and Rehme (1983). Measurements of velocity, turbulence structure using hot wire anemometer (Rehme, 1976, 1984a, b) and wall shear stress are carried out in a rod arrays for different p/d (1.036, 1.07, 1.148) and wide range of w/d (1.045, 1.048, 1.072, 1.074, 1.096, 1.118, 1.222, 1.252) ratios (Rehme, 1977, 1980b, c, 1982a, b, c, 1983a, b, 1984, 1985, 1986). A rectangular channel with four parallel rods is used for the experiments as shown in Fig. 2.8.

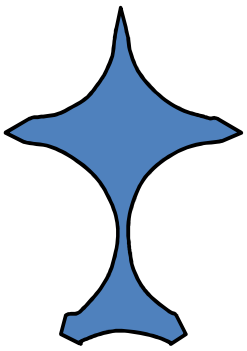

Fig. 2.3 Cross section of test section

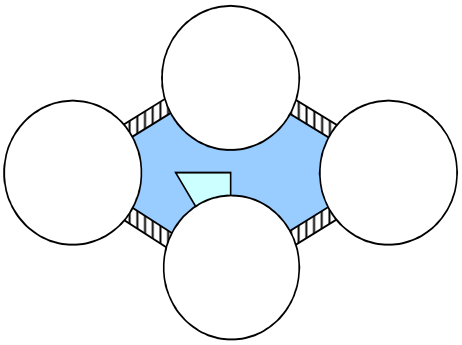

Fig. 2.4 Cross section of test section used by Eiffler and Nijsing for velocity field measurement (1967)

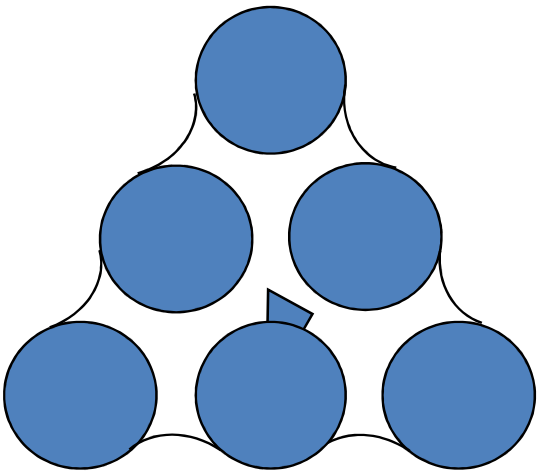

Fig. 2.5 Cross section of test section used by Kejellstrom, 1972, (p/d=1.217)

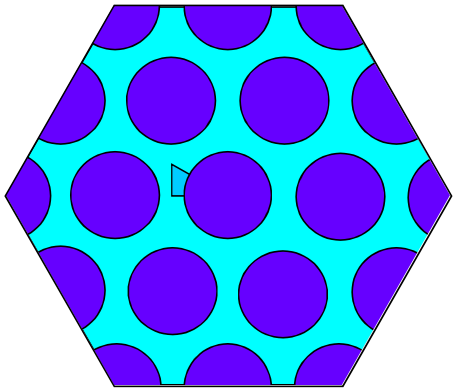

Fig. 2.6 Cross section of test section used by Trupp and Azad (1973)

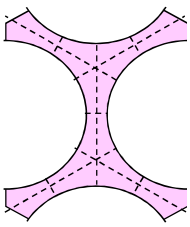

Fig. 2.7 Cross section of test section used by Carajilescov

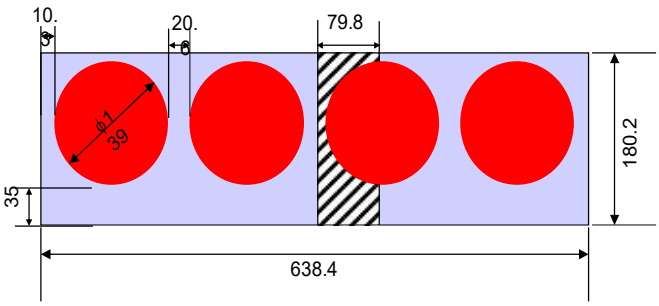

Fig. 2.8 Cross Section of the test channel used by Rehme

The experimental findings reveal that the structure of turbulent flow through rod bundles is different from that of circular tubes, at least for p/d and w/d ratios less than 1.2. They concluded that energetic and almost periodic azimuthal turbulent velocity component directed through the gap is responsible for the increased mixing process. The periodic pulsation is apparently generated by incompressible-flow parallel-channel instability. The long length scales of the axial and azimuthal turbulent-velocity components, relative to the gap width, emphasize the anisotropy of the turbulent transport processes in the gaps of rod bundles. The anisotropy of turbulent transport not only depends on the p/d and w/d ratios but also on its geometrical location inside the flow channels of rod bundles.

Experimental investigation of mass exchange under two-phase flows between two laterally interconnected sub-channel is carried out by Tapucu et al. (1994). The exchange of air/water mixtures flowing in two parallel, square, communicating channels is used for the initial testing and validation of ASSERT code. Channel geometries used in experimental setup are given in Fig. 2.9. The experiments were conducted at the same initial nominal mass flux in both sub-channels, but for different initial voids and different orientations. The key parameters, such as pressure, void fractions, and liquid and gas flow rates in both channels, were measured at several axial locations and the developed code was validated. The code is capable of computing distribution of flow and phases in horizontal channels and fuel bundles, and the onset of subcooled boiling in bundles. However further, investigations are required to improve the constitutive relationships describing the void generation, condensation, and drift.

Nicolas Silin and Luis Juanico (2006) carried out an experimental study for the dependency of Reynolds number with turbulent mixing between fuel-bundle sub-channels is studied. The physical configuration used in the experimental setup is depicted in Fig. 2.10. The measurements were done on a triangular array bundle with a p/d = 1.20 and 10 mm rod diameter, in a low-pressure water loop, for a range of Reynolds numbers between 1.4×10^3 to 1.3×10^5. The high accuracy of the results is obtained by a recently developed thermal tracing technique. It is also observed that there is a marked increase in the mixing rate for lower Reynolds numbers. The weak theoretical base of accepted Reynolds number dependence is pointed out in light of the later findings and its ambiguous supporting experimental data. The recent results also provide indirect information about the dominant large scale flow pulsations at different flow regimes.

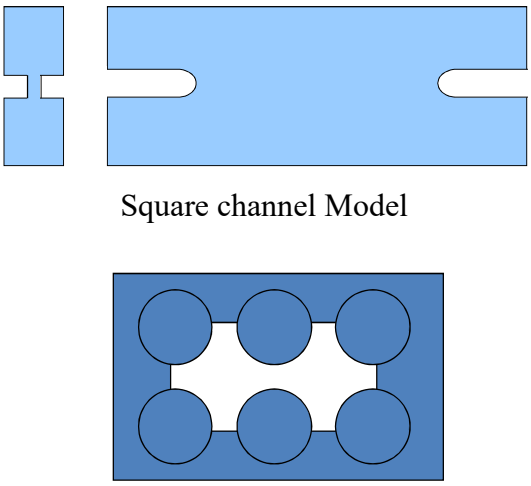

Fig. 2.9 Cross section of test Section used by Tapucu (1977)

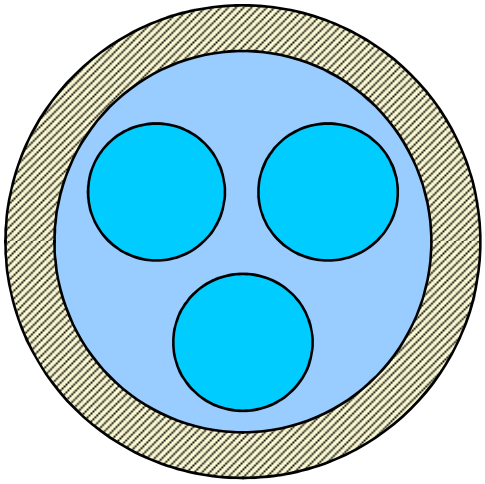

Fig. 2.10 Test section used in mixing experiments

Experimental works of turbulent diffusion of heat transfer between connected flow passages in the geometries shown in Fig. 2.11 are carried out by Seale (1979). The measurement of turbulent quantities in rod bundles is performed to assess the effect of turbulent inter-channel mixing due to the structure of turbulence, the effect of secondary flow (0.5% of axial flow velocity) and effective diffusivity in the circumferential direction. This study is concerned with mixing due to turbulent diffusion and secondary flow between sub-channels formed by bare smooth rods.

The experimental results confirm that inter sub-channel mixing is considerably higher than that predicted by simple turbulent diffusion theory. Further, effective diffusivity through the gap is also observed to be strongly anisotropic in nature.

The contours of axial velocity and temperature do not suggest any disturbances which could be attributed to secondary flow. The enhanced mixing rate through the gap is diffusive in nature and is due to a marked anisotropy in the gap region. Secondary flow appears to be much less significant in the ducts of the current type compared to that believed earlier. The source of marked anisotropic diffusivity remains a major unanswered question.

Fully developed turbulent flow of air in five-rod sector of 37-rod bundle CANDU type fuel assembly (Fig. 2.12) is conducted to measure the mean velocity, Reynolds stress and turbulent scales at the wall and inner sub-channel (Ouma and Tavoularis, 1991). The study was conducted by moving the central rod inside wise as well in rotated conditions, thereby, creating the rod-to-rod and rod-to-wall contacts. The aim of the study was oriented towards the understanding of heat transfer characteristics under

distorted geometrical conditions. The measurements show that the local friction factor varied appreciably than the average friction factor based on sub-channel bulk velocity.

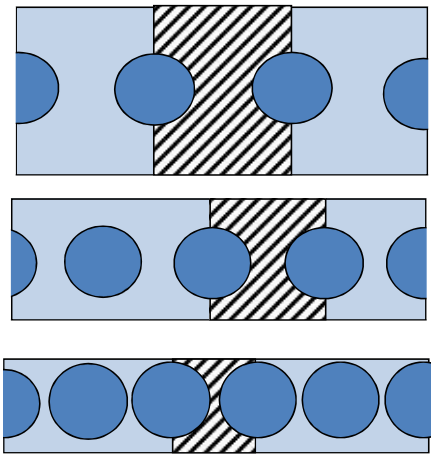

Fig. 2.11 Cross section of Seale's facility (Seale, 1979)

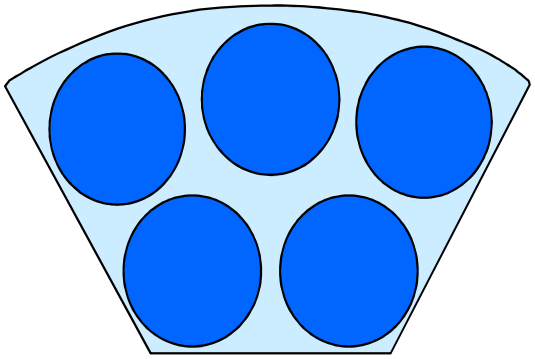

Fig. 2.12 Cross section of Five rod sector of 37 rod bundle test section.

Measurements of enthalpy and flow distributions at the outlet of a square-lattice bundle (Fig. 2.13) at 69 bar (BWR Operating conditions) are carried out in the General Electric (GE) 9-rod bundle (Lahey et al., 1970). Similarly, two-phase flow distribution tests were conducted in ISPRA-16 rod bundle under PWR operating conditions. These tests were used to assess the inter-channel mixing models used in the COBRA-IV codes (2000).

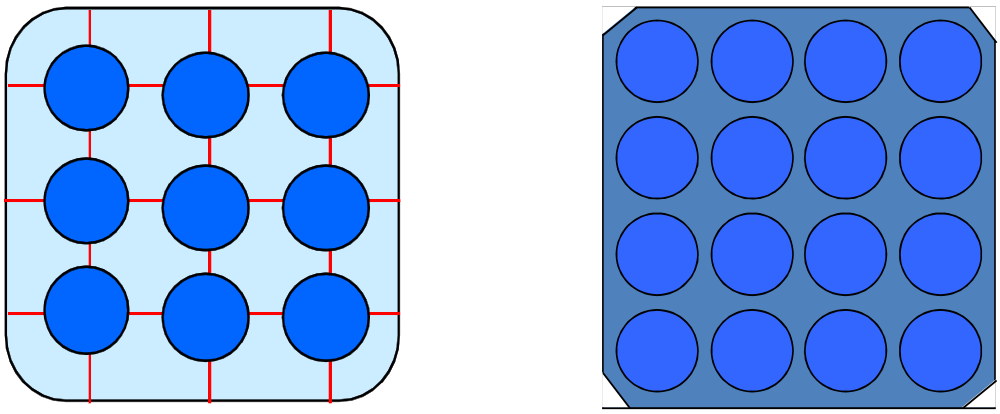

Fig. 2.13 GE-9 rod and ISPRA-16 rod two phase flow distribution test bundles.

Experimental and theoretical investigations of critical heat flux and turbulent mixing in hexagonal tight lattice 7-rod bundles (Fig. 2.14) were investigated by Cheng and Muller (1998) using Freon-12 as a working fluid. It has been found that the two-phase mixing coefficient increases with decreasing mass flux for the test conditions considered. Similar experiments in the two-phase flow regime were conducted in a 7-rod bundle with the circular channel by many other researchers to study the effect of channel wall flow distribution (Carver et al., 1984).

Phenomenological investigations on the turbulent flow structures in a 5 × 5 rod bundle array (Fig. 2.15) with mixing devices is carried out by Chang et al. (2008), in MATIS-H facility. This experiment was conducted in the cold test loop at Korea Atomic energy research institute (KAERI) using Laser Doppler Anemometry (LDA) to measure the velocities and the turbulent quantities. The measurement and CFD predictions indicated that the split type spacer grid is more effective for mixing between neighboring sub-channels rather than mixing within a sub-channel. Swirl type mixing vane has better performance for mixing within a sub-channel.

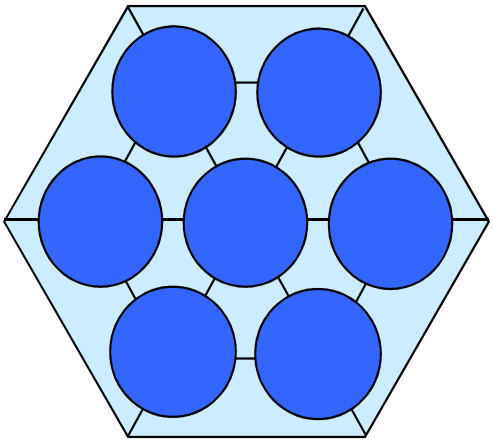

Fig. 2.14 Test section used in CHF and mixing experiment.

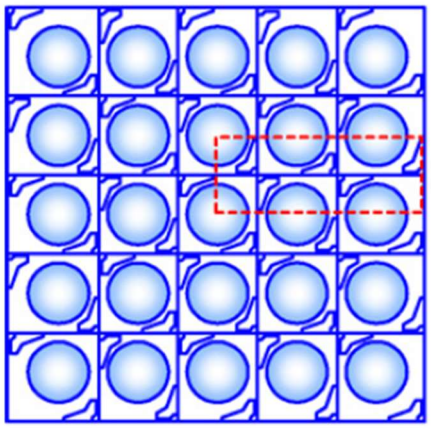

Fig. 2.15 Rod bundle with mixing vanes.

2.4.2 Theoretical studies of fuel assembly sub-channels

The analytical works related to the turbulent inter-channel mixing, sub-channel analysis, fluid flow and heat transfer characteristics of rod bundles were surveyed from the literature and some of the literature relevant to inter-channel mixing and sub-channel analysis is discussed in this section.

The analytical findings on rod bundles were aimed at predicting rod bundle's hydraulic and heat transfer characteristics under single and two-phase flow conditions in the fuel bundles of different types of reactors. The sub-channel analysis is aimed at predicting flow, velocity and temperature distributions in bare as well as wire wrapped rod bundle (Bishop and Todreas, 1979; Rehme, 1982; Hooper and Rehme, 1984; Hooper and Wood, 1984; Rapley and Gosman, 1986; Kaiser and Zeggel, 1987; Lee and Jang, 1997; Kriventsev and Ninokata, 1999; Misawa et al., 2003; Chang and Tavoularis, 2007; Kazuyuki and Ninokata, 2007; Ninokata et al., 2009) and also for blocked sub-channels (Ang et al., 1987; Hooper and Wood, 1983). The analysis included the prediction of pressure drop across fuel assemblies and the friction factors (Rehme, 1972, 1973a, b; Marek et al., 1973; Marek and Rehme, 1979; Lee, 1995; Jian et al., 2002; Su and Freire, 2002; Schikorr et al., 2010) of different types of sub-channels (Cheng and Todreas, 1986) such as central, wall and corner in rod bundles. The evaluation of flow distribution, coolant mixing within the bundle due to inter-channel mixing under single phase (Castellana et al., 1974; Jeong et al., 2006) and two-phase flow conditions (Lahey and Schruab, 1969; Carlucci et al., 2004; Kawahara et al., 2006) with different geometrical parameters (Jeong et al., 2007) of bare rod assembles (Hee, 1970), assemblies with grid spacers, wire wrapped spacers (Ginsberg, 1971) and mixing vanes (Lee and Choi, 2007) were carried out using different mixing models in sub-channels

analysis codes (Tapucu et al., 1994; Dae-Hyun et al., 2000). Different mixing models and correlations were studied to estimate the turbulent mixing rate and turbulent energy exchange between sub-channels for water (Petrunik, 1973; Ramm et al., 1974; Ninokata and Todreas, 1975; Rehme, 1979b; Rehme, 1980; Eiff and Lightstone, 1996; Wu, 1995) and low Prandtl number fluids (Rehme, 1992; Kim and Chung, 1999, 2001). The influence of wall sub-channels on turbulent flow and temperature distributions are also studied analytically (Rehme, 1978a, b; Mohanty and Sahoo, 1986).

The coolant mixing within the reactor pressure vessel and outlet plenum were examined to assess the flow through the fuel bundle (Todreas, 1979, 1985) and also the influence of wall and upper tie plate on flooding in rod bundle (Okhawa and Lahey, 1980; Spatz and Mewes, 1987). Apart from flow distributions, turbulent heat transfer characteristics is also studied numerically using various turbulent models in bare rod and wire wrapped bundles (Axford, 1967; Baglietto and Ninokata, 2003; Khan et al., 1975; Lewis and Buettiker, 1974; Matiur and Ahmad, 1982; Tae Sun and Todreas, 1988; Thompson and Holy, 1975).

The analytical works on the temperature and heat flux distribution in the tightly packed liquid metal cooled pin bundle are carried out by many researchers (Dwyer, 1966; Nijsing et al., 1964, 1966, 1975; Subbotin et al., 1961; Subbotin et al., 1971; Levchenko et al., 1967; Hofmann, 1970; Zaiyong Ma et al., 2012). Analysis of liquid metal heat transfer in closely spaced fuel rods assemblies is carried out by Nijsing and Eifler (1969). A theoretical evaluation of two-dimensional temperature and heat flux distribution for turbulent axial flow at relatively low Peclet numbers is reported. In the analysis, turbulent, fully developed axial flow and heat transfer conditions are considered for heat transfer in infinite triangular or rectangular array of fuel rods cooled

by liquid metal. It was assumed that the coolant turbulent heat transport is negligible with respect to heat conduction due to liquid metal and close rod spacing. The results were presented for dimensionless rod spacing p/d in the range of 1.0 to 1.15 and various rod material combinations of practical interest. Theoretical predictions were compared with experimental data and found to be in good agreement.

A review of heat transfers to liquid metals flowing in-line through un-baffled rod bundles is presented by Dwyer (1969) for fully developed heat transfer to liquid metals flowing turbulently and longitudinally through closely spaced un-baffled rod bundles (Dwyer et al., 1972). The pins were arranged in a triangular pitch, and rod spacing, rod design, and ranges of independent variables covered were chosen with reference to liquid-metal-cooled nuclear reactor applications. Three different sets of thermal boundary conditions were considered i.e. (i) uniform heat flux in the axial direction with uniform temperature in the circumferential direction, on the outer surface of the cladding, (ii) uniform heat flux in both directions on the outer surface of the cladding, and (iii) uniform heat flux in both directions on the inner surface of the cladding. The rod-average heat-transfer coefficients and circumferential variations of temperature and heat flux on the rod surface were presented as functions of p/d and Pe. Different methods of estimating eddy diffusivity of momentum in the circumferential direction were employed, and the reference method i.e. equality of the eddy diffusivities of momentum in both the circumferential and radial directions appears to give satisfactory predictions.

A numerical analysis of heat transfer in turbulent longitudinal flow through assemblies of un-baffled fuel rods is presented by Pfann (1972). The solution applied to triangular or rectangular arrays of fuel rods with fully developed velocity and temperature profiles, for fluids $Pr \leq 1$. In the case of liquid metals, the thermal resistance of the cladding and

bond were considered. However, the turbulent heat transport component is neglected. For common liquids, the circumferential turbulent heat transfer is considered. Results are compared in the range of dimensionless rod spacing of 1.0–1.6. The experimental results of other authors were found to be in good agreement with these calculations.

An analytical method of evaluating the circumferential variations of temperature and heat flux fields inside and around a displaced fuel rod in triangular rod bundles in turbulent flow were presented with examples by Hishida (1974). The analysis mainly consists of the derivation of simultaneous solutions of a set of heat conduction equations for fuel, cladding, and coolant for fully developed flow and heat transfer conditions. The local coolant velocity distribution, which is necessary for deriving the temperature field in the coolant, is determined by solving the Navier-Stokes equation and the turbulent mixing of coolant is taken into consideration. The results show how the circumferential variations in the temperature and heat flux fields on the outer surface of the cladding increases with lowering the p/d ratio and the larger the fuel rod displacement due to thermal conduction and peripheral coolant flow velocity distribution.

The calculation of heat transfer developments in the fuel bundle is carried out by Vonka and Boonstra (1974). Two elementary modes of heat transports in a rod bundle geometry were investigated, namely, the transport from a fuel rod surface into the adjacent sub-channel and from one sub-channel into the next one. The first transport is characterized in terms of the Nusselt or Stanton numbers, while the later in terms of the Stanton gap number or mixing factor. Hydraulically developed flow is assumed, with no feedback of heat transport on the flow condition. A three-dimensional numerical calculation by means of the finite difference method is applied. The comparison of

available experimental data and with theoretical predictions, it is found that the heat transfer between sub-channels is developed considerably slower in comparison with the development of the heat transport from fuel rod to sub-channel.

Solving the conservation equations in fuel rod bundles exposed to parallel flow by means of curvilinear-orthogonal coordinates is carried out by Meyder (1975). A unique method is described for constructing a curvilinear-orthogonal mesh grid. A method to perform calculations in such a mesh grid is illustrated and demonstrated for the problem of laminar flow in rod bundle geometries. Further, for prediction of turbulent velocity and temperature distribution in the central sub-channel of rod bundles (Meyder, 1975), the method was presented to calculate local heat transfer coefficients, temperatures, mixing rates, friction factors and wall shear stress distribution. This model led to a satisfactory agreement between experimental and theoretical results. The methods outlined here for the central sub-channel in a fuel element could now be applied in an analogous way to corner and wall channels. By coupling the different channel types, it would be possible to give a complete and economic description of the geometry in a fuel element or in a test section.

Some recent computations of rod bundle thermal hydraulics using boundary-fitted coordinates were presented by Chen et al. (1980). In this paper, the status of development of two computer codes for benchmark rod bundle thermal hydraulic analysis using the boundary-fitted coordinate method are described. A classification of the flow in rod bundles is made and details of computer codes are given. The codes solved essentially, identical sets of conservation of mass, momentum, and energy. However, one of them treated the fully-elliptic set of equations, and the other neglects the axial diffusion of momentum and heat. The ignorance of stream wise diffusion made

the flow partially elliptic and brought significant reductions in computer storage and modest savings in required computer time. Results of some validation calculations were presented with applications to possible reactor geometries.

Three dimensional distributed resistance modeling of wire-wrapped rod bundles were developed by Ninokata et al. (1987). The model is developed mainly for replacing the forced crossflow models that are currently in wide use in sub-channel analysis codes. The models specifically account for the presence of the wire-wrap spacer and might be used for any lumped parameter thermo-hydraulic analysis. Validation studies of the hydrodynamic resistance models were also performed using a sub-channel code ASFRE (Yoshika et al., 1981; Ninokata et al., 1985). The models were tested against sub-channel velocity and temperature data taken from bundles of triangular rod array configurations with wire-spacers. Overall the models performed satisfactorily, predicting the most important qualitative trends for flows in wire-wrapped rod bundles.

Turbulent flow and heat transfer in rod bundle sub-channels is analyzed using two-dimensional eddy diffusivity and a higher order K-I model proposed by Mohanty and Sahoo (1988). The eddy diffusivity was a generalization of the Reichardt's model for a concentric annulus. The K-I model is used to examine the effects of anisotropic turbulent diffusion. Fully developed flow and thermal conditions were assumed with the rod surface subjected to uniform heat flux in triangular and square arrangements of rods were investigated. The pitch to diameter ratio (p/d) is varied from 1.1 to 1.5. The algebraic eddy diffusivity was found to reproduce literature information, including those attributed to anisotropy or secondary flow effects. Thermal calculations have been carried out both for constant and variable values of turbulent Prandtl number.

2.4.3 CFD analysis of rod bundles

In recent times, as discussed earlier due to the advancement of computational resources and CFD techniques, the efforts are taken up by researchers to reduce the experimental works and apply CFD for the simulation of the flow characteristics in rod bundles. The literature on application of CFD technique for the study of rod bundle flow distributions and heat transfer characteristics were surveyed. The application of different CFD techniques and turbulence models were discussed in this section.

The CFD simulations were carried out by various researches, in PWR fuel assemblies, for the single-phase turbulent flow simulations to estimate the velocity and temperature fields (Ninokata and Merzari, 2007), secondary flow in rod bundles (Baglietto and Ninokata, 2004), turbulent flow structures and mixing across the narrow gap between rod bundle sub-channels (Biemüller et al., 1996; Chang and Tavoularis, 2008). In these simulations, various models of CFD techniques were studied. These include RANS (Chandra et al., 2009) or URANS (Merzari et al., 2007, 2008) with different turbulent models k-ε (Baglietto and Ninokata, 2005; Lee and Jang, 1997), LES (Biemüller et al., 1996) and DNS (Ninokata et al., 2004; Baglietto et al., 2006). The applications of CFD for the prediction of two-phase flow velocity, sub-cooled boiling (Krepper et al., 2007) and for void distribution. Further, these analyses were extended in the rod bundle (Carver et al., 1984; Anglart and Nylund, 1996). The CFD modeling was attempted for all types of reactors such as PWR (Conner et al., 2010; Cinosi and Walker, 2016), LMFBR (Cheng and Tak, 2006; Gajapathy et al., 2009; Chandra et al., 2009) and SCWR (Gu et al., 2008; Zhi, 2009; Zhi and Simon, 2010). The applications using computational fluid dynamics for the simulation rod bundles of next-generation nuclear systems are being developed worldwide (Angel et al., 2015).

On the discussions of turbulence models for rod bundle flow computations (Gabor Hazi, 2005) using commercial computational fluid dynamics codes, there are more than one turbulence models built in. It is the user responsibility to choose one of those models, suitable for the problem being studied. A common feature in a number of those simulations is that they were performed using the standard k–ε turbulence model without justifying the choice of the model. The authors have highlighted that the flow in a fuel rod bundles as a case study and discuss why the application of the standard k–ε model fails to give reasonable results in this situation. It was shown that the k–ε model could not reproduce the basic characteristics of such flows and demonstrated that the Reynolds-stress model predicts, accurate modeling of rod bundles flows.

A numerical study using CFD is carried out to estimate pressure loss in a strap and mixing vane structures and fluid hot spot locations in 5 × 5 fuel rod bundle (Ikeda et al., 2006). A CFD simulation under single phase flow condition is conducted for one specific condition in a water departure from nucleate boiling (DNB) test to examine the applicability of the CFD model for predicting the CHF rod position. Energy flux around the rod surface in a water DNB test is the sum of the intrinsic energy flux from a rod and the extrinsic energy flux from other rods, and increments of the enthalpy and decrements of flow velocity near the rod surface were assumed to affect CHF performance. CFD makes it possible to model the complicated flow field consisting of a spacer grid and a rod bundle and evaluate the local velocity and enthalpy distribution around the rod surface, which are assumed to determine the initial conditions for the two-phase structure. The results of this study indicated that single-phase CFD can play a significant role in designing PWR spacer grids for improved CHF performance.

CFD analysis for thermal-hydraulic behavior of heavy liquid metal flows, especially lead-bismuth eutectic, in sub-channels of both triangular and square lattices is carried out by Cheng and Tak (2006). The sensitivity of different turbulence models and the effect of pitch-to-diameter ratio, on the thermal–hydraulic behavior is investigated. Among the turbulence models selected, only the second order closure turbulence models reproduce the secondary flow. For the entire parameter range studied in this paper, the amplitude of the secondary flow is reported less than 1% of the mean flow. A strong anisotropic behavior of turbulence is observed. The turbulence behavior is similar in both triangular and square lattices. The average amplitude of the turbulent velocity fluctuation across the gap is about half of the shear velocity. It is only weakly dependent on the Reynolds number and p/d ratio. A strong circumferential non-uniformity of heat transfer is observed in tight rod bundles, especially in square lattices. Related to the overall average Nusselt number, CFD codes found to reproduce results for both triangular and square rod bundles. Comparison of the CFD results with bundle test data in mercury indicated that the turbulent Prandtl number for heavy liquid metal (HLM) flows in rod bundles is close to 1.0 at high Peclet number conditions, and increases by decreasing Peclet number. Based on the present results, the Speziale-Sarkar-Gatski (SSG) Reynolds stress model with semi-fine mesh structures ($y_1^+ < 15$) is recommended for the application of HLM flows in rod bundle geometries.

CHF experiments and CFD analysis in a 2 × 3 rod bundle with mixing vane is performed by (Shin and Chang, 2005, 2009) and In et al., 2008. The CHF enhancement using various mixing vanes is evaluated and the flow characteristics are investigated through the CHF experiments and CFD analysis. The detailed flow characteristics were also investigated by CFD analysis using the same conditions as the CHF tests. To calculate

the subcooled boiling flow, the wall partitioning model is applied to the wall boundary and various two-phase parameters were also considered. The reliability of the CFD analysis in the boiling is confirmed by comparing the average void fractions of the analysis and the experiments, the results agreed well. From the CFD analysis, the void fraction flattening as a result of the lateral velocity induced by the mixing vane is observed. By the lateral motion of the liquid, the void fraction in the near wall is decreased and that of the core region is increased resulting in the void fraction flattening. The decrease of the void fraction in the near wall region promoted liquid supply to the wall and consequently, the CHF increased. For the quantification of the void flatness, an index is developed and the applicability of the index in the CHF assessment is confirmed.

CFD analysis of flow field in a triangular rod bundle is investigated in sub-channels of VVER-440 pressurized water reactor fuel assemblies for a triangular lattice of p/d 1.35 by Toth and Aszodi (2010). The effect of mesh resolution and turbulence model is studied to obtain guidelines for CFD calculations of VVER-440 rod bundles. Results were compared to measurement data published by Trupp and Azad (1975). The study pointed out that RANS method with BSL Reynolds stress model using a sufficiently fine grid can provide an accurate prediction for the turbulence quantities for such types of the lattice. Applying the experiences of the sensitivity study thermal hydraulic processes were investigated in VVER-440 rod bundle sections. Based on the examinations they reported that the spacer grids have significant effects on the cross-flows, axial velocity and outlet temperature distribution of sub-channels. Therefore, they have to be modeled satisfactorily in CFD calculations. Some deviations were reported between them. The differences probably were caused by the deficiencies of the

COBRA model (inaccurate flow resistance and turbulent mixing coefficients, etc.) and CFD model gave a more accurate prediction. However, it must be mentioned that the suitability of the applied mesh and turbulence models were uncertain, therefore, further investigations were suggested. CFD modeling methodology and validation for steady state single-phase flow in PWR fuel assemblies for normal operation was investigated by Conner et al. (2010). This work was part of a program that is developing a CFD modeling methodology and predicting single-phase and two-phase flow conditions downstream of structural grids.

The three-dimensional CFD simulations of turbulent flow in a wire wrapped 19-pin rod bundle of an LMFBR for the pressure drop and heat transfer characteristics have been investigated by Natesan et al. (2010). The predicted results of eddy viscosity based turbulence models (k–ε and k–ω) and the Reynolds stress model were compared with those of experimental correlations for friction factor and Nusselt number for a different range of Re and for the ratio of the helical pitch of wire wrap to the rod diameter. All three turbulence models considered yielding similar results. The friction factor increases with reduction in the wire-wrap pitch while the heat transfer coefficient remains almost unaltered.

The numerical simulation of the thermal hydraulic characteristics within the fuel rod bundle using CFD methodology is carried out by Liu and Ferng (2010). This localized information, including flow, turbulence, and heat transfer characteristics, assist in the design and the improvement of rod bundles for nuclear power plants which is difficult to measure in actual geometry. A three-dimensional CFD analysis with the Reynolds stresses turbulence model is proposed to simulate these characteristics within the rod bundle and subsequently to investigate the effects of different types of grids on the

turbulent mixing. Heat transfer enhancement is studied in detail. Based on the CFD simulations, the secondary flow could be reasonably captured in the rod bundle with the grid. The CFD simulation results clearly showed that split-vane pair grid would enhance both the flow mixing and the heat transfer capability more than the standard grid. In addition to the comparison of the results of experiment and correlation, the present predicted result for the Nusselt (Nu) number distribution downstream the grid shows reasonable agreement for the standard grid design. However, there is a discrepancy in the decay trend of Nu number between the prediction and measurement for the split-vane pair gird. This would be significantly improved by adopting the finer mesh ($y^+ < 1$) simulation and Low-Reynolds number turbulence model.

Large Eddy Simulation (LES) and Unsteady Reynolds averaged Navier-Stokes (URANS) simulations of turbulent flow in 4-rod bundles in ocean environment to simulate the rolling motion is investigated by Yan et al. (2009, 2011). The effect of rolling motion consists of two parts, the axial additional force which causes velocity oscillation and the radial additional force. The analysis indicates that in the ocean environment, the effect of rolling motion on the flowing similarity is considerable and cannot be neglected for proper prediction of flow and heat transfer.

Numerical simulation of the coherent structures and turbulent mixing in a tight lattice is investigated by Yan et al. (2012). The calculation results were first validated with experimental data and then the effects of Reynolds number, Prandtl number, and pitch to diameter ratio on the coherent structure and turbulent mixing were analyzed. They reported that the effect of Prandtl number on the coherent structure and turbulent mixing is more limited than that of Reynolds number. The effect of pitch to diameter ratio on the coherent structure is most significant. The critical pitch to diameter ratio for this

lattice is 1.03. As the pitch to diameter ratio decrease from a large number to the critical value, the coherent structure becomes more significant which is beneficial to the local flow and heat transfer. However, as the pitch to diameter ratio continues to decrease from this critical value to a very small value, the coherent structure becomes weaker and weaker, and the local flow and heat transfer also becomes poorer.

Performing the full bundle CFD analysis is computationally intensive and more time consuming, hence, simulating the fuel assemblies with low-resolution CFD approaches is investigated by Roelofs et al. (2012). In addition to the traditional fuel assembly simulations using system codes, sub-channel codes or porous medium approaches, as well as detailed CFD simulations to analyze single sub-channels, a low-resolution Geometry Resolving (LRGR) CFD approach and a Coarse-Grid CFD (CGCFD) approach are considered in their work. Both methods were based on a low-resolution mesh that allows the capture of large and medium scale flow features such as recirculation zones, which are difficult to be reproduced by the system codes, sub-channel codes and porous media approaches.

2.5 Fluid Flow and Heat Transfer Characteristics in Sub-Channel Geometries

The convective flow and heat transfer in circular and non-circular channels are of considerable importance in many industrial applications and especially in the nuclear reactor fuel bundles. The knowledge of pressure drop, flow, and temperature distribution in these geometries are required, especially for the thermal hydraulic design calculations and safety-related studies of a reactor core. Extensive numerical simulations are required to estimate the thermal hydraulics safety margins as well as the safe limiting power of operation, under different conditions of the nuclear reactor core. Traditionally, the safety margins are estimated by sub-channel analysis codes, which

are applied at the bundle level as well as the partial symmetry of the core requiring a very large computational time. In past, the conservative estimates of the coolant and fuel temperatures were carried out by sub-channel analysis using semi-empirical correlations. Experimental and computational fluid dynamics works can reveal the actual velocity and temperature distributions in these sub-channels as compared to the sub-channel averaged coolant temperatures and to predict the hot spot regions. In the sub-channel analysis, the key input parameters like sub-channel loss coefficients and inter-channel loss coefficients are required to calculate the flow distribution within the fuel bundle. These are obtained experimentally on simple geometries.

Even today, the application of CFD for thermal hydraulics analysis of full bundle is a challenge due to limitations of computational resources and a large number of design calculations for different nuclear reactor operating regimes. However, CFD can be applied to the sub-channel level geometries to get more insight into the flow and temperature distribution within the rod bundle. During the emergency situations like Loss of Coolant Accident (LOCA), there can be a less cooling of fuel pins leading to ballooning, neighboring fuel pins can touch each other and can form the cusped sub-channel (Duck and Turner, 1987). Gunn and Darling (1963) measured the friction factors in cusped channels of square pitched four pin bundles. An experimental investigation of peripheral temperature variation on the wall of a non-circular duct was carried out by Barrow et al. (1984).

An experimental investigation of the turbulent flow and heat transfer characteristics in a four cusped channel with uniform wall temperature was studied in detail by Dutra et al. (1991). Mixed convection in 4-cusped duct was carried out for the estimation of fRe

and average Nusselt number by Dong and Ebadian (1994). Hassan and Hunaehn (2008) numerically studied the incompressible flow and heat transfer in 2-cusped and 3-cusped ducts of wall channels. Rheme (1973) has proposed a simple method of predicting friction factor of turbulent flow in non-circular channels on the basis of geometry factor (fRe) for laminar flow.

The experimental and analytical data of laminar friction factor and forced convection heat transfer in non-circular ducts were given by Shah and London (1971, 1978). CFD analysis of a non-circular duct similar to rod bundle sub-channel, requires a distinct wall boundary conditions like, axially uniform wall heat flux with uniform wall temperature in the periphery (H1 boundary condition), uniform wall heat flux in both axial and circumferential direction (H2 boundary condition) or uniform wall temperature (T1 boundary conditions). Numerical analysis of this kind of heat flux boundary conditions on the rectangular geometry were carried out by Spiga and Morini (1996) and Barletta et al. (2003). Also, the forced turbulent heat convection in a square duct with non-uniform wall temperature was carried out by Rivas et al. (2011).

In recent times, due to advancement of computational power and CFD techniques, the fluid flow and heat transfer characteristics of the rod bundle are studied using CFD (Kaiser et al. 1987; Lee et al. 1997; Baglietto et al. 2005 and 2006; Cheng et al. 2006; Rui Guo et al. 2015). Even today the application of CFD for thermal hydraulics analysis of full bundle is very difficult due to the computational resources and the design time (Hu and Fanning, 2011). In recent past, rod bundle has been simulated using different turbulent models. It was shown that the k–ε model could not reproduce the basic

characteristics of such flows rather than Reynolds-stress model, which can predict accurate modeling of rod bundle flows (Gábor Házi, 2005).

From the above literature survey, it is clear that the functional forms of fRe and average Nusselt number ($\overline{Nu}$) are available only for conventional geometries like circular and non-circular shapes. However, the application of these functional forms for analysis of nuclear fuel bundles does not hold good as the bundles possess complex geometry and boundaries. Hence, applying these functional forms to nuclear fuel bundles lead to large uncertainties in fRe and average Nusselt number ($\overline{Nu}$). This, in turn, leads to an inaccurate prediction of fluid flow and heat transfer characteristics of the fuel bundle as well as sub-channel geometries. Therefore, the present thesis is also focused to apply the CFD model on 2D geometry representing the non-circular rod bundle sub-channels by solving the out-of-plane flow velocities rather than a conventional 3D CFD analysis.

2.6 Summary and Future Directions of Research

Thermal-hydraulic investigations on the reactor core for different geometries of the fuel assemblies are being carried out since the beginning of the nuclear power program worldwide. Researchers have used different sub-channel analysis codes, experimental techniques, analytical and computational tools for the estimation of key parameters on rod bundle mixing to determine reactor safety margins. In this chapter, the works carried out by different groups of researchers in rod bundle sub-channel analysis is reviewed extensively. More than 300 research papers on this topic were referred. The major findings and the limitations were critically reviewed. Based on the understanding from the vast literature available in open sources. It was found that the most of the studies focused on the effect of key mixing parameters such as beta, gaps, p/d ratio and other parameters characterizing the single-phase mixing between sub-channels are brought

out. These studies emphasize the importance of predicting the accurate local conditions such as flow rate, velocities, and temperature distribution in the rod bundles. Further, these studies are oriented towards establishing reliable thermal-hydraulic safety parameters and thermal margins on CHF and CPR as discussed above.

Based on the literature survey of the subject, it is also noted that various experimental tests on turbulent mixing under different fluid conditions, sub-channel, and CFD analysis can be carried out to simulate those experiments. Thus reliable predictions of the mixing by CFD can be established. Further, design exploration studies of various parameters affecting the inter-channel mixing using the CFD techniques and to extend the mixing models for a wide range of operating and geometrical conditions can be approached. From the investigations on turbulent inter-channel mixing, improved understanding on the estimation of mixing parameters to characterize the key thermal-hydraulic safety margins at different states of the operational and transient conditions of the core can be evaluated. All these sub-channel codes require a large amount of data processing of sub-channel geometry, rod to sub-channel connectivity details, fluid properties, power distribution, and operating conditions. Therefore, the research shall be directed in the following gap areas of sub-channel analysis for reliable estimation of the safety margins of the nuclear reactor core.

a. Improved thermal hydraulic models of heat transfer and mixing correlations,
b. Reliable sub-channel analysis tools,
c. limitations for the calculation speed,
d. Improved code to handle a large number of sub-channels and fuel rods,
e. Code to include the verification and validation of earlier research works,
f. Non-linear variation of the properties of coolant, fuel, and clad materials.

The development of software framework to automate the entire core thermal-hydraulic analysis procedure and the presentation of thermal hydraulic results and hence, the safe reliable and accurate predictions of the thermal hydraulic safety margins is suggested. This will certainly improve the speed, accuracy and the repeatability of the sub-channel analysis and hence, the reliable estimation of the safety margins of the nuclear reactor core.

2.7 Motivation

From the review of the literature presented above, it is clear that ensuring the safety of nuclear reactor core under normal operating conditions and anticipated operational occurrences are at most importance and the safety is ensured by performing the detailed sub-channel thermal hydraulic analysis. The accurate estimation of local flow conditions inside the rod bundles is of more importance in evaluating the available thermal margins such as critical heat flux (CHF) and critical power ratio(CPR), fuel surface temperature and fuel centerline temperature to find out the limiting safety system settings and limiting conditions of operation of the reactor. The analysis of typical nuclear reactor core also requires a tremendous amount of calculations by varying the coolant pressure, inlet temperature, coolant flow rate, geometrical parameters, and power distributions etc. Hence, in this thesis, it is decided to develop a general purpose automated sub-channel analysis framework to carry out the sub-channel analysis. Perform the fluid flow and heat transfer analysis to estimate the pressure drop and fluid distribution in a non-circular sub-channel and fuel bundle geometries. Also to carry out the investigations on the effect of turbulent cross-flow mixing within a nuclear fuel bundle on the local conditions of the coolant. An automated

and validated analysis framework is required to identify the state of the core under different operating conditions to minimize the core design time with reliable and improved accuracy of the thermal-hydraulic analysis. The framework developed in this thesis helps us to carry out the detailed core thermal-hydraulic analysis of a nuclear reactor core in an efficient way with less human intervention.

2.8 Objective and Scope of the Present Work

The present thesis is focused to understand the flow distribution of coolant in a nuclear reactor fuel pin bundle and its effect on the thermal hydraulic safety margins of the nuclear reactor core.

The main objective of the thesis is,

(i) to develop a general-purpose automated sub-channel analysis framework

(ii) to understand fluid flow and heat transfer characteristics in the nuclear fuel bundle

(iii) investigation of coolant mixing on the predicted thermal-hydraulic safety margins by studying the effect of key parameters such as p/d ratio, w/d ratio, bundle size, turbulent inter-channel mixing parameters, mass flux, and power distribution.

2.9 Closure

An extensive review of literature relevant to the present study was presented in this chapter. The objectives and scope of the present investigation were also clearly brought out. The next chapter presents the mathematical formulation and the method of solution adopted in the present work.

CHAPTER-3

MATHEMATICAL FORMULATION AND METHOD OF SOLUTION

CHAPTER-3

3 MATHEMATICAL FORMULATION AND METHOD OF SOLUTION

3.1 Introduction

This chapter is devoted to a complete discussion on the governing equations and the methods of solution for the fluid flow and heat transfer in non-circular sub-channel geometries of the nuclear fuel bundle. First, the formulation of the governing equations and the solution methodology are explained. The investigations of cross-flow mixing are studied using the sub-channel analysis methodology and the governing equations used in the sub-channel analysis are also discussed in this chapter. The validation studies of the numerical results and the grid independent study tests of the problem studied are presented in the respective chapters for better appreciation and hence, are not discussed here.

3.2 Governing Equations of Fluid Flow

The flow and heat transfer through the fuel bundle geometry considered in this study are three dimensional in nature. The conservative or divergence form of the system of equations which governs the time dependent three-dimensional fluid flow and heat transfer of a compressible Newtonian fluid is as follows,

The continuity equation in conservative form is

$$\frac{\partial \rho}{\partial t} + \nabla \cdot \left(\rho \vec{U}\right) = 0 \tag{3.1}$$

The momentum equations in conservative form is

x-momentum of the fluid particle

$$\frac{\partial(\rho u)}{\partial t} + \nabla \cdot \left(\rho u \vec{U}\right) = -\frac{\partial p}{\partial x} + \nabla \cdot (\mu \nabla u) + S_{mx} \tag{3.2}$$

y-momentum of the fluid particle

$$\frac{\partial(\rho v)}{\partial t} + \nabla \cdot \left(\rho v \vec{U}\right) = -\frac{\partial p}{\partial y} + \nabla \cdot (\mu \nabla \mathrm{v}) + S_{my} \tag{3.3}$$

z-momentum of the fluid particle

$$\frac{\partial(\rho w)}{\partial t} + \nabla \cdot \left(\rho w \vec{U}\right) = -\frac{\partial p}{\partial z} + \nabla \cdot (\mu \nabla \mathrm{w}) + S_{mz} \tag{3.4}$$

The energy equation in conservative form is

$$\frac{\partial(\rho h)}{\partial t} + \nabla \cdot \left(\rho h \vec{U}\right) = -p \nabla \cdot \vec{U} + \nabla \cdot (\mathrm{k} \nabla \mathrm{T}) + \Phi + S_h \tag{3.5}$$

The Reynolds averaging of the instantaneous velocity in the Navier Stokes equations are decomposed into the mean (time-averaged) and the fluctuating components of the velocity are

$$u_i = \bar{u}_i + u_i' \tag{3.6}$$

Where, $\bar{u}_i$ and u_i' are the mean and fluctuating velocity components (i=x,y,z).

Likewise, for pressure and other scalar quantities

$$\phi = \phi_i + \phi_i' \tag{3.7}$$

Where $'\phi'$denotes a scalar such as pressure, energy, turbulence kinetic energy and specific dissipation rate. Substituting the expressions of this form for the flow variables into the instantaneous continuity and momentum equations and taking the time average (and dropping the bar on the mean velocity, $\bar{u}$) yields the Reynolds averaged equations of mass, momentum and energy in a tensor notations is as follows,

$$\frac{\partial U_i}{\partial x_i} = 0 \tag{3.8}$$

$$\frac{DU_i}{Dt} = -\frac{1}{\rho}\frac{\partial P}{\partial x_i} + \frac{\partial}{\partial x_j}\left(\frac{\mu}{\rho}\frac{\partial U_i}{\partial x_j} - \overline{u_i u_j}\right) \tag{3.9}$$

$$\frac{DT}{Dt} = \frac{\partial}{\partial x_j}\left(\alpha\frac{\partial T}{\partial x_j} - \overline{T' u_j}\right) \tag{3.10}$$

The time averaged equations have some additional unknown variables i.e. Reynolds stress in the momentum equations and turbulent heat flux in the energy equations and no exact equations are available for the evaluation of these additional quantities and the set of RANS equations is not closed. The turbulent models are required to determine these variables in terms of the known quantities. Unfortunately, no single turbulence model is universally accepted and appropriate selection of turbulence models depends on the physical nature of the problem considered. The choice depends on the physics of the flow, available computational resources and the time available for the simulations. There are many turbulence models are available in the literature such as Linear eddy viscosity models such as Zero equation models, one equation model, two equation models and the nonlinear eddy viscosity models such as Reynolds Stress Transport models (RSM) and Large Eddy Simulation (LES) and the Direct Numerical Simulation (DNS) of the turbulent flow equations.

The following conservation equations of Reynolds Averaged Navier Stokes equations (RANS) is solved with the standard k-ε turbulent closure models.

The continuity equation:

$$\frac{\partial(\rho u)}{\partial x} + \frac{\partial(\rho v)}{\partial y} + \frac{\partial(\rho w)}{\partial z} = 0 \tag{3.11}$$

The x-momentum equation:

$$\frac{\partial(\rho u)}{\partial t}+\frac{\partial(\rho uu)}{\partial x}+\frac{\partial(\rho vu)}{\partial y}+\frac{\partial(\rho wu)}{\partial z}=-\frac{\partial p}{\partial x}+\frac{\partial}{\partial x}\left[2\mu_{eff}\frac{\partial u}{\partial x}\right]$$
$$+\frac{\partial}{\partial y}\left[\mu_{eff}\left(\frac{\partial u}{\partial y}+\frac{\partial v}{\partial x}\right)\right]+\frac{\partial}{\partial z}\left[\mu_{eff}\left(\frac{\partial u}{\partial z}+\frac{\partial w}{\partial x}\right)\right] \tag{3.12}$$

The y-momentum equation:

$$\frac{\partial(\rho v)}{\partial t}+\frac{\partial(\rho uv)}{\partial x}+\frac{\partial(\rho vv)}{\partial y}+\frac{\partial(\rho wv)}{\partial z}=-\frac{\partial p}{\partial y}+\frac{\partial}{\partial x}\left[\mu_{eff}\left(\frac{\partial v}{\partial x}+\frac{\partial u}{\partial y}\right)\right]$$
$$+\frac{\partial}{\partial y}\left[2\mu_{eff}\frac{\partial v}{\partial y}\right]++\frac{\partial}{\partial z}\left[\mu_{eff}\left(\frac{\partial v}{\partial z}+\frac{\partial w}{\partial y}\right)\right] \tag{3.13}$$

The z-momentum equation:

$$\frac{\partial(\rho w)}{\partial t}+\frac{\partial(\rho uw)}{\partial x}+\frac{\partial(\rho vw)}{\partial y}+\frac{\partial(\rho ww)}{\partial z}=-\frac{\partial p}{\partial z}+\frac{\partial}{\partial x}\left[\mu_{eff}\left(\frac{\partial w}{\partial x}+\frac{\partial u}{\partial z}\right)\right]$$
$$+\frac{\partial}{\partial y}\left[\mu_{eff}\left(\frac{\partial w}{\partial y}+\frac{\partial v}{\partial z}\right)\right]+\frac{\partial}{\partial z}\left[2\mu_{eff}\frac{\partial w}{\partial z}\right] \tag{3.14}$$

The Reynolds stress terms are modelled by the help of turbulent kinetic energy and turbulent dissipation rate equations. For the k-ε model, the kinetic energy and the dissipation rates of the turbulence equations are:

The k equation:

$$\frac{\partial(\rho k)}{\partial t}+\frac{\partial(\rho uk)}{\partial x}+\frac{\partial(\rho vk)}{\partial y}+\frac{\partial(\rho wk)}{\partial z}=\frac{\partial}{\partial x}\left[\left(\mu+\frac{\mu_t}{\sigma_k}\right)\frac{\partial k}{\partial x}\right]$$
$$+\frac{\partial}{\partial y}\left[\left(\mu+\frac{\mu_t}{\sigma_k}\right)\frac{\partial k}{\partial y}\right]+\frac{\partial}{\partial z}\left[\left(\mu+\frac{\mu_t}{\sigma_k}\right)\frac{\partial k}{\partial z}\right]+P_k+G_k-\rho\varepsilon \tag{3.15}$$

The ε equation:

$$\frac{\partial(\rho\varepsilon)}{\partial t}+\frac{\partial(\rho u\varepsilon)}{\partial x}+\frac{\partial(\rho v\varepsilon)}{\partial y}+\frac{\partial(\rho w\varepsilon)}{\partial z}=\frac{\partial}{\partial x}\left[\left(\mu+\frac{\mu_t}{\sigma_\varepsilon}\right)\frac{\partial \varepsilon}{\partial x}\right]$$
$$+\frac{\partial}{\partial y}\left[\left(\mu+\frac{\mu_t}{\sigma_k}\right)\frac{\partial \varepsilon}{\partial y}\right]+\frac{\partial}{\partial z}\left[\left(\mu+\frac{\mu_t}{\sigma_k}\right)\frac{\partial \varepsilon}{\partial z}\right]+[C_{\varepsilon 1}(P_k+C_{\varepsilon 3}G_k)-C_{\varepsilon 3}]\frac{\varepsilon}{k} \tag{3.16}$$

Where P_k and G_k are shear and buoyant production of turbulent kinetic energy respectively and given as

$$P_k = \mu_t \left[2\left(\frac{\partial u}{\partial x}\right)^2 + 2\left(\frac{\partial v}{\partial y}\right)^2 + 2\left(\frac{\partial w}{\partial z}\right)^2 + \left(\frac{\partial u}{\partial x} + \frac{\partial v}{\partial y} + \frac{\partial w}{\partial z}\right)^2 \right] \tag{3.17}$$

$$G_k = \frac{\mu_t}{\sigma_T} g\beta \frac{\partial T}{\partial y} \tag{3.18}$$

$$\mu_{eff} = \mu + \mu_t \tag{3.19}$$

$$\mu_t = C_\mu \frac{\rho k^2}{\varepsilon} \tag{3.20}$$

$$k_{eff} = k_f + \frac{\mu_t C_P}{\sigma_T} \tag{3.21}$$

The empirical constants used in the turbulence model are listed in Table 3.1

Table 3.1 Empirical constants used in the turbulence model

C_μ	$C_{\varepsilon 1}$	$C_{\varepsilon 2}$	$C_{\varepsilon 3}$	σ_T	σ_k	σ_ε
0.09	1.44	1.92	1.0	1.0	1.0	1.3

3.3 Boundary Conditions

For the solution of the governing equations described in the previous section, the boundary conditions for the velocity components and temperature, k and ϵ need to be specified on all the boundaries of the domain. As regards the momentum conditions are subjected to the boundary conditions, u=0, v=0, w=0 on the solid wall. On the wall the temperature or the heat flux boundary conditions are applied on the wall of the pin and these are discussed in respective chapters for better appreciation.

3.4 Hydrodynamic Model of Non-Circular Geometry

The steady state fully developed Newtonian fluid flow and heat transfer are simulated by solving conservation equation of mass and momentum. For the simulation of steady state fully developed laminar Newtonian flow through an arbitrary shaped cross-section

of constant flow area straight ducts, the momentum equations are reduced to the Poisson's equation. The source term in Poisson's equation is the modified pressure gradient along the length of the duct (Bahrami et al., 2005). The resulting governing equations for fully developed flow in non-circular ducts is simulated in 2-D cross-section normal to the flow direction.

$$\frac{\partial^2 w}{\partial x^2} + \frac{\partial^2 w}{\partial y^2} = \frac{1}{\mu}\frac{\partial P}{\partial z} \qquad \text{and } w = 0 \quad \text{on domain boundary } (\Gamma) \tag{3.22}$$

The fully developed flow in circular ducts is generally simulated in reduced dimensions using 1-D or 2-D axi-symmetric model. In the case of non-circular ducts, such flow can be simulated in 2-D cross-section normal to the flow direction. Solution of the Poisson's equation with modified pressure gradient as the source term and no-slip boundary condition on domain walls leads to the longitudinal velocity distribution $w(x, y)$.

Integrating the velocity over the domain gives the average velocity as follows,

$$w_a = \frac{1}{A}\int_{\Gamma} w dA \tag{3.23}$$

Similarly integrating the wall shear stress on the boundaries of the domain gives the average wall shear stress as

$$\overline{\tau_w} = \frac{\int_{\Gamma} \tau ds}{\int_{\Gamma} ds} \tag{3.24}$$

The skin friction coefficient is estimated as

$$f = \frac{2\overline{\tau_w}}{\rho w_a^2} \tag{3.25}$$

and the frictional pressure drop is calculated from the wall shear stress as

$$\Delta P = \overline{\tau_w}\frac{SL}{A} \tag{3.26}$$

From the frictional pressure drop relationship, the product of friction factor (f) and Reynolds number (Re) gives a constant value and is called the Poiseuille number (fRe) in laminar flow regime. It is the Eigen value of Poisson's equation also called as geometry factor. This factor is solely determined from the geometrical cross section of the flow domain (Rehme, 1973).

3.4.1 Heat transfer model with prescribed wall heat flux

The energy equation:

$$w\frac{\partial T}{\partial z} = \alpha\left(\frac{\partial^2 T}{\partial x^2} + \frac{\partial^2 T}{\partial y^2} + \frac{\partial^2 T}{\partial z^2}\right) \tag{3.27}$$

For a fully developed flow through non-circular ducts with prescribed uniform axial heat flux and uniform circumferential temperature boundary conditions (H1 boundary condition), the energy equation (Eqn. 3.27) is reduced to a Poisson's equation. The source term is estimated from velocity profile and the prescribed heat flux as formulated by Barletta et al. (2003). The variables required for the estimation of source term in equation (3.28) are calculated using the internal variables, defined using the component coupling feature, in COMSOL. The momentum and the energy equations are solved simultaneously to get the velocity and temperature profile.

$$\left(\frac{\partial^2 T}{\partial x^2} + \frac{\partial^2 T}{\partial y^2}\right) = \frac{4\bar{q}_w}{kdw_a}w \tag{3.28}$$

On solving equation (3.28) with prescribed heat flux and temperature boundary condition on the flow domain, the temperature field T (x, y) is obtained.

The bulk average temperature (T_b) of the fluid in the domain is estimated as

$$T_b = \frac{\iint Twdxdy}{\iint wdxdy} \tag{3.29}$$

The average wall temperature (T_w) is calculated by integrating the temperature on the domain boundaries as,

$$T_w = \frac{\int_\Gamma T ds}{\int_\Gamma ds} \tag{3.30}$$

From the average wall temperature (T_w), bulk fluid temperature (T_b) and average heat flux around the wall ($\bar{q}_w$), the average Nusselt Number ($\overline{Nu}$) is estimated as follows,

$$\overline{Nu} = \frac{hd_h}{k} = \frac{\bar{q}_w d_h}{(T_w - T_b)k} \tag{3.31}$$

3.5 Sub-Channel Analysis

The derivations of the governing equations of the fluid flow and heat transfer in nuclear fuel bundle is discussed in this section.

3.5.1 Sub-channel model and governing equations

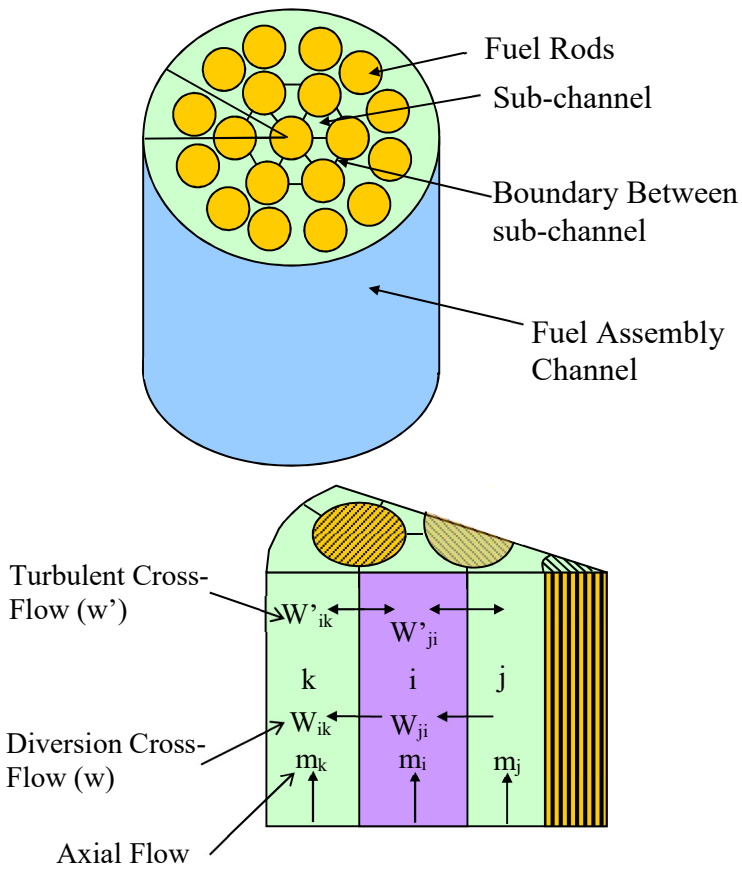

Fig. 3.1 Schematic of fuel assembly and sub-channel connectivity

3.5.2 Equation of continuity

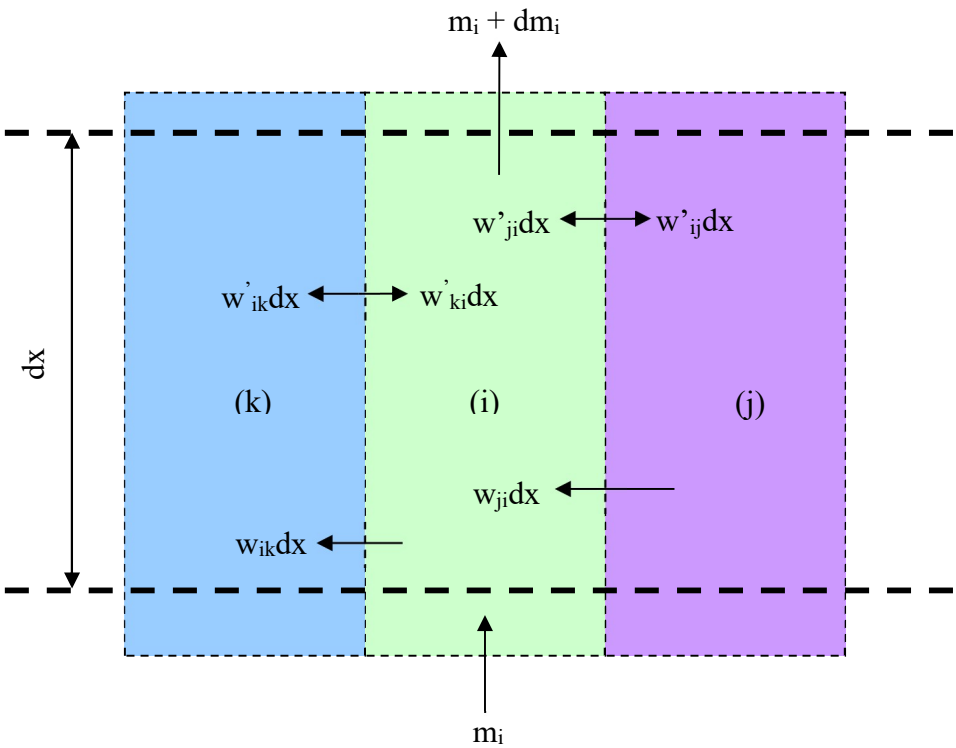

Fig. 3.2 Control volumes with neighboring sub-channel connectivity for mass balance

Mass balance on sub-channel i is

$$m_i + w_{ji}dx + w'_{ji}dx + w'_{ki}dx = m_i + dm_i + w_{ik}dx + w'_{ik}dx + w'_{ij}dx \tag{3.32}$$

definition of turbulent cross-flow gives

$$w'_{ij} = w'_{ji} \text{ and } w'_{ik} = w'_{ki} \tag{3.33}$$

$$\frac{dm_i}{dx} = w_{ji} - w_{ik} \tag{3.34}$$

$$\frac{dm_i}{dx} = -w_{ij} - w_{ik} \tag{3.35}$$

$$\frac{dm_i}{dx} = -\sum_{j=1}^{N} w_{ij} \qquad i = 1, 2, \dots, N \tag{3.36}$$

3.5.3 Equation of energy

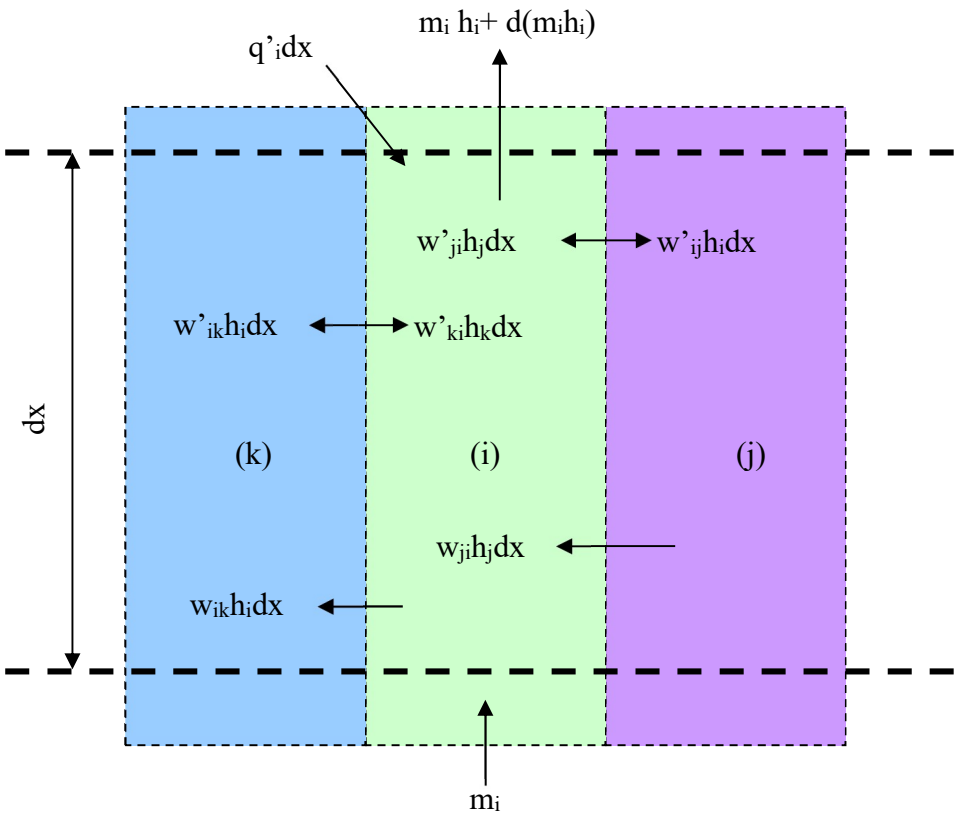

Fig. 3.3 Control volumes with neighboring sub-channel connectivity for energy balance

Energy balance on sub-channel (i) gives

$$m_i h_i + w_{ji} h_j dx + w'_{ji} h_j dx + w'_{ki} h_k dx + q'_i dx = m_i h_i + d(m_i h_i) + w_{ik} h_i dx + w'_{ik} h_i dx + w'_{ij} h_i dx \tag{3.37}$$

$$d(m_i h_i) = w_{ji} h_j dx + w'_{ji} h_j dx + w'_{ki} h_k dx + q'_i dx - w_{ik} h_i dx - w'_{ik} h_i dx - w'_{ij} h_i dx \tag{3.38}$$

$$w'_{ij} = w'_{ji} \; and \; w'_{ik} = w'_{ki} \tag{3.39}$$

$$\frac{d(m_i h_i)}{dx} = w_{ji}h_j - w_{ik}h_i + w'_{ij}(h_j - h_i) + w'_{ik}(h_k - h_i) + q'_i \tag{3.40}$$

$$\frac{d(m_i h_i)}{dx} = w_{ji}h_j - w_{ik}h_i + \sum_{j=1}^{N} w'_{ij}(h_j - h_i) + q'_i \tag{3.41}$$

$$m_i \frac{dh_i}{dx} + h_i \frac{dm_i}{dx} = w_{ji}h_j - w_{ik}h_i + \sum_{j=1}^{N} w'_{ij}(h_j - h_i) + q'_i \tag{3.42}$$

Substitute the equation of continuity into the above equation we get

$$m_i \frac{dh_i}{dx} + h_i(-w_{ij} - w_{ik}) = w_{ji}h_j - w_{ik}h_i + \sum_{j=1}^{N} w'_{ij}(h_j - h_i) + q'_i \tag{3.43}$$

$$m_i \frac{dh_i}{dx} - w_{ij}h_i - w_{ik}h_i = w_{ji}h_j - w_{ik}h_i + \sum_{j=1}^{N} w'_{ij}(h_j - h_i) + q'_i \tag{3.44}$$

$$m_i \frac{dh_i}{dx} = w_{ji}h_j + w_{ij}h_i + \sum_{j=1}^{N} w'_{ij}(h_j - h_i) + q'_i \tag{3.45}$$

$$m_i \frac{dh_i}{dx} = -w_{ij}h_j + w_{ij}h_i + \sum_{j=1}^{N} w'_{ij}(h_j - h_i) + q'_i \tag{3.46}$$

$$m_i \frac{dh_i}{dx} = -w_{ij}(h_j - h_i) + \sum_{j=1}^{N} w'_{ij}(h_j - h_i) + q'_i \tag{3.47}$$

$$m_i \frac{dh_i}{dx} = q'_i + \sum_{j=1}^{N} w'_{ij}(h_j - h_i) - \sum_{j=1}^{N} \begin{Bmatrix} 0 & ; if \quad w_{ij} \geq 0 \\ w_{ij}(h_j - h_i) & ; if \quad w_{ij} < 0 \end{Bmatrix} \tag{3.48}$$

$$i = 1,2, \dots, N$$

3.5.4 Equation of axial momentum

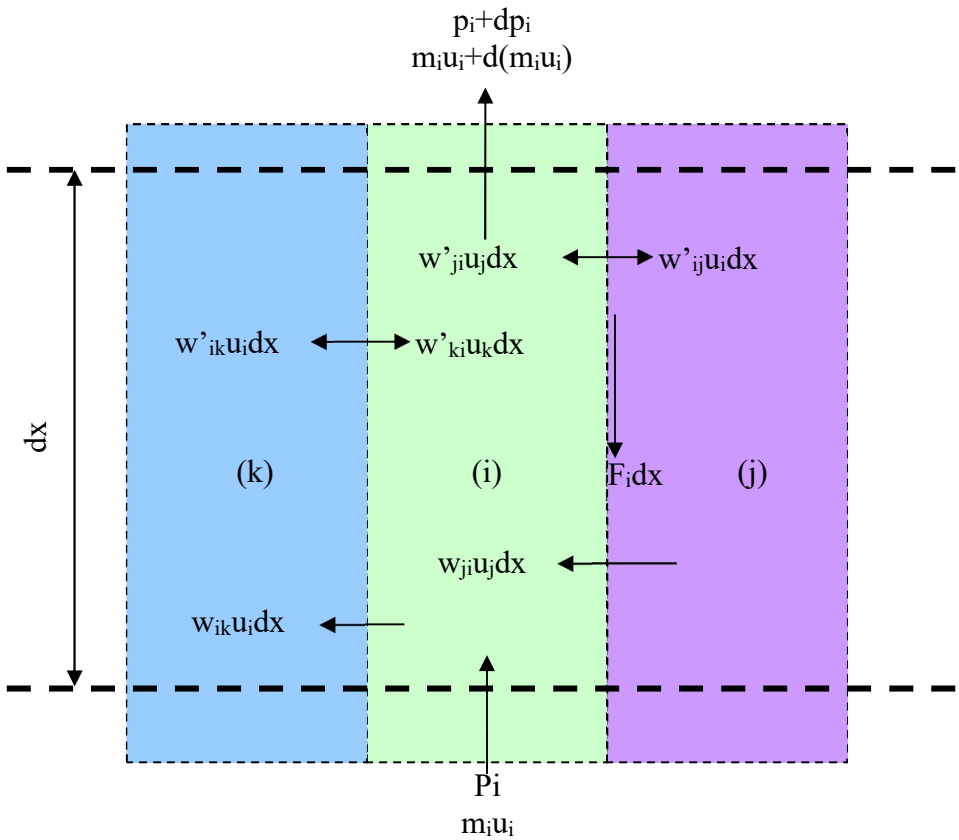

Fig. 3.4 Control volumes with neighboring sub-channel connectivity for equation of axial momentum

The momentum in two phase flow streams is

$$\frac{AG^2V'}{g_c} = \frac{AV'}{g_c}\left(\frac{m}{A}\right)^2 = \frac{mu}{g_c} \tag{3.49}$$

$$u = \frac{mV'}{A} \tag{3.50}$$

Equating the forces acting upon sub-channel (i) in X direction to the change in momentum gives

$$\begin{aligned} g_c(A_ip_i - F_idx - A_i(p_i + dp_i) - A_i\rho_i cos\theta dx) \\ = \left[f_D w_{ik}u_idx + f_T w'_{ik}u_idx + f_T w'_{ij}u_idx + m_iu_i + d(m_iu_i)\right] \\ - [m_iu_i + f_D w_{ji}u_jdx + f_T w'_{ki}u_kdx + f_T w'_{ji}u_jdx] \end{aligned} \tag{3.51}$$

$$g_c A_i dx\left(-\frac{F_i}{A_i}-\frac{dp_i}{dx}-\rho_i cos\theta\right)$$
$$= dx\left[f_D w_{ik}u_i - f_D w_{ji}u_j + f_T w'_{ik}(u_i-u_k) + f_T w'_{ij}(u_i-u_j) + d(m_i u_i)\right] \tag{3.52}$$

$$\left(-\frac{F_i}{A_i}-\frac{dp_i}{dx}-\rho_i cos\theta\right)$$
$$= \frac{f_D w_{ik}u_i}{g_c A_i} - \frac{f_D w_{ji}u_j}{g_c A_i} + \frac{f_T w'_{ik}}{g_c A_i}(u_i-u_k) + \frac{f_T w'_{ij}}{g_c A_i}(u_i-u_j) + \frac{u_i}{g_c A_i}\frac{dm_i}{dx} + \frac{m_i}{g_c A_i}\frac{du_i}{dx} \tag{3.53}$$

$$u_i = \frac{m_i V'_i}{A_i} \tag{3.54}$$

$$\frac{du_i}{dx} = \frac{d}{dx}\left(\frac{m_i V'_i}{A_i}\right) = \frac{1}{A_i}\left(m_i\frac{dV'_i}{dx} + V'_i\frac{dm_i}{dx}\right) \tag{3.55}$$

$$\frac{du_i}{dx} = \left(\frac{m_i}{A_i}\frac{dV'_i}{dx} + \frac{V'_i}{A_i}\frac{dm_i}{dx}\right) \tag{3.56}$$

$$\frac{m_i}{g_c A_i}\frac{du_i}{dx} = \frac{m_i^2}{g_c A_i^2}\frac{dV'_i}{dx} + \frac{m_i V'_i}{g_c A_i^2}\frac{dm_i}{dx} \tag{3.57}$$

$$\frac{m_i}{g_c A_i}\frac{du_i}{dx} = \frac{1}{g_c}\left(\frac{m_i}{A_i}\right)^2\frac{dV'_i}{dx} + \frac{u_i}{g_c A_i}\frac{dm_i}{dx} \tag{3.58}$$

$$\left(-\frac{F_i}{A_i}-\frac{dp_i}{dx}-\rho_i cos\theta\right) = \frac{f_D w_{ik}u_i}{g_c A_i} - \frac{f_D w_{ji}u_j}{g_c A_i} + \frac{f_T w'_{ik}}{g_c A_i}(u_i-u_k) + \frac{f_T w'_{ij}}{g_c A_i}(u_i-u_j) + \frac{u_i}{g_c A_i}\frac{dm_i}{dx} + \frac{1}{g_c}\left(\frac{m_i}{A_i}\right)^2\frac{dV'_i}{dx} + \frac{u_i}{g_c A_i}\frac{dm_i}{dx} \tag{3.59}$$

$$\left(-\frac{F_i}{A_i}-\frac{dp_i}{dx}-\rho_i cos\theta\right)=\frac{f_D w_{ik}u_i}{g_c A_i}-\frac{f_D w_{ji}u_j}{g_c A_i}+\frac{f_T w'_{ik}}{g_c A_i}(u_i-u_k)$$
$$+\frac{f_T w'_{ij}}{g_c A_i}(u_i-u_j)+\frac{2u_i}{g_c A_i}(-w_{ij}-w_{ik})+\frac{1}{g_c}\left(\frac{m_i}{A_i}\right)^2\frac{dV'_i}{dx} \tag{3.60}$$

$$-\frac{dp_i}{dx}=\frac{F_i}{A_i}+\rho_i cos\theta+\frac{f_T w'_{ik}}{g_c A_i}(u_i-u_k)+\frac{f_T w'_{ij}}{g_c A_i}(u_i-u_j)$$
$$+\frac{f_D w_{ik}u_i}{g_c A_i}-\frac{2w_{ik}u_i}{g_c A_i}-\frac{f_D w_{ji}u_j}{g_c A_i}-\frac{2w_{ij}u_i}{g_c A_i}+\frac{1}{g_c}\left(\frac{m_i}{A_i}\right)^2\frac{dV'_i}{dx} \tag{3.61}$$

$$-\frac{dp_i}{dx}=\frac{F_i}{A_i}+\rho_i cos\theta+\frac{f_T w'_{ik}}{g_c A_i}(u_i-u_k)+\frac{f_T w'_{ij}}{g_c A_i}(u_i-u_j)$$
$$+\frac{w_{ik}u_i}{g_c A_i}(f_D-2)+\frac{w_{ji}}{g_c A_i}(2u_i-f_D u_j)+\frac{1}{g_c}\left(\frac{m_i}{A_i}\right)^2\frac{dV'_i}{dx} \tag{3.62}$$

Frictional forces along the sub-channel wall is

$$\frac{F_i}{A_i}=\frac{f_i\phi_i}{2g_c\rho_f D_i}\left(\frac{m_i}{A_i}\right)^2 \tag{3.63}$$

$$\alpha=\alpha(h,\rho)$$

$$V'=\frac{(1-x^2)}{(1-\alpha)\rho_f}+\frac{x^2}{\alpha\rho_g} \tag{3.64}$$

$$V'_i=V'_i(p_i,h_i)$$

$$\frac{dV'_i}{dx}=\frac{\partial V'_i}{\partial p}\frac{dp_i}{dx}+\frac{\partial V'_i}{\partial h}\frac{dh_i}{dx} \tag{3.65}$$

$$-\frac{dp_i}{dx} = \frac{f_i\phi_i}{2g_c\rho_f D_i}\left(\frac{m_i}{A_i}\right)^2 + \rho_i cos\theta + \frac{f_T w'_{ik}}{g_c A_i}(u_i - u_k) + \frac{f_T w'_{ij}}{g_c A_i}(u_i - u_j)$$

$$+\frac{w_{ik}u_i}{g_c A_i}(f_D - 2) + \frac{w_{ji}}{g_c A_i}(2u_i - f_D u_j) \tag{3.66}$$

$$+\frac{1}{g_c}\left(\frac{m_i}{A_i}\right)^2\left(\frac{\partial V'_i}{\partial p}\frac{dp_i}{dx} + \frac{\partial V'_i}{\partial h}\frac{dh_i}{dx}\right)$$

$$-\left(1 + \frac{1}{g_c}\left(\frac{m_i}{A_i}\right)^2\frac{\partial V'_i}{\partial p}\right)\frac{dp_i}{dx} = \frac{f_i\phi_i}{2g_c\rho_f D_i}\left(\frac{m_i}{A_i}\right)^2 + \rho_i cos\theta$$

$$+\frac{f_T w'_{ik}}{g_c A_i}(u_i - u_k) + \frac{f_T w'_{ij}}{g_c A_i}(u_i - u_j) + \frac{w_{ik}u_i}{g_c A_i}(f_D - 2) \tag{3.67}$$

$$+\frac{w_{ji}}{g_c A_i}(2u_i - f_D u_j) + \frac{1}{g_c}\left(\frac{m_i}{A_i}\right)^2\left(\frac{\partial V'_i}{\partial h}\right)\frac{dh_i}{dx}$$

If we consider all possible sub-channels connected to (i) then

$$-\left(1 + \frac{1}{g_c}\left(\frac{m_i}{A_i}\right)^2\frac{\partial V'_i}{\partial p}\right)\frac{dp_i}{dx} = \frac{1}{g_c}\left(\frac{m_i}{A_i}\right)^2\left(\frac{f_i\phi_i}{2\rho_f D_i} + \left(\frac{\partial V'_i}{\partial h}\right)\frac{dh_i}{dx}\right)$$

$$+\rho_i cos\theta + \frac{1}{g_c A_i}\sum_{j=1}^{N} f_T w'_{ij}(u_i - u_j) \tag{3.68}$$

$$+\frac{1}{g_c A_i}\sum_{j=1}^{N}\begin{matrix} w_{ik}u_i(f_D - 2) & ; if \quad w_{ij} \geq 0 \\ w_{ji}(2u_i - f_D u_j) & ; if \quad w_{ij} < 0 \end{matrix}$$

$$i = 1,2, \dots, N$$

3.5.5 Transverse momentum equation

If we assume cross-flow velocity only occurs in the gap between adjacent sub-channels and the cross-flow velocity is small compared to the axial velocity.

$$p_i - p_j = C_{ij} w_{ij}|w_{ij}| \qquad i = 1,2, \dots, N \tag{3.69}$$

C_{ij} is a loss function, which accounts for the transverse resistance to flow and any other unrecoverable losses.

The summary of the governing equations of fluid flow and heat transfer characteristics used in sub-channel analysis are as follows,

Equation of Continuity

$$\frac{dm_i}{dx} = -\sum_{j=1}^{N} w_{ij} \qquad i = 1, 2, \dots, N \tag{3.70}$$

Equation of Axial Momentum

$$-\left(1 + \frac{1}{g_c}\left(\frac{m_i}{A_i}\right)^2 \frac{\partial V_i'}{\partial p}\right)\frac{dp_i}{dx} = \frac{1}{g_c}\left(\frac{m_i}{A_i}\right)^2 \left(\frac{f_i \phi_i}{2\rho_f D_i} + \left(\frac{\partial V_i'}{\partial h}\right)\frac{dh_i}{dx}\right)$$

$$+ \rho_i cos\theta + \frac{1}{g_c A_i}\sum_{j=1}^{N} f_T w_{ij}'(u_i - u_j) \tag{3.71}$$

$$+ \frac{1}{g_c A_i}\sum_{j=1}^{N} \begin{matrix} w_{ik} u_i (f_D - 2) & ; if \quad w_{ij} \geq 0 \\ w_{ji}(2u_i - f_D u_j) & ; if \quad w_{ij} < 0 \end{matrix}$$

$$i = 1,2, \dots, N$$

Equation of Transverse Momentum

$$p_i - p_j = C_{ij} w_{ij} |w_{ij}| \qquad i = 1,2, \dots, N \tag{3.72}$$

Equation of Energy

$$m_i \frac{dh_i}{dx} = q_i' + \sum_{j=1}^{N} w_{ij}'(h_j - h_i)$$

$$- \sum_{j=1}^{N} \begin{Bmatrix} 0 & ; if \quad w_{ij} \geq 0 \\ w_{ij}(h_j - h_i) & ; if \quad w_{ij} < 0 \end{Bmatrix} \tag{3.73}$$

$$i = 1,2, \dots, N$$

Turbulent Inter-Channel Mixing Model

$$w'_{ij} = \beta s_{ij} \frac{1}{2}\left(\frac{m_i}{A_i} + \frac{m_j}{A_j}\right) \tag{3.74}$$

$$w'_{ij} = \beta s_{ij} \overline{G_{ij}} \tag{3.75}$$

Where,

$$\beta = c\frac{d}{s} Re^{-0.1} \tag{3.76}$$

The governing equations of the sub-channel analysis methodology are implemented using the control volume approach and solved using COBRA solver.

3.6 Closure

The mathematical formulations adopted in the thesis was explained in this chapter. The governing equations in Cartesian coordinate system for the solution fluid flow and heat transfer in any geometry is discussed. Also, the governing equations of fluid flow and heat transfer in and out of plane flow problem has been discussed. The derivations of the governing equations of mass momentum and energy for the sub-channel analysis are also detailed. The numerical procedure adopted for the solution of governing equations are highlighted. The equations are solved using the finite element techniques available in a commercial code COMSOL multi physics. The sub-channel analysis is carried out using the developed framework. The subsequent chapters make use of the formulations discussed in this chapter.

CHAPTER-4

DEVELOPMENT OF FRAMEWORK FOR SUB-CHANNEL ANALYSIS

CHAPTER-4

4 DEVELOPMENT OF FRAMEWORK FOR SUB-CHANNEL ANALYSIS

4.1 Introduction

In this chapter, the necessity for the development of sub-channel thermal hydraulic analysis framework is elucidated and various features of the software framework are discussed in detail. The thermal hydraulic analysis of the nuclear reactor core is carried out traditionally by using the sub-channel analysis codes such as COBRA and its modified versions. These codes are written in FORTRAN language. The analysis involves the preparation of a sub-channel layout, which contains geometric details of fuel pin and sub-channel connectivity details. The parameters of relevance in safety analysis are i) size and geometry of bundle, p/d, w/d ratio, ii) Reactor pressure, iii) coolant flow rate, iv) coolant inlet temperature, v) core power vi) axial and radial power profile with and without xenon load for entire life of core etc. For analysing different conditions of the reactor, a large number of input conditions are considered and many changes in the input data are required to be made. The input data are also to be edited manually. The results of sub-channel codes are in the form of large text files, which provide details of sub-channels and rods in tabular form. During the design and optimization phases of the reactor core, a large number of analysis are to be carried out to estimate coolant temperature, fuel surface and centerline temperatures, the available safety margins, and operating power limits. For a typical reactor with 160 fuel sub-assemblies and reduced to 40 zones of fuel sub-assemblies with similar power generation, a systematic analysis demands around 80,000 simulations. Manual feeding

of input data and interpretation of the output are prone to human errors. In other words, identifying the fuel bundle to be analysed for hot spot requires scanning through the reactor physics calculations. Further, manual processing of these data for the evaluation of available thermal-hydraulic safety margins are also difficult. It takes a considerable amount of time in using the benchmarked sub-channel analysis codes for analyzing all the fuel assemblies for the entire range of operating power and at different flow regimes and transients. Considering the complexity of the rod bundle geometry, different turbulent scales and limitations of computational resources, it is difficult to perform the full scale thermal hydraulic analysis of reactor core using computational fluid dynamic (CFD) techniques. In recent times, the user-friendliness of sub-channel analysis codes were also improved to reduce the amount of efforts required with improved reliability of calculations (Burtak et al. 2006, Jaretag et al., 2015, Billings et al. 2015, Lassmann, 2015). In the present work, a general purpose automated sub-channel thermal hydraulic analysis framework is developed to make this process simple, fast and reliable to perform the sensitivity studies of different parameters affecting the thermal margins of the nuclear reactor core.

4.2 Sub-channel Thermal Hydraulic Analysis

The nuclear reactor core fuel assemblies are of different shapes typically, like, square, hexagonal or circular in cross-section as shown in Fig. 1.3 (Ginox, 1978; Todreas and Kazimi, 2001). Typical Pressurized Water Reactor (PWR), Boiling Water Reactor (BWR) and Liquid Metal Fast Breeder Reactor (LMFBR) fuel pins are assembled in the form of regular arrangements/patterns and are called fuel assemblies/bundles. Inside the fuel assembly, fuel pins are arranged either in square or triangular lattice configuration. In pressure tube type reactors such as PHWR, fuel pins arranged in the form of small

bundles without fuel channel cover but the coolant flow is restricted within the coolant channel. In old PWR designs as well as the recent large commercial PWR designs, the fuel assemblies are not covered with a channel or the fuel channel cover might contain the openings along the channel in the flow direction between the assemblies. This kind of arrangement causes the inter-channel mixing of coolant between assemblies along the axial direction. Deliberately the mixing is allowed between the assemblies to reduce the hot channel temperatures. These fuel assemblies constituting the nuclear reactor cores are generally called open channel core. In some configurations, the fuel assemblies are fully covered by the zircalloy channels which prevent the inter-channel mixing of the coolant among the assemblies. This kind of fuel assemblies constituting the nuclear reactor cores are called closed channel core. Thermal-hydraulic analysis of nuclear reactor core is carried out to estimate the detailed flow and temperature distribution within the fuel assembly. In the case of open channel assemblies, the entire core or symmetric sector of the core is to be analyzed to estimate the flow and temperature distribution within the core. In the case of closed channel assemblies, individual assemblies can be analyzed separately after getting the fuel assembly flow distribution.

The thermal hydraulic safety analyses of nuclear reactor are performed in two ways. First, the system level thermal hydraulic analysis is carried out using the system codes like RELAP, RETRAN, ATHLET to get the system behaviors under different steady state and transient operating conditions. Second, the results of this analysis gives the boundary conditions for the core/component level analysis. The detailed analysis of the reactor core is performed using the sub-channel thermal hydraulic codes like COBRA

(Rowe, 1967), VIPRE (Stewart et al., 1993) to estimate the thermal hydraulic safety margins of nuclear reactor core under steady state and transient conditions. A sub-channel is defined as a flow passage formed between number of rods or some rods and wall of channel/shroud tube. The sub-channels can be formed by either the coolant centered sub-channels or the rod centered sub-channels as shown in Fig. 4.1. The sub-channels can be either square or triangular in shape depending on the type of fuel pin arrangements either in square or in triangular pitch arrangements of the fuel assembly. The concept of sub-channel analysis method is an important tool for predicting the thermal hydraulic performance of rod bundle nuclear fuel element. It considers a rod bundle to be a continuously interconnected set of parallel flow sub-channels which are assumed to contain one-dimensional flow coupled to each other by cross-flow mixing. The axial length is divided into a number of increments such that the whole flow space of a rod bundle is divided into a number of control volumes/nodes.

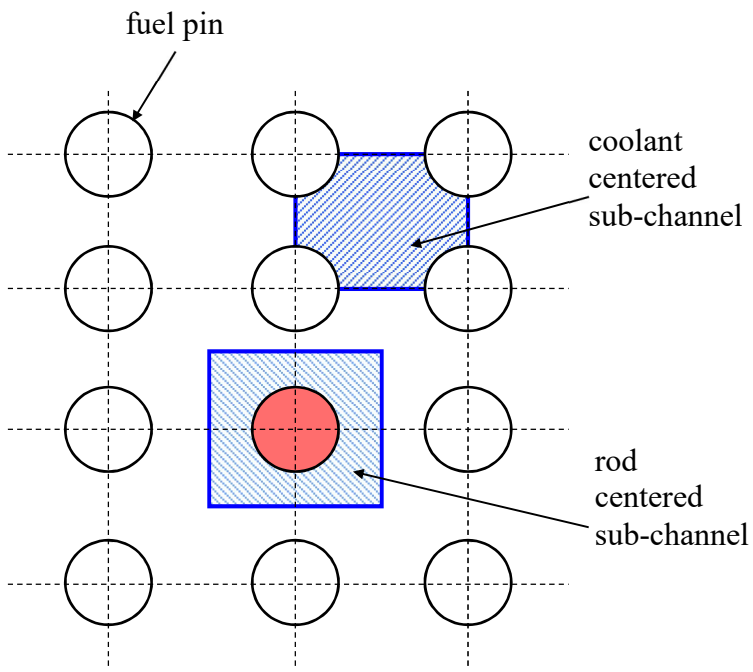

Fig. 4.1 Definition of fuel assembly sub-channels

The sub-channel thermal hydraulic analysis basically solves the conservation equations of mass, momentum and energy on the specified control volumes. The one-dimensional control volumes are connected in both axial and radial directions to get the three-dimensional effect of the core. Performing the detailed CFD kind of analysis for the entire core or a single fuel assembly is very difficult even with the present-day computing resources. Hence, most of the nuclear reactor cores are designed based on the sub-channel analysis codes. The detailed predictions of the sub-channel codes are greatly improved by taking into consideration of the effect of inter-channel mixing model to account for the flow exchange between the fuel assembly sub-channels. The relation between sub-channel flow rate, which is the mass flow rate in an axial direction through sub-channel area and diversion cross-flow, which is the mass flow in a transverse direction resulting from local pressure differences between two sub-channels is strongly governed by momentum balance in a transverse direction. A correct formulation of momentum equations and good knowledge of the mixing process between sub-channels are an absolute necessity, for obtaining reliable predictions of coolant local conditions using sub-channel methodology.

In the basic design of the fuel assembly, the spacers are provided at different locations of the fuel pin, to avoid hotspots, to maintain proper coolant flow area and to control flow-induced vibrations (FIV). The spacers also offer more pressure drop as compared to the bare assembly which improves the coolant redistribution inside the fuel assembly. Most of the improvements of the spacers were considered to reduce the pressure drop and improve the mixing between sub-channels by providing mixing vanes in the spacer. Due to the geometrical complexity of the spacer and the complexity of flow distribution downstream of the spacer, the spacer models are derived from both experiments and

CFD analysis to account for the proper flow diversion in the lateral momentum balance equation. These models are implemented in the sub-channel analysis codes to include the effect of different type of spacers on flow distribution. In case of transients and at higher power levels near the critical heat flux conditions the mixing within the assemblies are greatly affected by the local conditions due to two-phase flow formations. Hence, the proper predictions of the local conditions are important in the estimation of the critical power of the assembly and therefore, the temperature of the fuel pin surface. In this way, sub-channel type of thermal hydraulics analysis codes is applied to the practical design of the nuclear reactor core even today.

4.3 Architecture of Sub-Channel Analysis Framework

An **A**dvanced **S**ub-Channel **T**hermal **Hy**draulic **An**alysis **S**ystem (**ASTHYANS**) framework is developed based on the object oriented technology used in the advanced computer simulation programs for carrying out nuclear reactor core design and analysis. The graphical user interface (GUI) is created using Visual Basic (VB) with .Net framework. The architecture of the framework is shown in Fig. 4.2. The developed framework is used for defining the reactor core based on the arbitrarily shaped fuel assembly and performing the thermal hydraulic analysis for the estimation of thermal hydraulic safety parameters like fuel temperatures, critical heat flux and critical power margins. Figure 4.3 shows the schematic flow chart of the process of carrying out the sub-channel analysis inside the software framework. This framework consists of different modules for creating the objects like fuel pins and non-fuel pins. The pins are assembled in a specified lattice configuration as a fuel assembly. An object representing the typical fuel bundles are assembled together to form a nuclear reactor core.

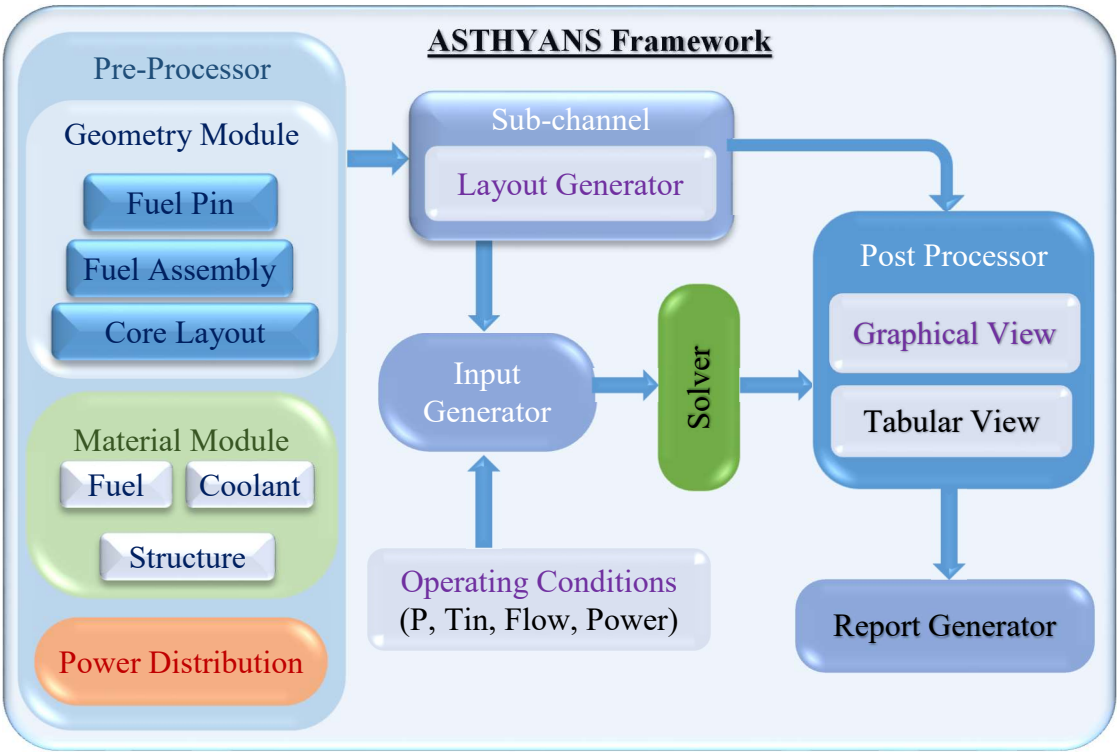

Fig. 4.2 Architecture of advanced sub-channel analysis framework

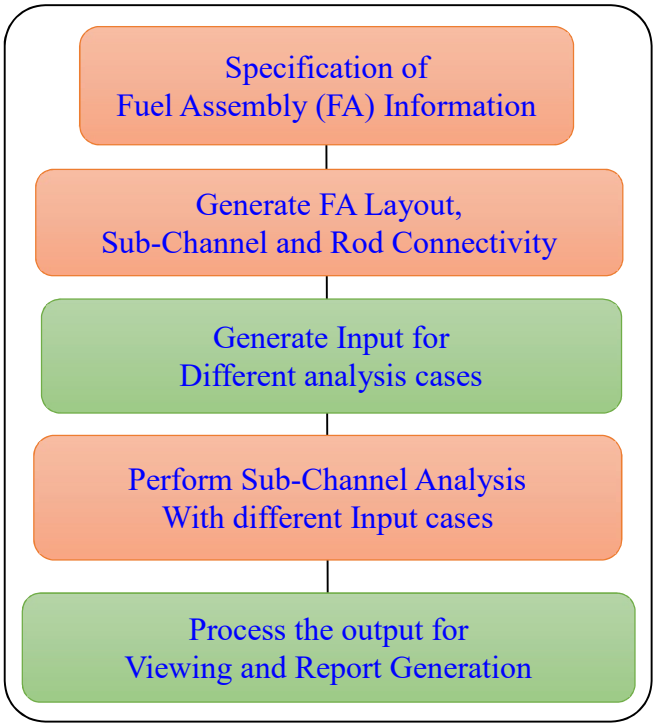

Fig. 4.3 Schematic flow chart of sub-channel analysis framework

Further, the basic geometrical and assembly details are converted to the required form for input to the sub-channel level thermal hydraulic analysis. The reactor core power distribution can be specified either uniform or non-uniform. Based on the core configuration, fuel assembly, and pin layout, the power distributions are estimated both at assembly level and sub-channel level. The fluid properties (water and steam) required for the analysis are estimated using the **I**nternational **A**ssociation for **P**roperties of **W**ater and **S**team (IAPWS) codes available in the form of VB routines. The code is written as a general purpose tool for the analysis of a typical nuclear reactor core with square pitched fuel assemblies or triangular pitched hexagonal fuel assemblies.

The screenshot of the various features of the ASTHYANS workbench is shown in Fig. 4.4. The framework consists of various modules which are programmed in such a way that the entire core thermal-hydraulic analysis of nuclear reactor is fully automated. The analysis process involves the pre-processing module for fuel assembly definition, core layout generation, sub-channel layout generation, assigning the power profile and definitions of material and fluid properties. The analysis module used for the estimation of pin power distribution, specifying operating conditions, generating inputs for various case studies to perform the sub-channel analysis. The post-processing and report generation module is used to process the analysis results. The developed framework and automated layout generation program is aimed at generating the input file required for the sub-channel analysis code in an efficient way with minimum human intervention. This helps in minimizing human error apart from reducing the analysis time.

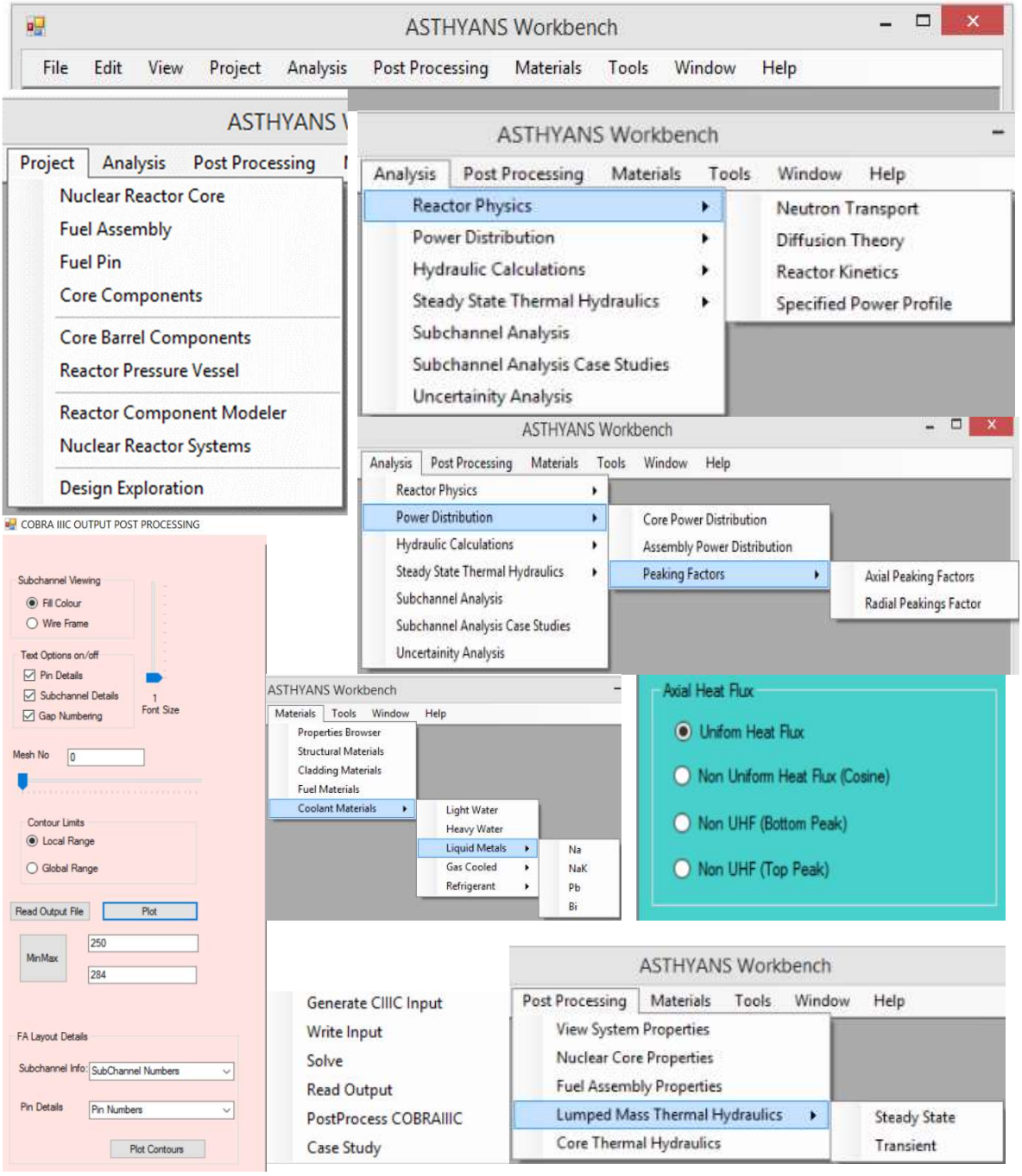

Fig. 4.4 Screen shot of ASTHYANS workbench showing various features.

4.4 Fuel Assembly Layout Generator Module

An automated fuel assembly layout generator code is used to generate the sub-channel layout for triangular and square pitched arrays of hexagonal and square shaped fuel assembly. The screen short view of the layout generator is shown in Fig. 4.5. Typical sub-channel layout for the triangular and square pitched rod array of different sizes of fuel bundles generated using the fuel assembly sub-channel layout generator is depicted in Fig. 4.6 and Fig 4.7. These figures clearly indicate the sub-channel layout and rod connectivity details for the interior, side and corner channels along with gap numbering. Once the layout is generated, the pin diameters and the power profile are specified. The basic geometric features of fuel assemblies like pin diameter, pitch, rod to wall gap and the number of rows of the pins in the square layout are specified. The details required for the sub-channel layout such as area, wetted perimeter, heated perimeter, sub-channel to sub-channel connectivity information, rod to sub-channel connectivity information and power distribution to each sub-channel are generated. After generation of fuel assembly details, layout information is redirected for preparation of the input to the sub-channel code. As the code is written based on the object-oriented methodology, different types of fuel assembly can be generated. The generated assemblies are used to create the reactor core layout.

4.5 Core Layout Generator Module

The core layout generator module is used to generate a typical reactor core consists of either square or hexagonal shaped fuel assembly. The screenshot of the typical core layout of 3x3 square fuel assembly is shown in Fig 4.8. Each square assembly object can be assigned to a fuel assembly object of any array sizes of the square pitched fuel bundle which is generated using the fuel assembly layout generator module.

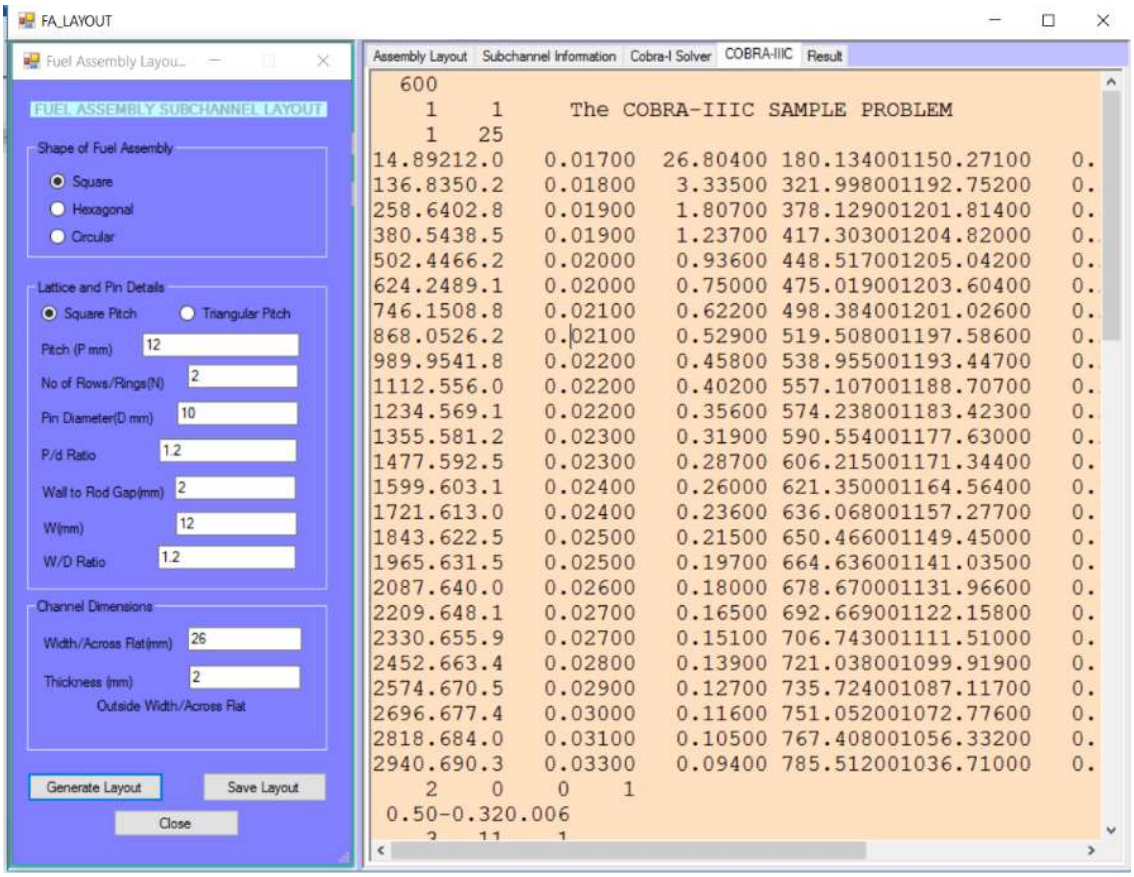

Fig. 4.5 Schematic of the layout generator

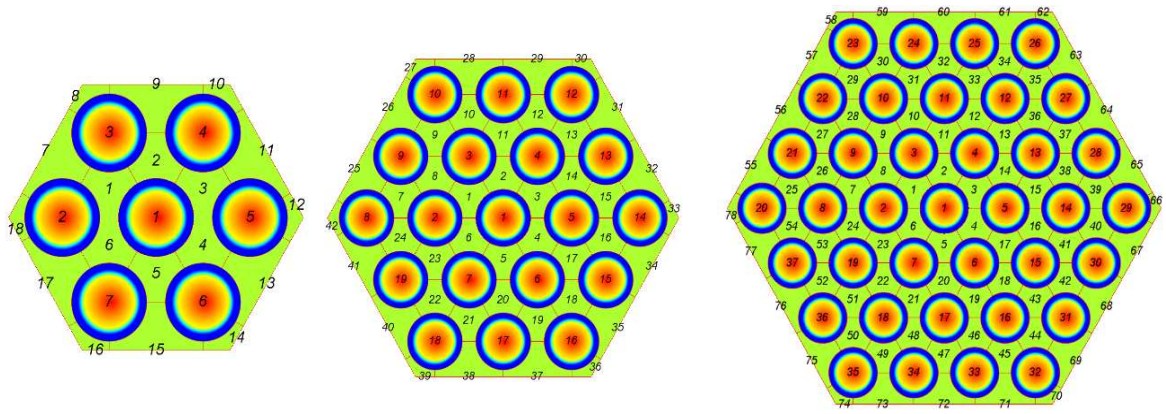

7 pins
(18 Sub-channels)

19 pins
(42 Sub-channels)

37 pins
(78 Sub-channels)

Fig. 4.6 Layout of the fuel pin and sub-channel arrangements in different sizes of hexagonal fuel assembly generated using fuel bundle layout generator

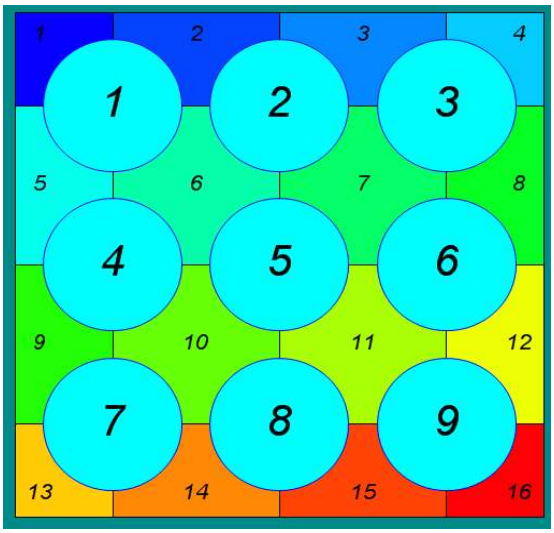

3 x 3 Fuel Bundle
(9 Pins, 16 Sub-channels)

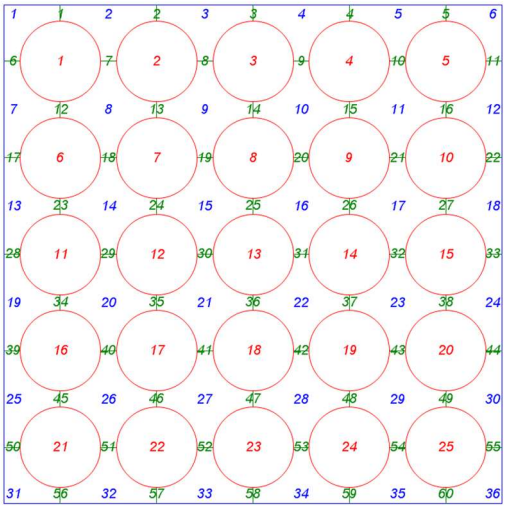

5 x 5 Fuel Bundle
(25 Pins, 36 Sub-channels, 60 Gaps)

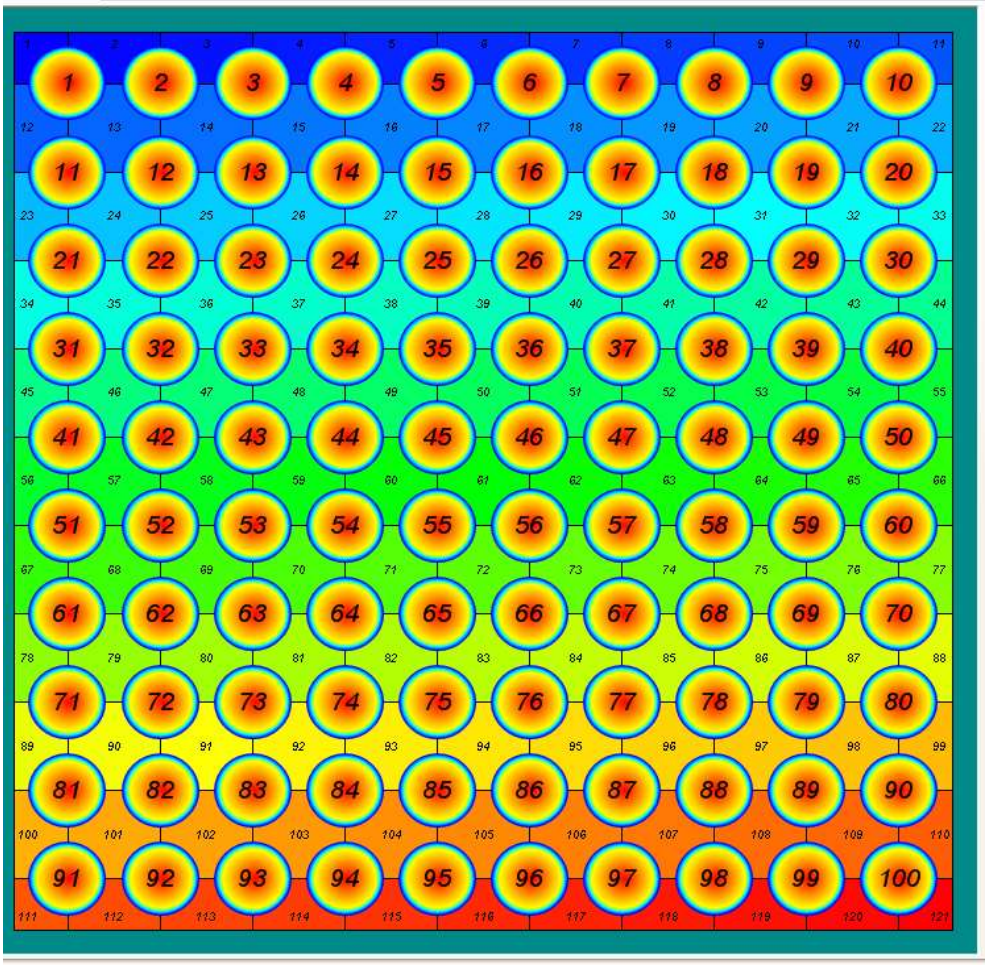

10 x 10 Fuel Bundle
(100 Pins, 121 Sub-channels, 220 Gaps)

Fig. 4.7 Typical sub-channel layout of square pitched fuel bundle generated using fuel bundle layout generator

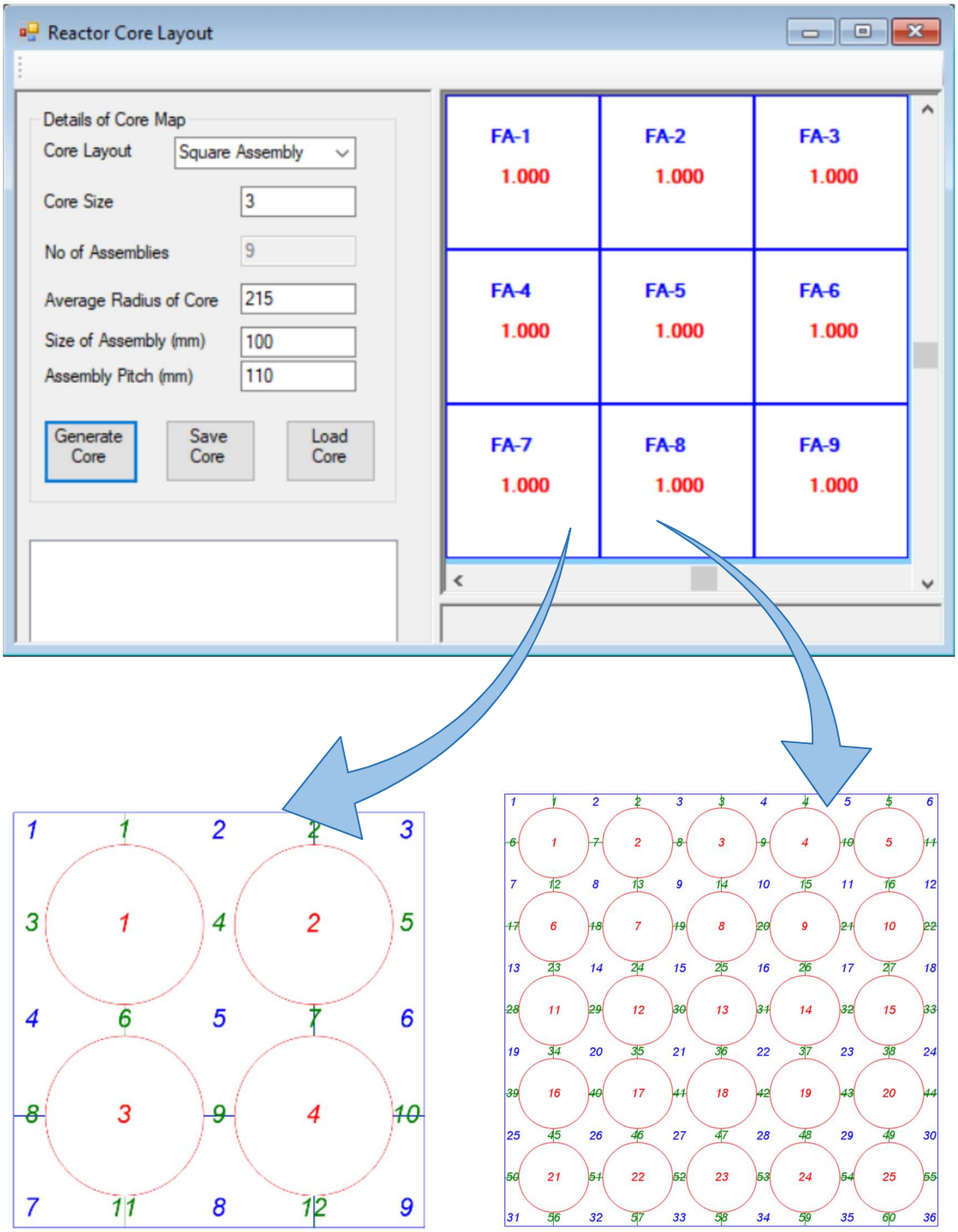

Fig. 4.8 Typical core layout of square pitched fuel assembly

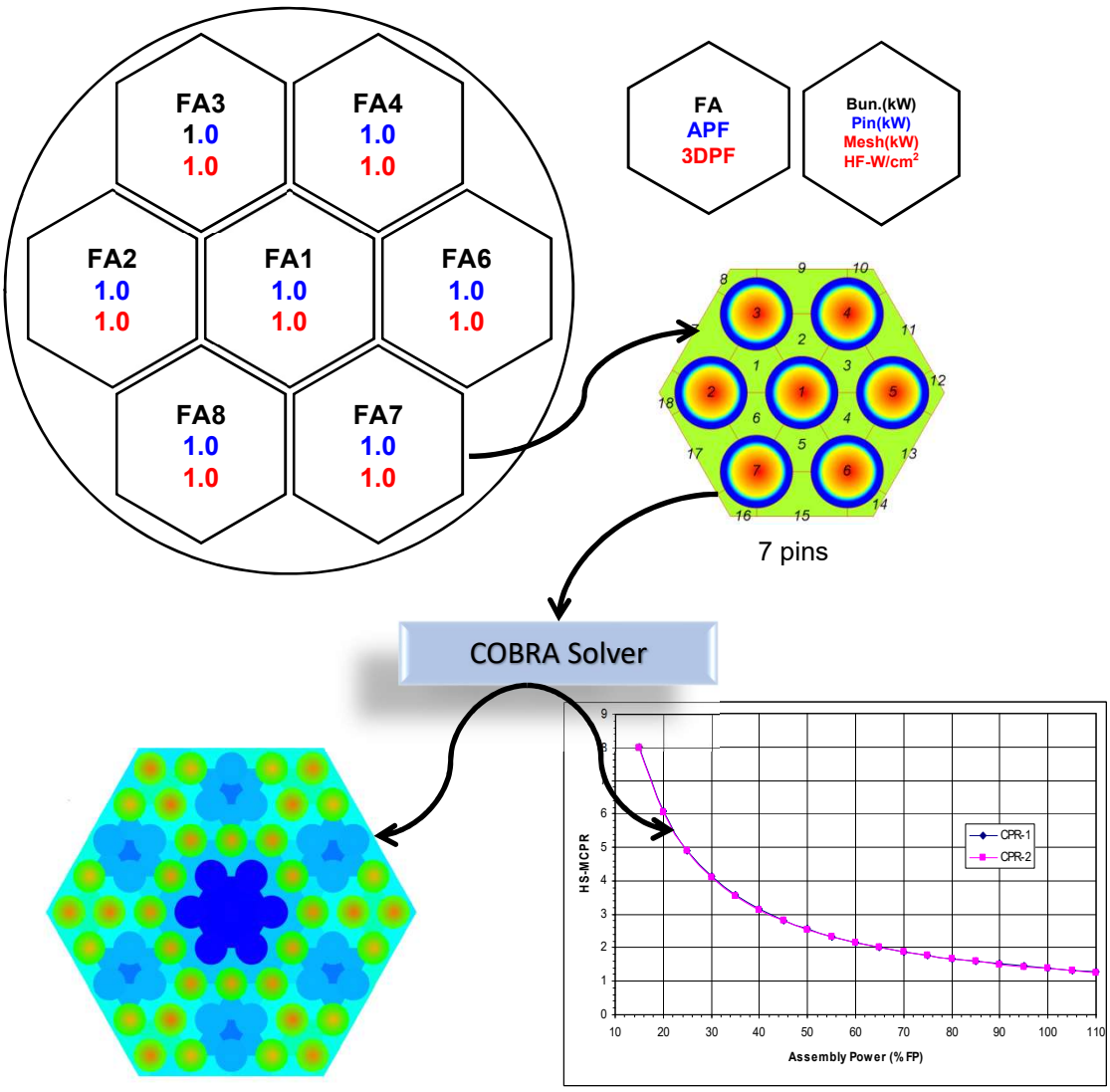

Fig. 4.9 Typical core layout of hexagonal fuel assembly, the Contours of fuel pin and Sub-channel temperatures and HS-MCPR values of the fuel assembly at different power.

The same reactor core layout module is used to generate the reactor core layout consists of a triangular pitched hexagonal fuel assembly. Typical layout of the reactor core with hexagonal fuel assembly is shown in Fig. 4.9. Similar to the reactor core with square pitched fuel assembly, various sizes of the hexagonal fuel assembly objects generated using the fuel assembly layout generator can be mapped to the fuel assemblies of the reactor core. As the sub-channel analysis framework is written based on the object-

oriented methodology, the software object written for the layout generation of a single fuel assembly is inherited to represent the various fuel assemblies in the entire reactor core. The power profiles of individual assemblies are assigned separately. Each fuel assembly has got its own power profile associated with the fuel assembly object. The sub-channel connectivity information between the assemblies is to be included by renumbering the neighbouring sub-channels and their connectivity. In this way, the layout generation program is used to generate the sub-channel layout for the entire reactor core.

4.6 Power Profile Module

The fuel assembly power profile can be considered to be varying either uniform or non-uniform in both radial and the axial direction. The actual nuclear reactor power profile is non-uniform in both radial and axial direction. The power profile generated from the reactor physics calculations are assigned to the respective fuel assembly. The power profile module is written to either generate the power profiles or read different power profiles from a text file and is assigned to a typical fuel assembly. The detailed 3-D power profiles are further reduced to the radial, axial, 3-D peaking factors. The peaking factors are defined as the ratio of local power to the average power. The 3-D peaking factor is defined as the ratio of mesh power to the core average mesh power. The 3-D peaking factor is used to estimate the local heat flux generated in the fuel pins at different mesh locations. The assembly peaking factors are also estimated from the 3-D peaking factors to estimate the power generated by the fuel assembly. Once the 3-D peaking factors are known, the bundle power, pin power, mesh power and heat flux are estimated. The power profile module also used to generate the axial and radial peaking factors of different assemblies which are required for the sub-channel analysis.

4.7 Analysis Module

In this module, the nominal operating conditions such as pressure, inlet temperature, flow rate, and the core power are specified. Once all the information of material properties, sub-channel to sub-channel connectivity, sub-channel to rod connectivity details and power profiles details are available, the data required for the sub-channel analysis code is assembled to prepare the typical input case file. This module also contains the routines for the generation of case studies. Here, to perform the parametric study on the effect of the change in the different input parameters, we can specify different input parameters varying in a specified range and interval. Different input files are generated according to the case studies using the sub-channel layout and connectivity information. The sub-channel analysis solver is invoked to perform the sub-channel analysis using the generated case files.

4.8 Post Processing and Report Generation Module

This module is used to post-process the output generated from the sub-channel analysis codes. The output data of sub-channel and pin details obtained from different cases studies for all the fuel assemblies of entire core is read for post-processing. The details of sub-channel output such as the fuel surface, central temperature, coolant conditions such as temperature, mass flow rate, quality etc., the critical heat flux of the channel and critical power of the assembly at different power levels and operating conditions are generated. The graphical representations of the sub-channel and rod details are generated using this module. The screenshot of the three-dimensional view of the fuel assembly peaking factors generated using the power profile viewer is shown in Fig. 4.10. The results can be viewed for each fuel assembly from the inlet to outlet at different mesh locations. The compilation of various output data in the form of tables is

also generated to view the numerical data in tabular form. The report generation module also contains the software routines to redirect all the details of the reactor core and fuel assembly and sub-channel details into a word document.

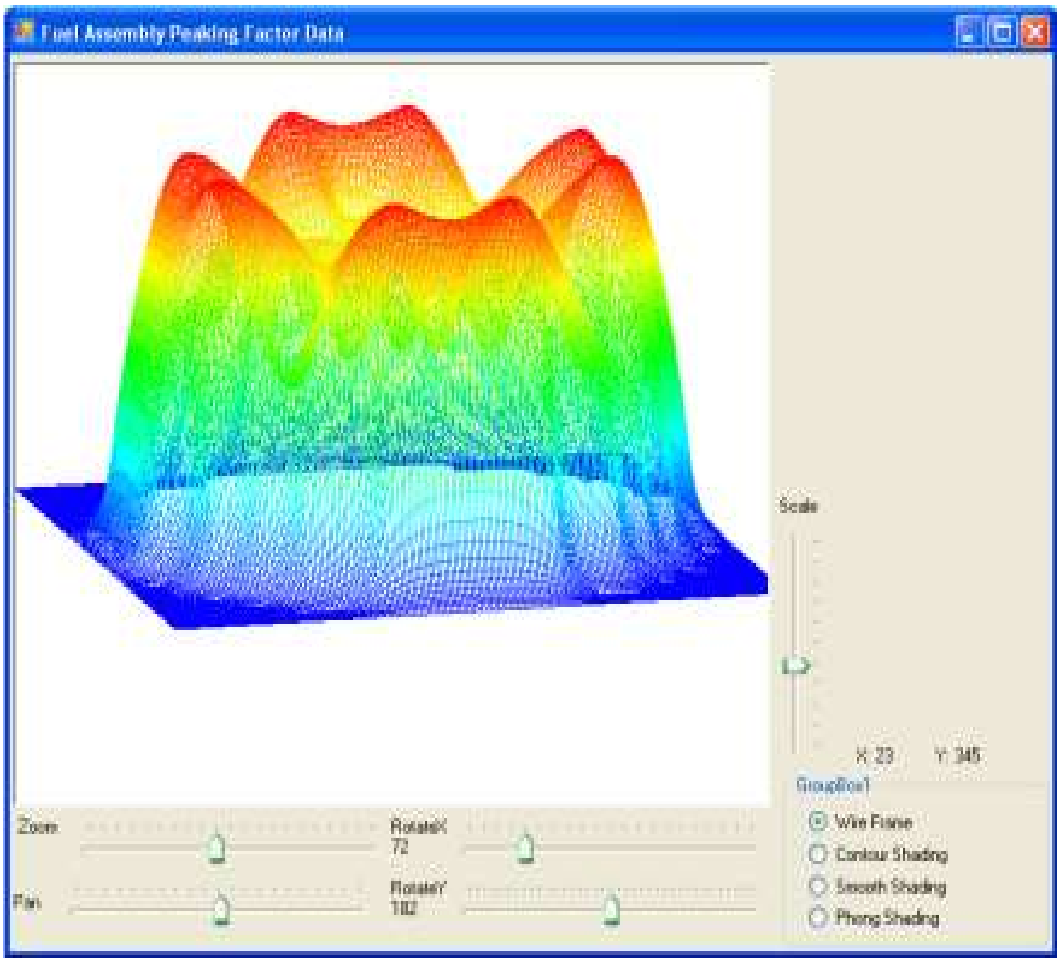

Fig. 4.10 The three dimensional fuel assembly peaking factors and power profile viewer.

4.9 Summary

An advanced general-purpose fully automated sub-channel analysis framework ASTHYANS is developed using an object-oriented methodology. An automated sub-channel layout generation program is developed to generate different configurations of a typical fuel bundle. The architecture and the various features of the modules are discussed. The sub-channel analysis framework developed in the present study can be

used to perform the thermal hydraulic analysis of nuclear reactor core in an efficient way with minimum human intervention.

4.10 Closure

In this chapter, the requirement and the development of the general purposed automated sub-channel thermal hydraulic analysis framework is discussed. The various features of the framework have been demonstrated. The developed framework is used to perform the investigation of cross-flow mixing in a typical nuclear reactor fuel pin bundle and the details of the investigations are discussed in chapter 7.

CHAPTER-5

FLUID FLOW AND HEAT TRANSFER CHARACTERISTICS IN SUB-CHANNEL GEOMETRIES

CHAPTER-5

5 FLUID FLOW AND HEAT TRANSFER CHARACTERISTICS IN SUB-CHANNEL GEOMETRIES

5.1 Introduction

This chapter discusses about the fluid flow and heat transfer characteristics in sub-channel geometries in laminar and turbulent flow conditions. Steady-state fully developed laminar flow in constant cross-section non-circular sub-channel geometries of rod bundles are studied. The study is focused to apply the CFD model on 2D geometry representing the non-circular rod bundle sub-channels by solving the out-of-plane flow velocities rather than a conventional 3D CFD analysis. Extensive validation of developed out-of-plane 2-D CFD model is also included in this chapter. Analyses are carried for different pitch to diameter (p/d) ratios to estimate the laminar friction factor and average Nusselt number. The influence of pitch to diameter (p/d) and width to diameter (W/d) ratio on fluid friction in square and hexagonal fuel bundle geometries are also investigated in detail. The turbulent flow simulations are also carried out for non-circular sub-channel geometry using a 3-D model for different Reynolds number. In this chapter, the results of flow and heat transfer simulations are discussed in detail.

5.2 Laminar Flow and Heat Transfer in Sub-Channel Geometry

5.2.1 Geometry of rod bundle sub-channels

The geometry of the computational domain considered in the present study is depicted in Fig. 5.1 (a-b). The regular non-circular geometries are modified at the corners, by considering the fuel pins, to represent a square/triangular pitched sub-channel as shown

in Fig. 5.1. The p/d equal to 1 represents a cusped channel and p/d equal to infinity represents a square/triangular channel. The four-pin square pitched and seven-pin triangular pitched fuel bundles are also considered for analysis. These pin bundles are selected as it represents of all types of sub-channels in rod bundles, i.e. interior, wall, and corner sub-channels. The geometries of square pitched pin bundle of size 2x2 to 10x10 are also generated and investigated the effect of bundle size on flow and heat transfer characteristics.

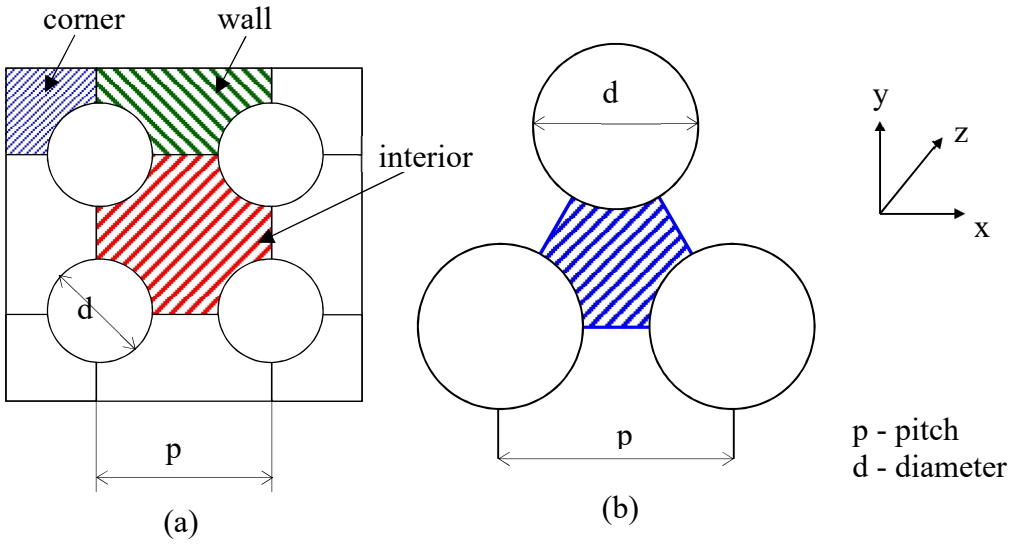

Fig. 5.1 (a) Four pin bundle with three different sub-channels of square assembly and (b) Triangular pitched sub-channel geometry

5.3 Numerical Simulation

The CFD simulations are carried out using COMSOL 4.0 multi-physics code. The governing equations are implemented using Poisson's equation. The classical partial differential equations interface is used to implement the Poisson's equation with modified pressure gradient $\left(\frac{1}{\mu}\frac{\partial P}{\partial z}\right)$ as the source term. These equations are discretized using the finite element method (FEM) and the Dirichlet boundary conditions are applied on the boundary wall. The model is meshed and solved using stationary

segregated solver with a relative tolerance of 10^{-4}. The model consists of two independent variables such as axial velocity (w) and temperature (T). The other quantities such as average velocity and wall shear stress are derived from the independent variables and its derivatives by defining the new internal variables in the COMSOL code. The integration of velocity over the domain and averaging of wall shear stress on the domain boundaries are carried out by using the component couplings, average, and integration operators. The simulations were carried out for different geometrical configurations using the developed computational model. Sufficiently fine meshes are used in the simulations to get the grid independent solutions.

5.4 Grid Independence Study and Validation

To test the grid independence of the numerical scheme, solutions have been obtained on different non-uniform grid patterns. The regular and non-circular geometry are created using the parametric model. The computational domain is meshed using physics controlled mesh by selecting the various meshing options inbuilt in COMSOL. The number of elements used in the models are varied from 50000 to 100000 for different shapes of the domain analysed. The results of grid independence study on the computed fRe for circular, square and triangular cross sections are given in Fig. 5.2. After careful examination, the fine grid size is chosen to get the grid independent solution of the variables. It is observed that even with the coarse mesh, the computed fRe variation with mesh size is within 2.5 % with respect to the theoretical solution (Fig. 5.2).

The developed numerical model is validated against the available analytical, numerical and experimental benchmark data in the literature. The computational time required for the 3-D problems of regular geometry was of the order of ~20 min with sufficiently fine mesh. The same problem solved using the out-of-plane flow approach requires very less

time (< 1 min) even for a large size of the bundle. The contours of the non-dimensional velocity (u/u_{max}) and shear stress (τ/τ_{max}) profiles in a regular circular and non-circular geometries are shown in Fig. 5.3(a-e). The axial velocity is integrated over the domain to get the average velocity (eqn. 3.23). The average wall shear stress is obtained by averaging the shear tress on the domain boundary (eqn. 3.24). The friction factor (eqn. 3.25) is estimated from the wall shear stress profiles and the average velocity. The geometry factor (fRe) and average Nusselt number ($\overline{Nu}$) obtained in the present study are compared with the data of Shah and London, 1971 for circular, square, equilateral triangular and for three and four cusped ducts and given in Table 5.1. It is observed that the results obtained from the computational model are in good agreement with the benchmark data available in the literature with an error of <0.5%.

These validation studies demonstrate that the developed model is capable of predicting the fully developed laminar flow and heat transfer characteristics of circular and non-circular geometries.

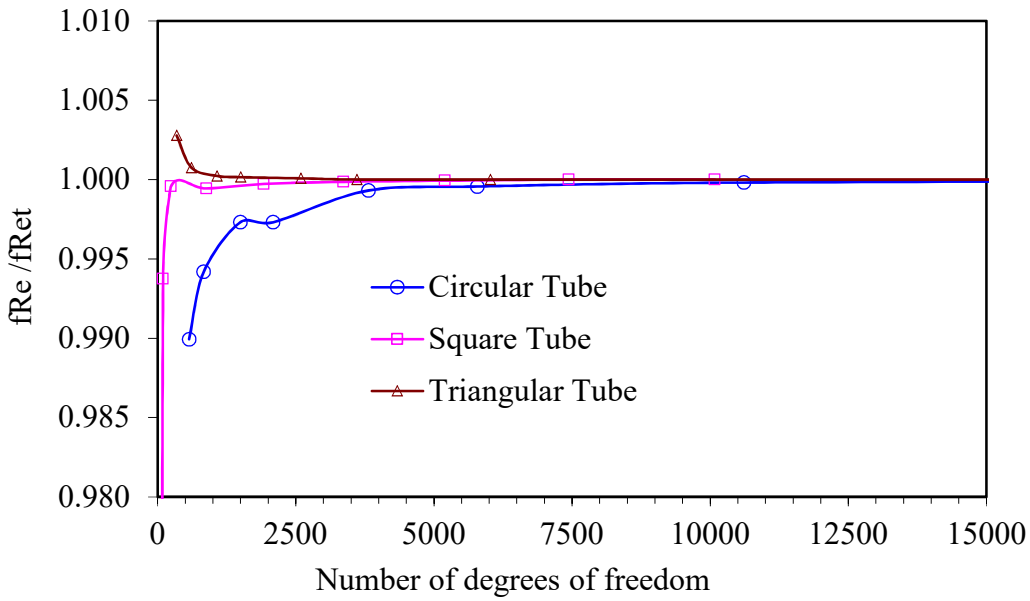

Fig. 5.2 Grid independence study of circular, square and triangular tube fRe with various sizes of mesh

Velocity Contours Shear Stress Contours

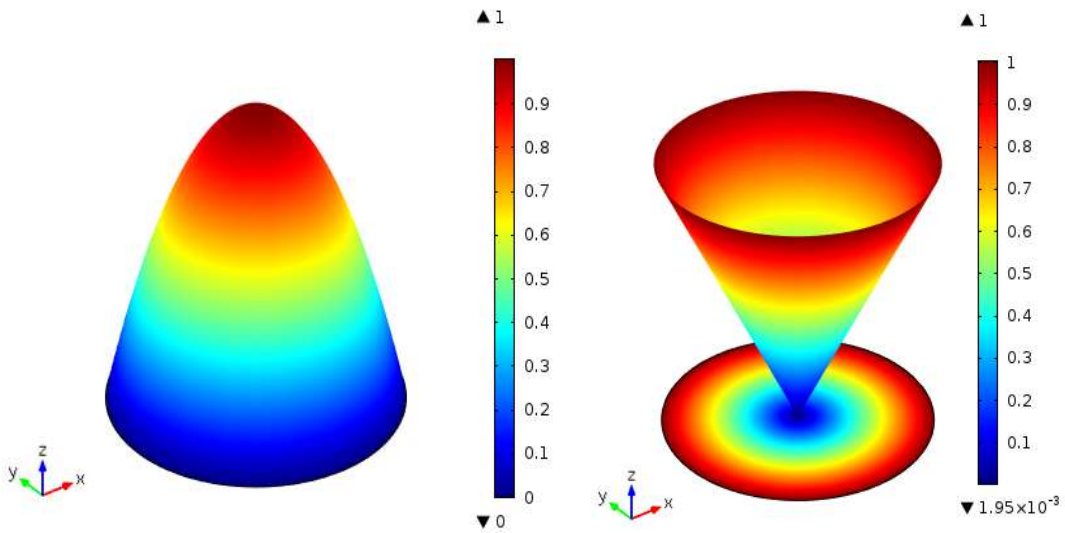

(a) Circular

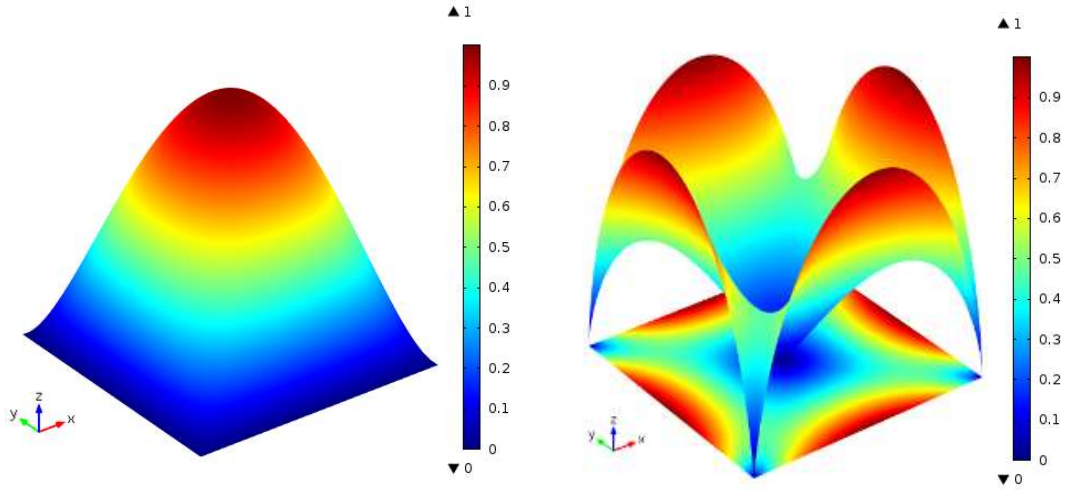

(b) Square

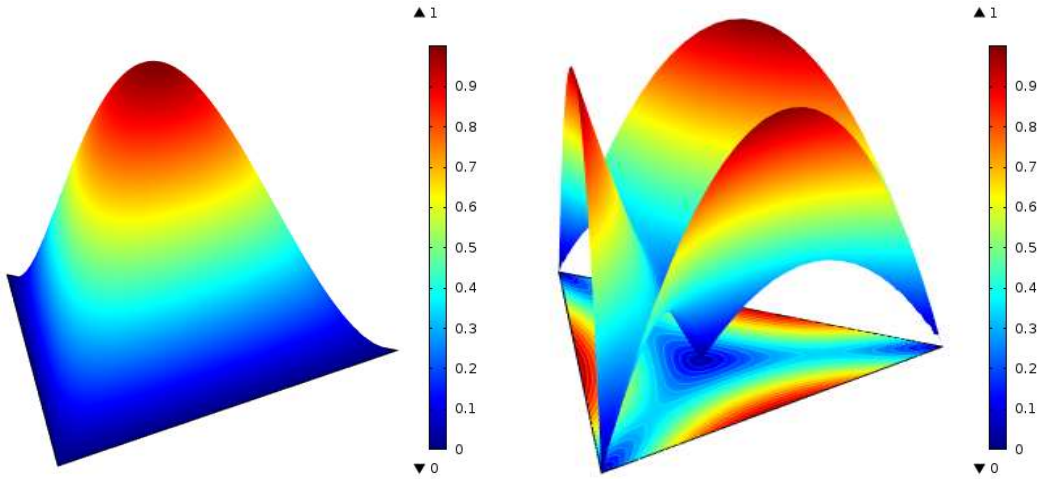

(c) Triangular

Velocity Contours Shear Stress Contours

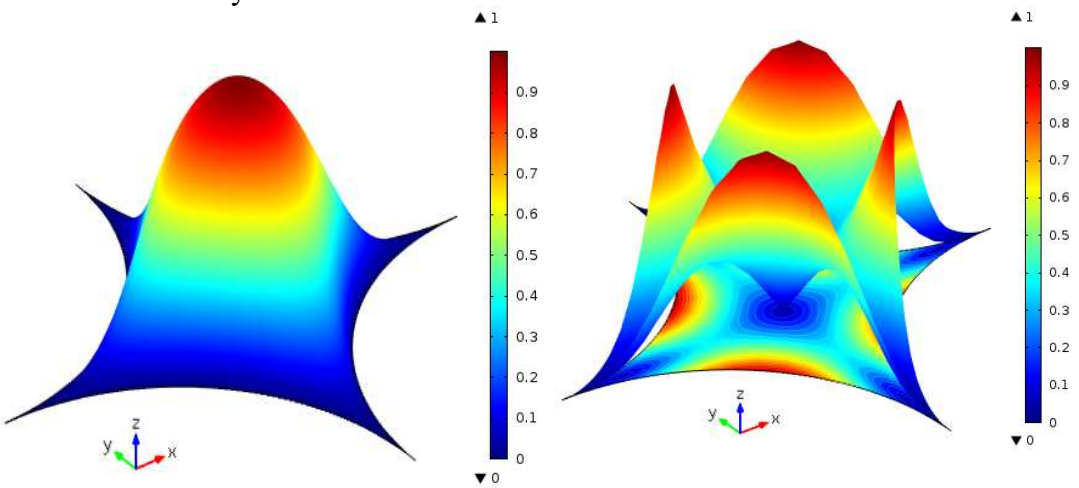

(d) 4-Cusped

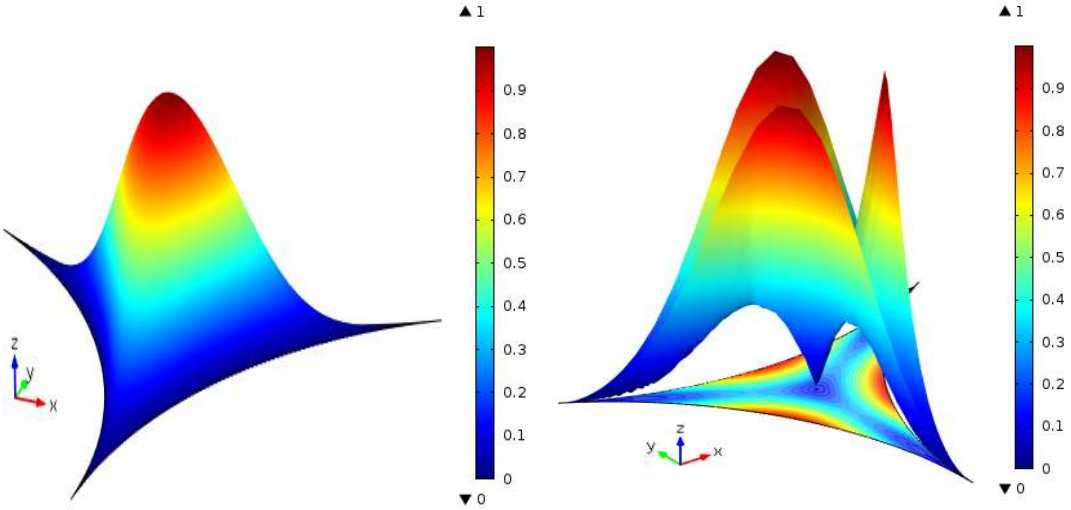

(e) 3-Cused

Fig. 5.3 The contours of non-dimensional velocity and shear stress profiles in regular non-circular geometries

Table 5.1 Comparison of the friction factor (fRe) and average Nusselt number ($\overline{Nu}$)

Geometry	*Present Study*			*Shah & London,1971*			*%Deviation*		
	fRe	$\overline{Nu}_{H1}$	$\overline{Nu}_{H2}$	fRe	$\overline{Nu}_{H1}$	$\overline{Nu}_{H2}$	fRe	$\overline{Nu}_{H1}$	$\overline{Nu}_{H2}$
Circular	16.000	4.364	4.364	16.000	4.364	4.364	0.00	0.00	0.00
Square	14.223	3.608	3.090	14.227	3.607	3.091	0.03	0.03	0.03
Triangular	13.333	3.111	1.889	13.333	3.102	1.892	0.00	0.29	0.16
3-Cusped	6.502	1.189	0.200	6.503	-	-	0.02	-	-
4-Cusped	6.605	1.354	0.380	6.605	-	-	0.00	-	-

5.5 Results and Discussion

Fully developed steady-state laminar flow and heat transfer characteristics in a constant cross-section of non-circular sub-channel geometries (Fig. 5.1) of rod bundles are considered in the analysis. The effect of bundle size on the fluid flow in a square pitched rod bundle for different p/d and W/d ratios are studied and discussed in this section.

In the fully developed laminar flow region of circular and non-circular tubes, the velocity profile does not change along the longitudinal direction. The longitudinal velocities are varying across the tube cross-section and there is no existence of cross-flow velocities in the fully developed laminar flow regime. In case of fully developed turbulent flow, the secondary velocities are induced in non-circular geometry and it remains unchanged in a longitudinal direction. Hence, the fully developed flow in circular and non-circular geometries are modeled in a two-dimensional plane across the tube cross-section and solving for the axial velocity in out-of-plane direction. The similar approach is used for analyzing the non-circular geometries of the nuclear fuel bundle. The characteristics of fully developed laminar flow and heat transfer in a large size of bare rod bundles are analysed easily using a two dimensional model. Hence, this justifies the use of two-dimensional models against a three-dimensional model which gives the same results with reasonably less computational efforts.

5.5.1 Analysis of sub-channel geometry

The developed computational model is used for the flow analysis of square and triangular pitched rod bundle sub-channels as well as the sub-channel shaped tubes for different p/d ratios. The numerical prediction of fRe and average Nusselt number $\overline{Nu}$ of square and triangular sub-channel for different p/d ratios varying from 1 to 2 are carried out and the results are given in Table 5.2. A reasonable comparison of the data obtained in the present study against the data available in the literature (Meyder, 1975; Rehme, 1971). With these comparison studies, the analyses are extended for the rod bundle sub-channel geometries. The parametric study of different p/d ratio on flow through square and triangular shaped sub-channel, as well as the sub-channel shaped tubes, are carried out and the trends of fRe with p/d is shown in Fig. 5.4 and Fig. 5.5.

Table 5.2 The effect of p/d ratio on Poiseuille Number (fRe) and average Nusselt number ($\overline{Nu}$)

ψ	Square Pitched Sub-channel					Triangular Pitched Sub-channel				
	Present			Meyder	Rehme	Present			Meyder	Rehme
p/d	fRe	$\overline{Nu}_{H1}$	$\overline{Nu}_{H2}$	fRe	fRe	fRe	$\overline{Nu}_{H1}$	$\overline{Nu}_{H2}$	fRe	fRe
1.0	6.61	1.354	0.380	-	-	6.502	1.189	0.200	-	-
1.1	14.69	2.846	1.686	14.65	14.75	20.36	4.557	2.936	20.925	20.80
1.2	20.26	4.599	3.684	20.25	20.25	24.92	7.436	6.905	25.000	25.25
1.3	24.17	6.377	5.819	-	-	27.39	9.164	9.041	27.500	27.50
1.4	27.19	8.007	7.705	-	-	29.28	10.32	10.29	-	-
1.5	29.73	9.448	9.289	29.75	30.00	30.98	11.24	11.23	31.250	30.50
2.0	40.29	15.06	15.05	-	-	39.31	15.27	15.27	-	-

It is clear that when the p/d ratio is 1.0, the sub-channel shaped tube and sub-channel approaches the same cusped geometry. The flow characteristics such as the velocity distribution and the shear stress distribution on the wall are the same for both the

geometries. As the p/d ratio increases greater than 1.0 the gap between the pins increases and the corresponding change in the flow velocity distribution in the sub-channel shaped tube with the corresponding increase in the wall shear stress and hence, the sharp increase in fRe (Fig.5.4). As p/d ratio increases more than 1.15 the wall shear stress contribution in the pin gap are increases and the contribution from the fuel pin wall decreases which causes a slight reduction in the fRe value. However, as p/d ratio approaches infinity, the geometry becomes the regular triangular and square channel and the corresponding fRe also approaches the value of triangular and square geometry. The fRe increases significantly from 6.5 to 24 for p/d ratio of 1 to 1.15 and then increases almost linearly with p/d ratio for the sub-channel shaped geometry (Fig.5.5). In the case of the sub-channel shaped duct of the same p/d ratio, the fRe increases sharply up to p/d ratio of 1.15

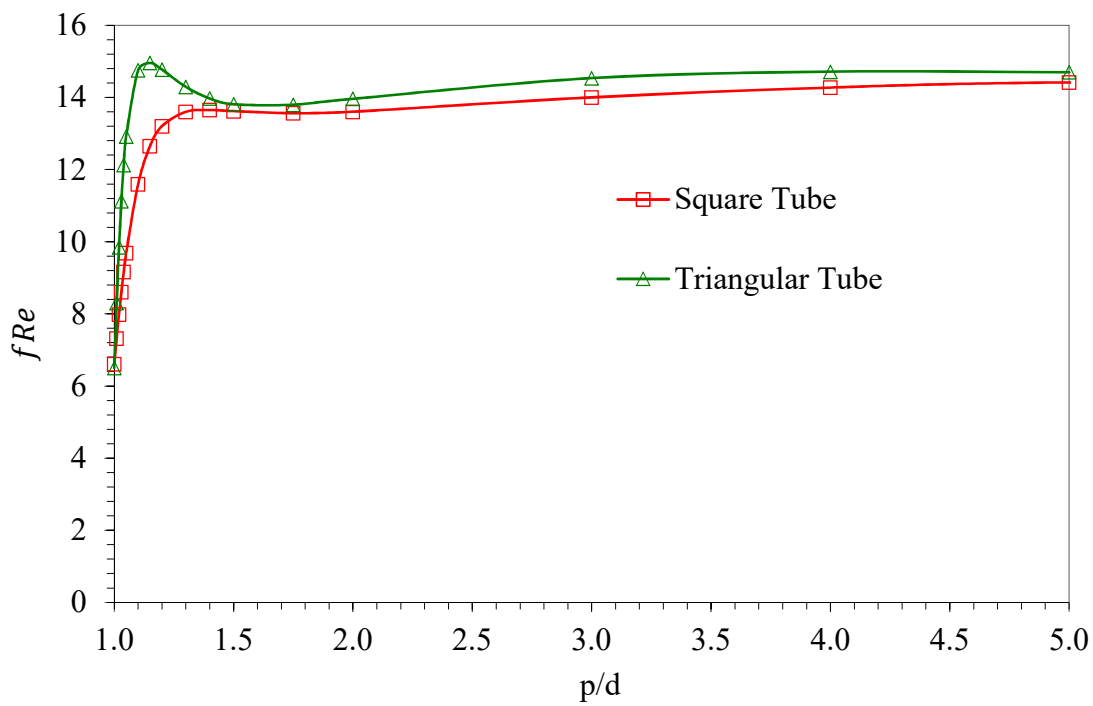

Fig. 5.4 Effect of p/d on fRe in square and triangular sub-channel shaped tube

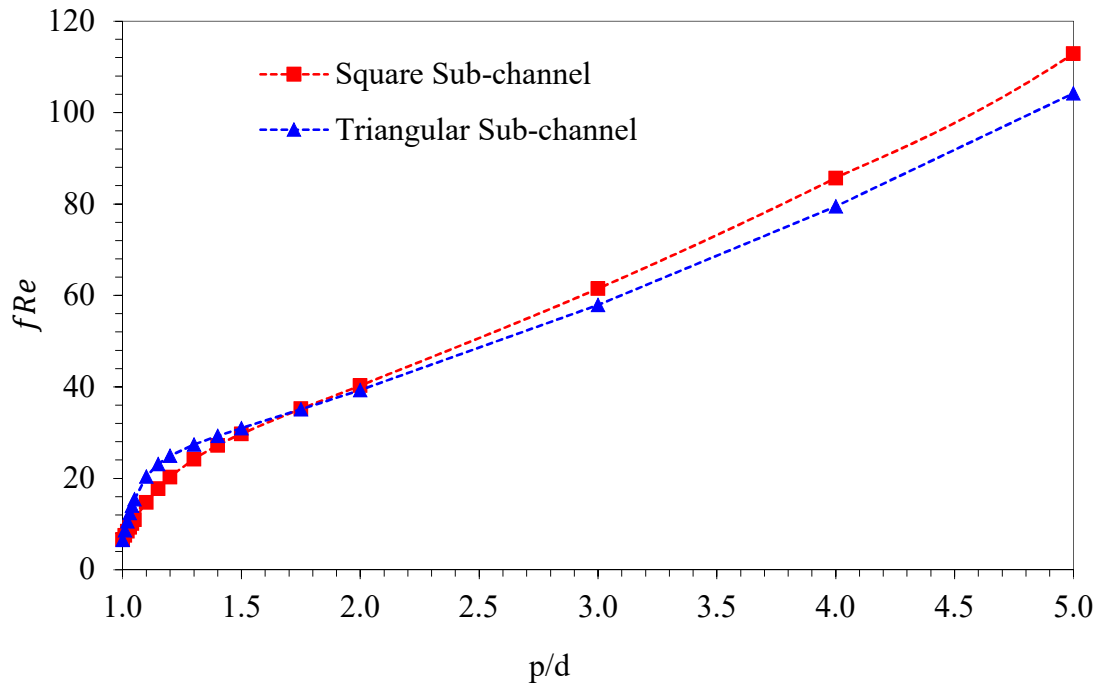

Fig. 5.5 Effect of p/d on fRe in square and triangular sub-channel

and then started decreasing slightly till the p/d of 1.5 and then relatively remains same and asymptotically approach the square and triangular tube value for the p/d ratio of infinity (Fig. 5.4).

Average Nusselt number for the H1 and H2 boundary conditions for square and triangular pitched sub-channel and sub-channel shaped ducts with different p/d ratio is evaluated. Figures. 5.6 to Fig. 5.9 depicts the Nusselt variation with p/d for sub-channel and sub-channel shaped tube respectively. It is observed that for p/d >1.5 for square pitched and p/d >1.3 for triangular pitched sub-channel, $\overline{Nu}_{\mathrm{H1}}$ and $\overline{Nu}_{\mathrm{H2}}$ are almost same and at lower p/d ratios, $\overline{Nu}_{\mathrm{H1}}$ is greater than $\overline{Nu}_{\mathrm{H2}}$ as depicted in Fig. 5.6 and Fig. 5.7. As the p/d ratio increases, the gap between pins increases causing the velocity and temperature profiles more uniform in the sub-channel in circumferential direction of pins. As a result, the average Nusselt number approaches to the same value for both boundary conditions. For the cusped channel (p/d=1), $\overline{Nu}$ is almost same for both

square and triangular sub-channels. In contrast to the rod bundle sub-channel, it is found that at higher p/d ratios greater than 1.5, the average $\overline{Nu}$ for square and triangular sub-channel shaped ducts remains constant and asymptotically approaches the square and triangular tube solutions (Fig. 5.8 and Fig 5.9). The three-dimensional contours of the non-dimensional velocity (u/u_{avg}) and shear stress (τ/τ_{wavg}) profiles in square and triangular sub-channel for p/d ratio of 1.1 are shown in Fig. 10 and Fig. 11. It is clearly seen that; the non-uniform wall shear stress profiles are present in the non-circular duct. The analysis also carried out for the 4 pin square pitched and 7 pin triangular pitched bundles and the corresponding non-dimensional velocity and shear stress profiles are shown in Fig. 5.12 (a and b). These figures also clearly indicate the nonlinear shear stress distribution on the wall in the non-circular geometries.

In the case of fuel bundle geometries, apart from the inner sub-channel which is described by p/d ratio, there is a wall and corner sub-channel. In addition to the p/d ratio, the wall channels are characterized by the W/d ratio. The study on the effect of p/d ratio and W/d ratio on the sub-channel flow distribution is carried out for 4 pin square and 7 pin hexagonal bundles. The effect of p/d and W/d ratio on velocity in hexagonal and square bundles is depicted in Fig. 5.13 and Fig. 5.14. It is clear from these figures that the W/d ratio significantly influences the flow characteristics in these bundle configurations. At lower p/d ratios the sub-channels are in isolated condition and as the p/d increases the strong interaction between the sub-channels takes place. Hence, these analyses show that there is an optimum W/d ratio for the given p/d ratio such that the average flow between the sub-channel is more or less same.

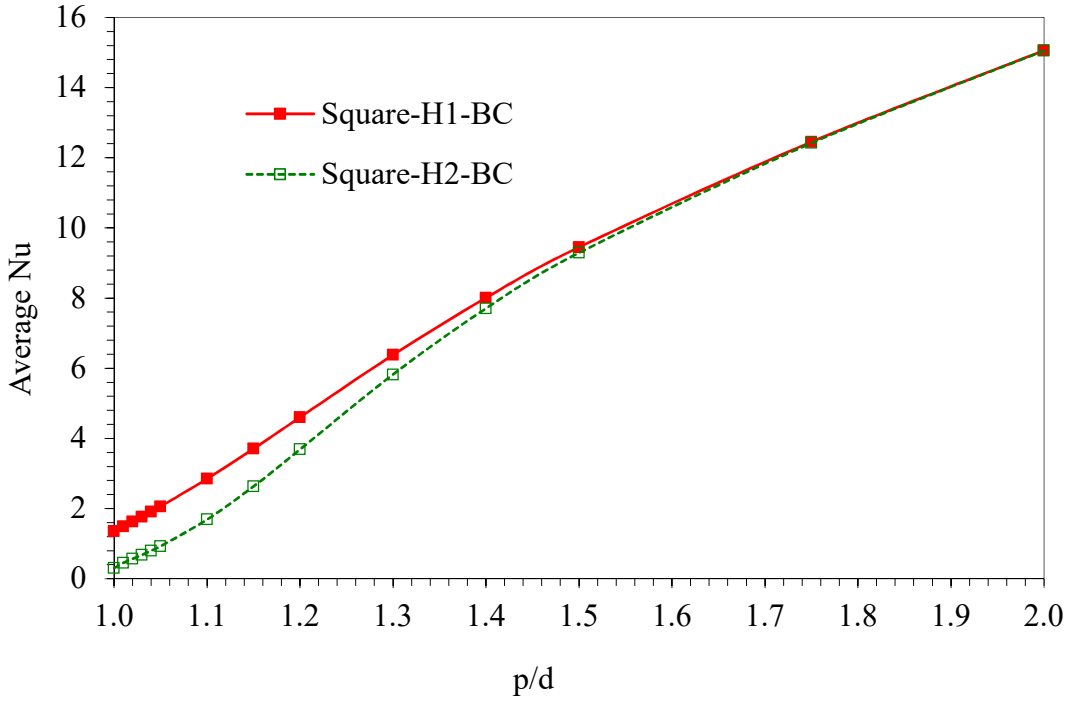

Fig. 5.6 Average Nusselt number for H1 and H2 boundary conditions of square pitched sub-channel

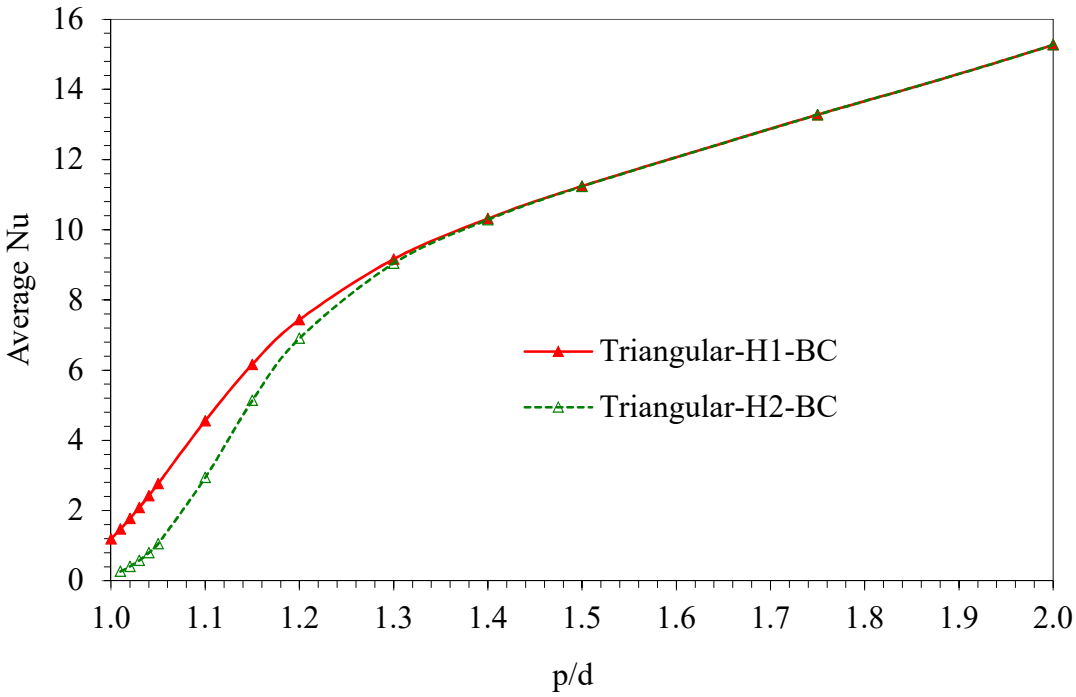

Fig. 5.7 Average Nusselt number for H1 and H2 boundary conditions of triangular pitched sub-channel

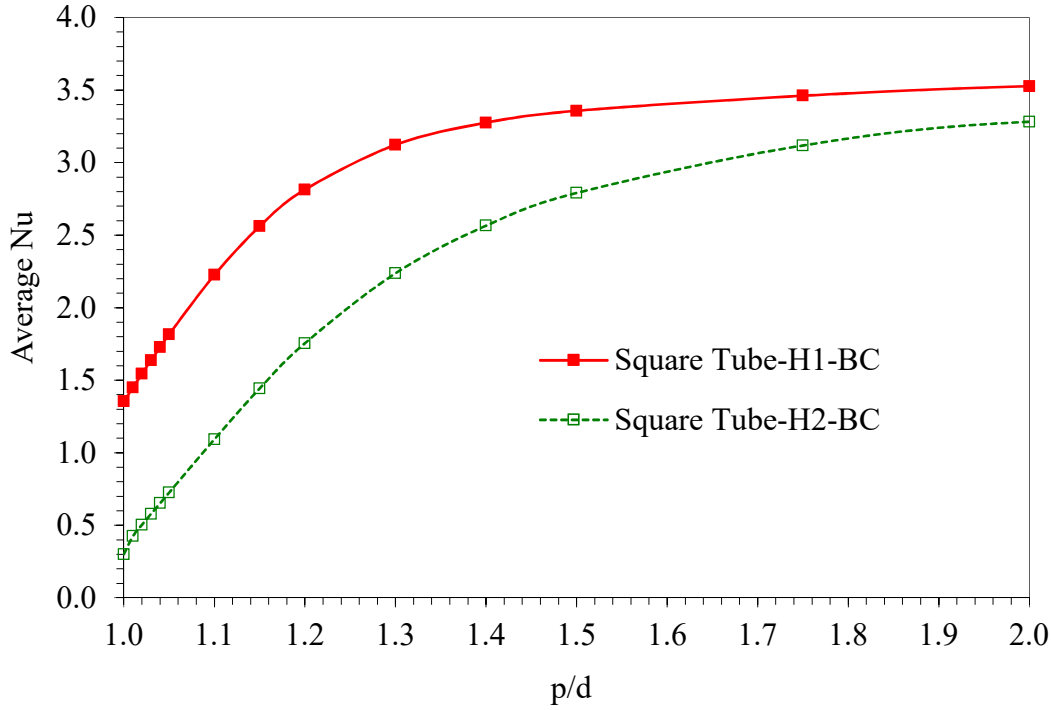

Fig. 5.8 Average Nusselt number for H1 and H2 boundary conditions of Square pitched sub-channel shaped tube

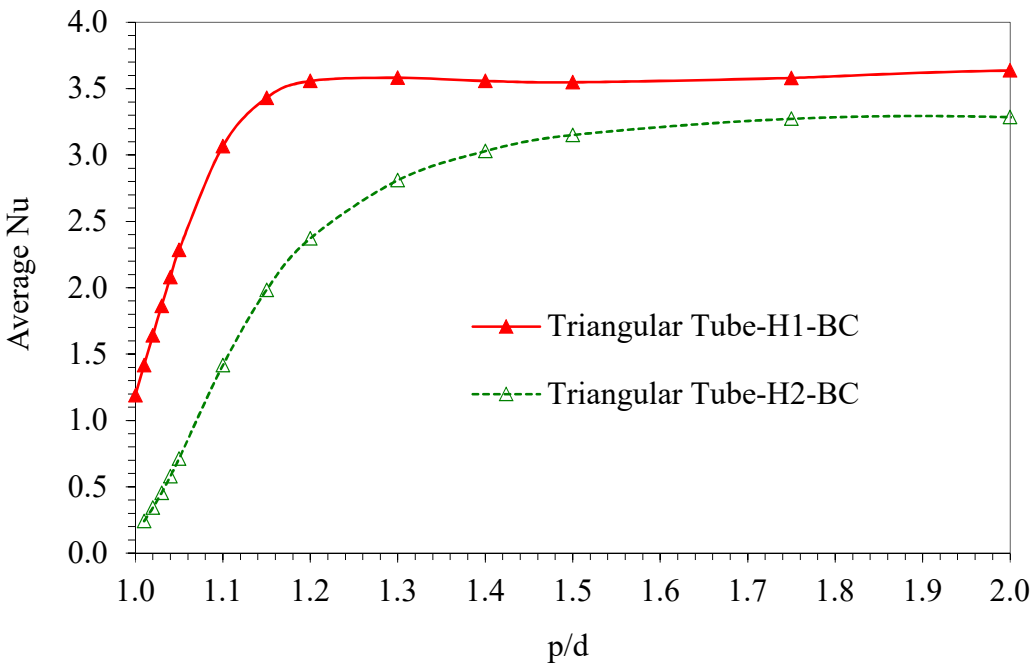

Fig. 5.9 Average Nusselt number for H1 and H2 boundary conditions of triangular pitched sub-channel shaped tube

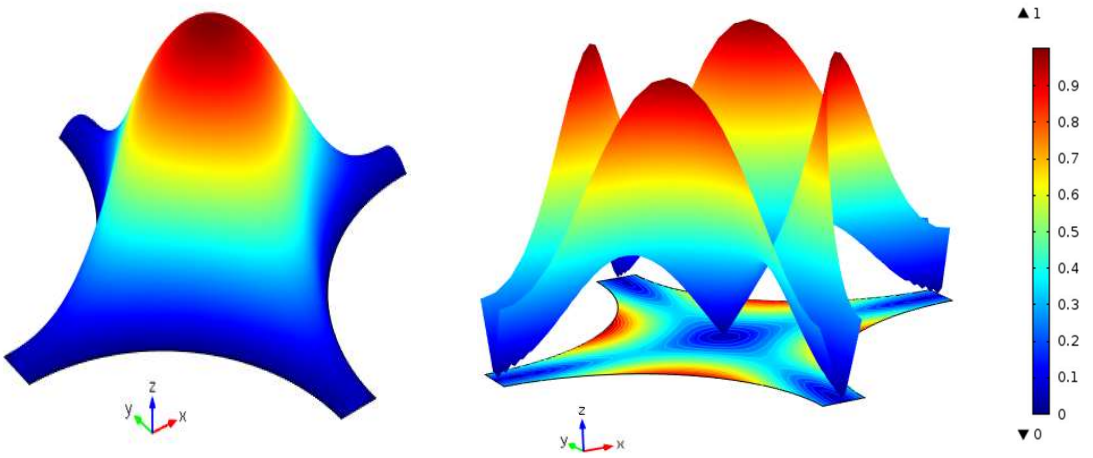

Fig. 5.10 Non-dimensional velocity and shear stress in interior square pitched sub-channel

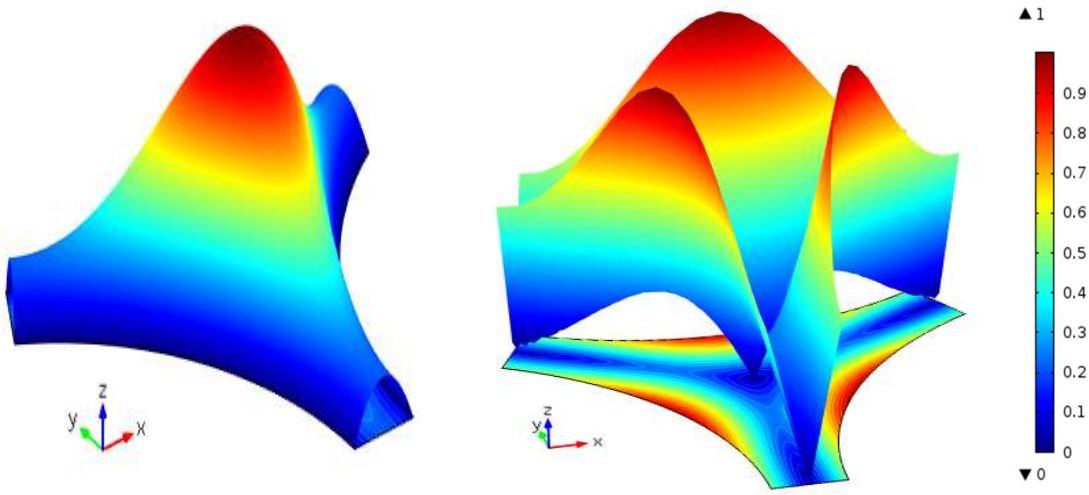

Fig. 5.11 Non-dimensional velocity and shear stress in interior triangular sub-channel

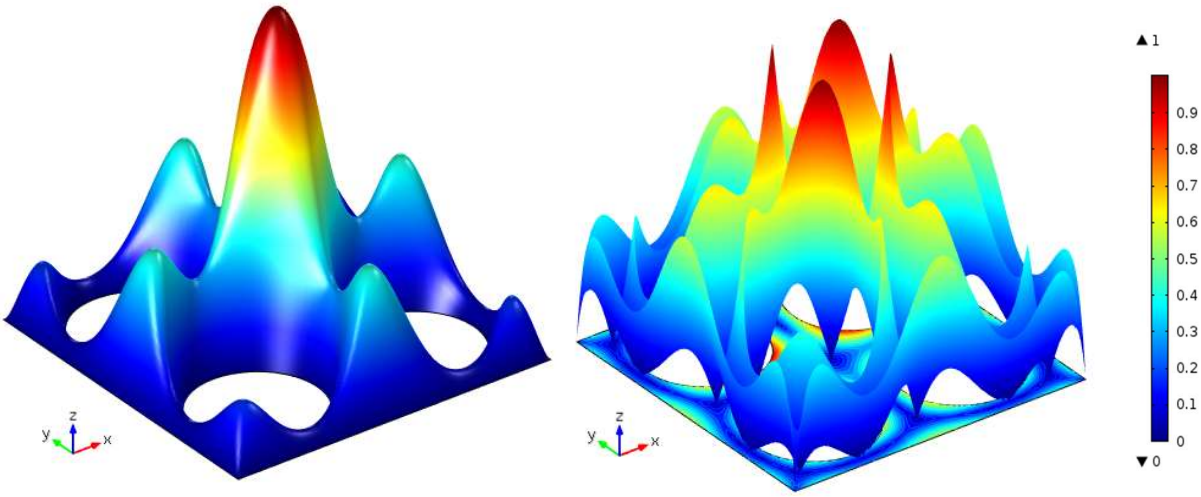

a) Square pitched 4 pin bundle

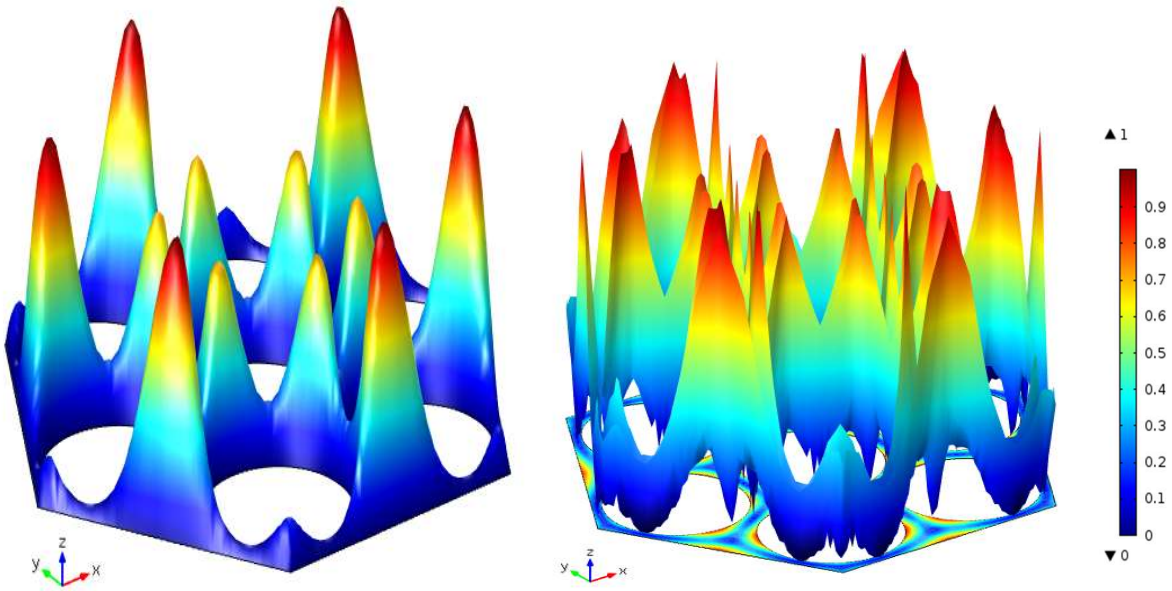

b) triangular pitched 7 pin bundle

Fig. 5.12 Non-dimensional velocity and shear stress in a) Square pitched 4 pin bundle b) triangular pitched 7 pin bundle

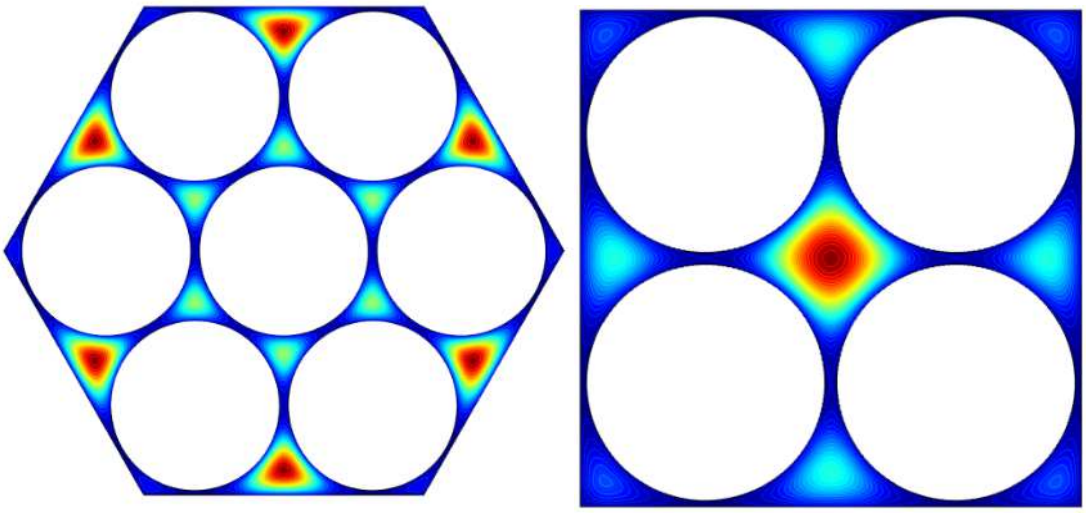

p/d = 1.05 and W/d = 1.025

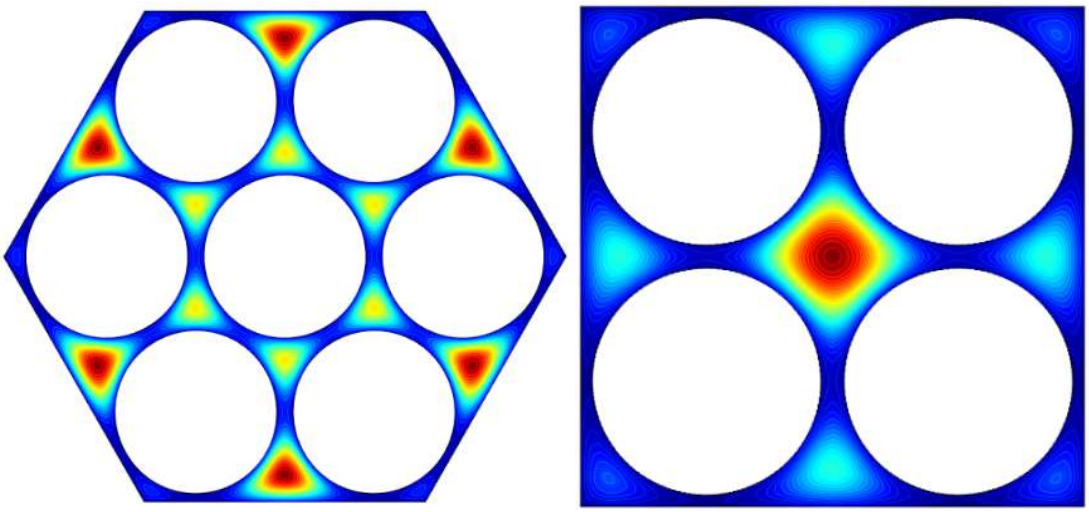

p/d = 1.1 and W/d = 1.05

Fig. 5.13 Effect of p/d and W/d ratio on non-dimensional velocity and shear stress in hexagonal and square bundle

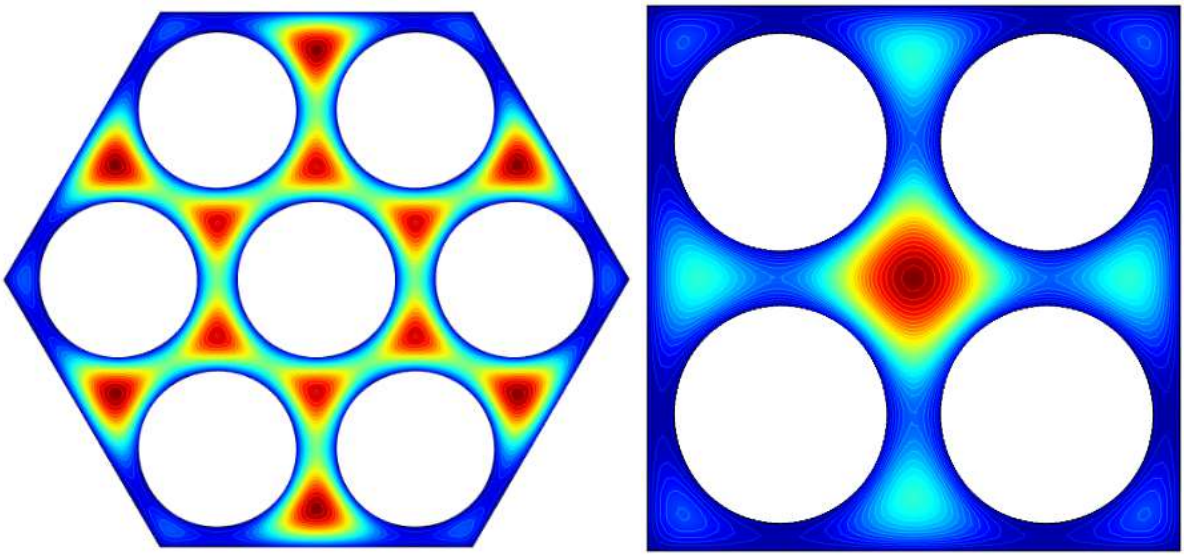

p/d = 1.25 and W/d = 1.125

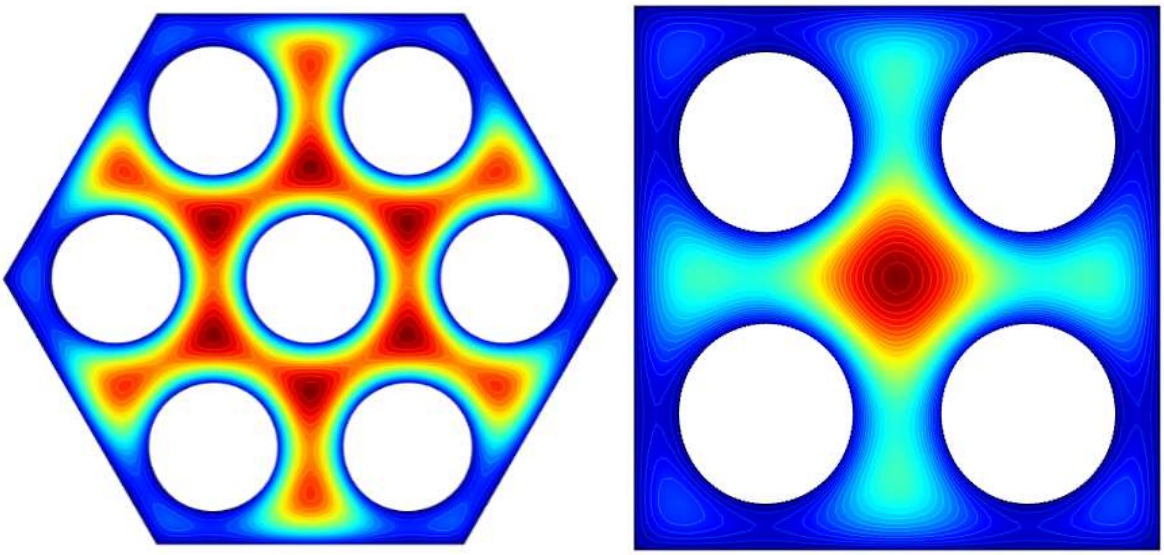

p/d = 1.5 and W/d = 1.25

Fig. 5.14 Effect of p/d and W/d ratio on non-dimensional velocity in hexagonal and square bundle

5.5.2 Correlations for Poiseuille number and average Nusselt number

In this section effect of p/d on the change in Poiseuille number (fRe) and the average Nusselt number $\overline{Nu}_{H1}$ and $\overline{Nu}_{H2}$ for the square pitched and triangular pitched sub-channels are presented in the form of the correlations. Based on the trends exhibited in the data, the following correlations are obtained by least square fitting of the numerical data.

The numerical data of fRe and the average Nusselt number correlated for triangular pitched sub-channel are given below,

$$fRe = \frac{42.70\left(\frac{p}{d}\right) - 41.18}{\left(\frac{p}{d}\right) - 0.7981} \tag{5.1}$$

$$\overline{Nu}_{H1} = \frac{21.41\left(\frac{p}{d}\right) - 20.96}{\left(\frac{p}{d}\right) - 0.5345} \tag{5.2}$$

$$\overline{Nu}_{H2} = \frac{22.37\left(\frac{p}{d}\right) - 22.64}{\left(\frac{p}{d}\right) - 0.5419} \tag{5.3}$$

The numerical data of fRe and the average Nusselt number, correlated for square pitched sub-channel are given below,

$$fRe = \frac{59.34\left(\frac{p}{d}\right) - 55.13}{\left(\frac{p}{d}\right) - 0.3881} \tag{5.4}$$

$$\overline{Nu}_{H1} = \frac{52.08\left(\frac{p}{d}\right) - 48.97}{\left(\frac{p}{d}\right) + 1.644} \tag{5.5}$$

$$\overline{Nu}_{H2} = \frac{51.20\left(\frac{p}{d}\right) - 51.22}{\left(\frac{p}{d}\right) + 1.358} \tag{5.6}$$

The numerical data agree within ±5 % with the correlation for $1.02 < p/d \leq 2.0$.

Similarly, the numerical data of fRe and the average Nusselt number $\overline{Nu}$ for H1 and H2 boundary conditions for the square and triangular sub-channel shaped tubes are correlated for a range of p/d ratio for 1.02 to 2.0 and the coefficients of the eqn. 5.7 are given Table 5.3.

$$f\left(\frac{p}{d}\right) = a\left(\frac{p}{d}\right)^{b} + c \qquad \text{for } 1.02 < \mathrm{p}/d \leq 2.0 \tag{5.7}$$

The comparison of the literature data with the present correlation for $\overline{Nu}_{\mathrm{H1}}$ and $\overline{Nu}_{\mathrm{H2}}$ in triangular sub-channel for different p/d ratio is shown in Fig. 5.15 and Fig. 5.16. The parity plots of the numerical data with the developed correlations of Poiseuille number and average Nusselt number ($\overline{Nu}$) for two different H1 and H2 boundary conditions for the rod bundle sub-channel geometries are shown in Fig. 5.17 and Fig 5.18. These plots clearly highlight the goodness of the fits.

Table 5.3 Coefficients of least square fit of fRe, $\overline{Nu}_{\mathrm{H1}}$ and $\overline{Nu}_{\mathrm{H2}}$ data of Square and triangular pitched sub-channel shaped tube

Geometry	a	b	c	R^2
Coefficients of Poiseuille Number (fRe)				
SPT	-7.300	-12.750	13.720	0.9978
TPT	-8.096	-33.240	14.320	0.9736
Coefficients of average Nusselt number $\overline{Nu}_{\mathrm{H1}}$				
SPT	-2.283	-5.753	3.583	0.9987
TPT	-2.572	-14.330	3.636	0.9919
Coefficients of average Nusselt number $\overline{Nu}_{\mathrm{H2}}$				
SPT	-3.450	-3.123	3.722	0.9987
TPT	-3.464	-6.106	3.421	0.9951

SPT - Square Pitched Tube, TPT - Triangular Pitched Tube

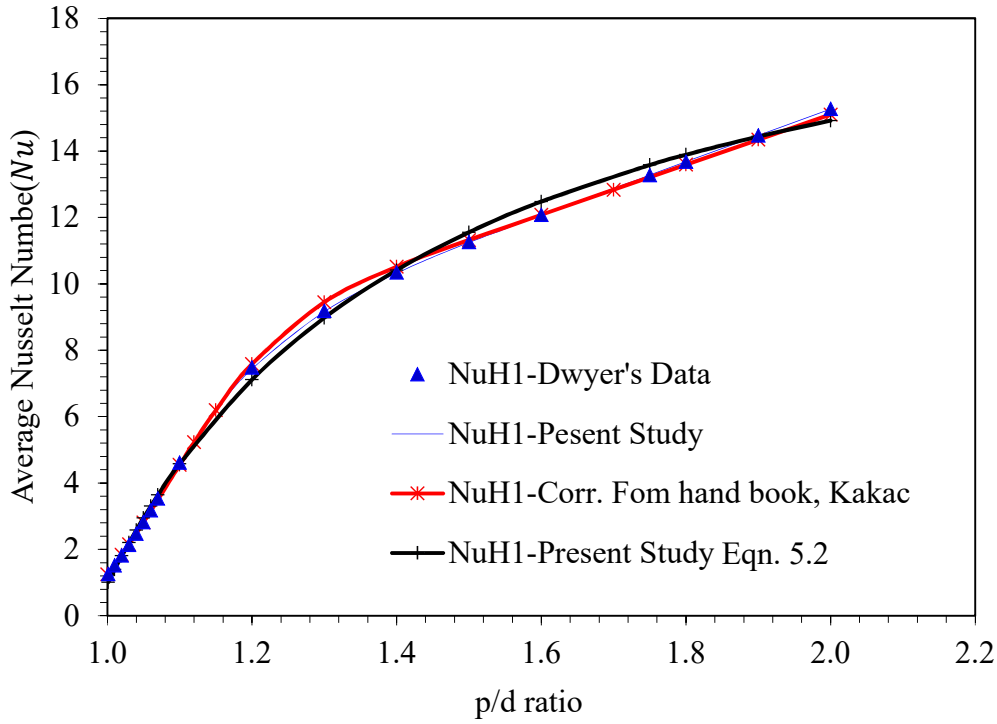

Fig. 5.15 Comparison of $\overline{Nu}_{\mathrm{H1}}$ with p/d for triangular pitched sub-channel

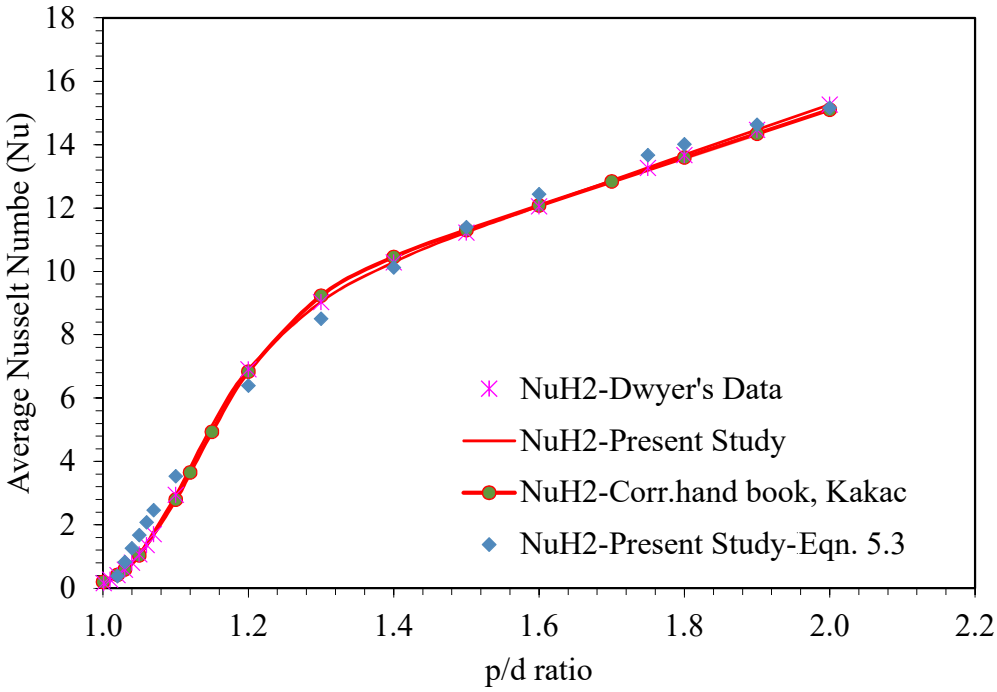

Fig. 5.16 Comparison of $\overline{Nu}_{\mathrm{H2}}$ with p/d for triangular pitched sub-channel

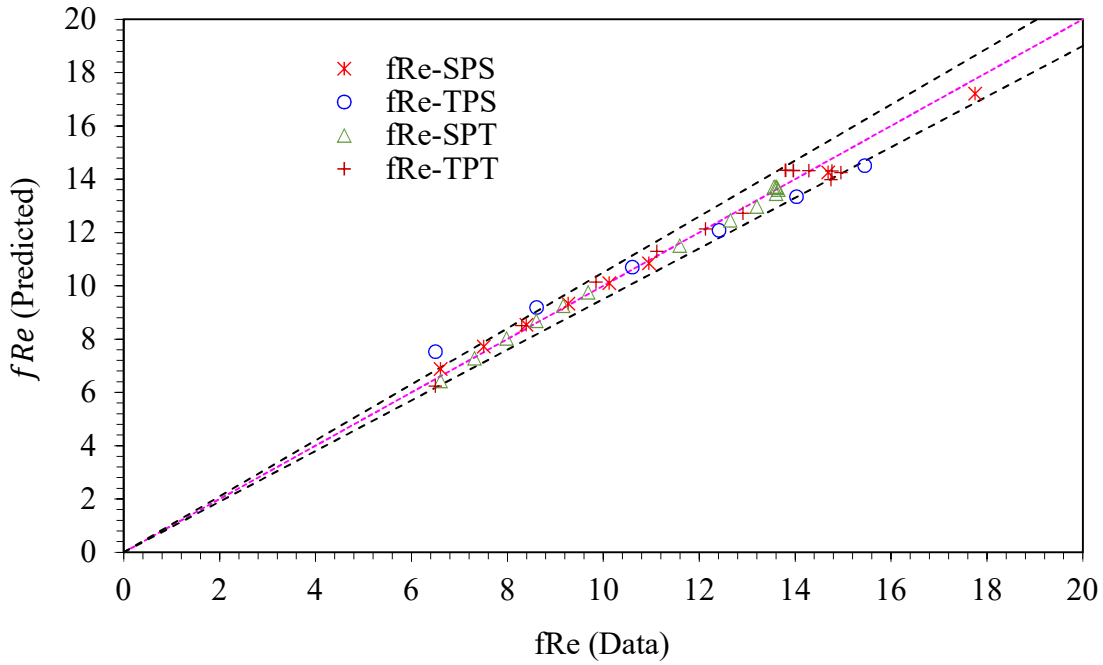

Fig. 5.17 Parity plot showing comparison of Poiseuille number (data) with Poiseuille number (predicted)

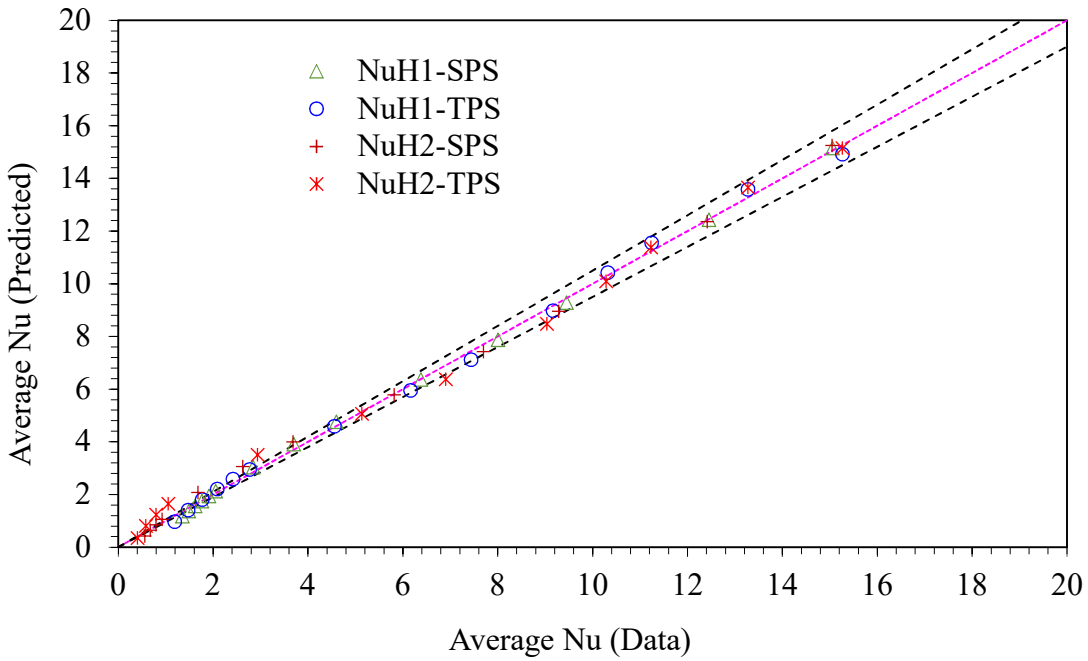

Fig. 5.18 Parity plot showing comparison of average Nusselt number (data) with average Nusselt number (predicted)

5.6 Analysis of Fuel Bundle

The estimation of the Poiseuille number (fRe) and hence, the frictional pressure drop in a 7 pin hexagonal bundle and 4 pin square pitched fuel bundles are carried out on a 2-D model. To validate the mathematical model, the present data are compared with the rod bundle tests carried out by Gunn and Darling (1963) for a 4 pin and 9 pin square pitched models. In the 4 pin model for 'p/d' ratio of 1.31 and W/d ratio of 1.157, fRe is found to be 15.09 and in 9 pin bundle of p/d ratio of 1.439 and W/d ratio of 1.495, fRe is found to be 25.19. It can be seen that the numerical predictions of fRe with experimental data compare well within the maximum deviation of 1%. After validation of the model with experimental data for rod bundles, the simulations are extended to predict the characteristics of the flow in the various sizes of the bundle. The effect of W/d on frictional pressure drop on the hexagonal and square pitched bundle for different p/d ratios are analysed. The pitch to diameter ratio is varied from 1.0 to 2.0 and the W/d ratio is varied from 1.05 to 1.4. The variation of fRe of triangular pitched 7 pin bundles for different p/d and W/d ratio is depicted in Fig. 5.19. It is observed from the figure that for a given W/d ratio, fRe increases as the p/d ratio increases and reaches a maximum and then starts decreases up to a p/d ratio of 2.0. The similar trend is observed at different W/d ratio. The maximum fRe occurs at a p/d ratio more or less equal to W/d ratio. As the W/d ratio increases more than 1.15, the change in the fRe for the p/d of 1.05 to 1.2 is very small and slightly decreases as the W/d ratio is further increased from 1.15 to 1.4. A similar analysis is carried out for the square pitched 4 pin fuel bundle. The variation of the fRe for different p/d and W/d ratio is shown in Fig. 5.20. In case of the square pitched fuel bundle also, the trend line is more or less similar to the triangular pitched bundle. However, the value of fRe is small as compared to the

triangular pitched bundle. In square pitched pin bundle also, initially, fRe increases with an increase in p/d and then starts decreasing. The frictional pressure drop increases for a given p/d with increases in the W/d ratio. When the W/d is increased more than 1.15, the change in the fRe of the square pitched pin bundle is insignificant between the p/d ratios of 1.0 to 1.2 similar to the case of triangular pitched seven pin bundle.

The analyses are also carried out to investigate the influence of p/d and W/d on fRe for different size of the fuel bundle. The p/d ratio is varied from 1 to 2 for three different W/d ratios of 1.05, 1.15 and 1.3. The variation of fRe with p/d for W/d=1.05 is depicted in Fig. 5.21. It can be seen that as the size of the bundle increases, the fRe also increases. For the smaller size of the bundle, it reaches a maximum value and then decreases with increase in p/d ratio. It is also seen that when the p/d ratio equals to W/d ratio, the change in the fRe is very small and more or less same for all sizes of the bundle. The effect of the change in fRe with p/d ratio, bundle size is also studied for two more W/d ratios of 1.15 and 1.30. The variation of fRe with p/d for two different W/d ratios of 1.15 and 1.3 are depicted in Fig. 5.22 and 5.23 respectively. In this case also when the p/d ratio close to the W/d ratio, the effect of bundle size vanishes and the value of fRe is equal for all sizes of the bundle. The change in fRe is of the order of 5% with change in the bundle size from 2x2 to 10x10 for a p/d and W/d ratio of 1.15 and 1.30 (Fig. 5.24). These results show that, as the bundle size increases for a given p/d and W/d ratios, fRe remains more or less same irrespective of the size of the bundle. The analysis of the influence of the bundle size on fRe also reveals that for all the p/d ratios less than W/d ratio, the value of fRe, is observed be insignificant and almost same for all bundles of size greater than 5x5. As the p/d ratio increases more than the W/d ratio, the bundle effect is significant on fRe and these are clearly observed in Figs. 5.21-23.

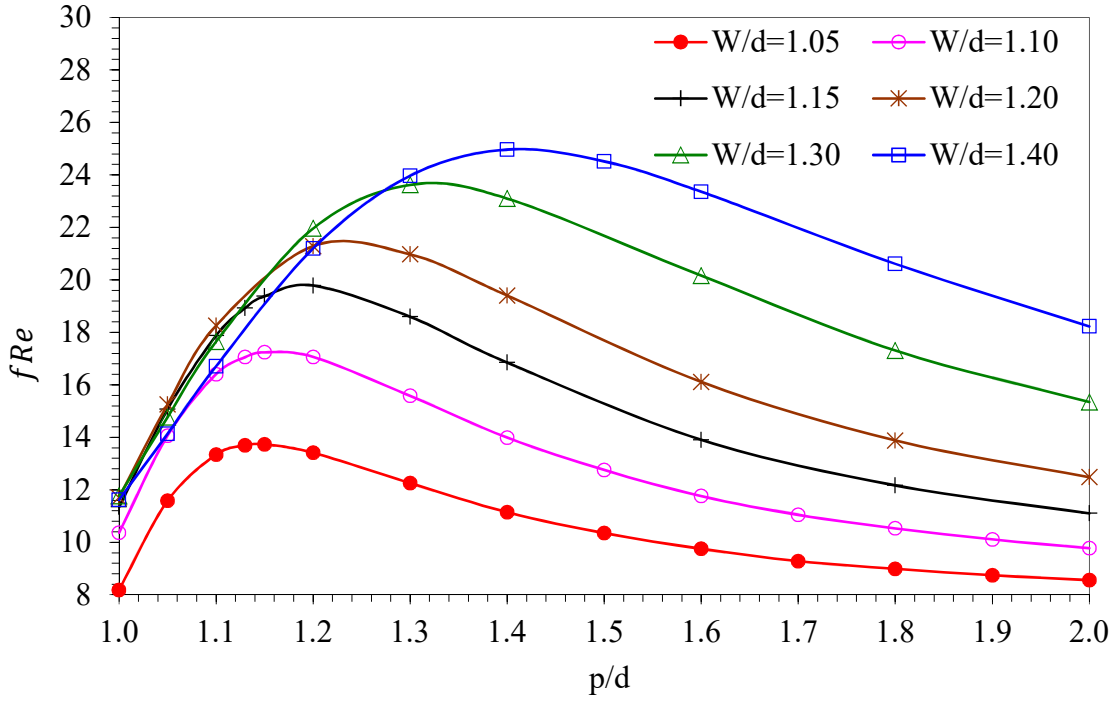

Fig. 5.19 Variation of fRe of triangular pitched 7 pin bundles for different p/d and W/d ratio

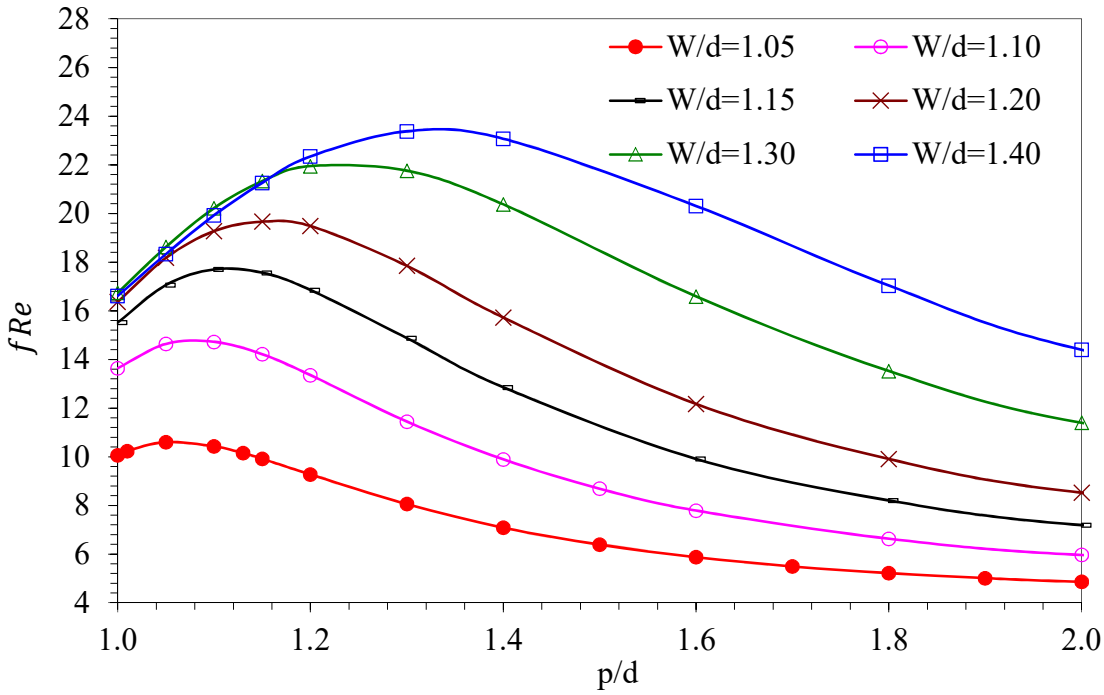

Fig. 5.20 Variation of fRe of square pitched 4 pin bundles for different p/d and W/d ratio

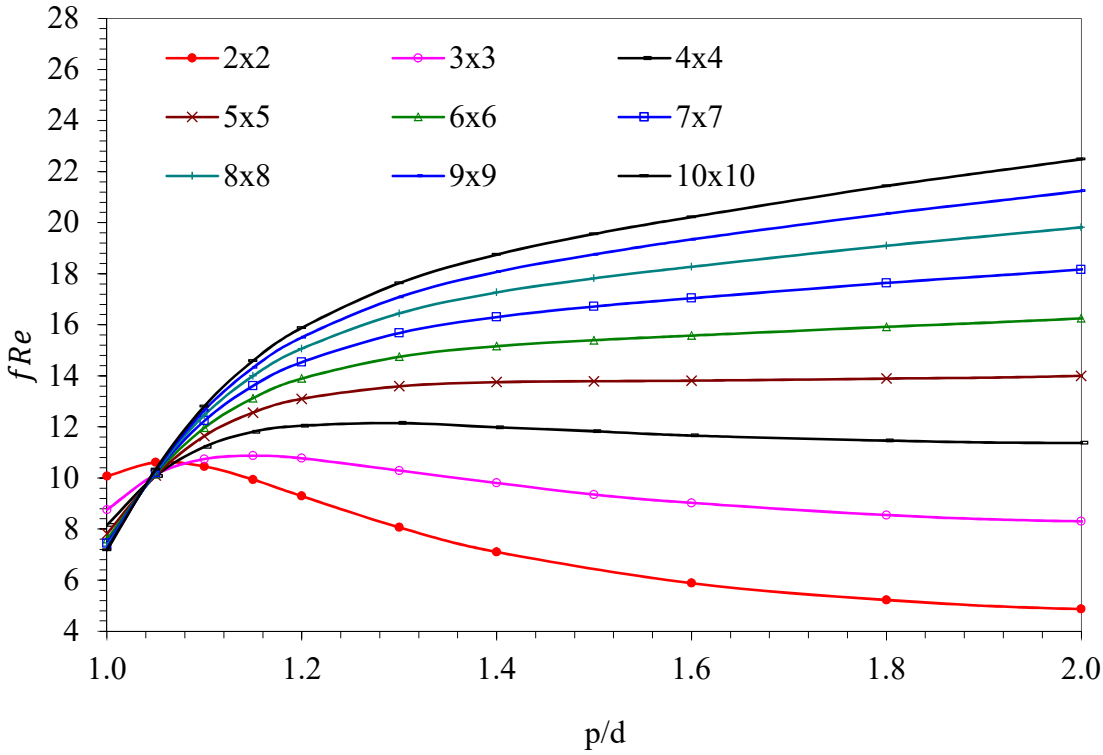

Fig. 5.21 The effect of different size of fuel bundle on fRe at different p/d ratios and W/d ratio of 1.05

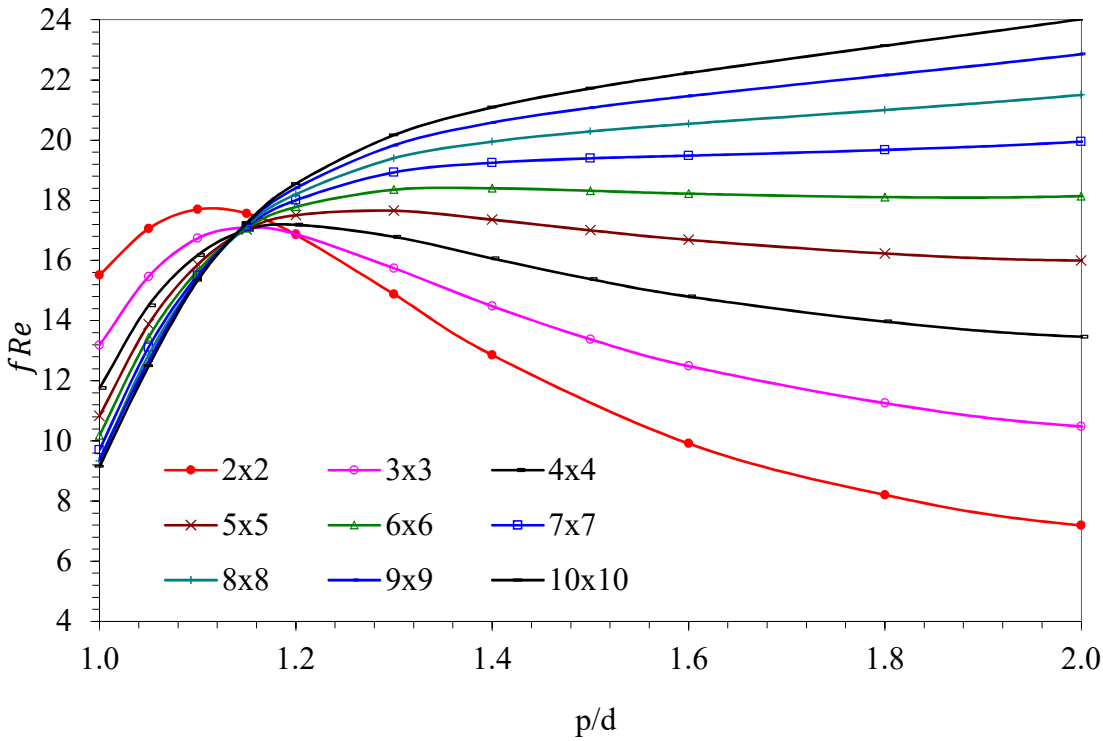

Fig. 5.22 Effect of different size of fuel bundle on fRe at different p/d ratios and W/d ratio of 1.15.

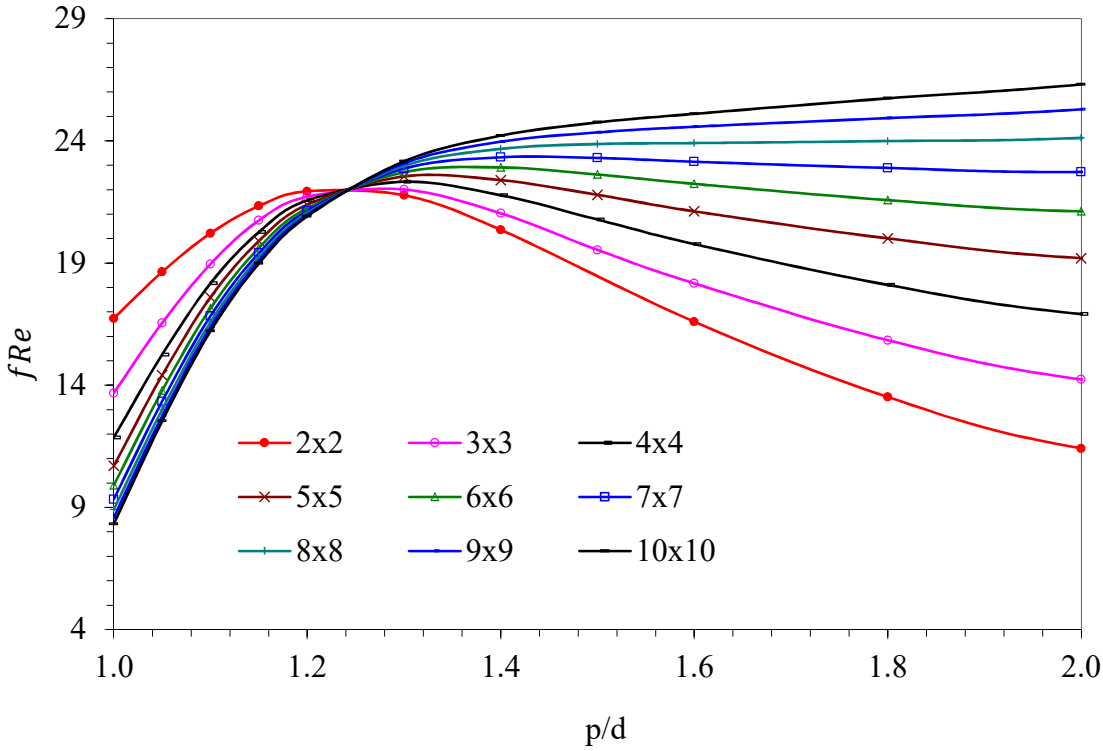

Fig. 5.23 Effect of different size of fuel bundle on fRe at different p/d ratios and W/d ratio of 1.3

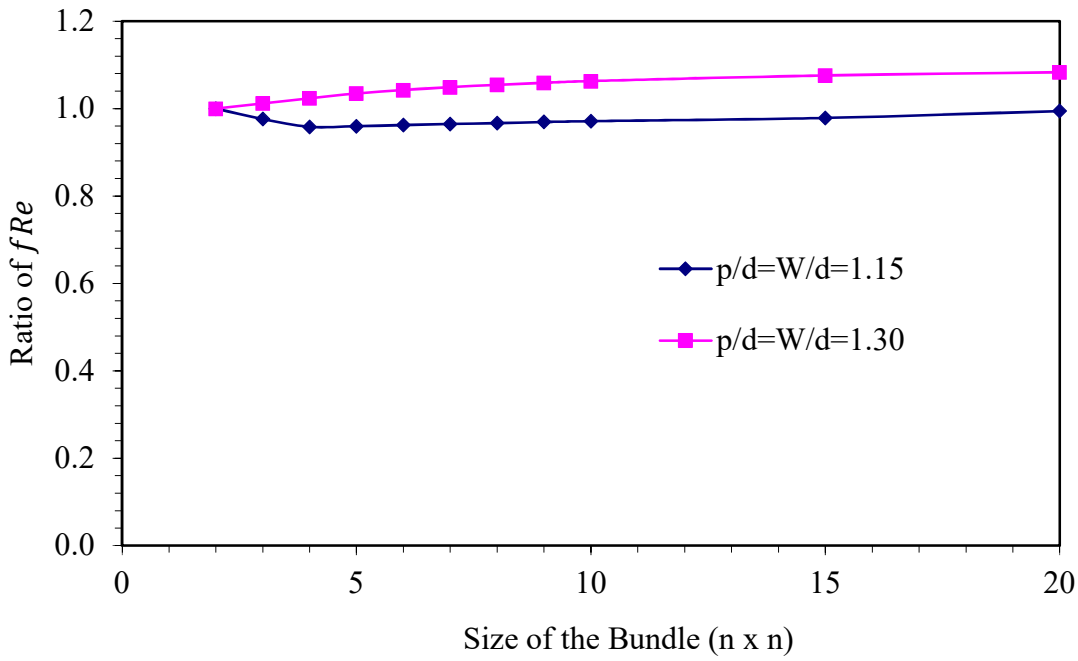

Fig. 5.24 Effect of bundle size on fRe for an equal p/d and W/d ratios of 1.15 and 1.30 (ratio with reference to 4 pin bundle)

5.7 Turbulent Flow and Heat Transfer in Sub-Channel Geometries

CFD analysis of turbulent fluid flow in a circular, square, triangular, non-circular sub-channel geometries are carried out using a 3-D model of a duct for the estimation of velocity and temperature fields. The turbulent flow calculations were carried out for different Reynolds numbers ranging from $2x10^4$ to $1x10^5$. The Sensitivity of two different turbulence models such as k-ε and Reynolds stress model were considered as turbulent closure model. It is found that RSM model predicts better secondary flow characteristics as compared to other model. Figure-5.25 shows the non-dimensionalised contours of velocity in different non-circular channels with secondary velocity vectors.

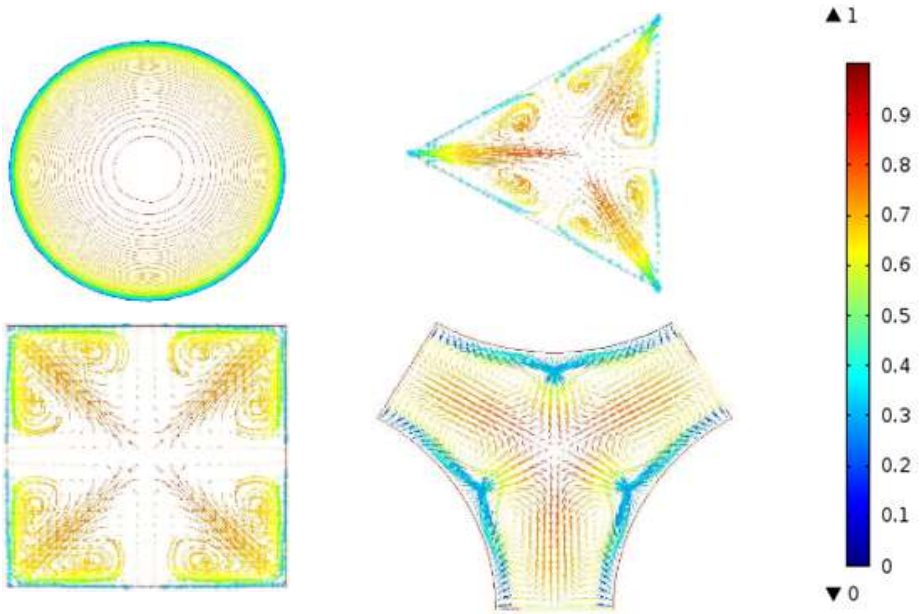

Fig. 5.25 The non-dimensionalised velocity in different non-circular channels with secondary velocity vectors.

From the wall shear stress, the frictional pressure drop is estimated for both the turbulent models. After the validation of the computational model with the regular geometries, the calculation of frictional pressure drop in a square and triangular pitched central sub-channel having a p/d ratio of 1.25 is carried out for different Reynolds number. The friction factor is estimated based on the frictional pressure drop and the average velocity

of the sub-channel and compared with the Blasius correlation. Fig. 5.25 shows the estimated friction factor for square and triangular pitched sub-channel for different Reynolds number.

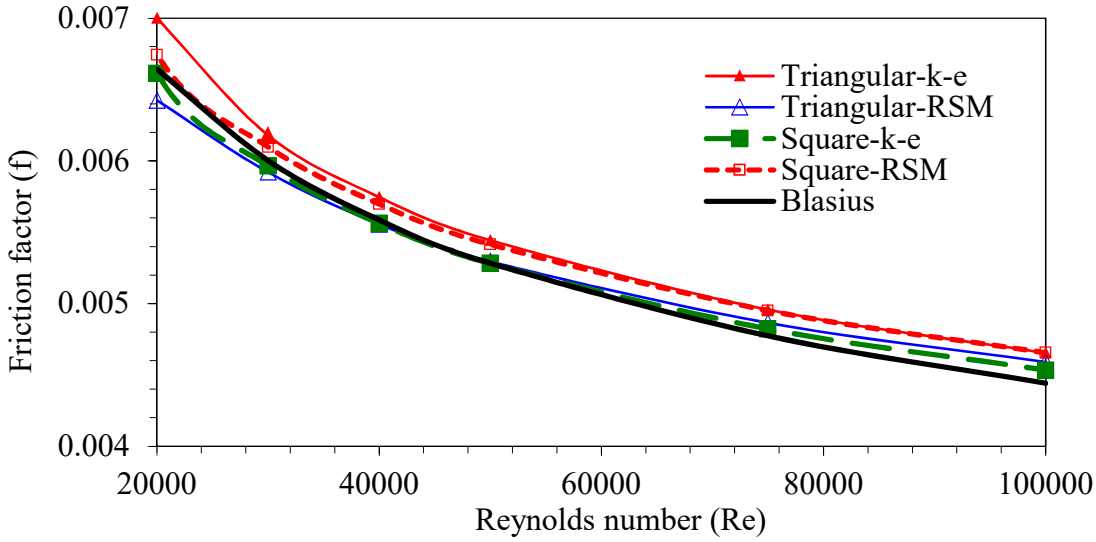

Fig. 5.26 Friction factor of square and triangular sub-channel at different Reynolds number with Blasius correlation for p/d =1.25.

Similar to the geometry factor fRe which is a constant for laminar flow for a given geometry, Rehme (1973) has proposed the geometry factor for turbulent flow (G) based on the Prandtl's velocity defect law. The geometry factor (G) is defined based on the three velocities i.e average, (U_{avg}), maximum (U_{max}) and friction velocity (U^*).

$$G = \frac{U_{max} - U_{avg}}{U^*} \qquad 5.1$$

Where,

$$U^* = \sqrt{\tau_w/\rho} \qquad 5.2$$

$$G = \frac{U_{max} - U_{avg}}{\sqrt{\frac{\tau_w}{\rho}}} \qquad 5.3$$

The variation of velocity ratio U_{avg}/U_{max} for a square and triangular pitched sub-channel geometry for a p/d ratio of 1.25 at different Reynolds number is given in Fig. 5.27. It is observed that, for both the geometry, the estimated velocity ratio based on RSM model is lower than that of k-ε model due to the secondary velocity. The friction velocity is also estimated based on the computed pressure drop. The variation of turbulent geometry factor for a square and triangular pitched sub-channel is shown in Fig. 5.28. It is observed that the geometry factor for turbulent flow is also comes out to be constant and is weak function of Re (Refer Fig.5.28).

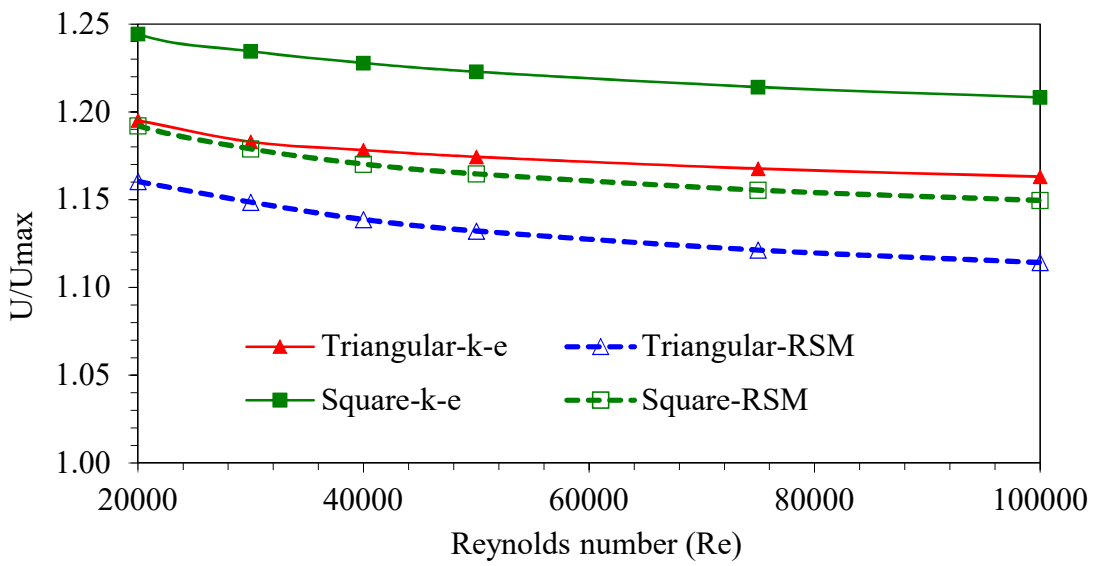

Fig. 5.27 the variation of velocity ratio U_{avg}/U_{max} for square and triangular pitched sub-channel having p/d ratio of 1.25 for different Reynolds number

The development of secondary velocity causes the increased mixing across the sub-channel and hence, the uniformity of velocity and temperature fields within the channel. The velocity fields obtained using two different turbulent models namely $k-\varepsilon$ and RSM for p/d = 1.25 and Re = $5x10^4$ are depicted in Fig. 5.29.

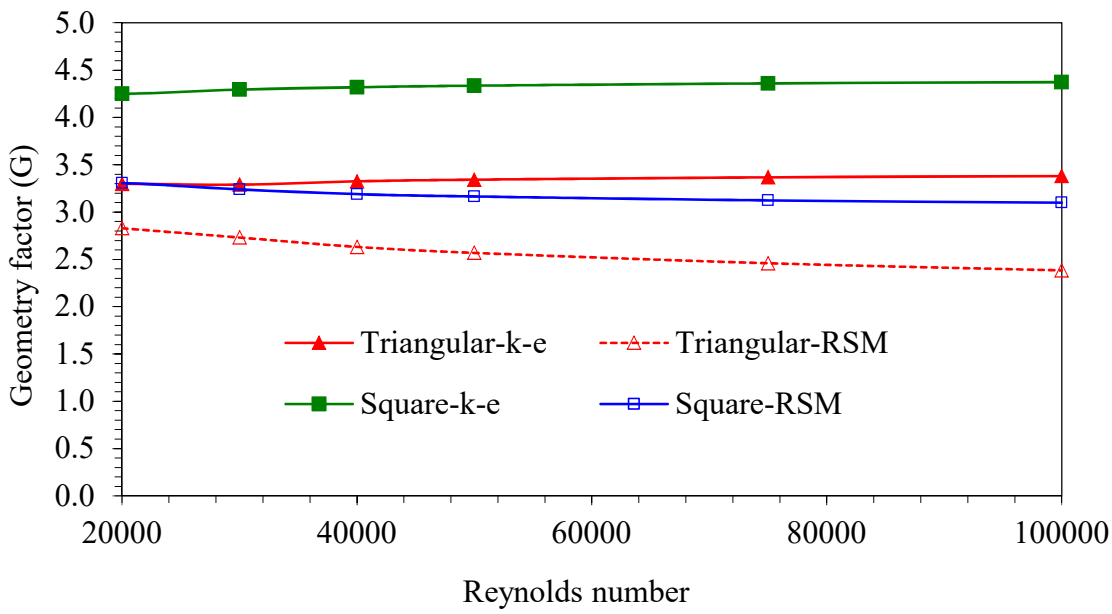

Fig. 5.28 Turbulent geometry (G) factor for square and triangular pitched sub-channel for p/d ratio of 1.25 for different Reynolds number.

The maximum velocity is observed to be 10.02 m/s in k-ε model as compared to 9.84 m/s in RSM model. The due to secondary velocity, the maximum velocity is less (1.8%) in RSM as compared to k-ε model. The effect of heat addition to different pins on the coolant temperature distribution is studied by applying uniform heat flux of 0.5 MW/m^2 on the fuel pin surface. The contours of isotherms at the outlet of a triangular sub-channel for different heat input to the channel is shown in Fig. 5.30. the average and maximum temperatures are observed to be different due to differences in the heat input to the channel. It is observed that, the non-uniform heating of pins in a sub-channel geometry causes the increase in fluid temperature near the gap region. In a sub-channel analysis, the average bulk temperatures which is used for the estimation of wall temperature which causes the under prediction of the fuel pin surface temperature as well as the energy exchange due to intermixing of coolant between sub-channels.

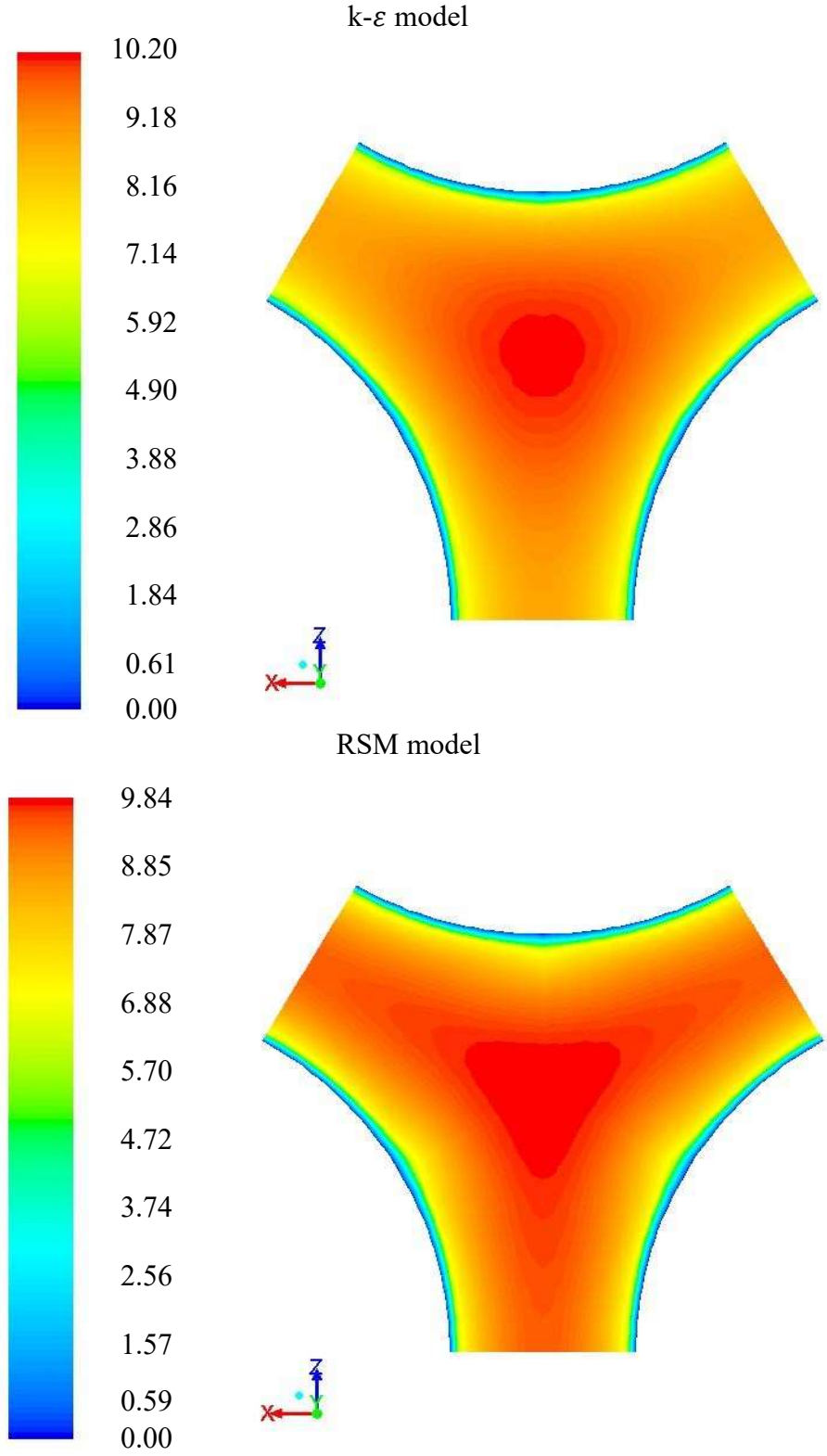

Fig. 5.29 The contours of velocity (m/s) in a triangular pitched non-circular sub-channel with p/d ratio of 1.25 at Re = $5x10^4$ with k-ε and RSM turbulent model

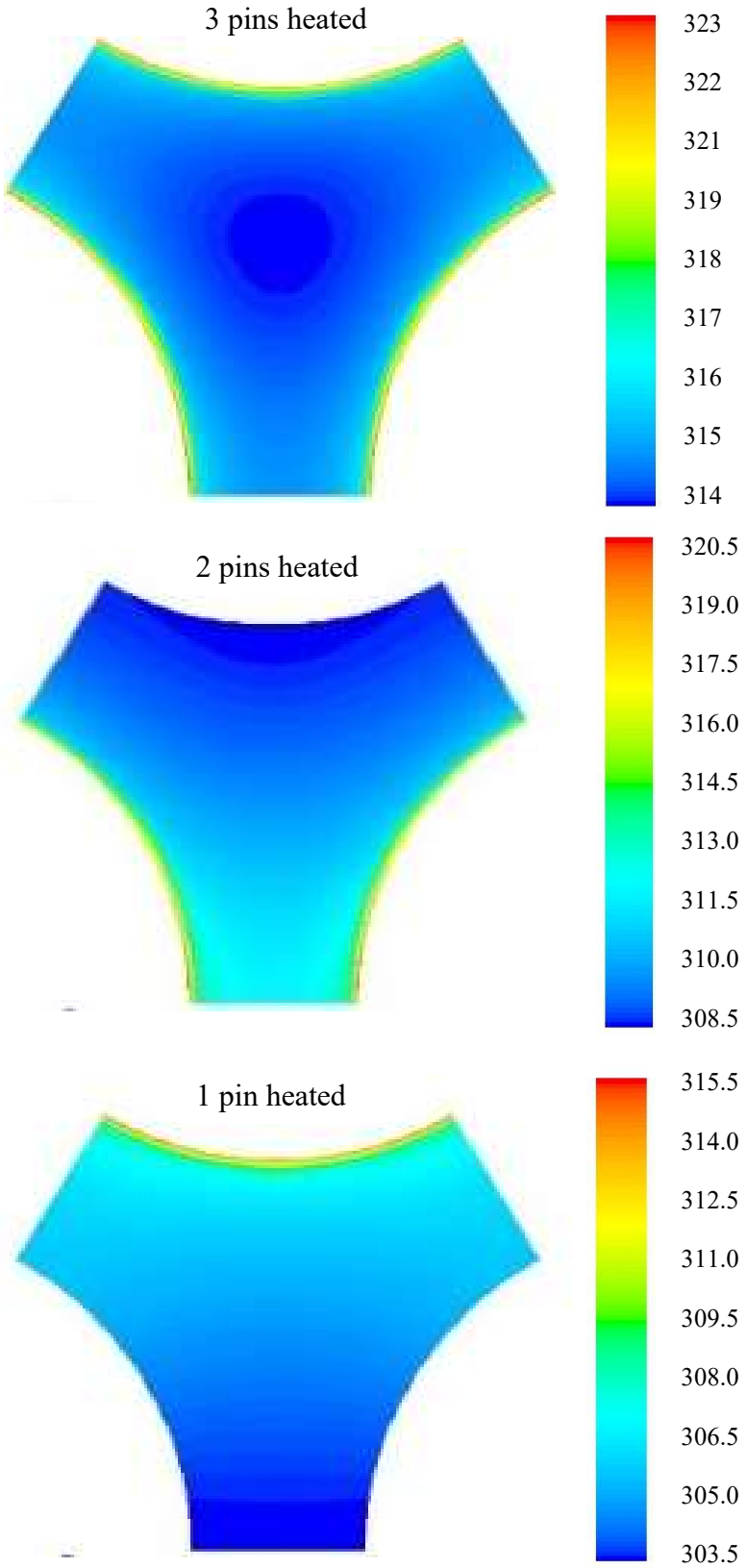

Fig. 5.30 The contours of temperature (K) distribution in triangular sub-channel for an input heat flux of 0.5 MW/m^2 for a p/d ratio of 1.25 at Re = 5x10^4 with k-ε model

5.8 Summary

Investigations of fully developed laminar and turbulent flow and heat transfer analysis in the non-circular and rod bundle sub-channel geometries is performed. The results are presented for different p/d and W/d ratios ranging from 1 to 2. The governing equations of the physical phenomena are simplified to Poisson's equation and implemented in COMSOL multi-physics solver. The non-circular geometries are solved for out-of-plane flow velocity on a 2-D cross-section as against the conventional CFD method. The extensive validation of the mathematical model is carried out for different non-circular ducts. The results obtained in the present study are in good agreement with the benchmark results reported in the literature. The parametric studies on the effect of p/d on geometry parameter (fRe) and average Nusselt number ($\overline{Nu}$) are carried out for square and triangular pitched sub-channel. It has been found that the fRe increases significantly for p/d ratio of 1 to 1.15 for the sub-channel shaped geometry. In case of the sub-channel shaped duct of the same p/d ratio, the fRe increases sharply up to p/d ratio 1.15 and then started decreasing slightly till the p/d of 1.5. In case of fuel bundle geometry, as the p/d ratio approaches the W/d ratio, the effect of bundle size on fRe vanishes. Furthermore, it turns out that the change in fRe is of the order of 5% with the size of bundle varying from 2x2 to 10x10 for an equal p/d and W/d ratios. The analysis also shows that for an equal p/d and W/d ratios, fRe remains more or less same. For engineering applications, the correlations have been developed by least square linear regression analysis to evaluate Poiseuille number and Nusselt number in terms of p/d for different sub-channel geometries. The results obtained from the present study are useful in the sub-channel analysis to estimate pressure loss coefficients, heat transfer characteristics of the sub-channel.

The fully developed turbulent flow analysis reveals that similar to the geometry factor for laminar flow, the geometry factor for turbulent flow exists and it comes out to be constant and is a weak function of Reynolds number. The effect of uniform and non-uniform heating of pins in triangular sub-channel is carried out to study the effect of secondary velocity on the change in the wall and bulk temperature of the fluid. The investigations of turbulent quantities in non-circular geometries reveals that an average developed length and the maximum velocity is reduced by 5% on considering the secondary velocities.

5.9 Closure

In this chapter, the fluid flow and heat transfer characteristics in sub-channel geometries in laminar and turbulent flow conditions is discussed. The fully developed laminar flow and heat transfer analysis in a square and triangular pitched sub-channel geometry, sub-channel shaped tube and a typical nuclear fuel bundle are carried out and the results of the investigations are discussed in detail. It is demonstrated that the approach of solving an out-of-plane fully developed flow problem, simplifies the complex 3D problem into a simple 2-D problem for non-circular sub-channel geometries of the nuclear fuel bundle. It is hoped that this kind of study greatly reduces the computational time and the accurate estimation of the flow distribution for different geometries of a typical fuel pin bundle. The turbulent flow analysis reveals that, similar to the geometry factor for laminar flow, there exists a geometry factor for turbulent flow and is independent of Reynolds number. The next chapter is devoted to the CFD investigations of cross-flow between adjacent sub-channels of a nuclear fuel bundle

CHAPTER-6

INVESTIGATIONS OF FLOW BETWEEN ADJACENT SUB-CHANNELS OF NUCLEAR FUEL BUNDLE

CHAPTER-6

6 INVESTIGATIONS OF FLOW BETWEEN ADJACENT SUB-CHANNELS OF NUCLEAR FUEL BUNDLE

6.1 Introduction

In a nuclear fuel bundle, the flow among adjacent sub-channels is mainly due to pressure gradient, turbulent mixing and other geometrical arrangements in a fuel bundle. To quantify the effect of pressure gradient on flow exchange, the estimation of local conditions of the coolant in the sub-channel is essential. This chapter reports the flow characteristics in a compound triangular sub-channel of a typical nuclear fuel bundle. The CFD model of two interacting compound sub-channel formed by nuclear reactor fuel/non-fuel pins arranged in triangular pitch is considered in the analysis for p/d ratios of 1.05 and 1.1. The mass exchange between sub-channels is studied by varying the inlet mass flux from 100 kg/m^{2}s to 600 kg/m^{2}s. The change in velocity fields along the channel is studied by varying the fuel pin heat flux on the flow distribution.

6.2 Computational Geometry of Triangular Sub-channel

The triangular pitched sub-channel geometry of a typical fuel bundle is considered for the analysis. The schematic of the computational geometry and the mesh of a two interconnected compound triangular sub-channel is shown in Fig. 6.1. Two types of triangular sub-channel with p/d ratios of 1.05 and 1.1 with a channel length of 1.5 m is considered for the analysis. The computational domain is split at different locations along the length of the sub-channel to estimate the average mass flux at different locations. It is also cut across the sub-channel for the mapped meshing of the domain.

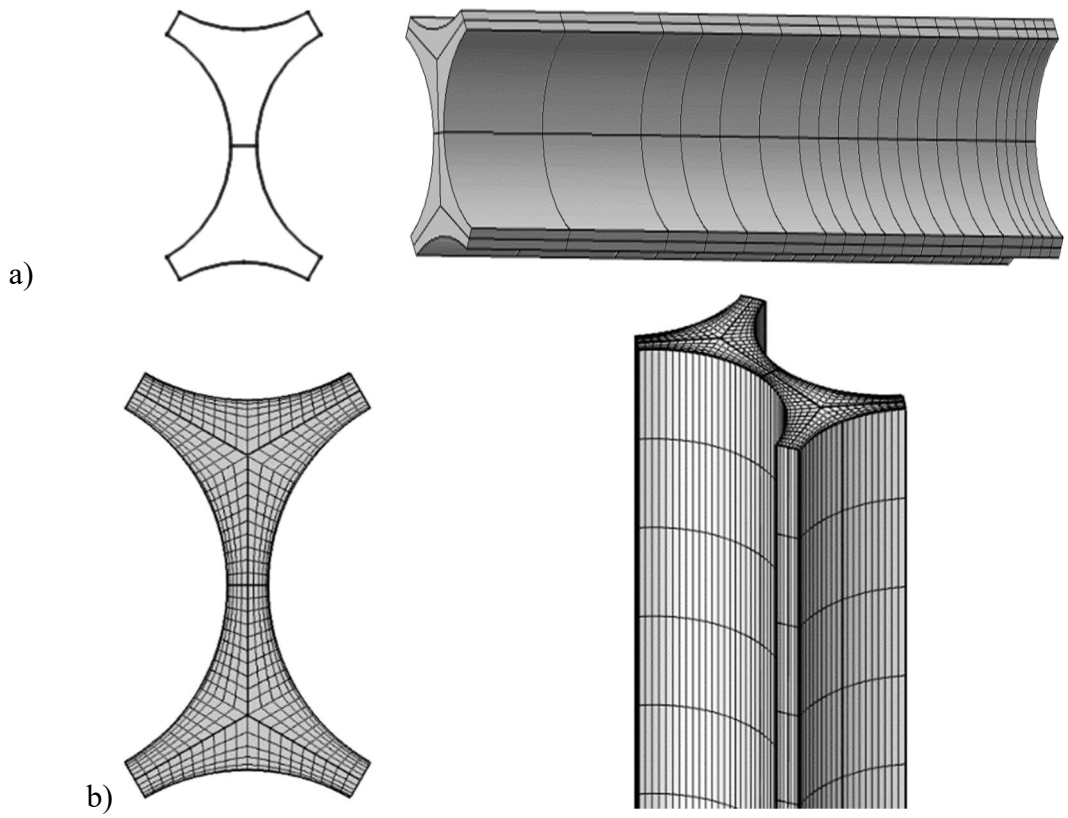

Fig. 6.1 Schematic of geometry and mesh of compound triangular sub-channel

6.2.1 Grid sensitivity analysis

A thorough grid sensitivity study has been carried out. Mapped meshing of the sub-channel is carried out to have the control of the number of meshes. Near wall gradients are used to have fine mesh closer to the wall. Around 200 elements along the length of the channels are used. The final meshed geometry is shown in Fig. 6.1(b). The computational domain consists of 4 lakhs elements and 4.5 lakhs vertices.

6.2.2 Boundary conditions and CFD simulation

The CFD simulations are carried out using COMSOL multi-physics software. The computational domain is solved using non-isothermal flow physics by considering the temperature variation of fluid properties of coolant (water). On the computational domain, velocity inlet and pressure outlet boundary conditions are specified. On the fuel

pins, wall boundary condition is applied and symmetry boundary condition is applied on the imaginary boundary formed between the pins. An interior boundary condition is also applied on the face connecting two sub-channels.

Initially, the effect of change in coolant inlet mass flow rate of neighboring channel is studied by keeping the mass flow rate of channel-2 at the inlet to zero for a p/d ratio of 1.05 to simulate a blocked sub-channel at the inlet. The mass flux of other channel is varied from 100 kg/m^{2}s to 600 kg/m^{2}s. The similar analysis is also carried out for a triangular sub-channel for p/d ratio of 1.1. In this case also, the mass flux at the inlet of channel-1 is varied and the Channel-2 is kept at zero. The effect of pressure gradient alone on the mass exchange is studied by varying the inlet mass flux of the sub-channels having an equal cross sectional area.

The effect of heat addition to one of the neighboring sub-channel on coolant flow distribution is also studied at higher mass flux in the turbulent regime for a p/d ratio of 1.1. The heat flux of 0.05 MW/m^2 is applied on the walls of one of the sub-channel. The effect of heat addition on the change in flow distribution and temperature along the stream wise direction is studied and discussed in the following sections.

6.3 Results and Discussion

6.3.1 Flow characteristics of triangular sub-channel of p/d ratio 1.05

The numerical analysis of flow distribution due to pressure gradient between the triangular sub-channels of equal cross sectional area along the axial direction is studied. The variation of the coolant velocity across the longitudinal cross section at the middle of the sub-channel is shown in Fig. 6.2(a) for a typical case of channel-1 inlet mass flux of 600 kg/m^{2}s. The average inlet velocity of the channel-1 is found to be 0.6 m/s,

However, the maximum velocity in the fully developed region is found to be 0.82 m/s. Internal redistribution of the flow at entry region is also clearly seen from these figures. The contours of the velocity at the outlet of the sub-channel are presented in Fig. 6.2(b).

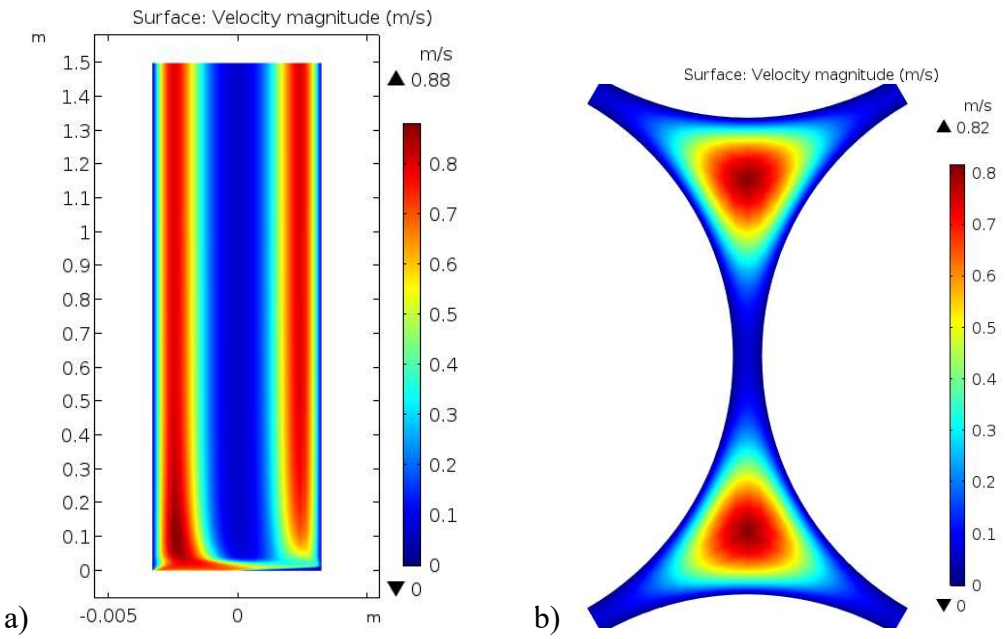

a) b)

Fig. 6.2 Contours of velocity across the sub-channel along the length and at the outlet of sub-channel for an inlet mass flux of channel-1 at 600 kg/m^{2}s and channel-2 at zero mass flux.

Also, the contours of flow velocity at higher mass flux under iso-thermal condition are shown in Fig. 6.3. The effect of change in the inlet mass flux on the flow development and the variation of the maximum velocity at the centre of the sub-channel are depicted in Fig. 6.4. It can be seen that the flow velocity of the high mass flux sub-channel gets reduced and the flow velocity of the low mass flux sub-channel is increased and indicates the cross-flow takes place between the sub-channel. It can be observed from the velocity change that, initially, flow velocity of both the channel is increased to achieve the flow distribution within the sub-channel along with cross-flow (Fig. 6.4.). As the flow distribution within the sub-channel is achieved, further flow development takes place with cross-flow.

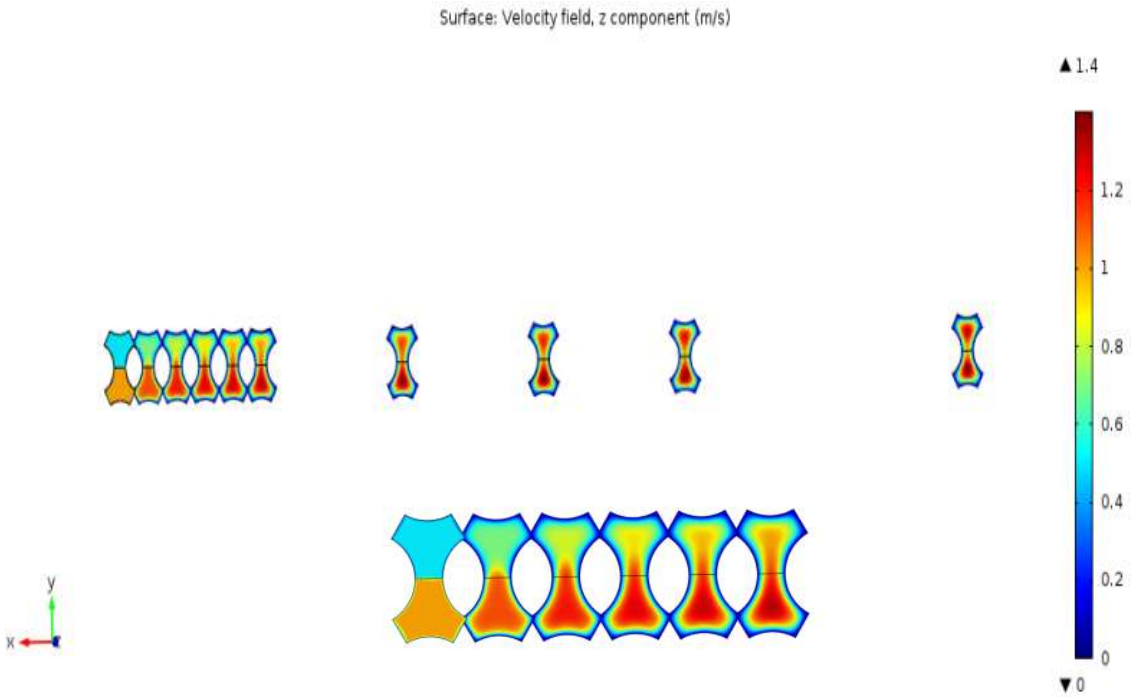

Fig. 6.3 Contours of the variation of coolant velocity along the flow direction in compound triangular sub-channel at isothermal condition.

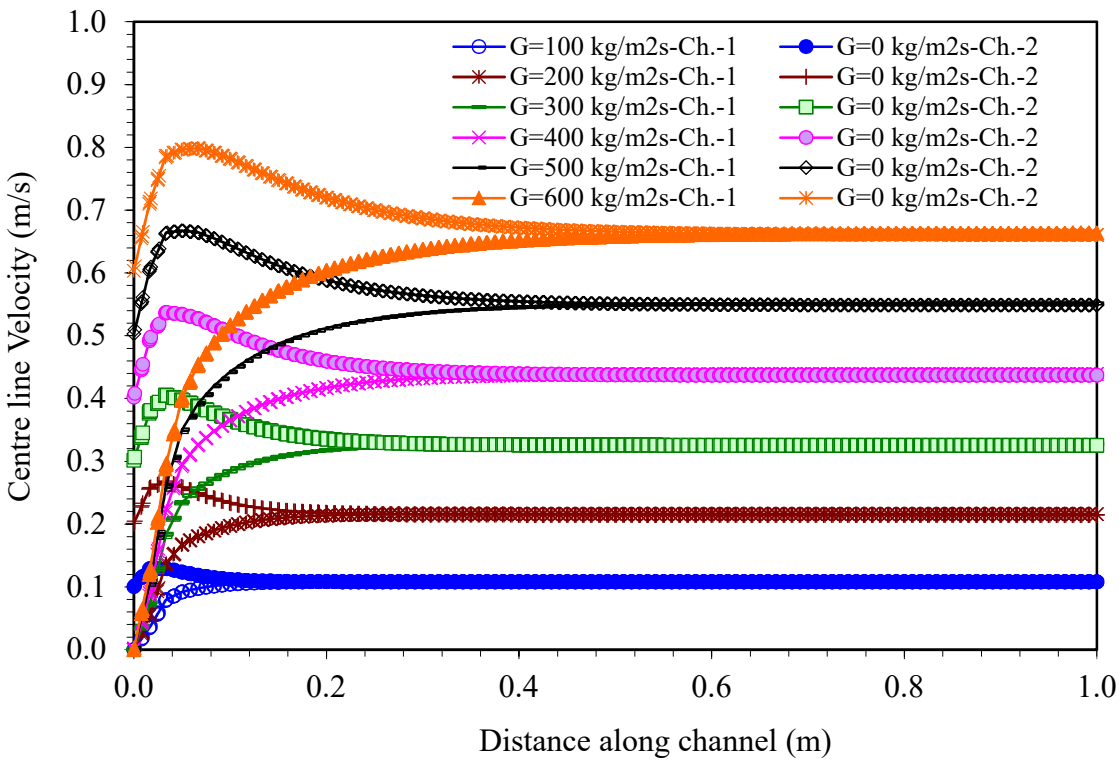

Fig. 6.4 Effect of change in the inlet mass flux of channel-1 on the flow development and the velocity at the centre of sub-channels. (Ch-1-channel-1, Ch-2- channel-2, G-inlet mass flux of respective channels)

The effect of change in the inlet mass flow rate on the flow development and inter mixing of coolant between sub-channels is established. Once flow distribution within the channel is established, cross-flow takes place almost at constant rate. However, beyond certain length, where the flow development is completed, the cross-flow due to pressure gradient is also negligible. Further, mixing with equal pressure gradient will be attributed to turbulent mixing and flow pulsation in the narrow gap.

The computed velocity profile is integrated across each sub-channel to estimate the variation of average mass flux along axis of the sub-channel (Fig. 6.5).

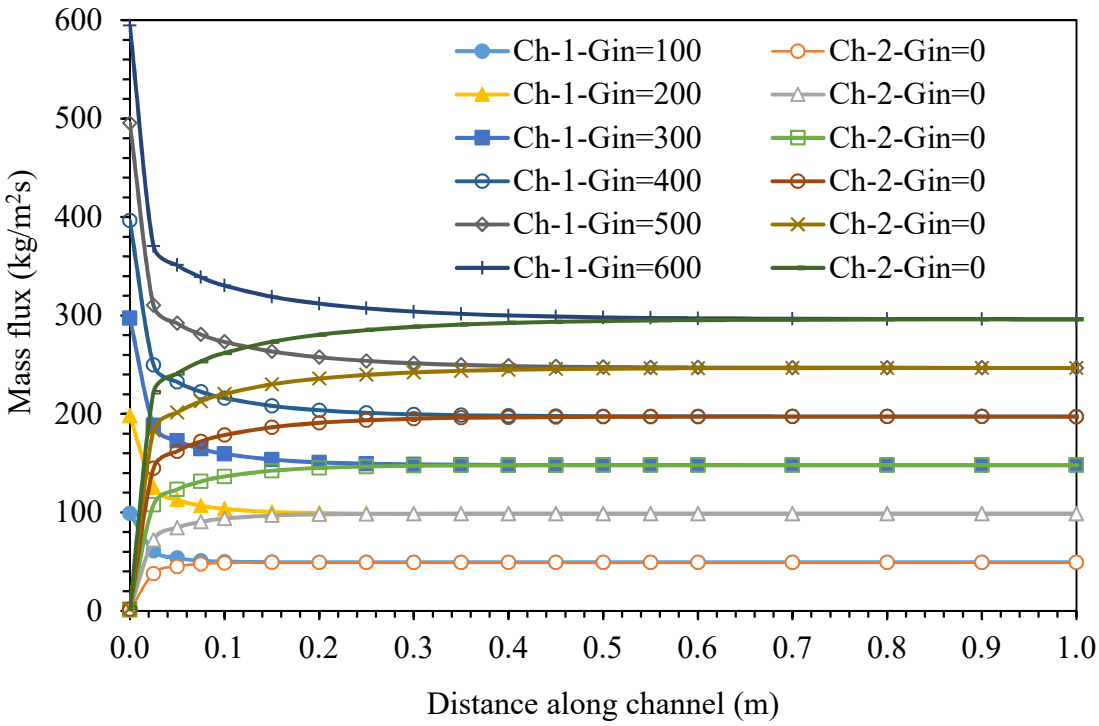

Fig. 6.5 Effect of change in the coolant mass flux along the sub-channels for p/d =1.05 (Ch-1-channel-1, Ch-2- Channel-2)

It is observed that both the channels are asymptotically reaching the equal mass flux. The flow exchange is higher at the entrance and after the initial redistribution, it gets gradually exchanged. The average developed length is observed to be a linear variation

with mass flux. As the flow passes from the channel, it redistributes to attain the equal mass flux between the channels.

6.3.2 Flow characteristics of triangular sub-channel of p/d ratio 1.10

The variation of coolant mass flux along the flow direction with isothermal condition are shown in Fig.6.6.

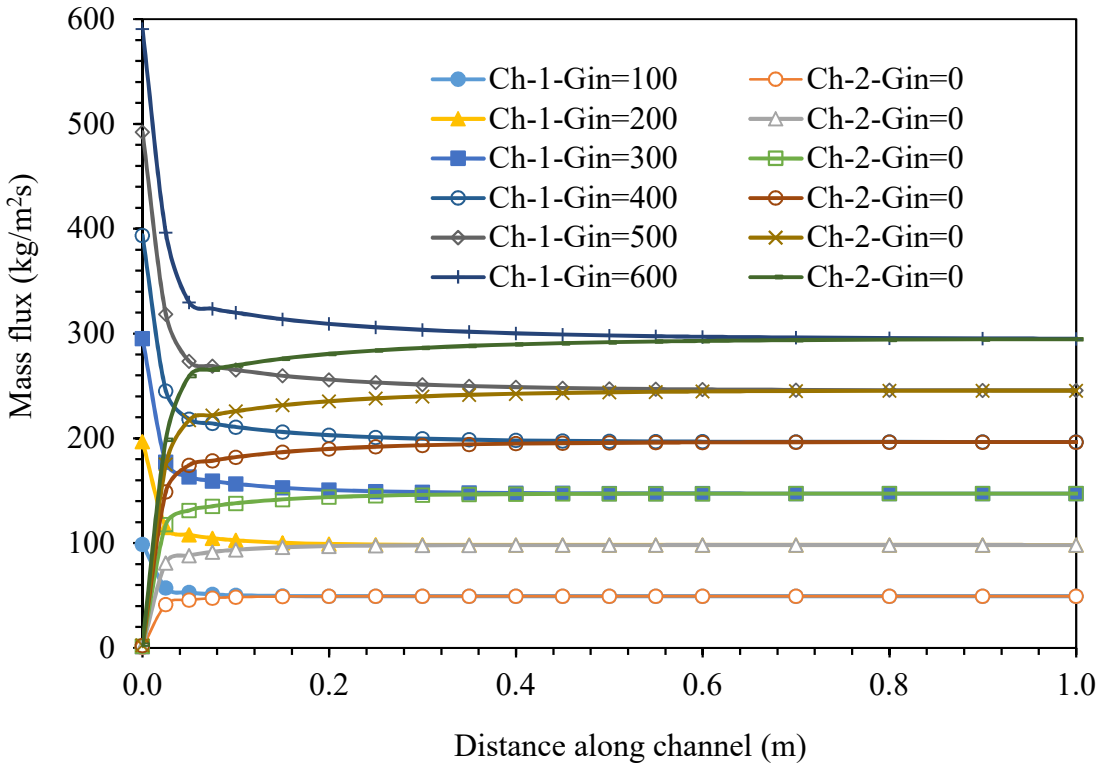

Fig. 6.6 Effect of change in the coolant mass flux along the sub-channels for p/d =1.10 (Ch-1-channel-1, Ch-2-channel-2)

It can be seen that, initially, flow uniformity takes place along with cross-flow due to pressure gradient and both sub-channels reach asymptotically the equal velocity and flow distribution after a sufficient developed length. The comparison of change in the mass flux channel for the p/d ratios of 1.05 and 1.1 is given in Fig. 6.7. It is clear that the mass exchange after initial distribution is more or less same for both the geometry

for a given inlet mass flux. However, it is varying insignificantly with the p/d ratio in case of mass exchange with pressure gradient alone.

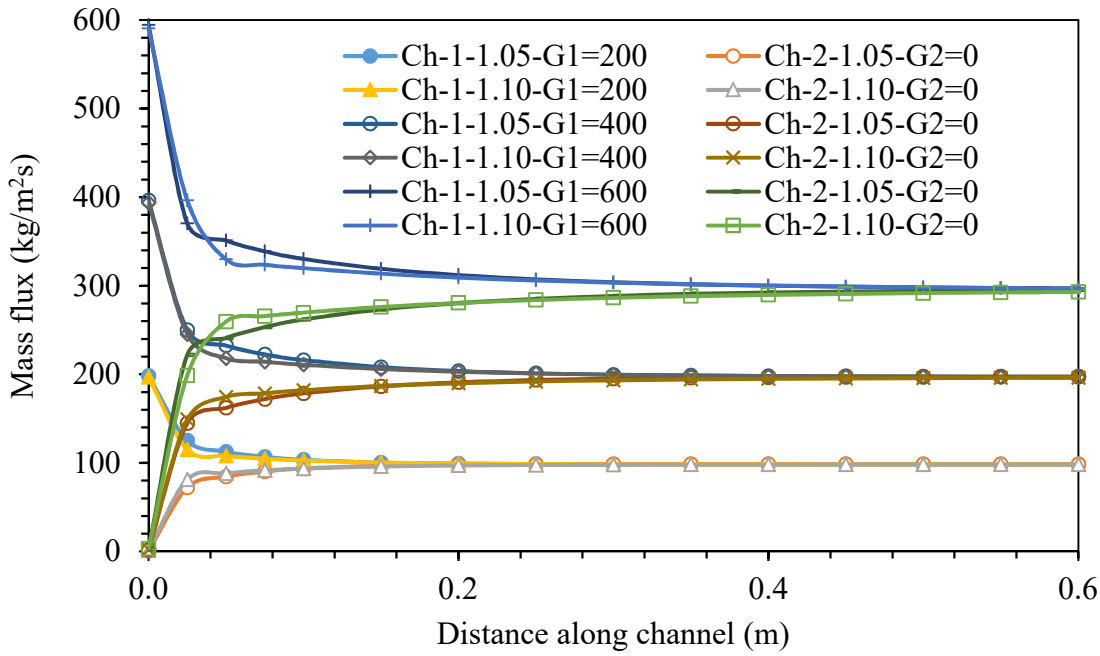

Fig. 6.7 Comparison of change in coolant mass flux along the channel for p/d ratio 1.05 and 1.10. (Ch-1-channel-1, G1- mass flux of Channel-1, G2-mass flux of channel-2)

6.3.3 Effect of heat flux on flow distribution

Apart from the inter-channel mixing due to pressure gradient by varying the mass flux under iso-thermal conditions, a study on the same model with heat input of 0.05 MW/m^2 is also carried out. The effects of heat flux on the flow distribution in a triangular sub-channel of p/d ratio 1.1 are presented in this section. The contours of the flow velocity in the triangular sub-channel with heat input are given in Fig. 6.8. The contours of coolant temperature along the length of the channels are shown in Fig. 6.9. These plots give the sequential evolution of flow velocity in both the sub-channels at different locations along the axis. It is found that due to heat addition to one of the sub-channel, the flow is not equalized across the channel and the mass flux continued to increase in the downstream of the sub-channel (Fig. 6.10.).

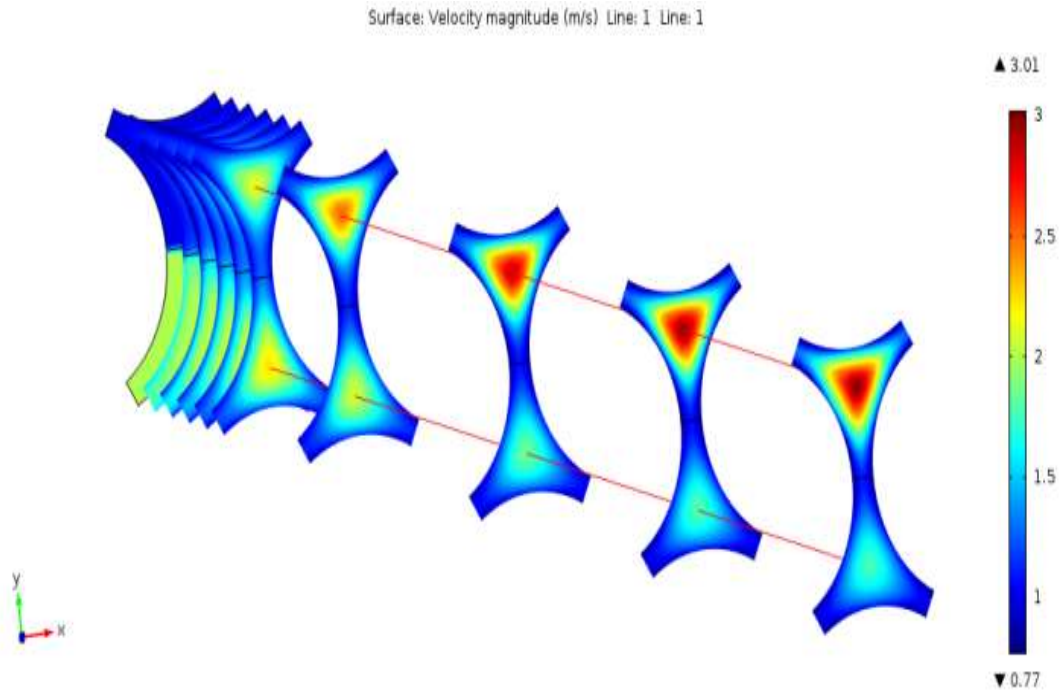

Fig. 6.8 Contours of the variation of coolant velocity in a compound triangular sub-channel with heating of one sub-channel

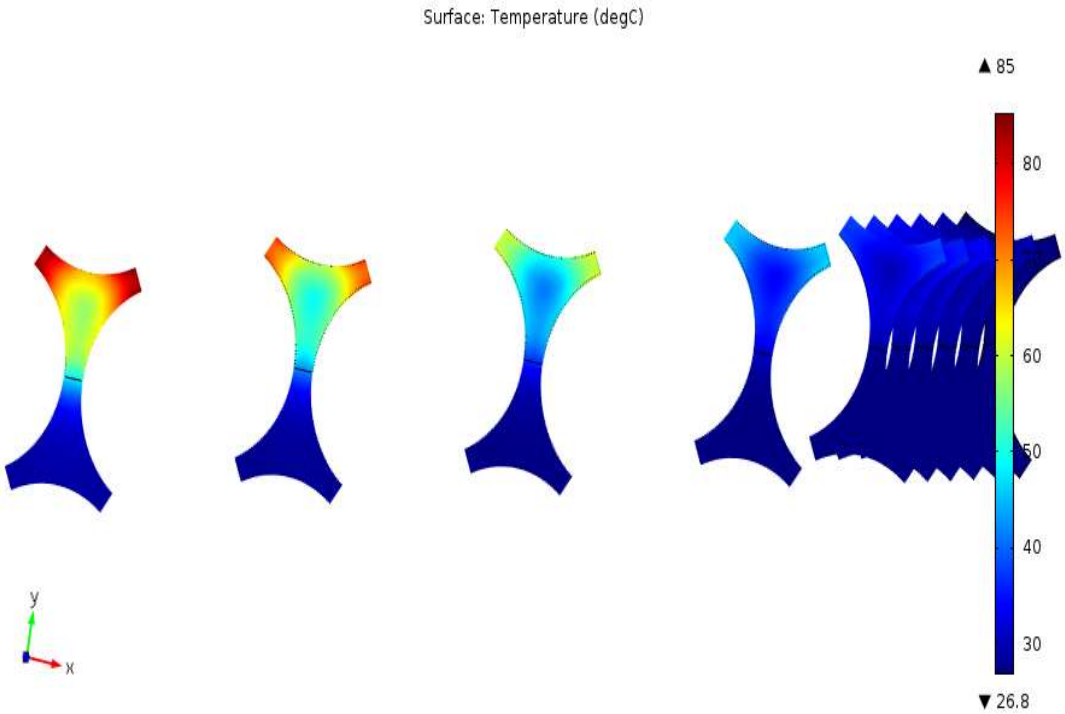

Fig. 6.9 Contours of coolant temperature variation along a compound triangular sub-channel with heating of one sub-channel

The coolant temperature is found to be increased from 27 ºC to maximum of 85 ºC. It is seen that, as the mass exchange takes place from cold channel to hot channel, the sequential change in temperature of cold channel is not appreciable. It is observed from Fig. 6.8 and Fig. 6.10 that, initially, the flow velocity increases in both low and high mass flux channels. As the heat is added to the low mass flux channel, the coolant density decreases and hence the continuous increase in the centre line velocity is observed (Fig. 6.10.). In the case of flow exchange in compound channels due to pressure gradient under iso-thermal conditions, both channels attain the same maximum and average velocity (Fig. 6.4.). In the case of the heat input, both channels attain the different velocity distribution. The high mass flux channel shows the decrease in velocity as compared to the low mass flux channels due to heat addition to the low mass flux channel. Further, the velocity and mass flux continue to increase in the hot channel as compared to cold channel.

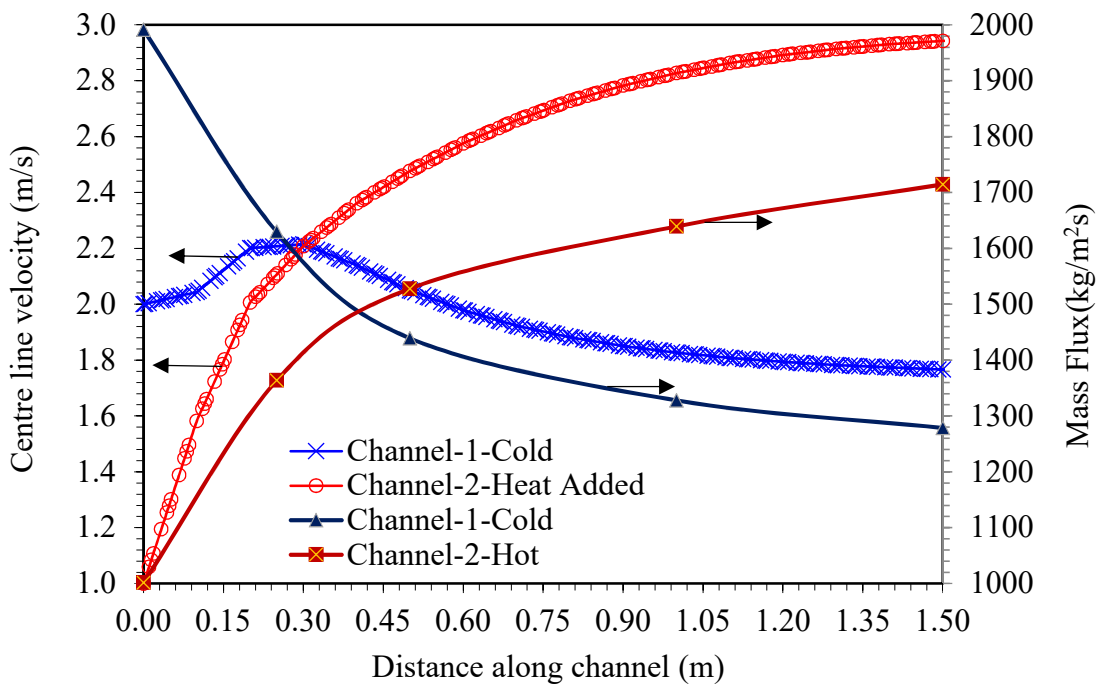

Fig. 6.10 Variation of coolant velocity along the centre line of the triangular sub-channel with heating of one sub-channel

6.4 Summary

Investigations are carried out to study the flow characteristics in a compound triangular sub-channel of a nuclear fuel bundle. The flow characteristics are studied in a triangular pitched sub-channel with p/d ratios 1.05 and 1.1, with and without heat addition. The mass flux between the sub-channels is varied from 100 kg/m^{2}s to 600 kg/m^{2}s. The study shows that the inlet mass flux does affect the average developed length and mass exchange between sub-channel irrespective of the p/d ratio (1.05 and 1.1) due to pressure gradient alone. It is found that at higher mass flux, deviations between the two interacting sub-channels causes a significant increase in the average developed length, average and maximum velocity along the compound channel. In case of the heat addition to one of the channel, both channels attain the different velocity distribution and high mass flux channel shows the lower velocity as compared to the low mass flux channel due to heat addition in low mass flux channel.

6.5 Closure

In this chapter, study of cross-flow mixing between compound triangular sub-channels is carried out. It was shown that the heat addition to the sub-channels significantly affects the mass exchange. The next chapter is devoted to the numerical investigations of coolant mixing in a nuclear reactor fuel pin bundle using the developed framework.

CHAPTER-7

INVESTIGATION OF CROSS-FLOW MIXING IN FUEL PIN BUNDLES

CHAPTER-7

7 INVESTIGATION OF CROSS-FLOW MIXING IN FUEL PIN BUNDLES

7.1 Introduction

In the earlier chapters, the results for the pressure drop and flow distribution in a typical nuclear reactor fuel pin bundle, sub-channel and sub-channel shaped tube are discussed in detail. The effect of p/d and w/d on the flow distribution for different size of the bundle is brought out in detail. This chapter presents the details of the investigations carried out to study the effect of cross-flow mixing on the coolant enthalpy rise in a typical nuclear reactor fuel pin bundle using the developed framework.

In a typical nuclear reactor of PWR, BWR and LMFBR the safety of reactor core is ensured by performing a detailed core thermal hydraulic analysis using a sub-channel analysis codes such as COBRA, CANAL, HAMBO, ENERGY etc. (Ref. Table. 2.2). The safety of nuclear reactor core is ensured based on accurate estimation of local conditions of the coolant in the fuel assembly/sub-channels. The coolant flow distribution among bundles is affected due to non-uniformity of entry conditions at the inlet plenum. The coolant local conditions are also affected very much due to the inter-channel mixing between sub-channels.

The coolant mixing among sub-channels is a combined effect of diversion cross-flow due to pressure gradient, turbulent mixing due to eddy diffusion, large scale flow pulsations and forced diversions due to spacer geometries, wire wraps or the shape of fuel pins. There are various uncertainties involved in manufacturing of fuel components, critical power correlations and measurements of parameters such as reactor power,

reactor pressure, coolant flow through the assembly and coolant inlet temperature etc. which, in turn, affects the estimated thermal hydraulic safety margins and fuel temperatures. Due to these uncertainties, both the local conditions and critical heat flux will differ from their nominal values which, in turn, affects critical power of bundle. Apart from the nominal core thermal hydraulic analysis, these uncertainties are accounted in the hot-spot and hot channel analysis. At the design and operating stage, large numbers of thermal hydraulic analysis are required to be carried out for different operating regimes of the reactor core. Traditionally COBRA kind of sub-channel analysis is performed which involves preparation of inputs for different operational conditions of the core and power distribution. This chapter details the investigation carried out on the effect of cross-flow mixing on rod bundle safety margins using the developed sub-channel analysis framework. The results of sub-channel analysis carried out by varying different parameters in this study are the size of the bundle, p/d ratio, intensity of turbulent mixing, mass flux, uniform and non-uniform axial power distribution. The sub-channel layouts for fuel bundles of different sizes varying from 2×2 to 10×10 and 17×17 for same p/d and w/d ratios of 1.05 to 1.3 were analyzed. The analyses are carried out by varying the intensity of turbulent mixing parameter (c) from 0 (no mixing) to 0.1 (high mixing) using the developed framework.

Therefore, with this objective, an automated sub-channel layout generation program is developed for square shaped, hexagonal and circular shaped fuel assembly. The general arrangement of square pitched fuel/non-fuel pin geometry of typical fuel bundle configuration is presented in this chapter. The inputs required for various case studies of different reactor operating parameters are generated to conduct the core thermal hydraulic analysis. The estimation of the coolant temperature, fuel pin surface

temperature and local quality are also carried out without considering the inter-channel mixing and compared with the change in the local conditions with different degree of mixing among the fuel bundle sub-channels. The post processing of the sub-channel and fuel conditions resulting from the thermal hydraulic analysis are also compared for different degree of turbulent interchannel mixing.

7.2 Core Thermal Hydraulic Analysis

7.2.1 Sub-channel analysis

Considering the complexity of the rod bundle geometry, different turbulent scales and limitations of computational resources, it is difficult to perform the full scale computational fluid dynamic analysis of reactor core. It is also time consuming. Hence, the thermal hydraulic safety margins of most of the operating reactors in the world are carried out using the sub-channel analysis codes. In these codes, the governing equations of mass, momentum and energy are solved in control volumes (nodes) which are connected in both radial and axial directions.

The governing equations for mass, momentum and energy are solved along with the turbulent inter-channel mixing model. The governing equations are discussed in chapter 3 in section 3.5.

7.2.2 Mixing of coolant between sub-channel

The prediction of the actual coolant conditions inside the rod bundle is very important. This helps to obtain fuel temperature as well as the limiting power that a fuel bundle can take under given operating conditions. Solving the one dimensional mass, momentum and energy equations, along the sub-channel with considering the cross-flow mixing between sub-channels can greatly reduce the computational resources and time. The cross-flow mixing between sub-channels is mainly due to natural effects like

pressure gradient between the sub-channel, turbulent mixing and forced effects due to spacer grids, wire wraps and mixing vanes. The forced mixing can be directional like flow sweeping and non-directional due to flow scattering. Also in recent times, it is identified that large scale flow pulsation between the sub-channels are also responsible for greater mixing among sub-channels (Meyer, 2010).

The flow distribution in the rod bundle geometry is estimated by considering lateral momentum balance and inter-channel mixing models (Eqn. 3.76) to account for the cross-flow (Eqn. 3.74) between the adjacent sub-channels. The accurate estimation of the local conditions of sub-channels are required to predict fuel temperature and power margins (Weismann and Ying, 1984). The turbulent mixing coefficient 'β'is estimated from Eqn. 3.76 for the prediction of thermal mixing of coolant between adjacent channels under single phase conditions. The prediction of turbulent mixing based on equal mass exchange model is suggested by Rowe and Angle (1967) and used in the similar form by various researchers (Seale, 1979; Castellana et al., 1974; Cheng and Todreas, 1984). The similar type of turbulent mixing model for the estimation of cross-flow under two phase flow conditions based on the void drift model is proposed by correcting the single phase mixing flow rate w'_{ij} using a two phase mixing multiplier (θ) (Beus, 1971; Bo Pang, 2013). The two phase turbulent mixing flow rates between the adjacent sub-channel is estimated as,

$$w'_{ij\,TP} = \theta\, w'_{ij\,SP} = \theta\beta s_{ij}\overline{G_{ij}} \tag{7.1}$$

The two phase turbulent mixing multiplier θ is estimated as follows,

$$\theta = 1 + (\theta_M - 1)\frac{x_{avg}}{x_c} \qquad \text{for bubbly flow regime}, \mathrm{x}_{avg} < \mathrm{x}_c \tag{7.2}$$

$$\theta = 1 + (\theta_M - 1)\frac{1 - \frac{x_o}{x_c}}{\frac{x}{x_c} - \frac{x_o}{x_c}} \qquad \text{for annular flow regime, } x_{avg} > x_c \tag{7.3}$$

Where, the parameters are

$\theta_M = 5$,

x_{avg} is the average quality of the adjacent sub-channel,

x_c is the slug-annular transition flow quality estimated as

$$x_c = \frac{0.4\frac{\sqrt{g\, D_{h\rho}\rho_l(\rho_l - \rho_g)}}{\overline{G_{lj}}} + 0.6}{\sqrt{\frac{\rho_l}{\rho_g}} + 0.6} \tag{7.4}$$

$\frac{x_o}{x_c}$ is calculated as a function of average Reynolds number,

$$\frac{x_o}{x_c} = 0.57 Re_{avg}^{0.0417} \tag{7.5}$$

These models are implemented in sub-channel codes for the prediction of turbulent mixing flow rates between adjacent sub-channels.

7.3 Geometrical Details and Boundary Conditions

The effect of turbulent inter-channel mixing on the coolant enthalpy rise/lowering in the rod bundle sub-channel is studied using the developed framework of fuel assembly layout generator. The sub-channel layout details, rod connectivity to sub-channels and power distribution details are generated for different sizes of the fuel bundles. The regular square pitched fuel bundles of size 2x2 to 10x10 and 17x17 were considered for the analysis. The sub-channel layout of square pitched fuel bundle of size 2x2, 3x3, 5x5 and 10x10 generated using the framework is shown in Fig.7.1(a to d). All the fuel bundles are of same configuration such as pitch to diameter (p/d) ratio, wall gap to

diameter (w/d) ratio of 1.2 and the pitch (p_t) of 12 mm. All pins are heated uniformly in radial as well as in axial direction. The sub-channel thermal hydraulic analysis is carried out to study effect of cross-flow mixing on different size of the bundle by varying the parameter (c) in the mixing correlation from 0 (no mixing) to 0.1 (high degree of mixing) and keeping the coolant inlet condition same. The coolant inlet mass flux is 1356 kg/m^{2}s with fuel pin average heat flux of 0.4732 MW/m^2 and system pressure of 155 bar is used in the analysis. The coolant inlet temperature of 250 ^{o}C is considered with uniform inlet mass flux. The mixing parameters are varied from 0 to 0.1 keeping all other parameters same, sub-channel analysis is carried out using COBRAIIIC. The output of the sub-channel analysis is processed using the framework.

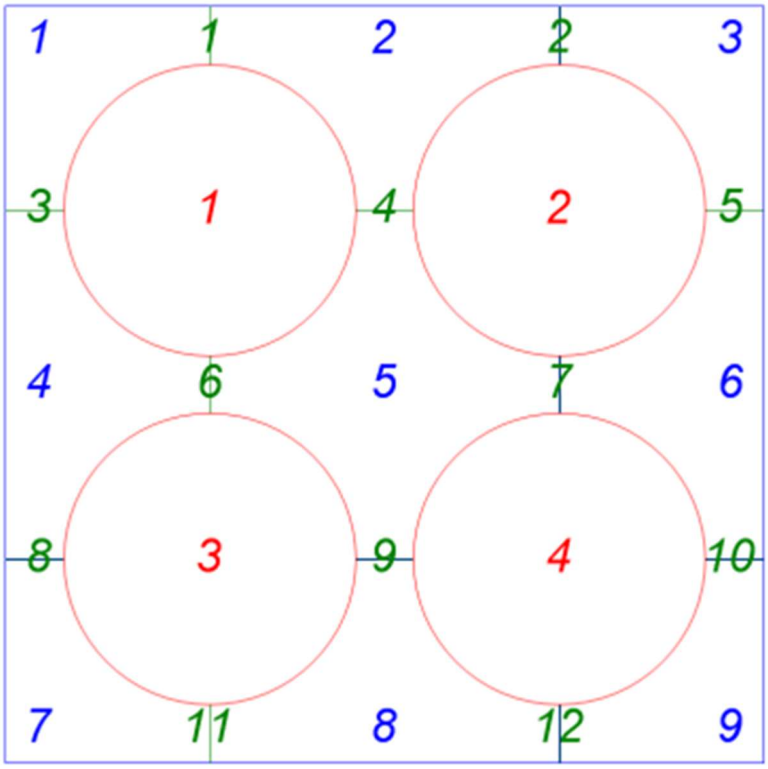

a) 2 X 2 Fuel Bundle
(4 Pins, 9 Sub-channels, 12 Gaps)

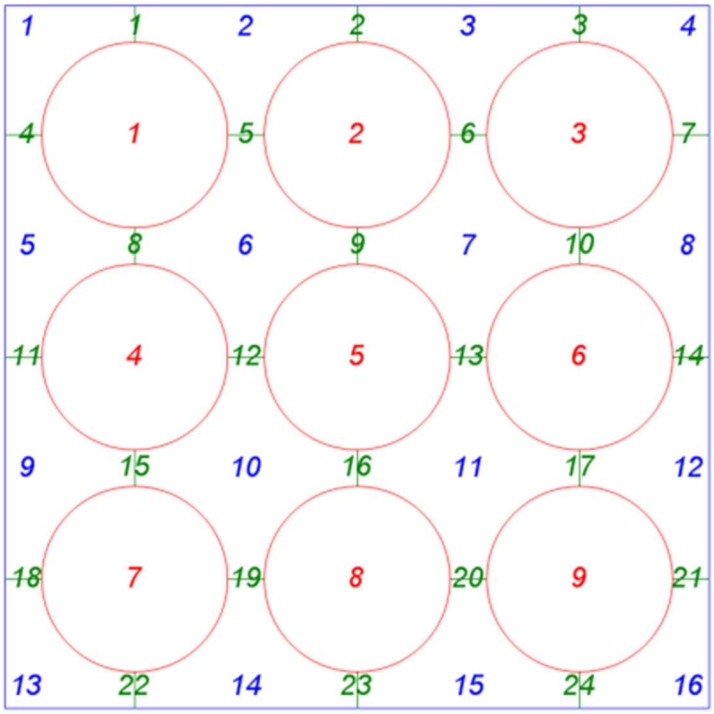

b) 3 X 3 Fuel Bundle
(9 Pins, 16 Sub-channels, 24 Gaps)

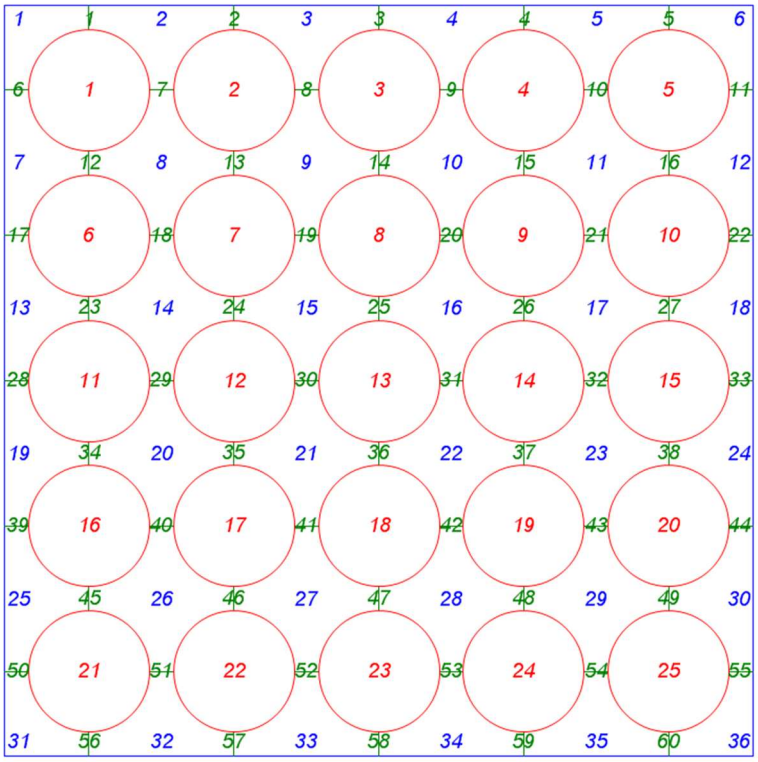

c) 5 X 5 Fuel Bundle
(25 Pins, 36 Sub-channels, 60 Gaps)

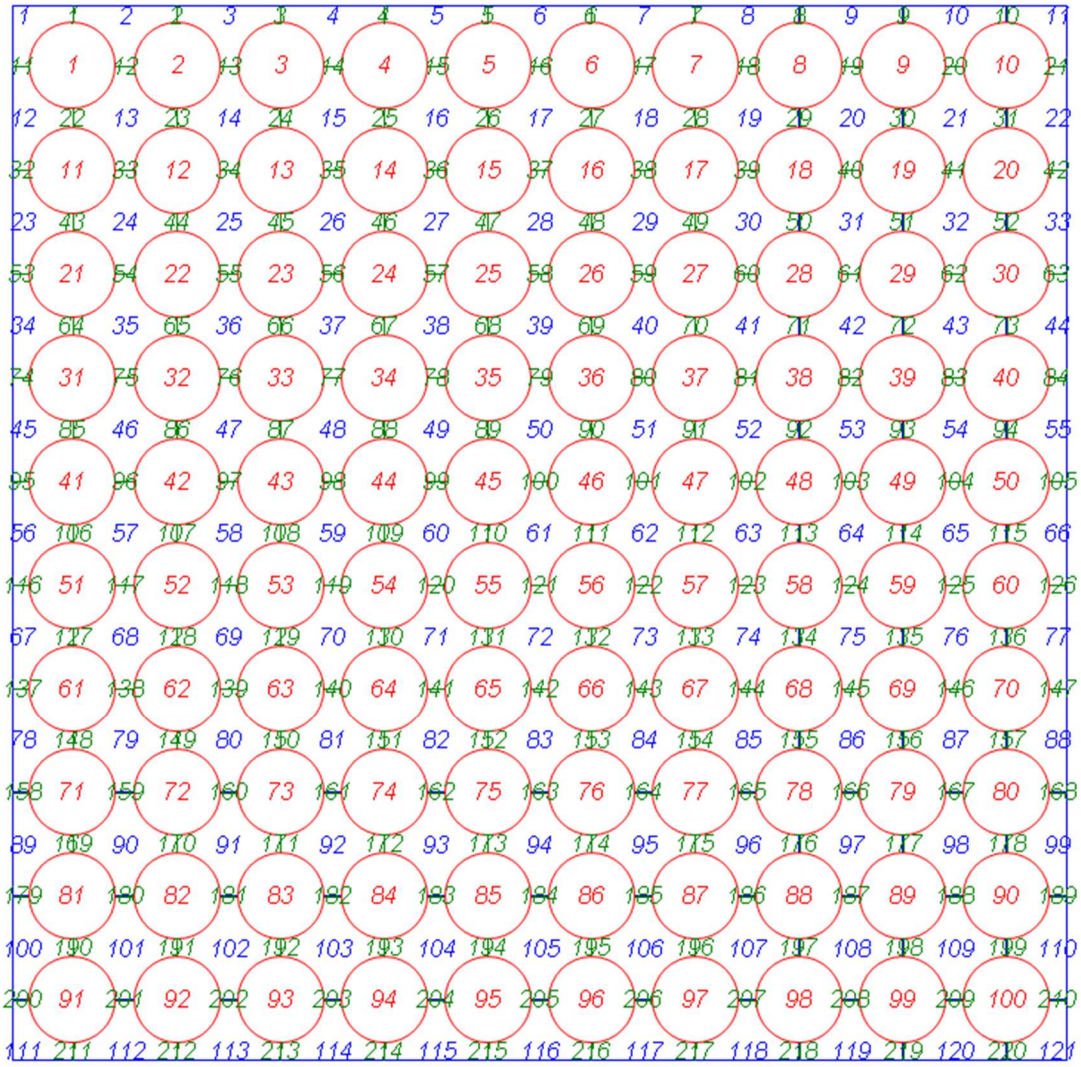

d) 10 X 10 Fuel Bundle
(100 Pins, 121 Sub-channels, 220 Gaps)

Fig.7.1. Typical sub-channel layout of square pitched fuel bundle generated using ASTHYAN Framework.

7.4 Comparison and Validation of Sub-Channel Analysis with CFD

The computational fluid dynamic analysis is carried out for two different sizes of square pitched array of 2x2 and 3x3 rod bundle with p/d and w/d of 1.2 using COMSOL multi physics code. The standard k-ε model is used to analysis turbulent flow characteristics through the bundle. A uniform velocity distribution is applied at the bundle inlet along

with heat flux of 0.4732 MW/m^2 on the surface of the fuel pin. The comparison of the outlet temperature of 2x2 and 3x3 pin bundle predicted by CFD and sub-channel analysis are given Fig. 7.2 and 7.3 respectively. The comparison of coolant temperature at the outlet of fuel bundle, centre, wall and corner sub-channel computed from the present developed code with CFD results is given in Table-7.1. The sub-channel analysis values are estimated based on considering no turbulent mixing. It can be seen that the agreement is very good, with a maximum deviation of only 1.05% in the coolant temperature at the outlet. These comparison studies demonstrate the capability of developed framework for predicting the flow and temperature distribution in rod bundle.

The validation of GE nine pin (3x3) bundle single phase turbulent mixing test cases under isothermal cases is also carried out. The results of computed mass flux are shown in Table-7.2. The CFD analysis of the same is also carried out using COMSOL multi physics. The contours of velocity at the outlet of the bundle for test point 1B is given in Fig. 7.4. The mass flux at the outlet of the individual sub-channel is computed by integrating the velocity over the sub-channel and multiplied by the density. The contours of mass flux from the sub-channel analysis reported by the COBRA code is given in Fig. 7.5. The analysis of other test points is also carried out in a similar manner and the results are given in Table-7.2. It is observed that the, the estimated error in the predicted outlet mass flux in a sub-channel is within 5% for both central and wall sub-channels. The 2x2 and GE 9-pin bundle validation cases using 3-D model requires approximately an hour of simulation time to get the convergence for a single test case. The same problem is analysed using the framework takes lesser time (< 1 min) using the sub-channel analysis approach.

CFD

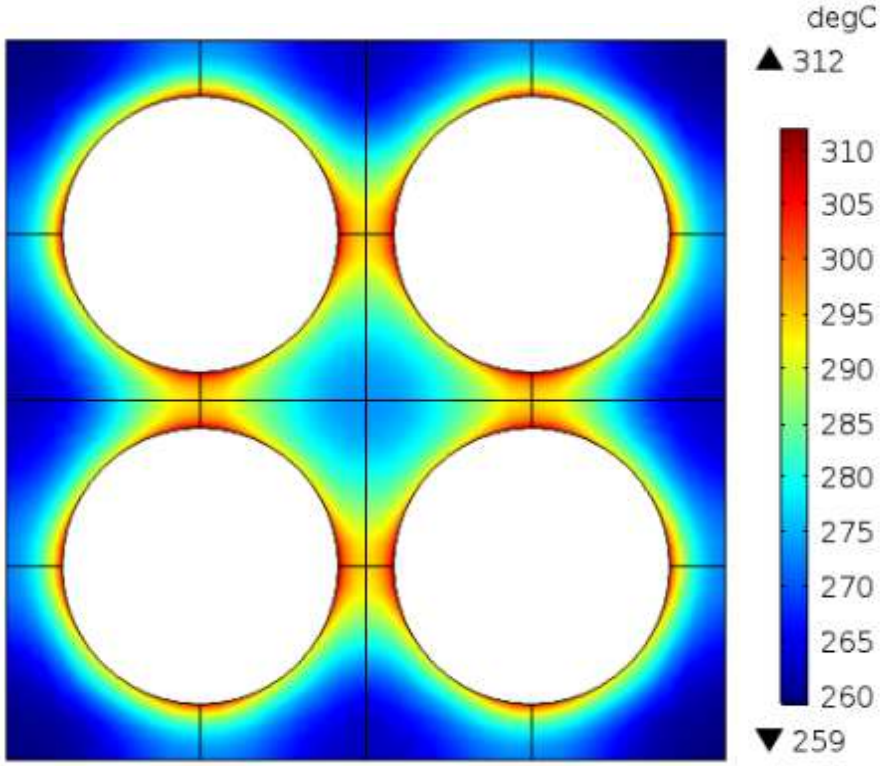

sub-channel

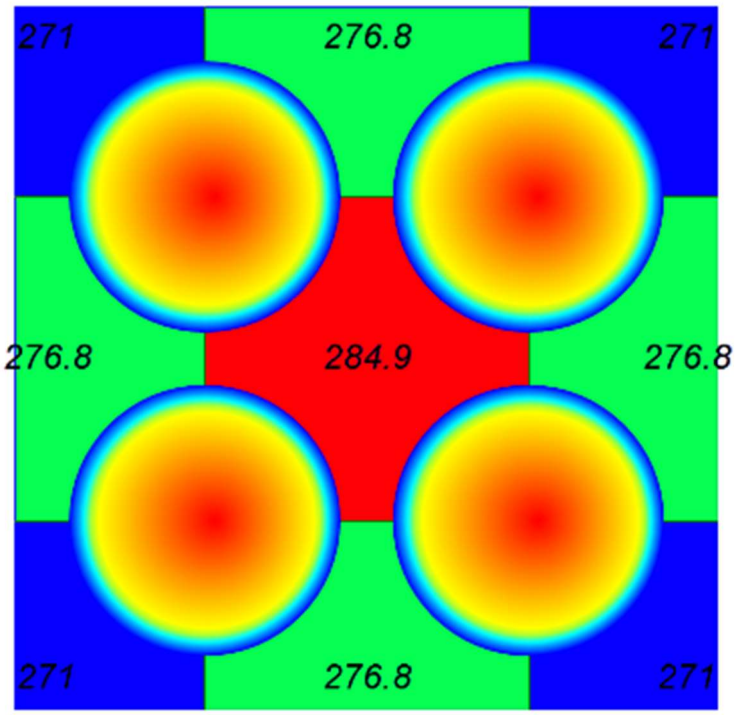

Fig. 7.2 Comparison of the outlet temperature of 2x2 pin bundle by CFD and sub-channel analysis

CFD

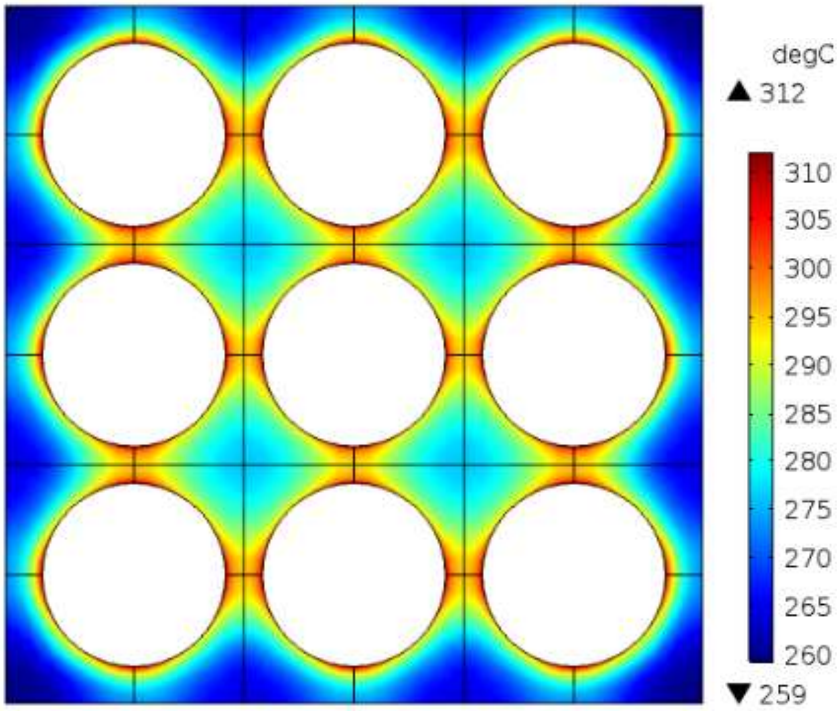

sub-channel

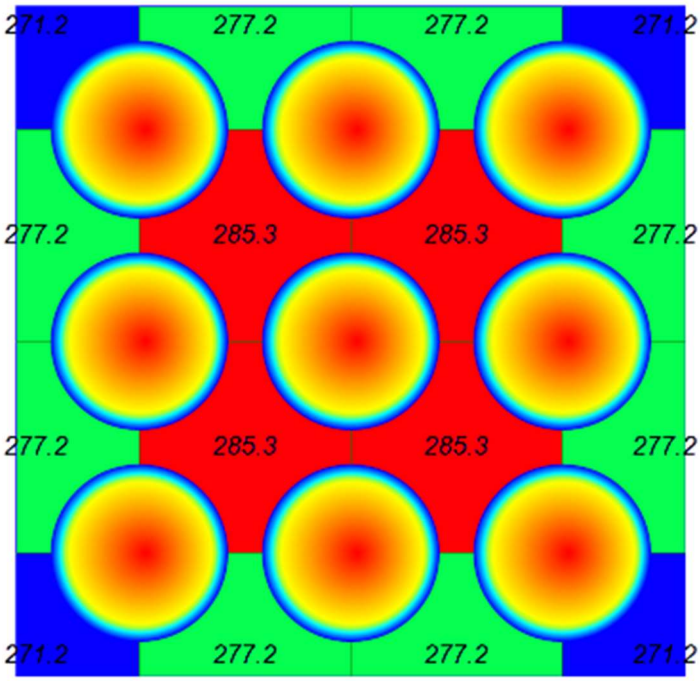

Fig. 7.3 Comparison of the outlet temperature of 3x3 pin bundle by CFD and sub-channel analysis

Table 7.1 Comparison of coolant temperature at the outlet of assembly

Outlet Location	2x2			3x3		
	CFD	Sub-channel	Error %	CFD	Sub-channel	Error %
Corner	271.7	271.0	0.24	272.0	270.1	0.24
Wall	276.2	276.8	-0.22	276.9	277.6	-0.22
Centre	283.8	284.9	-0.38	284.6	285.8	-0.38
Bundle	276.5	279.4	-1.05	279.2	279.4	-1.05

Table 7.2 Comparison of GE nine pin bundle test – Isothermal test cases

TEST POINT	Data From	Mass Flux at the outlet (kg/m^2/s)				**Error %**		
		Bundle	Corner	Wall	Center	Corner	Wall	Center
1B	Exp. Data	651.0	421.8	626.6	713.4			
	CFD Analysis	651.0	481.6	633.0	728.0	-14.19	-1.03	-2.05
	SUBCHANNEL	651.0	435.9	614.9	754.7	0.78	-0.52	2.00
1C	Data	1342.6	950.7	1273.5	1559.6			
	CFD	1342.6	1008.5	1307.1	1494.7	-6.09	-2.64	4.17
	SUBCHANNEL	1342.6	942.8	1280.3	1529.8	0.78	-0.52	2.00
1D	Data	2047.9	1485.0	1954.3	2292.0			
	CFD	2047.8	1552.1	1995.6	2273.0	-4.52	-2.11	0.83
	SUBCHANNEL	2047.9	1487.8	1963.8	2305.5	-0.17	-0.48	-0.60
1E	Data	2671.7	2197.0	2590.3	2970.1			
	CFD	2671.8	2036.5	2605.1	2959.8	7.31	-0.57	0.34
	SUBCHANNEL	2671.7	1971.9	2570.0	2989.1	11.05	0.78	-0.64

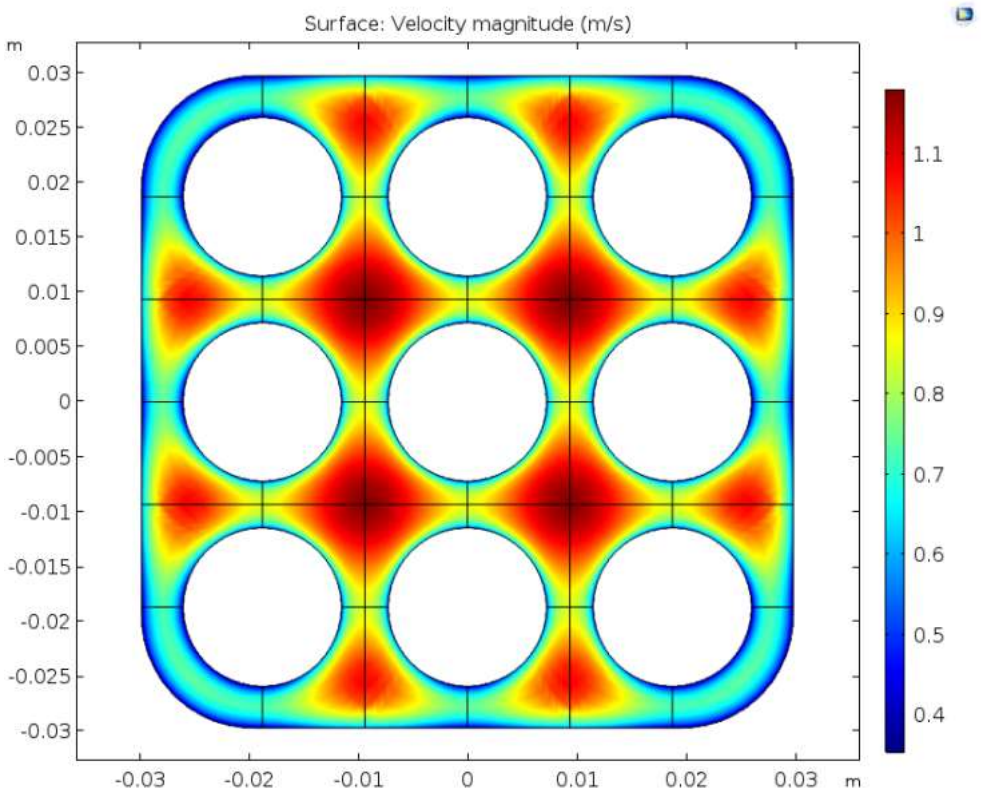

Fig. 7.4 The contours of velocity at the outlet of 3x3 GE nine pin Bundle

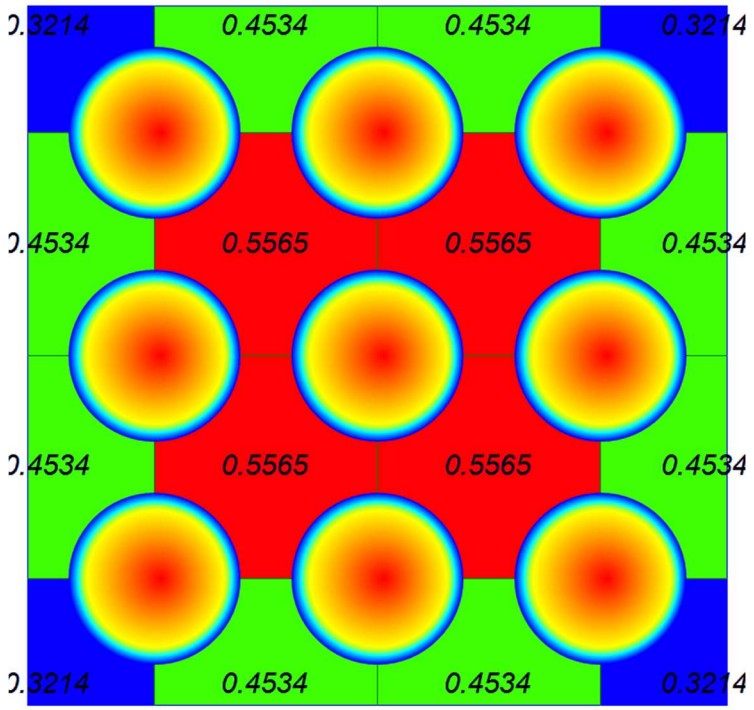

Fig. 7.5 The contours of mass flux (Mlb/hrft^2) at the outlet of 3x3 GE nine pin bundle from sub-channel analysis

7.5 Result and Discussion

7.5.1 Effect of cross-flow mixing on sub-channel temperature with bundle size

The comparison of the sub-channel outlet temperature in centre, wall and corner sub-channel of square pitched fuel assembly for 3x3, 10x10 and 17x17 are shown in Fig. 7.6. It is observed that for 3x3 bundle, the central sub-channel outlet temperature decreased from 287.5 ^{o}C for no mixing to 279.7^{o}C for high mixing, which is about 26.8% reduction in the average coolant temperature difference. The corner sub-channel outlet temperature increased from 270.0 ^{o}C (no mixing) to 279.0 ^{o}C (high mixing), which is around 31% increase on the cornel sub-channel temperature rise with respect to the bundle average outlet temperature. Similarly, for the wall channel, the outlet temperature increased from 277 ^{o}C (no mixing) to 279.2 ^{o}C, which is ~7% increase in coolant temperature difference for wall sub-channel. Similar comparison of the centre, wall and corner sub-channels of 10x10 and 17x17 large size bundle is also depicted in Fig. 7.6. It is observed that the centre sub-channel (hot channel) outlet temperature is not much affected. In case of the wall and corner sub-channel, the increase in outlet temperature in larger bundle is almost at the same order as in case of smaller bundle. When the parameter 'c' is greater than 0.04, the change in sub-channel outlet temperature is negligible for small sized fuel bundle.

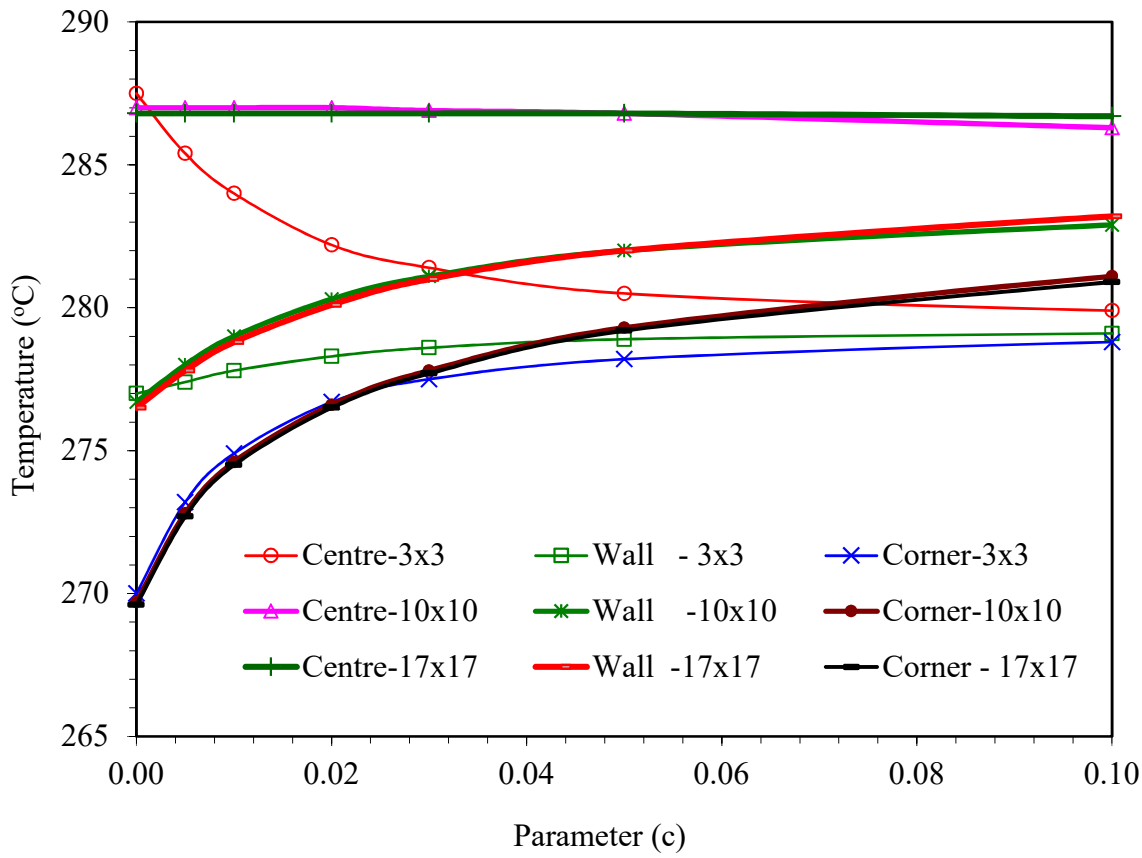

Fig. 7.6 Effect of change in the sub-channel outlet temperature with the parameter (c) in the mixing correlation for different size of the bundle

The effect of change in the bundle size on the centre sub-channel outlet temperature for a given degree of mixing is depicted in Fig. 7.7. For the centre channel, in case of smaller sized bundle, it is observed that there is a strong interaction between centre sub-channel to the wall and corner sub-channel which is evident from the sub-channel outlet temperature. The effect of bundle size on the wall sub-channel outlet temperature as a function of parameter 'c' is shown in Fig. 7.8.

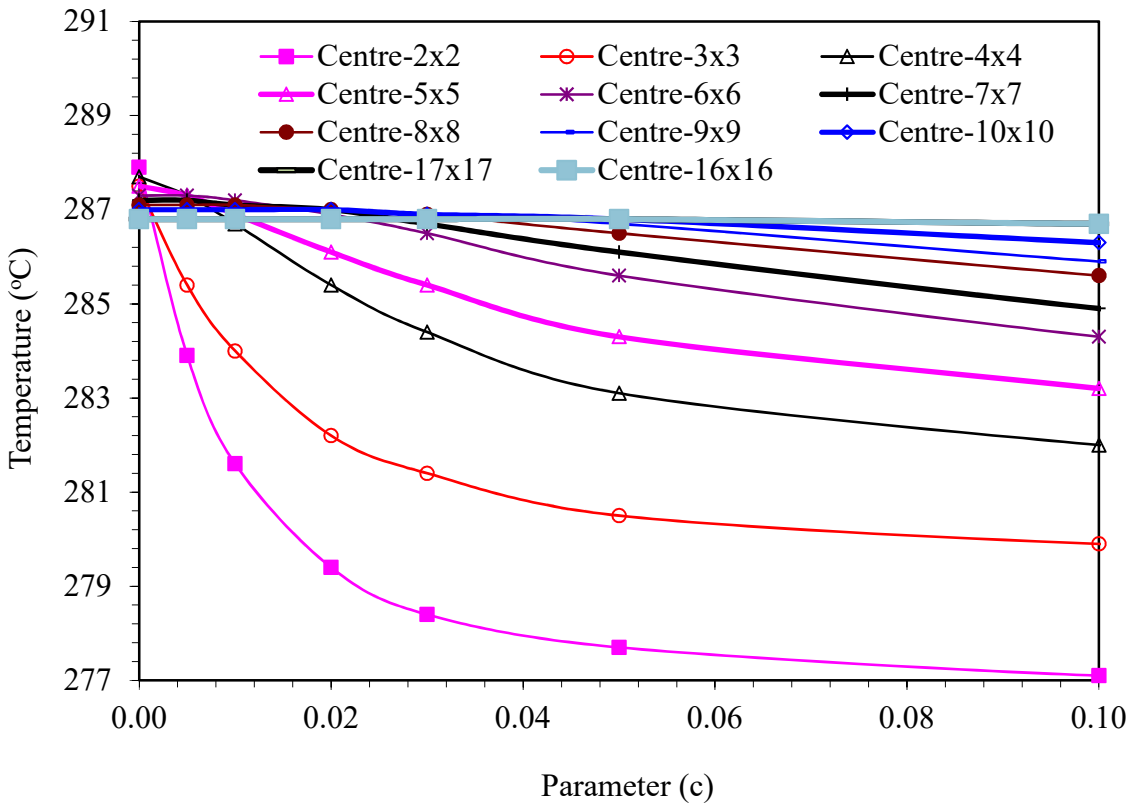

Fig. 7.7 Effect of bundle size on the center sub-channel outlet temperature with parameter (c) in the mixing correlation

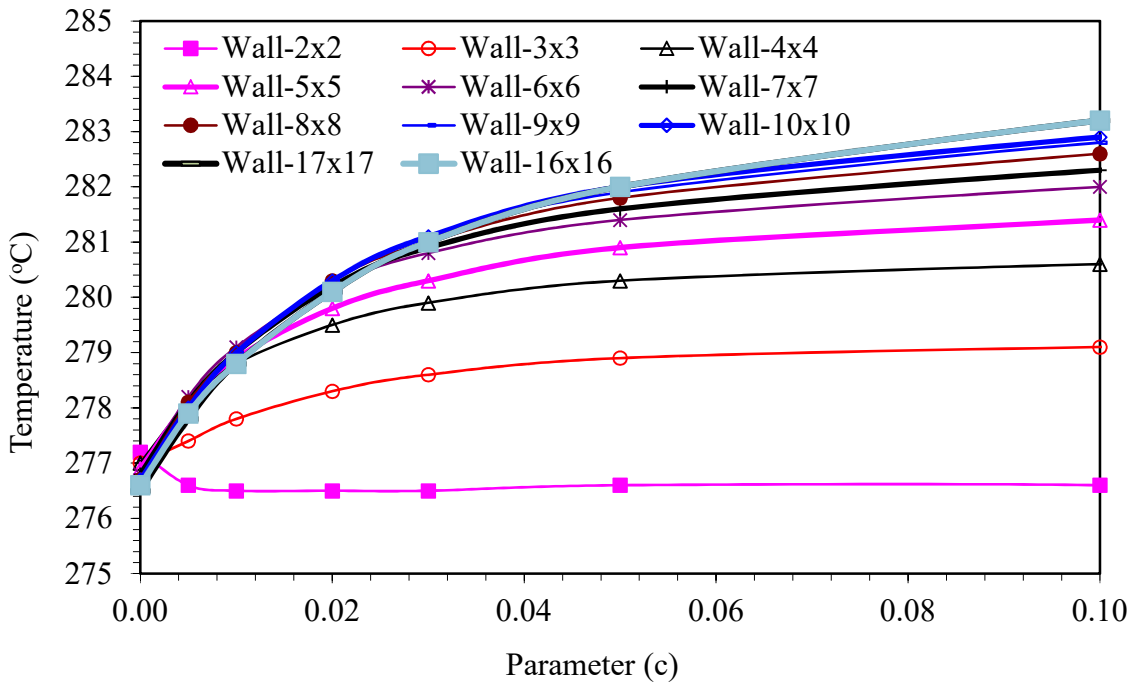

Fig. 7.8 Effect of bundle size on the wall sub-channel outlet temperature with parameter (c) in the mixing correlation

The increase in the wall sub-channel temperature is less in case of smaller sized bundle and as the bundle size increases, the corresponding increase in the wall sub-channel outlet temperature is observed. When the bundle size increases above 5x5, the wall sub-channel temperatures are more or less same irrespective of the bundle size. The effect of bundle size on the corner sub-channel outlet temperature is depicted in Fig. 7.9.

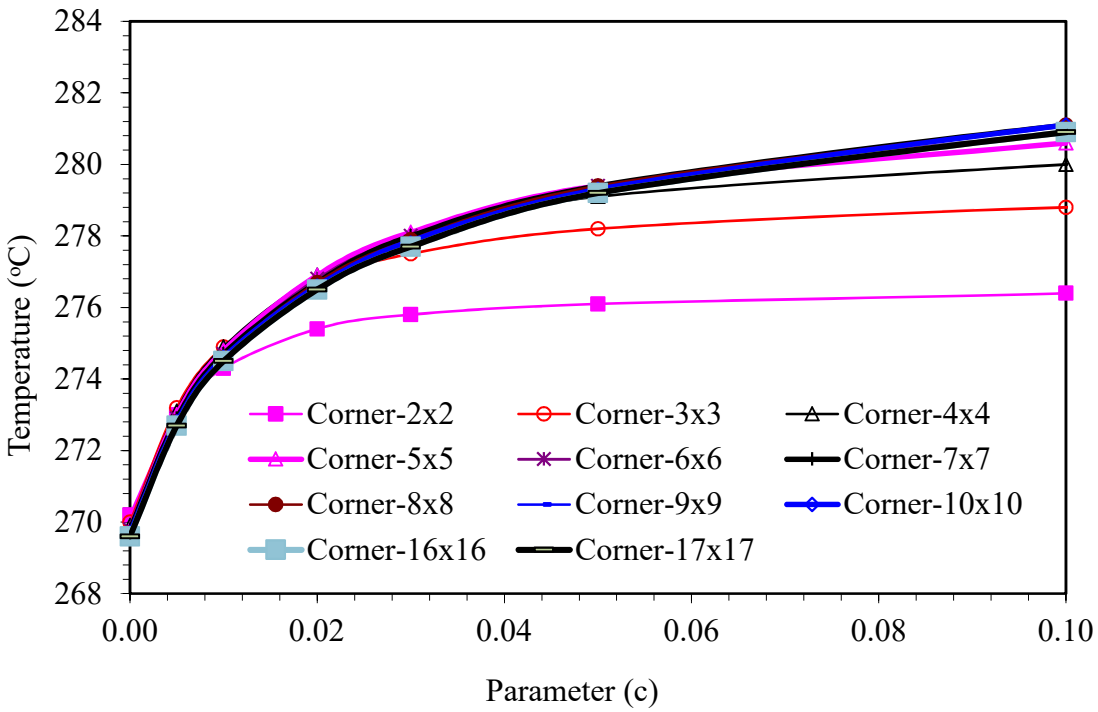

Fig. 7.9 Effect of bundle size on the corner sub-channel outlet temperature with parameter (c) in the mixing correlation

It is clear from this figure that the increase in sub-channel outlet temperature is more or less same and is independent of the size of the bundle (above 5x5) for a given degree of mixing. However, as the parameter (c) increases, the turbulent inter-channel mixing increases and the coolant between sub-channels gets mixed and more temperature

uniformity takes place. The parameter (c) depends on geometry as well as other flow and heat transfer conditions. Hence, for a given size and geometry of the bundle, proper degree of turbulent inter-channel mixing is to be used for realistic prediction of sub-channel temperatures. It is also evident that the interaction between centre and wall, corner sub-channel is strong in smaller size bundle (Fig. 7.7). In a larger size bundle, the centre sub-channel is less affected as compared to the wall and corner sub-channel. Also, due to mixing, the increase in the wall and corner sub-channel temperature is more for larger sized bundles as compared to the smaller sized bundle for the same length of fuel pin with similar flow and heat flux conditions as depicted in Figs. 7.7-7.9.

The contour plots of the sub-channel temperatures for 3x3 fuel assembly at the outlet plane of the assembly for different mixing parameters is shown in Figs. 7.10-7.11. It is clear from these figure that in case of isolated sub-channel (i.e. no cross-flow mixing) the difference in temperature between corner and central sub-channel is of the order of 15ºC at the outlet of the assembly. As mixing enhances, the temperature uniformity among the sub-channels is observed. Figures 7.10-7.13 and Fig. 7.14 depict the sub-channel outlet temperature at different mixing parameters for 10x10 and 17x17 fuel bundle respectively. It can be seen that, in the case of small bundle, more uniformity in outlet temperature takes place as compared to the large sized bundle. In large size bundle, the hot channel gets less affected in case of uniform heating of all the pins. The presence of non-fuel pins in the interior of the fuel assembly can change the hot channel temperature rise. The diffusion of heat from the inner sub-channel to wall is clearly observed from Figs. 7.13 and 7.14 with increase in mixing parameters.

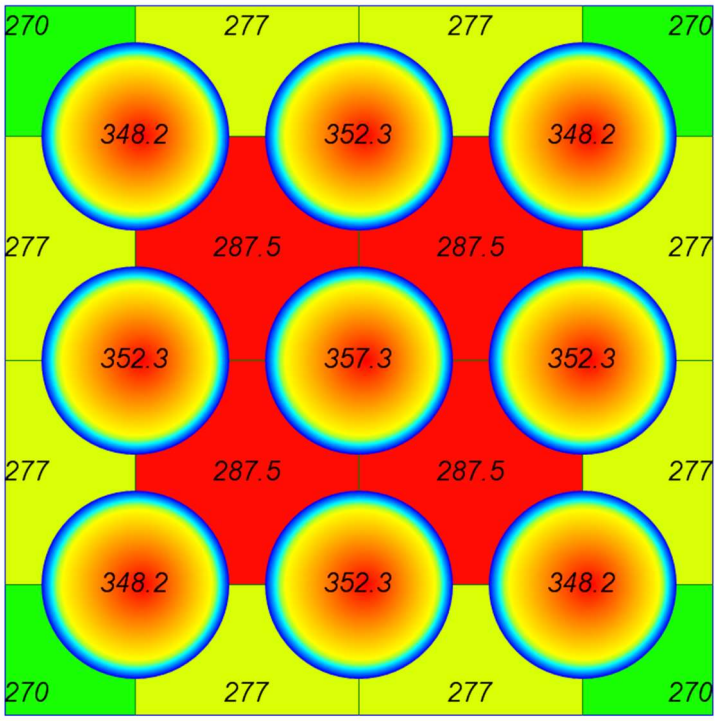

a) c=0.00
(Tsmin=270.0, Tsmax=287.5) (Tfmin=348.2, Tfmax=357.3)

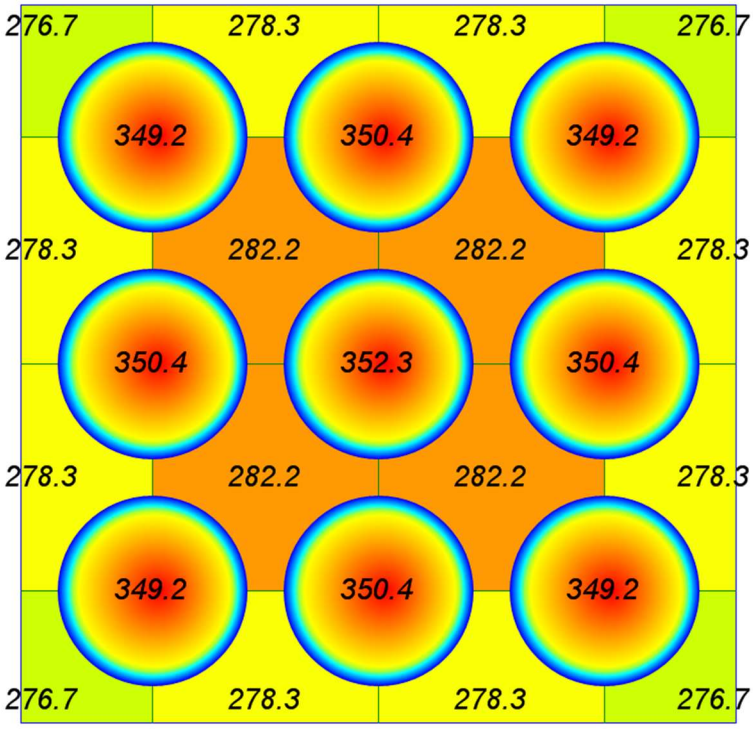

b) c=0.02
(Tsmin=276.7, Tsmax=282.2) (Tfmin=349.2, Tfmax=352.3)

Fig. 7.10 Contours of sub-channel temperature (ºC) at the outlet of 3x3 square pitched fuel assembly for mixing parameter (a) c = 0.00 and (b) c=0.02

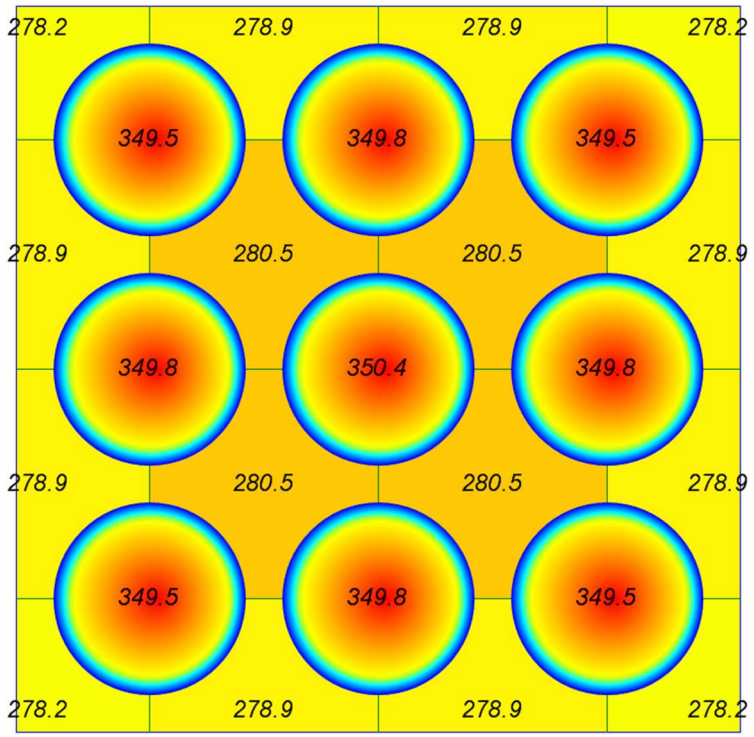

a) c=0.05
(Tsmin=278.2, Tsmax=280.5) (Tfmin=349.5, Tfmax=350.4)

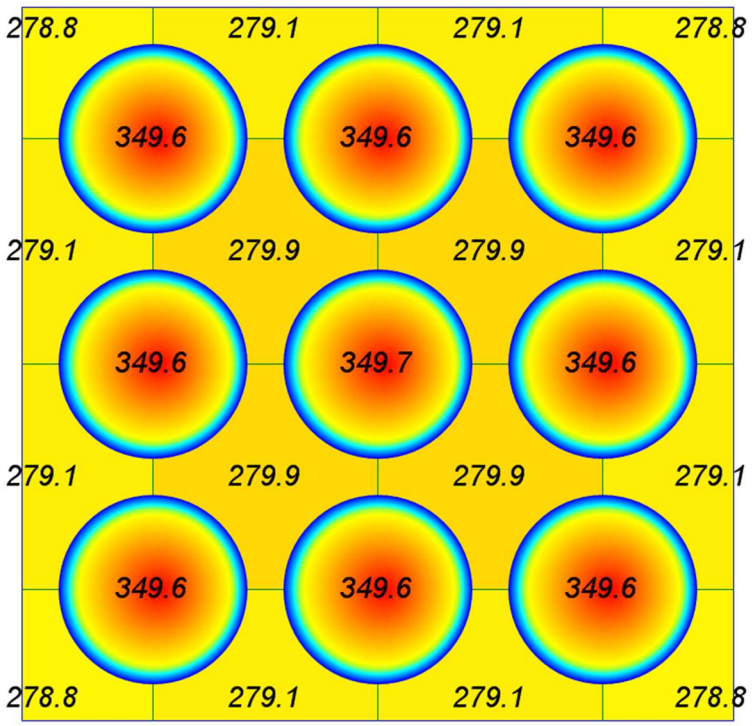

b) c=0.10
(Tsmin=278.8, Tsmax=279.9) (Tfmin=349.6, Tfmax=349.7)

Fig. 7.11 Contours of sub-channel temperature (ºC) at the outlet of 3x3 square pitched fuel assembly for mixing parameter (a) c=0.05 and (b) c=0.10

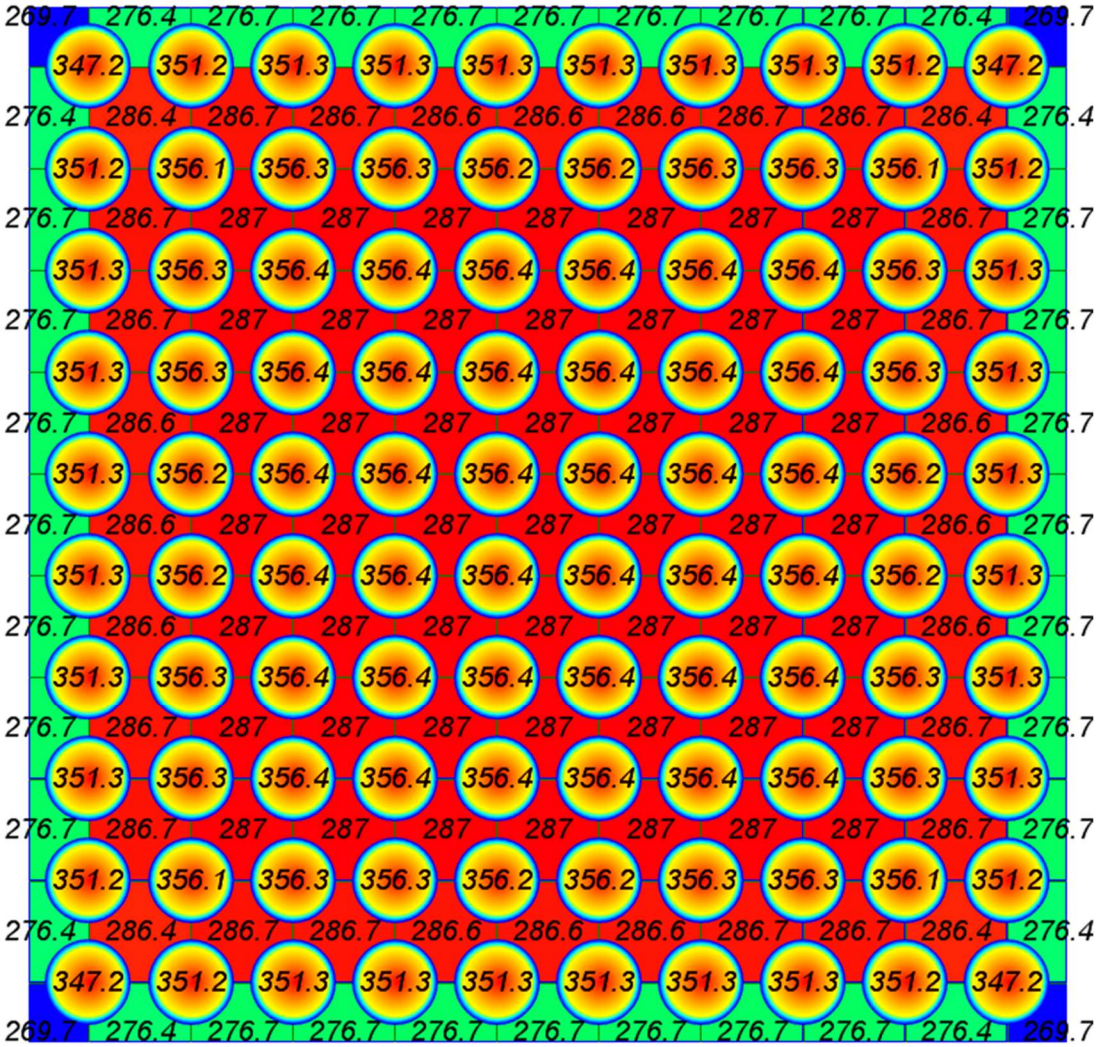

c=0.00

(Tsmin=269.7, Tsmax=287.0, Tfmin=347.2, Tfmax=356.4)

Fig. 7.12 Contours of sub-channel temperature (°C) at the outlet of 10x10 square pitched fuel assembly for mixing parameter c=0.00

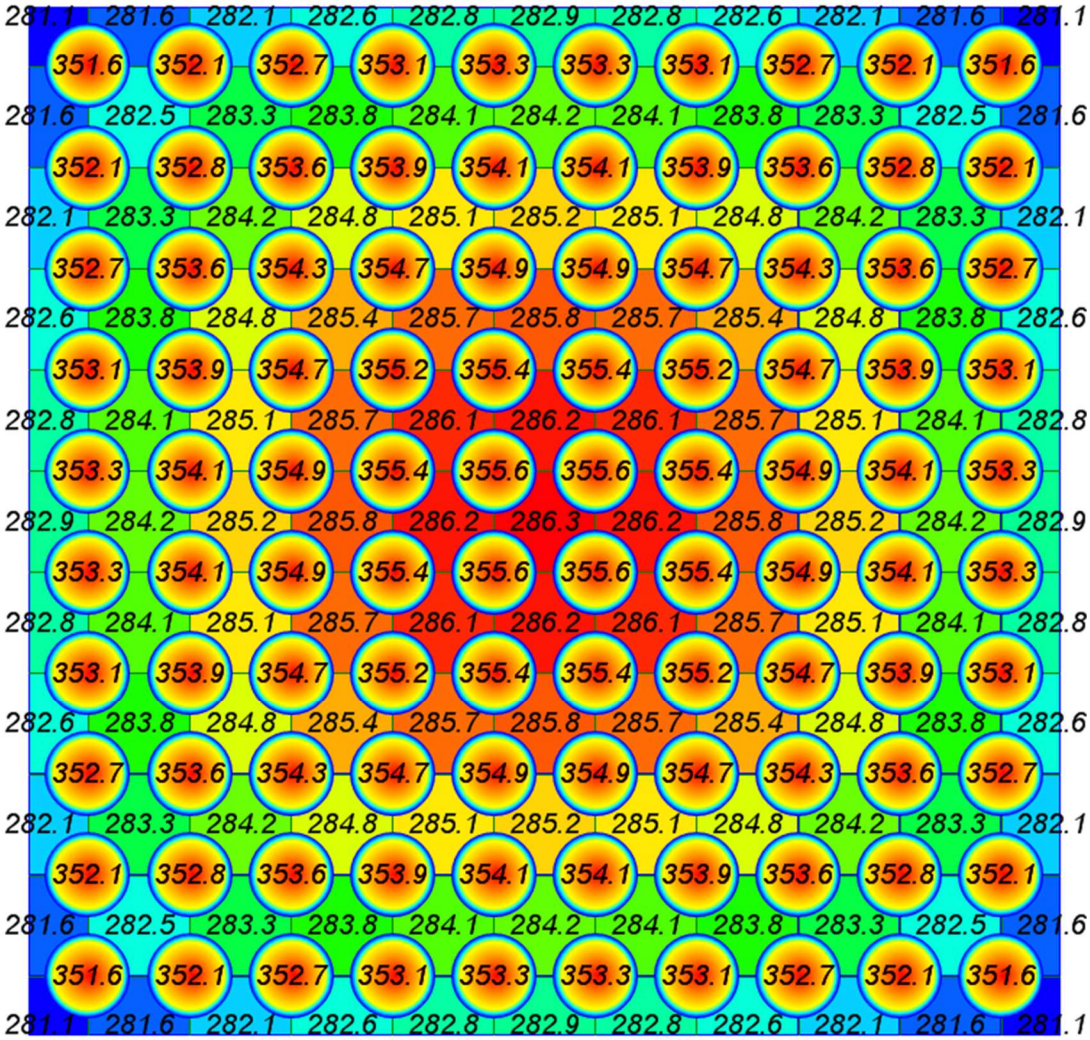

c=0.10

(Tsmin=281.0, Tsmax=286.3, Tfmin=351.6, Tfmax=355.6)

Fig. 7.13 Contours of sub-channel temperature (ºC) at the outlet of 10x10 square pitched fuel assembly for mixing parameter c=0.10

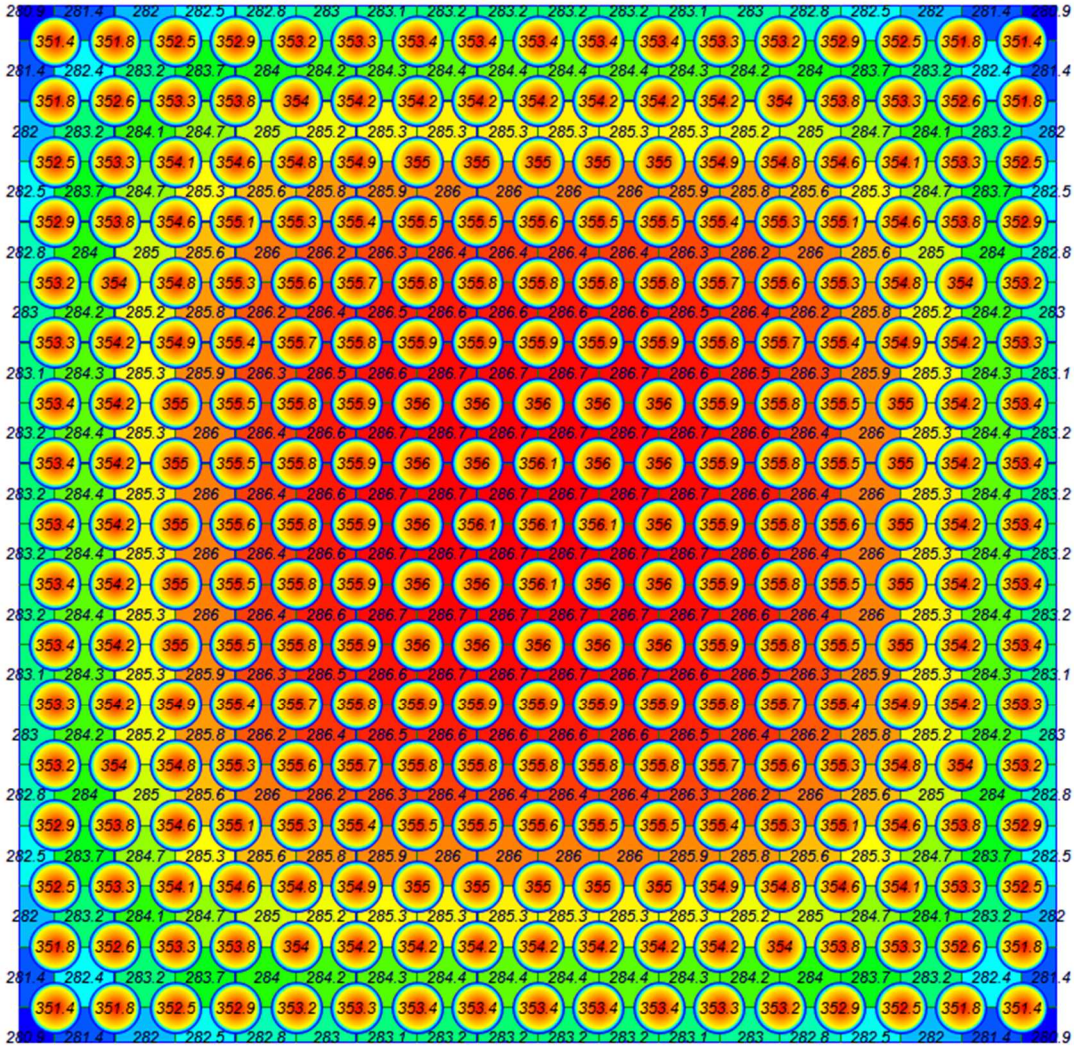

c=0.10 , (Tsmin=280.9, Tsmax=286.7, Tfmin=351.4, Tfmax=356.1)

Fig. 7.14 Contours of sub-channel temperature (ºC) at the outlet of 17x17 square pitched fuel assembly for mixing parameter c=0.10

The pin power distributions of actual nuclear reactor core are varying non-uniformly in radial as well as in axial directions. The axial power profile of bare core varies as chopped cosine form (Tong and Tang, 1997). In the actual core, due to presence of control rod, the axial power profile is skewed towards the bottom of the core at the beginning of life. As the burn up increases, the control rods goes up, to compensate the reactivity and towards the end of life the power profile are skewed at the top of the core. In the framework, non-uniform axial power profile was also specified as follows,

$$q''(z) = q''_o \left[A + B\, cos\left(2C\left(\frac{z}{L} - 0.5\right)\right)\right] \tag{7.7}$$

The constants A, B and C are chosen such that the average peaking factor of the channel is 1 and the maximum axial peaking factor is 1.61 at the middle of the core due the assumption of chopped cosine profile. The axial power profile considered in the present analysis is shown in Fig. 7.15.

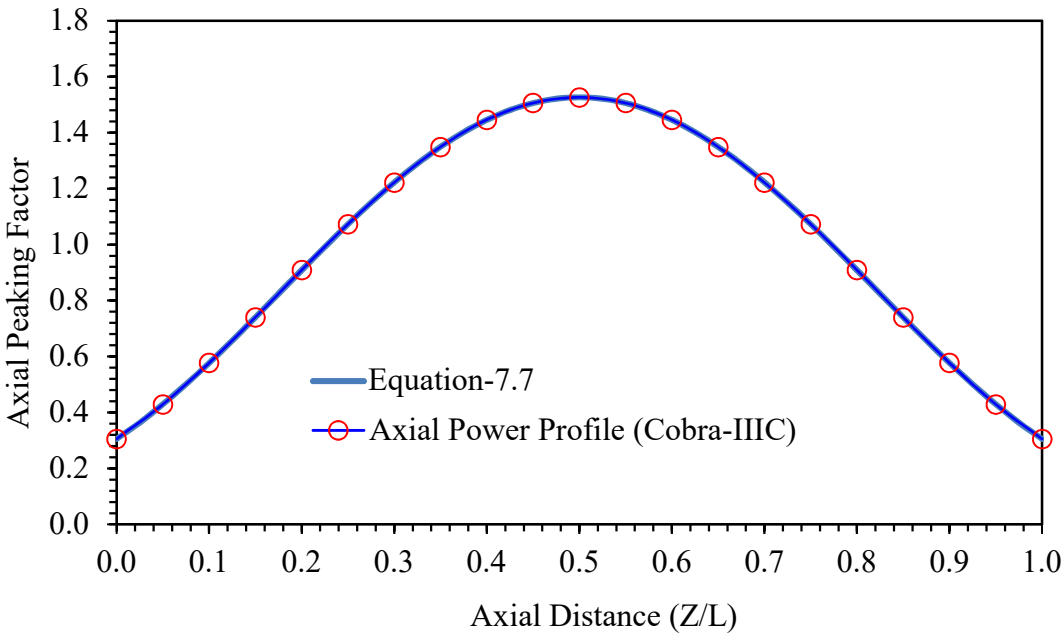

Fig. 7.15 Variation of Non-Uniform Axial Power Profile for 3X3 bundle

The effect of axially uniform and non-uniform power profile on the critical heat flux for 3x3 fuel bundle is studied by varying the mixing parameter. The critical heat flux is estimated based on the 1996 Lookup table method (Groeneveld et al. 1996, Lee, 2000). The variation of critical heat flux ratio (CHFR) with uniform and non-uniform axial power profile for 3X3 bundle is shown in Figs. 7.16 and 7.17 respectively. The CHFR is estimated using CHF Lookup table method and based on the local conditions of coolant in the sub-channel. As the power input to each sub-channel is same in both

uniform and non-uniform case, the sub-channel outlet temperature is observed to be same in both cases.

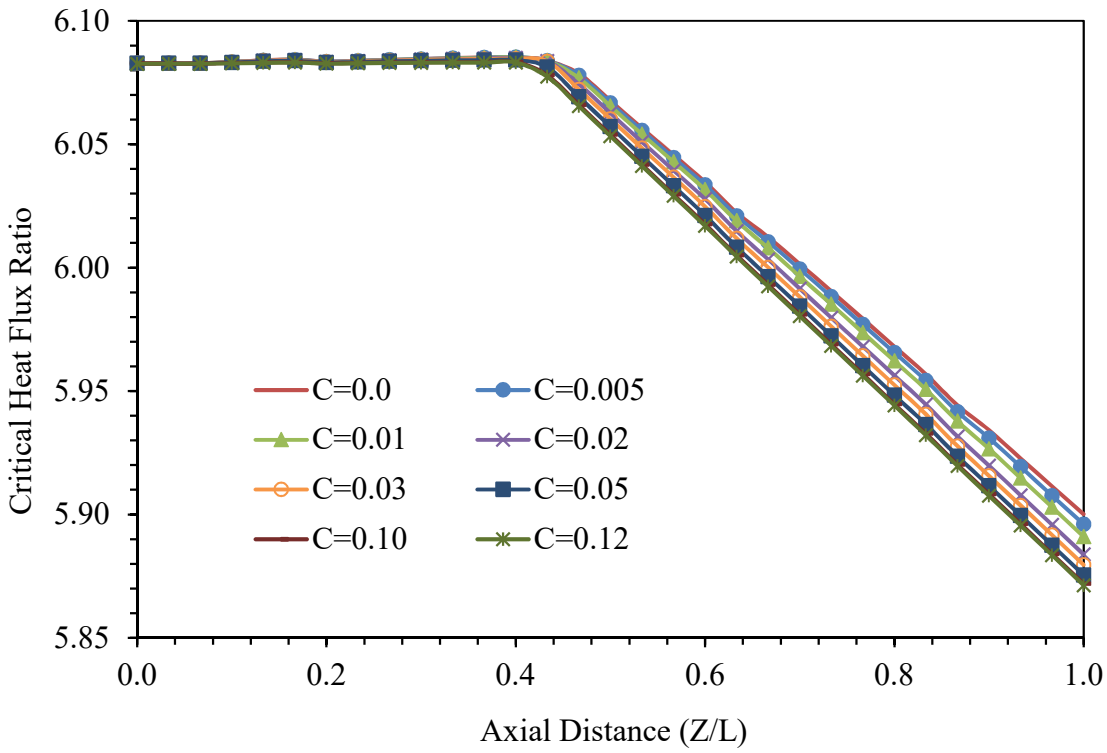

Fig. 7.16 Variation of critical heat flux ratio with uniform axial power profile for 3x3 bundle

In case of the uniform axial power profile, the minimum CHFR occurred at the outlet of the bundle as shown in Fig. 7.16. and the uniform value of CHFR of 6.08 for z/L<0.4 is also observed. Since, CHFR calculations are performed for all regions of core and the capping of CHFR for z/L<0.4 is due to equilibrium quality of sub-channel and high mass flux region of CHF look up table. In the present case the change in CHFR value is small and hence, the uniform CHFR value is observed. In case of non-uniform power profile, even though the change in CHFR values with the mixing parameters are small and more or less constant, there is a variation of the local heat flux and hence the reduction in the CHFR is observed for z/L<0.53 in Fig. 7.17.

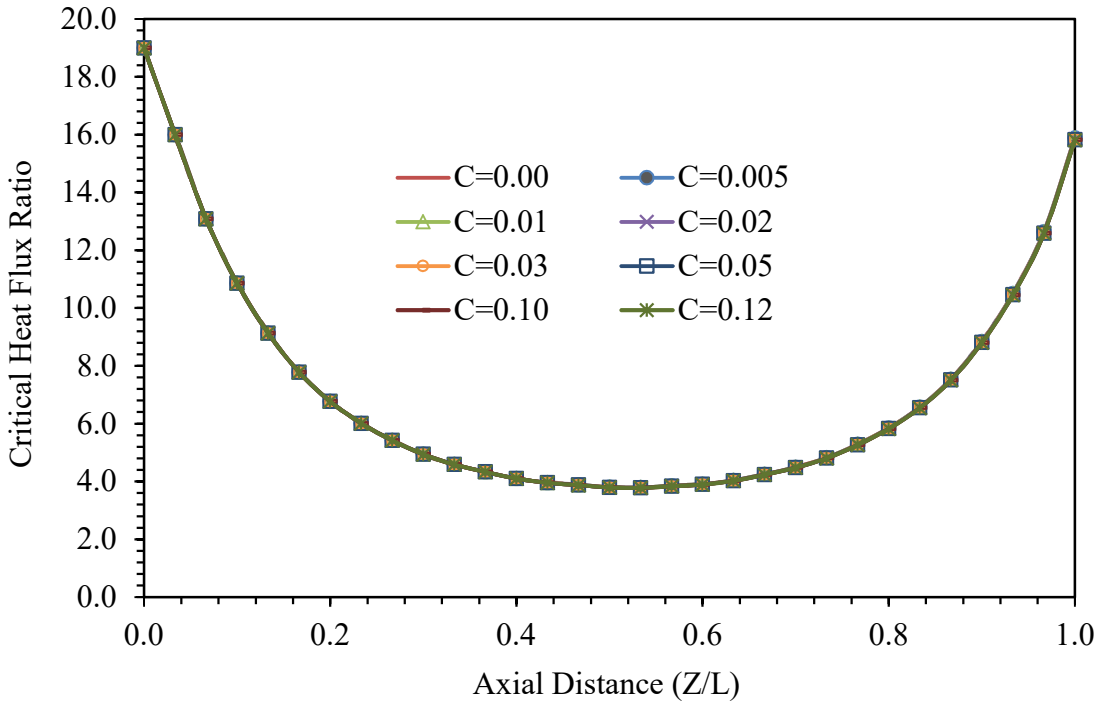

Fig. 7.17 Variation of critical heat flux ratio with non-uniform axial power profile for 3x3 bundle

In case of non-uniform power profile, the minimum CHFR occurred slightly above the middle of the core (z/L=0.53) where the local heat flux is maximum at the middle of core in the present case of the power distribution and operating condition. The actual characteristics of critical heat flux variation with operating conditions and power profile is more complex. In the present study, the effect of change in the CHFR with the mixing parameters is found to be within 0.5% for the operating conditions considered. As the power of the channel increases to the critical power of the assembly, variation in CHFR with mixing parameter is expected to be higher. It is observed that minimum CHFR is reduced from 5.90 for axially uniform heat flux to 3.79 for axially non-uniform heat flux case.

7.5.2 Effect of inlet mass flux on CHF with mixing parameter and bundle size

The study on effect of reduction in inlet mass flux on minimum critical heat flux ratio in a square fuel assembly for uniform radial and axial power distribution for various sizes of the assemblies is carried out. The calculated minimum CHFR as a function of mass flux is shown in Fig. 7.18 for bundles of size 3x3, 5x5 and 10x10 and for two different mixing parameters 'c' (0.02 and 0.05).

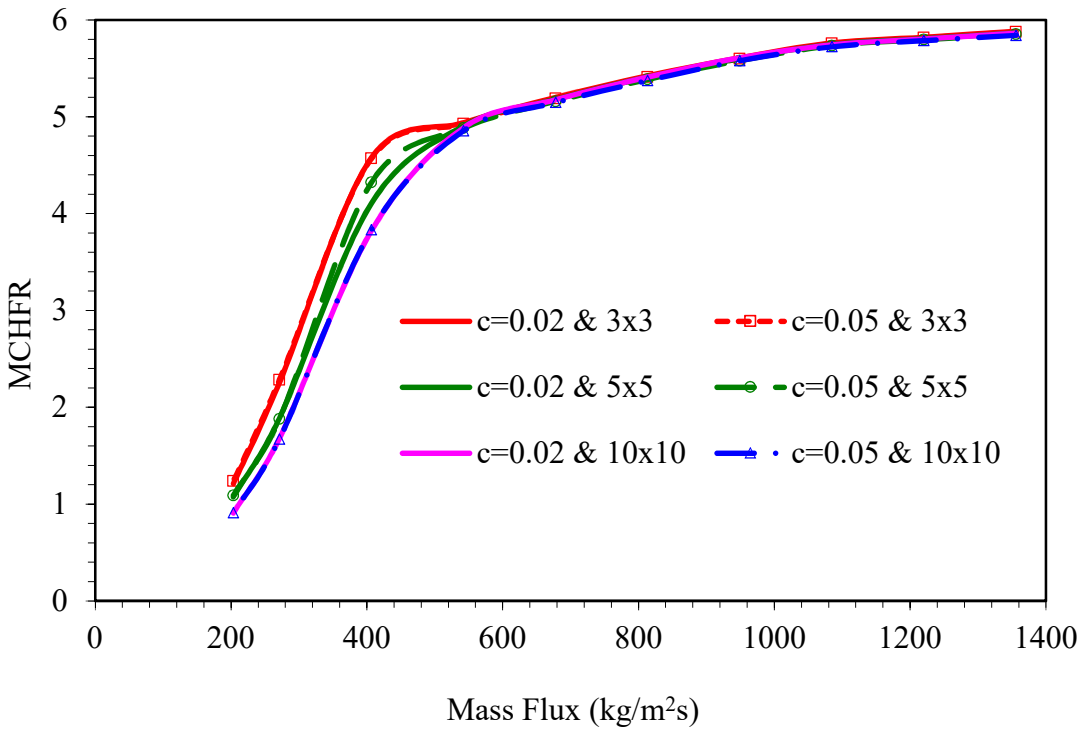

Fig. 7.18 Variation of minimum critical heat flux ratio with mass flux with uniform axial and radial power distribution for different size of bundle

The coolant inlet mass flux is varied from 1356 kg/m^{2}s to 200 kg/m^{2}s in a steps of 135 kg/m^{2}s. It is found that minimum CHFR decreases with decrease in inlet mass flux. At higher mass fluxes above 550 kg/m^{2}s, the reduction in MCHFR is observed to be insignificant. In the lower mass flux region i.e. from 550 kg/m^{2}s to 200 kg/m^{2}s, the reduction in MCHFR is observed to be significant. It is clear that in the high mass flux

region, the MCHFR is less affected even with bundle size and the mixing parameter and vice versa. The margin in MCHFR for the larger size of the bundle is lower as compared to smaller size of the bundle by ~25% in the low mass flux region. The results also indicate that for the uniform radial power distribution, change in MCHFR for a given size of the bundle is less affected with mixing parameter. It is due to the fact that the hot channel gets less affected even at increased mixing in larger size of the bundle.

7.5.3 Effect of p/d on sub-channel temperature with cross-flow mixing

The effect of cross-flow mixing on different bundle size by varying its p/d from 1.05 to 1.3 is analysed. It is assumed that the uniform mass flux is entering at the inlet of all sub-channels and is kept constant while varying the p/d ratio and the bundle size. The maximum outlet temperature for corner, wall and centre sub-channel is calculated at different degree of mixing for different sizes of the bundle. As the p/d ratio changes, the effective mass flow through the bundle gets affected and hence, the sub-channel outlet temperature. Therefore, a non-dimensional temperature (T^*) is defined (eqn. 7.8), for a comparison of the estimated sub-channel outlet temperature for different size of the bundle with given degree of mixing. The data is normalised based on average temperature rise in the bundle.

$$T^* = \frac{T_{subo} - T_{in}}{T_{avgo} - T_{in}} \tag{7.8}$$

Figures 7.19-7.22 shows the variation of the non-dimensional temperature for different p/d ratios as a function of mixing parameter (c). The comparison of non-dimensional temperature for a 2x2 bundle for different p/d ratio is given in Fig. 7.23. It is observed from the analysis that, as the p/d ratio increases, the non-dimensional temperature also increases. However, the non-dimensional temperature decreases with increase in the

degree of mixing among the sub-channel. It is also observed that, for a p/d ratio greater than 1.2, the change in non-dimensional temperature with increase in p/d ratio for a given mixing parameter is small for all the sub-channels (Fig. 7.23).

The above analysis carried out with the framework for different size of the bundle for different p/d ratio reveals that reactor fuel bundle can be constituted with different number of fuel pins for a given power rating. As the bundle size is smaller, the effective mixing between the inner and wall, corner sub-channel increases, which cause the reduction in the hot-channel temperature. In case of large sized bundle, the hot channel temperature is less affected and hence, that causes the limitation on the thermal margins.

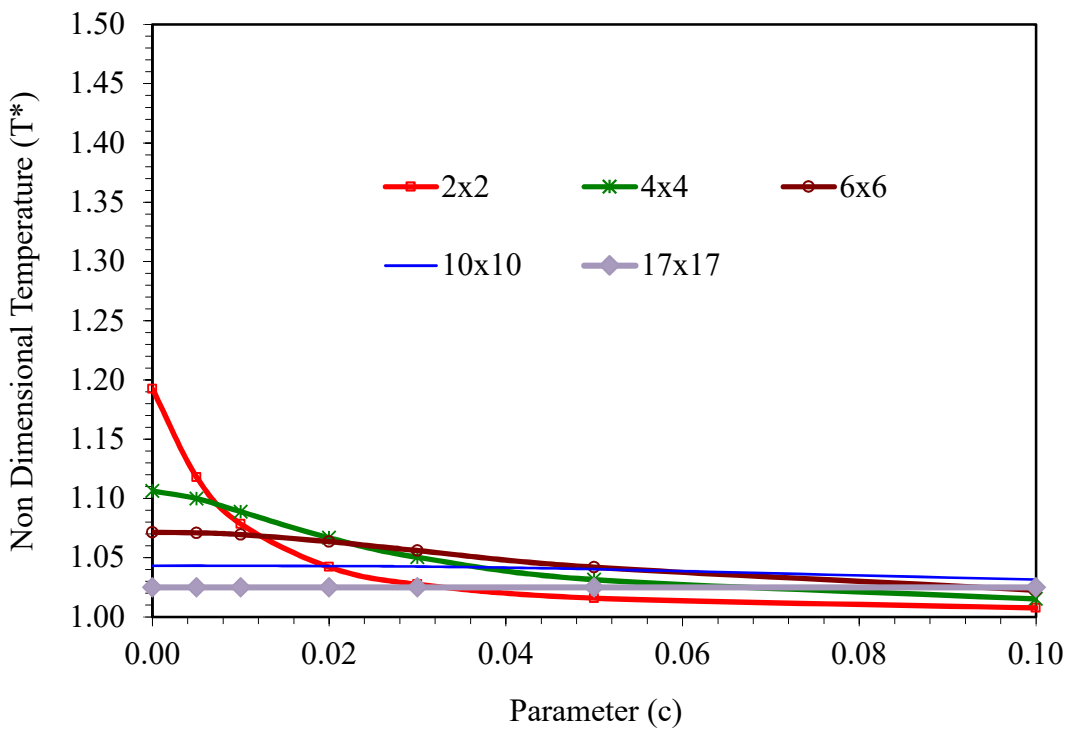

Fig. 7.19 Non-dimensional temperature of the center sub-channel for different p/d ratio of 1.05.

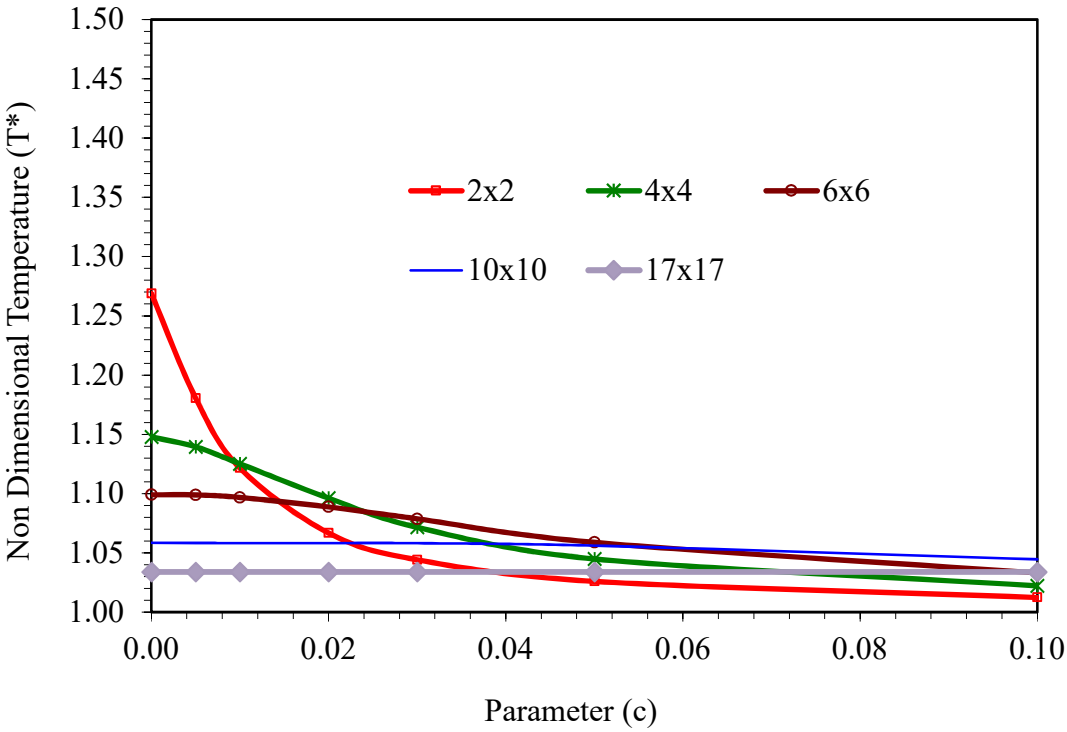

Fig. 7.20 Non-dimensional temperature of the center sub-channel for different p/d ratio of 1.10

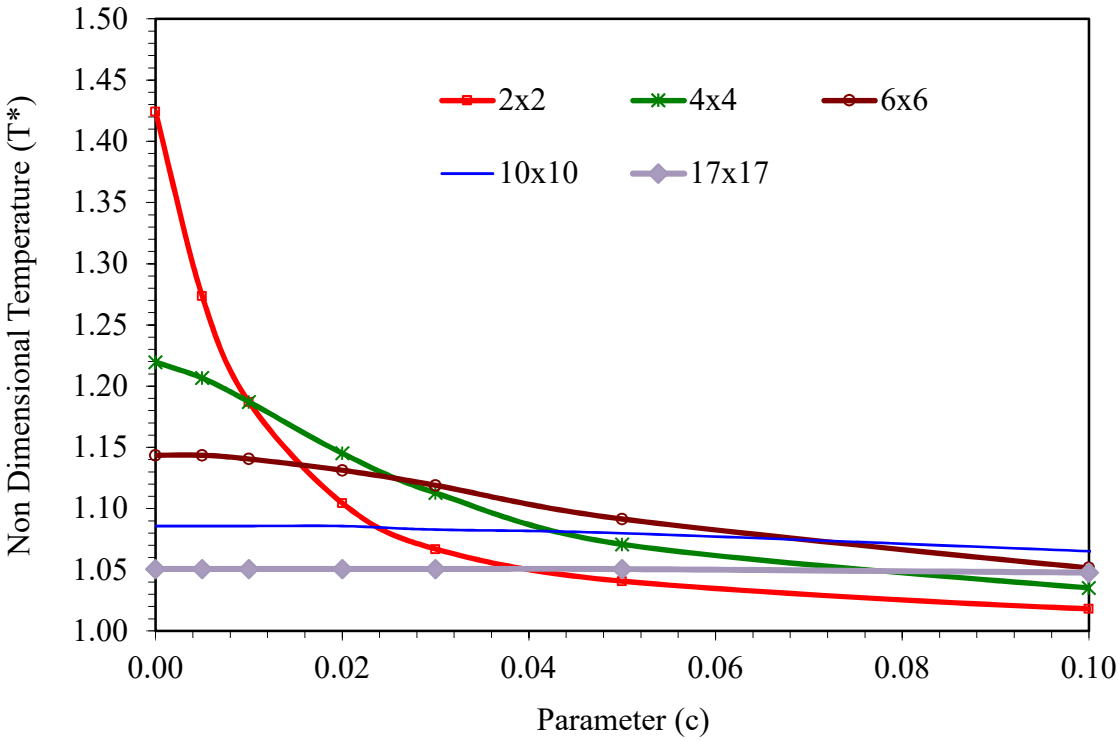

Fig. 7.21 Non-dimensional temperature of the center sub-channel for different p/d ratio of 1.20

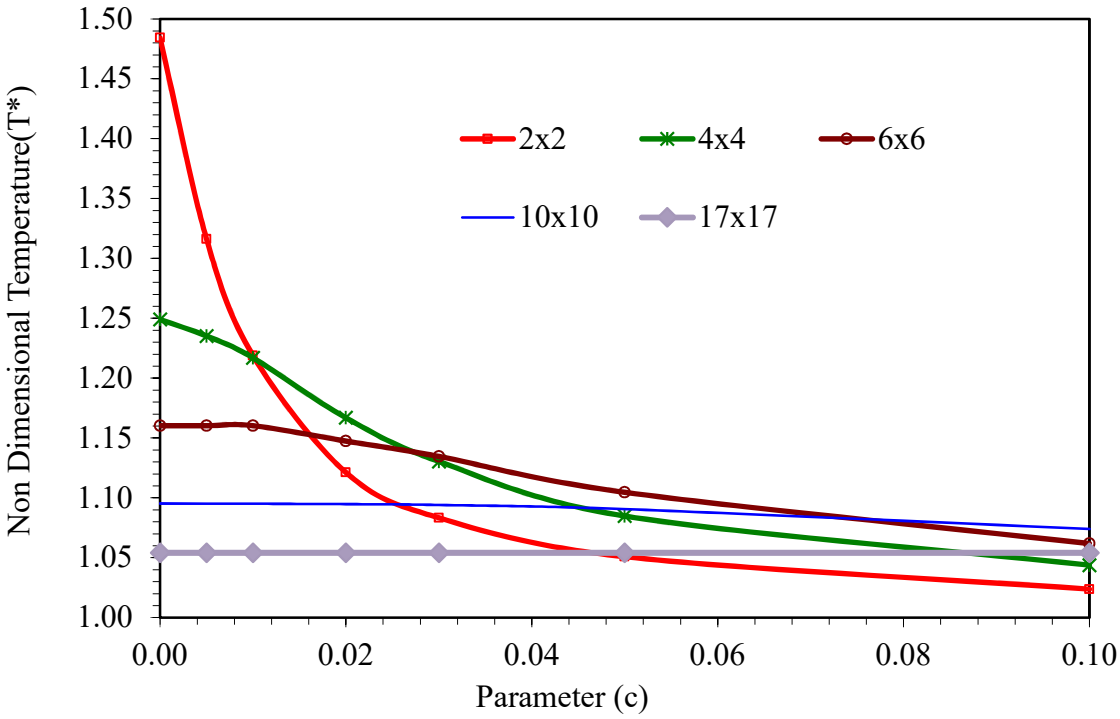

Fig. 7.22 Non-dimensional temperature of the center sub-channel for different p/d ratio of 1.30

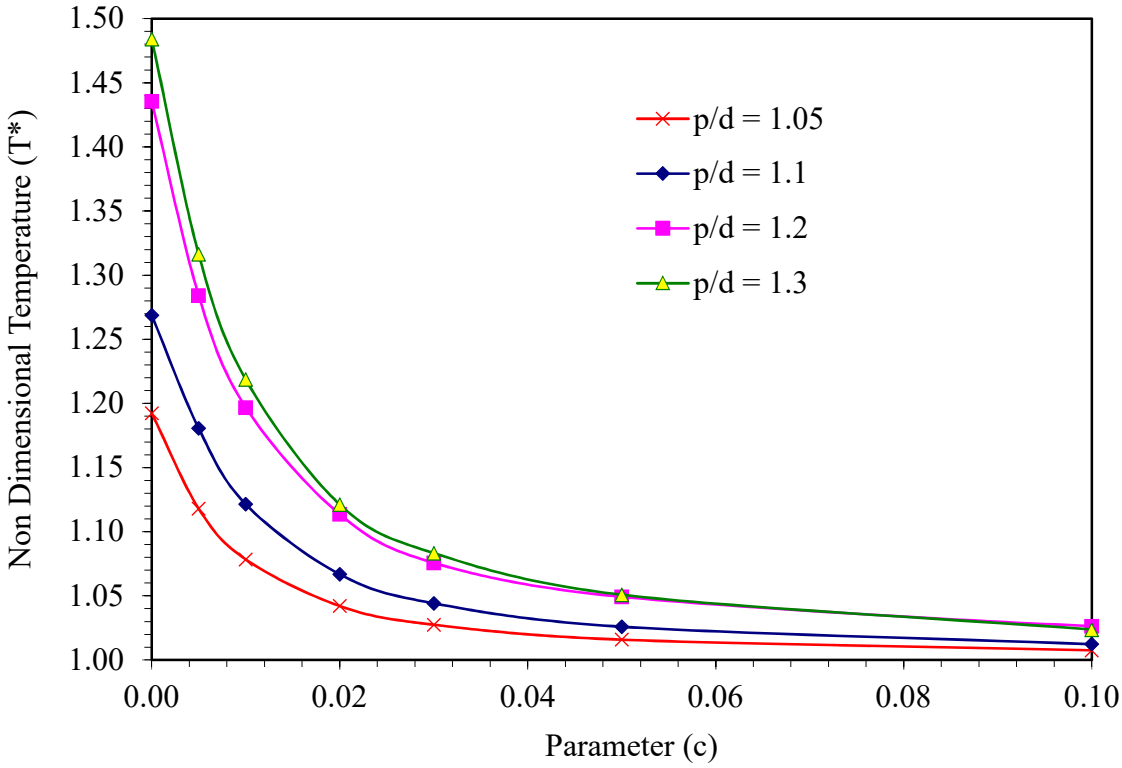

Fig. 7.23 Variation of non-dimensional temperature with parameter (c) for 2x2 pin bundle at different p/d ratios

7.6 Summary

Investigation on the effect of different degree of coolant mixing between the sub-channels for different p/d ratios in a square lattice fuel bundle is carried out to estimate the changes in the local conditions of the sub-channel. An automated sub-channel layout generation program is developed to generate different configurations of a typical fuel bundle. The comparison study demonstrates the capability of developed framework. The parametric study on the effect of cross-flow mixing parameter on coolant enthalpy rise in a fuel bundle is performed. It is found that there is ~30% increase in the temperature difference for corner sub-channels in case of complete mixing as compared to no mixing case. However, the increase in temperature difference at wall channel is only ~7%. For a large sized assembly, hot channel temperature is less affected as compared to smaller size assemblies. The hot channel temperature is decreased by 26% due to strong interaction between wall and corner channel. The wall distance significantly alters the inner sub-channel flow as well as the temperature in smaller bundle as compared to larger bundle. It is found that, for p/d ratio greater than 1.3, the non-dimensional temperature change in the central sub-channel is small irrespective of the degree of mixing. However, for the large sized bundles, the hot channel temperature is less affected thereby, putting a limitation on thermal margins. The present study is emphasizing the importance of sub-channel mixing on the thermal margins such as fuel, coolant temperature and hence, the critical heat flux. The sub-channel analysis framework developed in present study can be used to perform the thermal hydraulic analysis of nuclear reactor core in an efficient way with minimum human intervention.

7.7 Closure

In this chapter, the results of the investigations of coolant mixing in a typical nuclear reactor fuel pin bundle are discussed in detail. The special focus on the mixing parameter, the p/d ratio and the coolant inlet mass flux on the coolant temperature and flow distribution for different sizes of fuel bundle were studied and presented in this chapter. The validation of the developed code with the CFD analysis for 2x2 and 3x3 pin bundle was also demonstrated. The experimental data of isothermal flow distribution in a GE nine pin bundle tests were also used for the validation of the CFD and sub-channel analysis. The effect of non-uniform power distribution on the predicted CHF with mixing parameters for different size of the bundle is also carried out. The next chapter provides the general conclusions of the present study carried out on the investigations of coolant mixing in a typical nuclear reactor fuel pin bundles and the suggestions for future work.

CHAPTER-8

CONCLUSIONS AND SCOPE FOR FUTURE WORK

CHAPTER-8

8 CONCLUSIONS AND SCOPE FOR FUTURE WORK

8.1 Introduction

The previous chapters were devoted to the detailed description about (i) the development of the advanced sub-channel thermal hydraulic analysis framework, (ii) the fluid flow and heat transfer analysis of nuclear fuel pin bundle of both square and triangular pitched configurations and the useful correlations obtained from the study (iii) the investigations of coolant mixing in a nuclear fuel pin bundle using the developed framework. In this chapter, some of the highlights of the work and major conclusions drawn from the studies are presented. The scope for future work is also highlighted.

8.2 Highlights of the Present Study

The ultimate safety of the nuclear reactor core is ensured by performing the Sub-channel thermal-hydraulic Analysis of reactor core which involves the accurate estimation of coolant flow distribution within the fuel assembly sub-channels and hence, the accurate estimation of thermal margins of reactor core.

The CFD simulations of fluid flow and heat transfer in a square and triangular pitch fuel pin bundle are carried out using an out-of-plane flow problem. The solution of fuel bundle for different p/d and w/d ratio of square and triangular pitch pin bundle is demonstrated for a bare rod assembly instead of using a detailed 3D model. This saves a lot of computational time to find the optimum p/d and w/d ratios during the initial

design of reactor core. The detailed validation study confirms the adequacy of the model developed for studying the flow distribution in a typical nuclear fuel pin bundle.

The developed sub-channel analysis Framework was used to perform the investigation of a coolant mixing in a nuclear reactor fuel bundle and to study the effect of various geometrical parameters such as p/d, w/d and size of the bundle on coolant mixing. The different operating parameters such as pressure, inlet temperature, flow rate and power are considered in the analysis. The effect of turbulent mixing parameter on the coolant temperature change in a uniform and non-uniform power distribution is also studied.

The developed framework is extended to carry out the reliable calculations of sub-channel analysis with quick modelling approach and fast analysis methodology.

8.3 Broad Conclusions of the Present Study

8.3.1 Development of sub-channel analysis framework

i. An advanced ASTHYANS framework is developed to carry out simulations to obtain the data required for the sub-channel analysis code. This development helps in reduction of human error and reduce computer efforts.

ii. An automated sub-channel layout generation program is developed to generate different configurations of a typical fuel bundle. The comparison study demonstrates the capability of the developed framework.

8.3.2 Thermal hydraulics in sub-channel geometry of rod bundle

i. Investigations of fully developed fluid flow and heat transfer in the non-circular and rod bundle sub-channel geometries are carried out.

ii. The non-circular geometries are solved for out-of-plane flow velocity on a 2-D cross-section instead of the conventional CFD method.

iii. It has been found that the fRe increases significantly for p/d ratio of 1 to 1.15 for the sub-channel shaped geometry.

iv. In case of fuel bundle geometry, as the p/d ratio approaches the W/d ratio, the effect of bundle size on fRe vanishes.

v. For all the p/d<w/d ratio, the change in Poiseuille number is observed to be insignificant for bundle size greater than 5x5. For bundle size higher than 5x5, the effect is significant for all p/d>w/d.

vi. For engineering design applications, the correlations have been developed to evaluate Poiseuille number and Nusselt number in terms of p/d for different sub-channel geometries.

vii. The turbulent flow analysis reveals that, similar to the geometry factor for laminar flow, there exists a geometry factor for turbulent flow and is independent of Reynolds number.

viii. The study of flow in compound triangular sub-channel shows that the inlet mass flux affects the average developed length and mass exchange between sub-channel and is independent of the p/d ratios 1.05 and 1.1 due to pressure gradient.

ix. The heat addition to one of the channel shows that the mass exchange between channel continues to take place even after the pressure equalization and both channels attain different velocity distributions. The heat addition significantly affects the mass exchange.

8.3.3 Investigations of coolant mixing in rod bundle

i. Investigation on the effect of different degree of coolant mixing between the sub-channels for different p/d ratios in a square lattice fuel bundle is also carried out to estimate the changes in the local conditions of the sub-channel.

ii. It is found that there is ~30% increase in the temperature difference for corner sub-channels in case of complete mixing as compared to no mixing case. The increase in temperature difference at wall channel is only ~7%.

iii. For a large sized assembly, hot channel temperature is less affected as compared to smaller size assemblies. The hot channel temperature is decreased by 26% due to strong interaction between wall and corner channel in smaller sized assembly.

iv. It is found that, for p/d ratio greater than 1.3, the non-dimensional temperature change in the central sub-channel is small irrespective of the degree of mixing. However, for the large sized bundles, the hot channel temperature is less affected thereby, putting a limitation on thermal margins.

v. The present study is emphasizing the importance of sub-channel mixing on thermal margins such as fuel and coolant temperature and hence, critical heat flux.

8.4 Suggestions for Future Work

The study of out-of-plane flow problem can be extended to the fully developed turbulent flow simulations in a fuel bundle. The continued development in ASTHYANS framework can be taken up to include various features such as transient analysis, further incorporation of various CHF case studies. The coupled neutronic calculations can also be built-in along with the thermal hydraulic analysis. The framework can be extended to take care of the various uncertainties involved in the systems to account for the deviations in the flow, power, pressure, coolant inlet temperature and manufacturing tolerances on the estimated thermal hydraulic safety margins. The continued effort towards the code development with the object oriented methodology will help in the seamless integration of the sub-channel analysis with the system thermal hydraulics codes for the design and safety analysis of nuclear reactor core.

REFERENCES

1. Abdul-Razzak, A., Shoukri, M., Chan, A.M.C., **1992**. Rewetting of hot horizontal tubes. Nucl. Eng. Des. 138, 375–388.

2. Aly A. M. M., Trupp A. C., Gerrard A. D., **1978**. Measurements and prediction of fully developed turbulent flow in an equilateral triangular duct. Journal of Fluid Mechanics, 85, 57–83.

3. Ang M.L., Aytekin, A., Fox, A.H., **1987**. Analysis of flow distribution in a PWR fuel rod bundle model containing a 90% blockage., Nucl. Eng. Des. 103, 165-188.

4. Angel Papukchiev, Ferry Roelofs, Afaque Shams, Gregory Lecrivain, Walter Ambrosini., **2015**. Development and application of computational fluid dynamics approaches within the European project THINS for the simulation of next generation nuclear power systems. Nuclear Engineering and Design 290 (2015) 13–26.

5. Anglart, H., Nylund, O., **1996**. CFD application to prediction of void distribution in bubbly flows in rod bundles. Nucl. Eng. Des. 163 (1996) 81-98.

6. Anklam, T.M., White, M.D., **1981**. Experimental investigations of two-phase mixture level swell and axial void fraction distribution under high pressure, low heat flux conditions in rod bundle geometry., conf-810806-8.

7. AREVA NP, Inc., **2010**. "ANP-10311P, Revision 0, 'COBRA-FLX: A Core Thermal-Hydraulic Analysis Code Topical Report,'" March 31, 2010, ADAMS Accession No. ML101550172.

8. Axford, R.A., **1967**. Two-dimensional multi region analysis of temperature fields in reactor tube bundles, Nucl. Eng. Des. 6, 25.

9. Baglietto, E., Ninokata, H., **2003**. Turbulence models for heat transfer simulation in tight lattice fuel bundles. In: 10th International Topical Meeting on Nuclear Reactor Thermal Hydraulics (NURETH-10), Seoul, Korea, October-2003, 5–9.

10. Baglietto, E., Ninokata, H., **2004**. CFD Modeling of Secondary Flows in Fuel Rod Bundles. NUTHOS-6, Nara, Japan.

11. Baglietto, E., Ninokata, H., **2005**. A turbulence model study for simulating flow inside tight lattice rod bundles, Nucl. Eng. Des. 235 (2005) 773-784.

12. Baglietto, E., Ninokata, H., Misawa, T., **2006**. CFD and DNS methodologies development for fuel bundle simulations. Nucl. Eng. Des. 236, 1503–1510.

13. Bahrami, M., Yovanovich, M. M., and Culham, J. R., **2005**. Pressure drop of fully developed Laminar flow in micro channels of arbitrary cross-section. Proceedings of ICMM, 3rd international conference on Micro and mini channels, Toronto, Ontario, Canada.

14. Baratto, F., Bailey, S.C.C., Tavoularis, S., **2006**. Measurements of frequencies and spatial correlations of coherent structures in rod bundle flows., Nucl. Eng. Des.236, 1830-1837.

15. Barletta, A., Rossi di Schio, E. and Zanchini, E., **2003**. Combined forced and free flow in a vertical rectangular duct with prescribed wall heat flux. International Journal of Heat and Fluid Flow, 24, PP-874-887.

16. Barrow, H. Hassan, A. K. A., and Avgerinos, C., **1984**. Peripheral temperature variation in the wall of a non-circular duct - An experimental investigation., International Journal of Heat and Mass Transfer, 27(7), PP-1031-1037.

17. Basehore, K. L., Todreas, N. E., **1980**, SUPERENERGY-2: A Multi assembly, Steady-State Computer Code for LMFBR Core Thermal-Hydraulic Analysis., PNL-3379, C00-2245-57TR, August 1980.

18. Basile, D., Chierici, R., Beghi, M., Salina, E., and Brega, E., **1999**. "COBRA-EN, an Updated Version of the COBRA-3C/MIT Code for Thermal-Hydraulic Transient Analysis of Light Water Reactor Fuel Assemblies and Cores," Report 1010/1 (revised 1.9.99), ENEL-CRTN Compartimento di Milano.

19. Baumann, W., MISTRAL-II, **1972**. Thermohydraulische Mischströmungsalgorithmen für Stabbündel. KfK 1605, Juni 1972 (in German).

20. BAW-10156-A, Rev. 1, **1993**. LYNXT Core Transient Thermal-Hydraulic Program, B&W Fuel Company, August 1993.

21. Beus, S.G., **1970**. A Two-Phase Turbulent Mixing Model for Flow in Rod Bundles., WAPD-T-2438.

22. Beus, S. G., **1971**. A two-phase turbulent mixing model for flow in rod-bundle. Technical Report WAPD-T-2438, Bettis Atomic Power Energy.

23. Biemüller, M., Meyer, L., Rehme, K., **1996**. Large eddy simulation and measurement of the structure of turbulence in two rectangular channels connected by a gap. In: Heraklion, G.R., Rodi, W. (Publ.), Proc. 3rd Internat. Symp., Eng. Turbulence Modelling and Experiments, Elsevier, Amsterdam (u.a.), pp. 249–258.

24. Billings, Jay Jay, Deyton, Jordan H., Forest Hull III, S., Lingerfelt, Eric J., Wojtowicz, Anna, 2015. A domain-specific analysis system for examining nuclear reactor simulation data for light-water and sodium-cooled fast reactors., Annals of Nuclear Energy, 85, 856-868.

25. Bishop, A.A., Todreas, N.E., **1979**. Hydraulic characteristics of wire-wrapped rod bundles. Nucl. Eng. Des. 62, 271-293.

26. Bo Pang., **2013**. Numerical study of void drift in rod bundle with subchannel and CFD codes, Dissertation, KIT-SR-7669., Karlsuhe Institute of Technology.

27. Bowring R.W., **1968**. HAMBO, a computer programme for the subchannel analysis of the hydraulic and burnout characteristics of rod clusters, part 1: general description, AEEW-R524, 1967, and part 2: the equations, AEEW-R582, 1968.

28. Burns, C. J., Aumiller, D.L., **2007**. COBRA-IE evaluation by simulation of the NUPEC BWR full-size fine-mesh bundle tests (BFBT)., B-T-3653.

29. Burtak, F., Heinecke J., Gluck M., Kronenberg, J. Kollmann, T., **2006**. Advanced thermal hydraulic core and fuel assembly design with state-of-the-art subchannel codes, International meeting on LWR fuel performance, TopFuel-2006., Pg-127-131., Salamanca, Spain.

30. Carajilescov Pedro., **1975**. Experimental and analytical study of Axial Turbulent Flows in an interior subchannel of a bare rod bundle., PhD Thesis., Massachusetts Institute of Technology. MIT., March -1975.

31. Carajilescov, P., Todreas, N.E., **1976**. Turbulent diffusion of heat between connected flow passages. Nucl. Eng. Des. 54, 183–195.

32. Carelli, M., Curzio, G., Renieri, A., **1969**. A radioactive tracer technique for measuring coolant mixing in nuclear reactor fuel sub-assembly, Nucl. Eng. Des. 11, 93-102.

33. Carlucci, L.N., Hammouda, N., Rowe, D.S., **2004**. Two-phase turbulent mixing and buoyancy drift in rod bundles. Nucl. Eng. Des. 227, 65–84.

34. Carver, M.B., Tahir, A., Rowe, D.S., Tapucu, A., Ahmad, S.Y., **1984**. Computational analysis of two-phase flow in horizontal bundles, Nucl. Eng. Des. (1984).

35. Castellana, F.S., Adams, W.T., Casterline, J.E., **1974**. Single phase sub-channel mixing in a simulated nuclear fuel assembly., Nuclear Engineering and Design, 26, 242-249.

36. Castellani, F., Curzio, G., Pieve, L., Grazzini, R., **1975**. Experimental tests on the applicability of a radioactive tracer technique for measuring coolant mixing in nuclear reactor fuel subassemblies., Nucl. Eng. and Design-32-105-109.

37. CENPD-206-NP., Combustion Engineering Inc., **1977**. TORC Code, Verification and Simplification Methods, CENPD-206-NP, 1977

38. Chandra, L., Roelofs, F., Houkema, M., Jonker, B., **2009**. A stepwise development and validation of a RANS based CFD modelling approach for the hydraulic and thermal-hydraulic analyses of liquid metal flow in a fuel assembly. Nucl. Eng. Des. 239, 1988–2003.

39. Chang, D., Tavoularis, S., **2007**. Numerical simulation of turbulent flow in a 37-rod bundle. Nucl. Eng. Des. 237, 575–590.

40. Chang, D., Tavoularis, S., **2008**. Simulations of turbulence, heat transfer and mixing across narrow gaps between rod-bundle subchannels. Nucl. Eng. Des. 238,109–123.

41. Chelemer, H., Weisman, J., Tong, L.S., **1972**. Sub-channel thermal analysis of rod bundle cores, Nucl. Eng. Des. 21, 35-45.

42. Chelemer, H., Hochreiter, L.E., Boman, L.H., Chu, P.T., **1977**. An improved thermal-hydraulic analysis method for rod bundle cores., Nucl. Eng. and Des. 41, 219-229.

43. Chen and Todreas, N. E., **1975**. Prediction of the coolant temperature field in a breeder reactor including inter assembly heat transfer., Nuclear Engineering and Design, 35, no. 3, pp. 423-440 (1975).

44. Chen, B.C.J., Vanka, S.P., Sha, W.T., **1980**., Some recent computations of rod bundle thermal hydraulics using boundary fitted coordinates., Nucl. Eng. Des. 62, 123-135.

45. Cheng, S.K., Todreas, N. E., **1984**. Constitutive Correlations for Wire-Wrapped Subchannel Analysis under Forced and Mixed Convection Conditions., DOE/ET/37240-108TR, MIT, Cambridge, Massachusetts.

46. Cheng, S.K., Todreas, N.E., **1986**. Hydrodynamic models and correlation for bare, and wire-wrapped hexagonal rod bundles – bundle friction factor, subchannel friction factors and mixing parameters. Nucl. Eng. Des. 92, 227–251.

47. Cheng, X., Muller, U., **1998**. Critical Heat flux and turbulent mixing in hexagonal tight rod bundles. Int. Journal of Multiphase Flow. 24(1998)1245-1263.

48. Cheng. X., Muller. U., **2003**. Review on Critical Heat Flux in water cooled reactors. FZKA-6825., Forschngszentrum Karlsruhe GmbH, Karlsruhe.

49. Cheng, X., Tak, N.I., **2006**. CFD analysis of thermal–hydraulic behavior of heavy liquid metals in sub-channels. Nucl. Eng. Des. 236, 1874-1885.

50. Chi Young Lee, Chang Hwan Shin, Wang Kee In, **2013**. Effect of gap width on turbulent mixing of parallel flow in a square channel with a cylindrical rod., 2013. Experimental Thermal and Fluid Science, 47, 98-107.

51. Chieng, C.C., Lin, C., **1979**. Velocity distribution in the peripheral subchannels of the CANDU-type 19 rod bundle. Nucl. Eng. Des. 55, 389-394.

52. Chiu, R., Todreas, N., Morris, R., **1980**. Experimental techniques for LMCFBR assembly thermal/hydraulic tests, Nucl. Eng. Des. 62, 253-270.

53. Chu, P. T., Chelemer, H., Hochreiter, L. E., **1973**. THINC-IV, An improved program for thermal-hydraulic analysis of rod bundle cores, WCAP-7956, 1973.

54. Chun, S.-Y., Chung, H.-J., Moon, S.-K., Yang, S.-K., Chung, M.-K., Schoesse, T., Aritomi, M., **2001**. Effect of pressure on critical heat flux in uniformly heated vertical annulus under low flow conditions. Nucl. Eng. Des. 203, 159–174.

55. Cinosi, N., Walker, S.P., **2016**. CFD analysis of localized crud effects on the flow of coolant in nuclear rod bundles. Nucl. Eng. Des. 305, 28–38.

56. Collingam, R.E., Thorne, W.L., McCormack, J.D., **1971**. 217-pin wire-wrapped bundle coolant mixing test., TME 71-146.

57. Conner, M.E., Baglietto, E., Elmahdi, A.M., **2009**. CFD methodology and validation for single-phase flow in PWR fuel assemblies, Nucl. Eng. Des. (2009).

58. Dae-Hyun Hwang, Yeon-Jong Yoo, Wang-Kee In, Sung-Quun Zee., **2000**. Assessment of the inter channel mixing model with a subchannel analysis code for BWR and PWR conditions., Nucl. Eng. Des. 199, 257-272.

59. Dalle Donne, Marek, J., Martelli, A., Rehme, K., **1977**. BR2 bundle mockup heat transfer experiments, Nucl. Eng. Des. 40, No. 1, Special Issue GCFR (1977) 143-156.

60. Dalle Donne, M., Martelli, A., Rehme, K., **1979**. Thermo fluid dynamic experiments with gas-cooled bundles of rough rods and their evaluation with the computer code SAGAPO, Int. J. Heat Mass Transfer 22 (1979) 1355-1374.

61. Dobson, G.P., O'Neill, J.M., **1992**. SABRE, User Guide for Version 4, RSSD 261, AEA Technology.

62. DOE/ET-0009., **1977**. A Compendium of Computer Codes for the Safety Analysis of Fast Breeder Reactors.

63. Dong, Z. F. and Ebadian, M.A., **1994**. Mixed convection in cusped duct, Transactions of the ASME Journal of Heat Transfer, 116, PP. 250-253.

64. Duck, P.W. and Turner, J.T., **1987**. Pressurised water reactor blockage-prediction of Laminar flow and temperature distributions following loss of coolant accident. International Journal of Heat and Fluid Flow, 8(2), PP. 149-155.

65. Duffey, R.B., Porthouse, D.T.C., **1973**. The physics of rewetting in water reactor emergency core cooling. Nucl. Eng. Des. 25, 379–394.

66. Dutra, A. S., Souza Mendes, P. R., and Parise, J. A. R., **1991**. Transport coefficients for laminar and turbulent flow through a four-cusp channel., International Journal of Heat and Fluid Flow, 12, June, PP-99-101.

67. Dwyer, O.E., **1966**. Analytical study of heat transfer to liquid metals flowing in-line through closely packed rod bundies, Nucl. Sci. Eng. 25, 343.

68. Dwyer, O.E., **1969**, Heat transfer to liquid metals flowing in line through unbaffled rod bundles: a review, Nucl. Eng. Des. 10 (1969) 3-20.

69. Dwyer, O.E., Berry, H.C., **1972**. Heat transfer to liquid metals flowing turbulently and longitudinally through closely spaced rod bundles., Nucl. Eng. Des.23, 273-294.

70. Dwyer, O.E., Berry, H.C., Hlavac, P.J., **1972**. Heat transfer to liquid metals flowing turbulently and longitudinally through closely spaced rod bundles (part ii uniform heat flux at the inner surface of the cladding)., Nucl. Eng. Des. 23, 295-308.

71. Eichhorn, R., Kao, H.C., Neti, S., **1980**. Measurements of shear stress in a square array rod bundle, Nucl. Eng. Des. 56, 385-391.

72. Eiff, O.S., Lightstone, M.F., **1996**. On the modelling of single-phase turbulent energy transport in sub-channels.

73. Eifler, W., Nijsing, R., **1967**. Experimental investigation of velocity distribution and flow resistance in a triangular array of parallel rods, Nucl. Eng. Des. 5, 22-42.

74. Eifler, W., Nijsing, R., **1973**. VELASCO - Velocity field in asymmetric rod configurations, Ispra Report, EUR 4905e.

75. Engle, F.C., Minushkin, B., Atkins, R.J., Markley, R.A., **1980**. Characterization of heat transfer and temperature distributions in an electrically heated model of an LMFBR blanket assembly, Nucl. Eng. Des. 62 (1980) 335-347.

76. Eriksson. S.O., **1971**, SCEPTIC. A Fortran IV Computer Program for Temperature Analysis of Gas or Liquid Cooled Flow Passages with Heated Smooth or Roughened Surfaces. A user's Guide. EIR, TM-IN-H79, 16.7.1971

77. Faya. A., Wolft. L. and Todreas. N., **1979**, CANAL USER'S MANUAL, Energy Laboratory Report No. MIT-EL 79-028, November 1979

78. Forti. G. and Gonzalez-Santalo, J.M., **1973**. A model for subchannel analysis of BWR rod bundles in steady-state and transient", Int. Conf. Reactor Heat Transfer, Karlsruhe, Germany (1973).

79. Gabor Hazi., **2005**., On turbulence models for rod bundle flow computations., Annals of Nuclear Energy, 32, 755-761.

80. Gajapathy, R., Velusamy, K., Selvaraj, P., Chellapandi, P., Chetal, S., **2009**. A comparative CFD investigation of helical wire-wrapped 7, 19, 37 fuel pin bundles and its extendibility to 217 pin bundle. Nucl. Eng. Des. 239, 2279–2292.

81. George, T. L., Basehore K. L., Wheeler C. L. and Masterson. R. E., **1980**. COBRA-WC: A Version of COBRA for Single-Phase Multi-Assembly Thermal Hydraulic Transient Analysis., PNL-3259, Pacific Northwest Laboratory, Richland, WA.

82. Ginox, J.J., **1978**. Two-Phase flows and heat transfer with application to nuclear Reactor Design Problems., Hemisphere publishing corporation.

83. Ginsberg T., **1971**. Forced-flow interchannel mixing model for fuel rod assemblies utilizing a helical wire-wrap spacer system. Nucl. Eng. Des. 22, 28-42.

84. Gluck, M., **2007**. Sub-channel analysis with F-COBRA-TF – Code validation and approaches to CHF prediction, Nuclear Engineering and Design, 237, 655-667, 2007.

85. Grandjean, C., **2007**. Coolability of blocked regions in a rod bundle after ballooning under LOCA conditions. Main findings from a review of past experimental programmes. Nucl. Eng. Des. 237, 1872–1886.

86. Groeneveld, D.C., Leung, L.K.H., Kirillov, P.L., Bobkov, V.P., Smogalev, I.P., Vinogradov, V.N., Huang, X.C., Royer, E., **1996**. The 1995 look-up table for critical heat flux in tubes. Nucl. Eng. Des. 163, 1–23.

87. Grover, R.B., Venkat Raj, V., **1980**. Pressure drop along longitudinally-finned seven-rod cluster nuclear fuel elements. Nucl. Eng. Des. 58, 79.

88. Gu, H.Y., Cheng, X., Yang, Y.H., **2008**. CFD analysis of thermal hydraulic behavior in SCWR typical flow channels. Nucl. Eng. Des. 238, 3348-3359.

89. Guellouz, M.S., Tavoularis, S., **1992**. Heat transfer in rod bundle subchannels with varying rod-wall proximity. Nucl. Eng. Des. 132, 351-366.

90. Gunn, D. J. and Darling, M. D. **1963**. Fluid Flow and Energy Losses in Non-Circular conduits, Transactions of Institution of Chemical Engineers., 41, PP.163-169.

91. Hassan, A. A., Hunaehn, Q. K. **2008**. Numerical Study of incompressible flow and heat transfer in non-circular ducts with cusp corners. Journal of Engineering, 14(2), June, PP. 2571-2589.

92. Hee Cha Jong, Haeng Cho Moon., **1970**. A study on coolant mixing in multirod bundles subchannels., Journal of the Korean Nuclear Society, 2 (1970) 19-25.

93. Hirao S., Nakao N. **1974**. DIANA - A Fast and High Capacity Computer Code for Interchannel Coolant Mixing in Rod Arrays, Nuclear Science And Design. 1974. v.30, N3.

94. Hishida Hisashi, **1974**. an analytical method of evaluating the effect of rod displacement on circumferential temperature and heat flux distributions in turbulent flow through unbaffled rod bundles., Nucl. Eng. Des. 26, 408-422.

95. Hochreiter, L.E., Cheung, F.B., Lin, T.F., Frepoli, C., Sridharan, A., Todd, D.R., Rosal, E.R., **2010**. Rod bundle heat transfer test facility test plan and design., NUREG/CR-6975.

96. Hofmann, F., **1970**. Velocity and temperature distribution in turbulent flow in sodium cooled fuel elements with eccentric geometry, Nucl. Eng. Des. 14, 43.

97. Holloway, M.V., Beasley, D.E., Conner, M.E., **2008**. Single-phase convective heat transfer in rod bundles, Nucl. Eng. Des. 238, 848-858.

98. Hooper, J.D., **1980**. Developed single phase turbulent flow through a square pitch rod cluster, Nucl. Eng. Des. 60, 365-379.

99. Hooper, J.D., Rehme, K., **1983**. The structure of single-phase turbulent flows through closely spaced rod arrays, KfK Report 3467, Kernforschungszentrum Karlsruhe (1983).

100. Hooper, J.D. and Wood, D.H., **1983**. Flow recovery from a single subchannel blockage in a square-pitched array, Nucl. Eng. Des. 74, 91-103.

101. Hooper, J.D., Rehme, K., **1984**. Large-scale structure effects in developed turbulent flow through closely spaced rod arrays. J. Fluid Mech. 145, 305–337.

102. Hooper, J.D., Wood, D.H., **1984**. Fully developed rod bundle flow over a large range of Reynolds number, Nucl. Eng. Des. 83, 31-46.

103. Hu, R., Fanning, T.H., **2011**. Progress report on development of intermediate fidelity full assembly analysis methods. September-2011. ANL/NE-11/35.

104. Hudina, M., Markbczy, G., **1977**. The hexagonal bundle heat transfer and fluid flow experiment AGATHE HEX, Nucl. Eng. Des. 40, No. 1, Special Issue GCFR (1977) 121-131.

105. Hudina, M., Huggenberger, M., **1986**. pressure drop and heat transfer in gas-cooled rod bundles. Nucl. Eng. Des. 97, 347-360.

106. Huggenberger. M.,**1977**. SCRIMP A thermal-hydraulic subchannel analysis computer code., Eidg. Institut für Reaktorforschung Würenlingen (Switzerland)., EIR-Bericht Nr. 322., Würenlingen, June 1977.

107. Ibragimov, M.C., Usupov, I.A., Subbotin, V.I., **1967**. The calculation and experimental investigation of velocity distribution in noncircular channels of complex form (transl.), Liquid Metal. 234, Atomizdat (1967).

108. Ihle, P., Rust, K., **1987**. PWR reflood experiments using full length bundles of rods with zircaloy claddings and alumina pellets. Nucl. Eng. Des. 99, 223–237.

109. Ikeda, K., Makino Y., Hoshi M., **2006**. Single-phase CFD applicability for estimating fluid hot-spot locations in a 5×5 fuel rod bundle. Nucl. Eng. Des. 236, 1149–1154.

110. Imke. U., Sanchez. V., and Gomez. R., **2010**. SUBCHANFLOW: An empirical knowledge based subchannel code," in Proceedings of the Annual Meeting on Nuclear Technology, pp. 4–6, Berlin, Germany, May 2010.

111. In, W.K., Chun, T.H., Shin, C.H., Oh, D.S., **2008**. Numerical computation of heat transfer enhancement of a PWR rod bundle with mixing vane spacers, Nucl. Tech. 161, 69-79.

112. Jareteg Klas, Vinai Paolo, Sasic Srdjan, Demaziere Christophe, 2015. Coupled fine-mesh neutronics and thermal-hydraulics – Modeling and implementation for PWR fuel assemblies., Annals of Nuclear Energy, 84, 244-257.

113. Jeong, Hae-Young, Ha, Kwi-Seok, Kwon, Young-Min, Lee, Yong-Bum, Hahn, Dohee, 2007. A dominant geometrical parameter affecting the turbulent mixing rate in rod bundles. Int. Journal of Heat and Mass Transfer. 50, 908-918.

114. Jeong, Hae-Yong, Ha, Kwi-Seok, Kwon, Young-Min, Chang, Won-Pyo, Lee, Yong-Bum, 2006. A correlation for single phase turbulent mixing in square rod arrays under highly turbulent conditions. Nucl. Eng. Technol. 38, 809–818.

115. Jian, S., Atila, P., Silva, F., **2002**. Analytical prediction of friction factors and Nusselt numbers of turbulent forced convection in rod bundles with smooth and rough surfaces. Nucl. Eng. Des. 215, 111–127.

116. Kaiser, H.G., Zeggel, W., **1987**. Turbulent flows in complex rod bundle geometries numerically predicted by the use of fem and a basic turbulence model., Nucl. Eng. Des. 99, 351-363.

117. Kattchee, N., Reynolds, W.C.,**1962**., HECTIC II. An IBM 7090 FORTRAN Computer Program for Heat Transfer Analysis of Gas or Liquid Cooled Reactor Passages. ID0-28595, AGN, California, December 1962.

118. Kawahara, A., Sato, Y., Sadatomi, M., **1997**. The turbulent mixing rate and the fluctuations of static pressure difference between adjacent subchannels in a two-phase subchannel flow. Nucl. Eng. Des. 175, 97–106.

119. Kawahara, A., Sadatomi, M., Kudo, H., Kano, K., **2006**. Single and Two-Phase Turbulent mixing rate between subchannels in triangular Tight lattice rod bundle., JSME Int. Journal, Series B, 49(2006)287-295.

120. Kazuyuki Takase, Hisashi Ninokata., **2007**. Large-Scale Simulations on Thermal-Hydraulics in Fuel Bundles of Advanced Nuclear Reactors.., CH.3-Epoch-Making Simulation.

121. Kelly, J. E., **1980**. Development of Two-fluid Two-phase model for light water reactor subchannel Analysis., PhD Thesis.

122. Kelly, J.E., Kao, S.P., Kazimi, M.S., **1981**. THERMIT-2: A two-fluid model for light water reactor sub-channel transient analysis., MIT-EL-81-014, MIT.

123. Khan, E.U., Rohsenkow, W.M., Sonin, A.A., Todreas, N.E., **1975**. A porous body model for predicting temperature distribution in wire-wrapped fuel rod assemblies, Nucl. Eng. Des. 35, 1-12.

124. Khurrum Saleem Chaudri, Yali Su, Ronghua Chen, Wenxi Tian, Guanghui Su, Suizheng Qiu., **2012**, Development of sub-channel code SACoS and its application in coupled neutronics/thermal hydraulics system for SCWR., Annals of Nuclear Energy., Volume 45, July 2012, Pages 37–45.

125. Kim, Sin, Chung Bum, Jin., 1999. Estimation of the turbulent mixing rate for low Prandtl number flows through rod bundles., Int. Comm. Heat Mass Transfer, Vol. 26, No. 7, pp. 1009-1017, 1999.

126. Kim, Sin, Chung, Bum-Jin., 2001., A scale analysis of the turbulent mixing rate for various Prandtl number flow fields in rod bundles., Nucl. Eng. Des. 205, 281-294.

127. Kim W.S., Kim Y.G., Kim. Y.J., **2002**. A Subchannel analysis code MATRA-LMR for wire-wrapped LMR subassembly, Ann. Nucl. Energy, 29 (2002), pp. 303–321.

128. Krauss, T., Meyer, L., **1996**. Characteristics of turbulent velocity and temperature in a wall channel of a heated rod bundle., Experimental Thermal and Fluid Science, 1996; 12: 75-86.

129. Krauss, T., Meyer, L., **1998**. Experimental investigation of turbulent transport of momentum and energy in a heated rod bundle. Nucl. Eng. Des. 180, 185-206.

130. Krepper, E., Končar, B., Egorov Y., **2007**. CFD modelling of subcooled boiling-Concept, validation and application to fuel assembly design. Nucl. Eng. Des. 237, 716–731.

131. Kriventsev, V., Ninokata, H., **1999**. Calculation of detailed velocity and temperature distributions in a rod bundle of nuclear reactor. In: Proceedings of the Proceedings of the Ninth International Topical Meeting on Nuclear Reactor Thermal Hydraulics. NURETH-9, 3–8 October-1999, San Francisco, CA.

132. Lahey, R.T., Schruab, F.A., **1969**. Mixing, flow regimes, and void fraction for two-phase flow in rod bundles,

133. Lassmann, K., Schubert, A., Van de Laar, J., Van Uffelen P., **2015**. The 'Fuel Rod Analysis Tool Box': A general program for preparing the input of a fuel rod performance code., Annals of Nuclear Energy, 81, 332-335.

134. Lee, M., **2000**. A critical heat flux approach for square rod bundles using the 1995 Groeneveld CHF table and bundle data of heat transfer research facility. Nucl. Eng. Des. 197, 357–374.

135. Lee, C.M., Choi, Y.D., **2007**. Comparison of thermo-hydraulic performances of large scale vortex flow (LSVF) and small scale vortex flow (SSVF) mixing vanes in 17_17 nuclear rod bundle, Nucl. Eng. Des. 237, 2322-2331.

136. Lee, K.B., **1995**. Analytical prediction of subchannel friction factor for infinite bare rod square and triangular arrays of low pitch to diameter ratio in turbulent flow. Nucl. Eng. Des. 157, 197–203.

137. Lee, K.B., Jang, H.C., **1997**. A numerical prediction on the turbulent flow in closely spaced bare rod arrays by a nonlinear k–ε model. Nucl. Eng. Des. 172, 351–357.

138. Levchenko, J.D., Subbotin, V.I., Ushakow, P.A., **1967**. Coolant velocity and wall shear stress distribution in closely packed rods, Atomnaja Energija 22 (1967) 218-225.

139. Levchenko, Y.D., Subbotin, V.I., Ushakov, P.A., **1972**. Experimental investigation of averaged characteristics of turbulent flow in cells of rod packs. Atom. Energy 33 (5), 1035–1042.

140. Lewis, M.J., Buettiker, P., **1974**. Momentum losses and convective heat transfer in rod bundles - an overview., Nucl. Eng. Des. 31, 351-362.

141. Liu. C.C., Ferng. Y.M., **2010**. Numerically simulating the thermal-hydraulic characteristics within the fuel rod bundle using CFD methodology. Nucl. Eng. Des. 240, 3078-3086.

142. Macdougall, J.D., Lillington, J.N., **1984**. The SABRE code for fuel rod cluster thermohydraulics, Nucl. Eng. Des. 82, 171-190.

143. Marek, J., Rehme, K., **1979**. Heat transfer in smooth and roughened rod bundles near spacer grids. In: Fluid Flow and Heat Transfer Over rod or tube Bundles. ASME, Presented at the ASME Winter Annual Meeting, December 2–7, 1979, pp. 163–170.

144. Marek, J., Maubach, K., Rehme, K., **1973**. Heat transfer and pressure drop performance of rod bundles arranged in square arrays. Int. J. Heat Mass Transfer 16, 2215–2228.

145. Matiur Rahman, Ahmad, S.Y., **1982**. Finite element analysis of axial flow with heat transfer in a square duct., AMM-6-481-490.

146. Maubach, K., Rehme, K., **1973**. Pressure drop for parallel flow through a roughened rod cluster, Nucl. Eng. Des. 25, 369-378.

147. Merzari, E., Ninokata, H., Baglietto, E., **2007**. Unsteady Reynolds averaged Navier–Stokes simulation for an accurate prediction of the flow insight tight rod bundles. Proc. NURETH-12, Log number 213, Pennsylvania, USA.

148. Merzari, E., Wang, S., Ninokata, H., Theofilis, V., **2008**. Biglobar linear stability analysis for the flow in eccentric annular channels and a related geometry. Phys. Fluids, 20.

149. Merzari, E., Ninokata, H., Baglietto, E., **2008**. Numerical simulation of flows in tight lattice fuel bundles, Nucl. Eng. Des., 238, 1703-1719.

150. Merzari, E., Ninokata, H., **2009**. Anisotropic turbulence and coherent structures in eccentric annular channels. Flow Turbulence Combust. 82 (1), 93–120.

151. Meyder, R., **1975**. Solving the Conservation Equations in Fuel Rod Bundles Exposed to Parallel Flow by Means of Curvilinear-Orthogonal Coordinates. JCP-17-53-67.

152. Meyder, R., **1975**. Turbulent velocity and temperature distribution in the central subchannel of rod bundles, Nucl. Eng. Des. 35, 181-189.

153. Meyer, L., **1994**. Measurements of turbulent velocity and temperature in axial flow through a heated rod bundle. Nucl. Eng. Des. 146, 71–82.

154. Meyer, L., **2010**. From discovery to recognition of periodic large scale vortices in rod bundles as source of natural mixing between subchannels-A review. Nuclear Engineering and Design, 240, 1575-1588.

155. Meyer, L., Rehme, K., **1994**. Large scale turbulence phenomena in compound rectangular channels. Exp. Thermal Fluid Sci. 8, 286–304.

156. Meyer, L., Rehme, K., **1995**. Periodic vortices in flow through channels with longitudinal slots or fins. In: 10th Symp. Turbulent Shear Flows, The Pennsylvania State University, vol. 1, University Park, PA, August 14–16, pp. 1–55.

157. Misawa, T., Ninokata, H., Maekawa, I., **2003**. Calculation of detailed velocity and temperature distributions in a triangular pin bundle using pseudo direct numerical simulation. In: 10th International Topical Meeting on Nuclear Reactor Thermal Hydraulics (NURETH-10), Seoul, Korea, October 5–9.

158. Mohanty, A.K., Sahoo, K.M., **1986**. Laminar convection in wall sub-channels and transport rates for finite rod bundle assemblies by superposition. Nucl. Eng. Des. 92, 169-180.

159. Mohanty, A.K., Sahoo, K.M., **1988**. Turbulent flow and heat transfer in rod-bundle subchannels., Nucl. Eng. Des. 106, 327-344.

160. Moller, S.V., QASSIM, R.Y., **1985**. A resistivity tensor-concept model for three-dimensional fluid flow through rod bundles and the verification of its applicability., Nucl. Eng. Des. 88, 1-9.

161. Moller S. V., **1991**. On phenomena of turbulent flow through rod bundles. Experimental Thermal and Fluid Science, 4, 25–35, 1991.

162. Moller S. V., **1992**, Single-phase turbulent mixing in rod bundles, Experimental Thermal and Fluid Science, 5, 26–33.

163. Muto, S., Anegawa, T., Morooka, S., Yokobori, S., Ebata, S., Yoshimoto, Y., Suzuki, S., **1990**. An experimental study on rewetting phenomena in transient conditions of BWRs. Nucl. Eng. Des. 120, 311–321.

164. Natesan, K., Sundararajan, T., Narasimhan, A., Velusamy, K., **2010**. Turbulent flow simulation in a wire-wrap rod bundle of an LMFBR. Nucl. Eng. Des. 240, 1063-1072.

165. Neti, S., Eichhorn, R., Hahn, O.J., **1983**. Laser Doppler measurements of flow in a rod bundle., Nucl. Eng. Des.74, 105-116.

166. Nicolas Silin., Luis Juanico., **2006**. Experimental study on the Reynolds number dependence of turbulent mixing in a rod bundle. Nucl. Eng. Des. 236, 1860-1866.

167. Nijsing, R., **1966**. Temperature and heat flux distribution in nuclear fuel element rods, Nucl. Eng. Des. 4, 1.

168. Nijsing, R., Eifler, W., **1969**. Analysis of liquid metal heat transfer in assemblies of closed spaced fuel rods (A theoretical evaluation of two-dimensional temperature- and heat flux distribution for conditions of turbulent axial flow at relatively low Peclet numbers). Nucl. Eng. Des. 10, 21–54.

169. Nijsing, R., Eifler, W., **1971**. Temperature fields in liquid metals cooled rod assemblies, Int. Seminar on Heat Transfer in Liquid Metals, Trogie, Yugoslavia, EUR/C-IS/791/71.e (1971).

170. Nijsing, R., Eifler, W., **1972**. Temperature fields in liquid metal cooled rod assemblies, Int. Seminar on Recent Developments in Heat Exchangers, Torgir, Yugoslavia, 1972.

171. Nijsing, R., Eifler, W., **1973**, Temperature fields in liquid metal cooled rod assemblies, Progress in heat and mass transfer-1973-7-115-149.

172. Nijsing R., Eifler, W., and Delfau, B., **1975**. Lateral turbulent diffusion for longitudinal flow in a rectangular channel., Nuclear Engineering and Design, 32, 221-238.

173. Nijsing, R., Eifler, W., Delfan, B., Camposilvan, J., **1967**. studies on fluid mixing between subchannels in a bundle of finned tubes, Nucl. Eng. Des. 5, 229-253.

174. Nijsing, R., Gargantini, I., Eifler, W., **1964**. Fundamental studies of fluid flow and heat transfer in fuel element geometries, part I, EUR 2193.e, Joint Nuclear Research Centre, Ispra (1964).

175. Nijsing, R., Gargantini, I., Eifler, W., **1966**. Analysis of fluid flow and heat transfer in a triangular array of parallel heat generating rods., Nucl. Eng. Des. 4, 375-398.

176. Ninokata, H., Deguchi, A., Baba, K., **1985**. ASFRE-III: A computer program for triangular rod array thermo hydraulic analysis of fast breeder reactors, PNC Report, PNC-N941 85-106 (July 1985).

177. Ninokata, H., Atake, N., Baglietto, E., Misawa, T., Kano, T., **2004**. Direct numerical simulation of turbulence flows in a subchannel of tight lattice fuel pin bundles of nuclear reactors. http://www.Jamstec.go.jp/esc/publication /annual/annual2004/.

178. Ninokata, H., Merzari, E., Khakim, A., **2009**. Analysis of low Reynolds number turbulent flow phenomena in nuclear fuel pin subassemblies of tight lattice configuration. Nuclear Engineering and Design 239, 855–866.

179. Ninokata, H., Todreas, N.E., **1975**. Turbulent momentum exchange coefficients for reactor fuel bundle analysis. Report 000-2245-22TR, Nucl. Eng. Dep., MIT (1975).

180. Ninokata, H., Efthimiadis, A., Todreas, N.E., **1987**. Distributed resistance modeling of wire wrapped rod bundles. Nuc. Eng. & Dsgn.,104, 93–102.

181. Ninokata H. and Okano T., **1985**. SABENA: An advanced subchannel code for sodium boiling analysis," Proc. 3rd Int. Topical Meeting on Reactor Thermal Hydraulics, Newport, Rhode Island, Oct. (1985).

182. Ninokata, H. et al., **2001**. Development of the NASCA Code for Predicting Transient BT Phenomena in BWR Rod Bundles. NEA/CSNI/R (2001) 2, vol. 2.

183. Ninokata, H., Merzari, E., **2007**. Computational fluid dynamics and simulation based-design approach for tight lattice nuclear fuel pin subassemblies. In: Proc.NURETH-12, Log no: KN#6, Pennsylvania, USA.

184. Novendstern, E.H., **1972**. Turbulent flow pressure drop model for fuel rod assemblies utilizing a helical wire wrap spacer system, Nucl. Eng. Des., 22 (1972), pp. 19–27.

185. Nordsveen, M., Hoyer, N., Adamsson, C., Anglart, H., **2003**. The MONA Subchannel Analysis Code – Part A: Model and Description, Proceedings: Tenth International Meeting on Nuclear Reactor Thermal-Hydraulics (NURETH-10), Seoul, Korea.

186. Okhawa, K., Lahey, R.T., **1980**. The analysis of CCFL using drift-flux models, Nucl. Eng. Des., 61.

187. Ouma, B.H., Tavoularis, S., **1991**. Flow measurements in rod bundle subchannels with varying rod-wall proximity., Nucl. Eng. Des. 131, 193-208.

188. Pan Wu, Jianqiang Shan , Xiong Xiang, Bo Zhang, Junli Gou, Bin Zhang., **2016**. The development and application of a sub-channel code in ocean environment., Annals of Nuclear Energy., Volume 95, September 2016, Pages 12–22.

189. Petrunik, **1973**. Turbulent interchange in simulated rod bundle geometries for genetron-12., PhD Thesis.

190. Pfann Jaroslav., **1972**. Heat transfer in turbulent longitudinal flow through unbaffled assemblies of fuel rods., Nucl. Eng. Des.25, 217-247.

191. Pierre St. C. C., **1966**. SASS code 1, Subchannel Analysis for the Steady State. AECL-APPE-41 (1966).

192. Ramm, H., Johannsen, K., Todreas, N.E., **1974**. Single phase transport within bare-rod arrays at laminar, transition and turbulent flow condition, Nucl. Eng. Des. 30, 186-204.

193. Rapley, C.W., Gosman, A.D., **1986**. The prediction of fully developed axial turbulent flow in rod bundles. Nucl. Eng. Des. 97, 313–325.

194. Reynolds, W.C., Kattchee, N., **1961**., HECTIC, An IBM 704 Computer Program for Heat Transfer Analysis of Gas Cooled Reactors. Aerojet-General Nucleonics, AGN-TM381, May, 1961.

195. Rehme, K. **1971**. Laminarstromung in stabbundeln, Chem. Ing. Tech. 43, PP.962.

196. Rehme, K., **1972**. Pressure drop performance of rod bundles in hexagonal arrangements. Int. J. Heat Mass Transfer 15, 2499–2517.

197. Rehme, K., **1973a**. Simple method of predicting friction factors of turbulent flow in non-circular channels., International Journal of Heat and Mass Transfer, 16, 933-950.

198. Rehme, K., **1973b**. Pressure drop correlations for fuel element spacers. Nucl. Technol. 17, 15-23.

199. Rehme, K., **1976**. Hot-wire anemometry in subchannels of rod bundles, KTG-Fachtagung Experimentiertechnik in der Reaktor-Fluiddynamik, Berlin, 1976 (in German).

200. Rehme, K., **1977**. Measurements of the velocity, turbulence and wall shear stress distributions in a corner channel of a rod bundle, KfK 2512, Kernforschungszentrum Karlsruhe (1977, in German).

201. Rehme, K., **1978**. The structure of turbulent flow through a wall subchannel of a rod bundle, Nucl. Eng. Des. 45, 311-323.

202. Rehme, K., **1978a**. Turbulent flow through a wall subchannel of a rod bundle, KfK-2617, Kernforschungszentrum Karlsruhe (1978, in German).

203. Rehme, K., **1978b**, Distributions of velocity and turbulence of turbulent flow through a wall subchannel of a rod bundle, KfK-2637, Kernforschungszentrum Kaflsruhe (1978, in German).

204. Rehme, K., **1979**. The Structure of turbulent flow through subchannels of rod bundles, In: Fluid Flow and Heat Transfer Over Rod or Tube Bundles., eds. S.C. Yao and T.A. Psand (ASME, New York, 1979) pp. 67-76.

205. Rehme, K., **1979b**. Non-isotropic eddy viscosities in turbulent flow through rod bundles, in: turbulent Forced Convection in Channels and Bundles, Vol.I, eds S. Kakac and D.B. Spalding (Hemisphere/McGraw-Hill, New York, 1979) pp. 505-519.

206. Rehme, K., **1980**. Turbulent Momentum Transport In Rod Bundles. Nucl. Eng. Des. 62, 137-146.

207. Rehme, K., **1980a**. Experiments on the structure of turbulence in a wall subchannel of a rod bundle (P/D = 1.07), KfK 2983, Kernforschungszentrum Karlsruhe (1980, in German).

208. Rehme, K., **1980b**. Experimental investigations on the fluid flow through an asymmetric rod bundle (W/D = 1.096), KfK 3047, Kernnforschungszentrum Karlsruhe (1980, in German).

209. Rehme, K., **1980c**. Experimental investigations on the fluid flow through an asymmetric rod bundle (W/D = 1.048), KfK 3069, Kemforschungszentrum Karlsruhe (1980, in German).

210. Rehme, K., **1981**. Structure of turbulence in a wall subchannel of a rod bundle, KfK 3177, kernforschungszentrum Karlsruhe (1981, in German).

211. Rehme, K., **1982**. Distributions of velocity and turbulence in a parallel flow along an asymmetric rod bundle, Nucl. Technol. 59, 148-159.

212. Rehme, K., **1982a**. Experimental investigations on the fluid flow through an asymmetric rod bundle (W/D = 1.118), KfK 3318, Kernforschungszentrum Karlsruhe (1982, in German).

213. Rehme, K., **1982b**. Experimental investigations on the fluid flow through an asymmetric rod bundle, KfK 3324, Karlsruhe (in German) (1982).

214. Rehme, K., **1982c**. Experimental investigations on the fluid flow through a wall subchannel of a rod bundle (P/D= 1.036, W/D = 1.072), KfK 3361, Kernforschungszentrum Karlsruhe (1982, in German).

215. Rehme, K., **1983a**. Experimental investigations on the fluid flow through an asymmetric rod bundle (P/D =1.148, W/D=1.045), KfK 3597, Kemforschungszentrum Karlsruhe (1983, in German).

216. Rehme, K., **1983b**. Experimental investigation on the fluid flow through an asymmetric rod bundle (P/D =1.148, W/D=1.252), KfK 3598, Kernforschungszentrum Karlsruhe (1983, in German).

217. Rehme, K., **1984**. Experimental investigations on the fluid flow through an asymmetric rod bundle (P/D =1.148, W/D=1.074), KfK 3818, Kernforschungszentrum Karlsruhe (1984, in German).

218. Rehme, K., **1984a**. Computer-controlled rig for measurements of velocity and turbulence distributions by hot-wires, KfK 3744, Kernforsehungszentrum Karlsruhe (1984, in Germarn).

219. Rehme, K., **1984b**. Comparison between results obtained by different hot-wire methods, KfK 3813, Kernforschungszentrum Karlsruhe (1984, in German).

220. Rehme, K., **1985**. Experimental investigations on the fluid flow through an asymmetric rod bundle (P/D =1.148, W/D=1.222), KfK 3822, Kernforschungszentrum Karlsruhe (1985, in German).

221. Rehme, K., **1986**. Turbulence measurements in a wall subchannel of a rod bundle (P/D = W/D =1.148), KfK-Report 4027 (1986).

222. Rehme, K., **1987a**. The structure of turbulent flow through rod bundles, Nucl. Eng. Des. 99, 141-154.

223. Rehme, K., **1987b**. The structure of turbulence in wall sub-channels of a rod bundle, Atomkernenergie 49, 145-150.

224. Rehme, K., **1987b**. Convective heat transfer over rod bundles, in: Handbook of Single Phase Convective Heat Transfer, ed. S. Kakac, R.K. Shah and W. Aung (Wiley-Interscience, New York, 1987) pp. 7.1-7.62.

225. Rehme, K., **1989**. Experimental observations of turbulent flow through subchannels of rod bundles. Exp. Thermal Fluid Sci. 2, 341–349.

226. Rehme, K., **1992**. The prediction of turbulent Prandtl and Schmidt numbers. Int. J. Heat Mass Transfer 18, 1055-1069.

227. Rehme, K., **1992**. The structure of turbulence in rod bundles and the implications on natural mixing between subchannels. Int. J. Heat Mass Transfer 35, pp. 567–581.

228. Renksizbulut, M., Hadaller, G. I., **1986**. An experimental study of turbulent flow through a square-array rod bundle, Nucl. Eng. Des.91, 41-55.

229. Rivas, G. A., Garcia, E.C. and Assato, M. **2011**. Forced turbulent heat convection in a square duct with non-uniform wall temperature. International Communications in Heat and Mass Transfer, 38, PP.844-851.

230. Roidt, M., Pechersky, M.J., Markley, R.A., Vegter, B.J., **1973**. Experimental determination of turbulent exchange coefficients in a model reactor rod bundle. Conf-730803--2.

231. Roelofs F., Gopala V.R., Chandra L., Viellieber M., Class A., **2012**. Simulating fuel assemblies with low resolution CFD approaches. Nucl. Eng. Des. 250, 548–559.

232. Roidt, R.M., Bartholet, T.G., Harper, L.J., **1974**. Experimental determination of interior subchannel cross flow and axial flow in a model of the Clinch River breeder reactor fuel assembly rod bundle with wire wrap spacers.., conf-741107--4.

233. Roidt, R.M., Carelli, M.D., Markley, R.A., **1980**. Experimental investigations of the hydraulic field in wire-wrapped LMFBR core assemblies, Nucl. Eng. Des. 62, 295-321.

234. Rogers, J.T., Rosehart. R.G., **1972**. Mixing by turbulent interchange in fuel bundles. Correlations and interfaces., 72-HT-53.

235. Rogers, J. T., Tahir, A.E.E., **1975**. Turbulent interchange mixing in rod bundles and role of secondary flows., 75-HT-31.

236. Rowe. D.S., **1967**, Cross-Flow mixing between parallel flow channels during boiling Part-I COBRA-Computer program for coolant boiling in rod arrays. BNWL-371-Pt-I.

237. Rowe, D. S., Angle, C. W., **1967**. Experimental study of mixing between rod bundle fuel-element flow channels during boiling. Transactions of ANS-Vol.10, 655.

238. Rowe, D.S., Angle, C.W., **1967**. Cross flow mixing between parallel flow channels during boiling part ii measurement of flow and enthalpy in two parallel channels., BNWL-371-Pt-2.

239. Rowe, D.S., Angle, C.W., **1969**. Cross Flow mixing between parallel flow channels during boiling Part III -Effect of spacers on mixing between two channels, BNWL-371-Pt-3.

240. Rowe D.S., **1970**. Cobra-II: A digital computer program for thermal hydraulic subchannel analysis of rod bundle nuclear fuel elements, BNWL-1229 VC-80, February 1970.

241. Rowe D. S., **1973**. COBRA IIIC: A Digital Computer Program for Steady-State and Transient Thermal Analysis of Rod Bundle Nuclear Fuel Elements., BNWL-1695, Pacific Northwest Laboratory, 1973.

242. Rui Guo, Yoshiaki Oka., **2015**. CFD analysis of coolant channel geometries for tightly packed fuel rods assembly of Super FBR., Nucl. Eng. Des., 288, PP 119-129.

243. Sadatomi, M., Kawahara, A., Sato, Y., **1994**. Flow redistribution due to void drift in two-phase flow in a multiple channel consisting of two subchannels. Nucl. Eng. Des. 148, 463–474.

244. Sahu, S.K., Das, P.K., Bhattacharyya, S., **2010**. An experimental investigation on the quenching of a thin vertical tube by spray at high flow rate. Nucl. Eng. Des. 240, 1558–1568.

245. Schikorr, M., Bubelis, E., Mansani, L., Litfin, K., **2010**. Proposal for pressure drop prediction for a fuel bundle with grid spacers using Rehme pressure drop correlations. Nucl. Eng. Des. 240, 1830–1842.

246. Seale, W.J., **1979**. Turbulent diffusion of heat between connected flow passages. Nucl. Eng. Des. 54, 183-195.

247. Seale, W.J., **1979**. Turbulent diffusion of heat between connected flow passages; Part 2: Prediction using K - e turbulence model, Nucl. Eng. Des. 54, 197-209.

248. Sha, W.T., **1980**. An overview of rod-bundle thermal-hydraulic analysis, Nucl. Eng. Des. 62, 1-24.

249. Shah, R.K. and London, A.L. **1971**. Laminar Flow Forced Convection Heat Transfer in straight and curved ducts- A summary of Analytical Solutions. Technical Report-75, Department of mechanical engineering, Stanford University, California.

250. Shah, R.K. and London, A. L. **1978**. Laminar Flow Forced convection in ducts. New York: Academic Press.

251. Shin, B.S., Chang S.H., **2005**. Experimental study on the effect of angles and positions of mixing vanes on CHF in a 2×2 rod bundle with working fluid R-134a. Nucl. Eng. Des. 235, 1749–1759.

252. Shin, B.S., Chang, S.H., **2009**. CHF experiment and CFD analysis in a 2×3 rod bundle with mixing vane., Nucl. Eng. Des. 239, 899-912.

253. Silin, N., Juanico, L., Delmastro, D., **2004**. Thermal mixing between subchannels: measurement method and applications. Nucl. Eng. Des., 227, 51–63.

254. Skinner V. R., Freeman A. R., Lyall H. G., **1969**, Gas mixing in rod clusters. Int. J. Heat and Mass Transfer, 12, 265–278.

255. Spatz, R., Mewes, D., **1987**. The influence of walls and upper tie plate slots on the flooding mechanism in fuel elements with and without heat transfer between steam and water., Nucl. Eng. Des. 110, 413-422.

256. Spiga, M., Morini. G. L. **1996**. Nusselt numbers in laminar flow for H2 boundary conditions, International Journal of Heat and Mass Transfer., 39(6), PP.1165-1174.

257. Stewart, C.W., Wheeler, C.L., Cena, R.J., **1977**. COBRA-IV: the model and the method. In: Battelle Pacific Northwest Laboratories Richland, Washington, USA.

258. Stewart. C.W., Cuta. J.M., Montgomery. S.D., Kelly. J.M., Basehore. K.L., George. T.L, and Rowe. D.S., **1993**. VIPRE-01: A Thermal-Hydraulic Analysis Code for Reactor Cores, Volume 1: Mathematical Modeling, EPRI NP-2511-CCM, Electric Power Institute (1993).

259. Su, K., Freire, A.P.S., **2002**. Analytical prediction of friction factors and Nusselt numbers of turbulent forced convection in rod bundles with smooth and rough surfaces. Nucl. Eng. Des. 217, 111–127.

260. Subbotin, V.I., Ushakov, P.A., Gabrianovich, B.N., Zhukov, A.B., **1961**. Heat exchange during the flow of mercury and water in a tightly packed rod pile, Soviet J. Atom. Energy, 9, 1001-1009.

261. Subbotin, V.I., Ushakov, P.A., Levchenko, Y.D., Aleksandrov, A.M., **1971**. Velocity fields in turbulent flow past rod bundles, Heat Transfer, Soviet Res. 3, No. 2 (1971) 9-35.

262. Swindlehust, G. B., **1995**. A utility perspective on subchannel analysis. Nuclear Technology, 112, 1995.

263. Tachibana, F., Oyama, A., Akiyama, M., and Kondo, S., **1969**, Measurement of heat transfer coefficients for axial air flow through eccentric annulus and seven-rod cluster. Journal of Nuclear Science and Technology, 6, 207–214.

264. Tae Sun RO, Todreas, N.E., **1988**. Energy transfer mechanisms in LMFBR rod bundles under mixed convection conditions., Nucl. Eng. Des. 108, 343-357.

265. Tapucu, A., **1977**. Studies on diversion cross flow between two parallel channels communicating by a lateral slot: 1. Transverse flow resistance coefficient., Nuclear Engineering and Design, 42, 297–306.

266. Tapucu, A., Teyssedou, A., Tye, P., Troche, N., **1994**. The effect of turbulent mixing models on the prediction of subchannel codes. Nucl. Eng. Des. 149, 221–231.

267. Thompson, J.J., and Holy, Z.J., **1975**. Conjugate heat transfer and thermo elastic analysis of heat generating rods, Nucl. Eng. Des. 35, 247-268.

268. Thompson, T.S., **1974**. On the process of rewetting of hot surface by a falling liquid film. Nucl. Eng. Des. 31, 234–245.

269. Todreas, N.E., **1979**. Coolant mixing in LMFBR rod bundles and outlet plenum mixing transients., DOE/ET/37240-72.

270. Todreas N. E., **1985**. Coolant mixing in LMFBR rod bundles and outlet plenum mixing transients. DOE/ET/37240--109-PR.

271. Todreas, N.E., Kazimi, M.S., **2001**. Nuclear Systems II- Elements of Thermal Hydraulic Design., Taylor and Francis.

272. Tong, L. S. and Tang, Y. S., **1997**. Boiling Heat transfer and Two phase flow. Taylor and Francis, Washington DC., USA.

273. Toth, S., Aszodi, A., **2010**. CFD analysis of flow field in a triangular rod bundle. Nucl. Eng. Des. 240, 352–363.

274. Toumi. I., Bergeron A., Gallo D., Royer E., Caruge D., **2000**. FLICA-4: A 3D two-phase flow computer code with advanced numerical methods for nuclear applications, Nuc. Eng. Dsgn, 200, pp. 139-155, (2000)

275. Touran, Nick. "What is a Nuclear Reactor?" WhatIsNuclear, https://whatisnuclear.com/reactors.html. Accessed 29 August, 2018.

276. Trupp, A.C., Azad, R.S., **1975**. The structure of turbulent flow in triangular array rod bundles, Nucl. Eng. Des., 32, 47-84.

277. Tsutomu Ikeno, Takeo Kajishima, **2010**. Analysis of dynamical flow structure in a square arrayed rod bundle. Nucl. Eng. Des. 240, 305-312.

278. Tuzla, K., Unal, C., Chen, J.C., **1991**. An experimental study of bottom rewetting in a rod bundle geometry. Nucl. Eng. Des. 125, 189–200.

279. Tye, P., Teyssedou, A., Tapucu, A., **1994**. An investigation of the constitutive relations for inter subchannel transfer mechanisms in horizontal flows as applied in the ASSERT-4 subchannel code. Nucl. Eng. Des. 149, 207–220.

280. U.S.NRC, The Pressurized Water Reactor, https://www.nrc.gov/reading-rm/basic-ref/students/animated-pwr.html.

281. Van Der Ros, T., Bogaart, M., **1970**. Mass and Heat Exchange between Adjacent Channels in Liquid-Cooled Rod Bundles, Nucl. Eng. Des. 12, p. 259.

282. VIPRE-02, **1994**. VIPRE-02: A Two-Fluid Thermal-Hydraulic Code for Reactor Core and Vessel Analysis", Volume 1: Mathematical Modeling and Solution Methods, TR-103931-V1 Research Project, Final Report, June 1994

283. Vonka, V., **1988**. Measurement of secondary flow vortices in a rod bundle. Nucl. Eng. Des. 106, 191–207.

284. Vonka, V., Boonstra, B.H., **1974**. Calculated heat transfer development in bundles., Nucl. Eng. Des. 31, 337-345.

285. Walton, F.B., **1969**. Turbulent mixing measurements for single phase air, single phase water and two phase air-water flows in adjacent triangular subchannels. MS-Thesis.

286. Webb, B.J., **1988**. COBRA-IV PC: A Personal Computer Version of COBRA-IV-I for Thermal-Hydraulic Analysis of Rod Bundle Nuclear Fuel Elements and Cores., PNL-6476.

287. Weisman, J., Ying, S.H., **1984**. A theoretically based critical heat flux prediction for rod bundles at PWR conditions., Nucl. Eng. Des.85, 239-250.

288. Wheeler C. L., Stewart C. W., Cena R. J., Rowe D.S., Sutey A. M., **1976**. "COBRA-IV-I: An Interim Version of COBRA for Thermal Hydraulic Analysis of Rod Bundle Nuclear Fuel Elements and Cores," BNWL-1962, Pacific Northwest Laboratory.

289. Wolf, L., Fischer, K., Herkenrath, H., Hufschmidt, W., **1987**. Comprehensive assessment of the Ispra BWR and PWR subchannel experiments and code analysis with different two-phase models and solution schemes. Nucl. Eng. Des. 99, 329–350.

290. Wolf. L. Guillebaud, Louis Jean Marie, Faya A., **1978**. WOSUB - A Subchannel Code for Steady-State and Transient Thermal Hydraulic Analysis of BWR Fuel Pin Bundles. Volume I - Model Description", MIT-EL-78-023 (1978).

291. Wu, X., Trupp, A.C., 1994. Spectral measurements and mixing correlation in simulated rod bundle subchannels. Int. J. Heat Mass Transfer 37, 1277–1281.

292. Wu, Xiaohua., **1995**. On the transport mechanisms in simulated heterogeneous rod bundle subchannels., Nucl. Eng. Des. 158, 125-134.

293. Yadigaroglu, G., Anderani, M., Dreier, J., Coddington, P., **2003**.Trends and needs in experimentation and numerical simulation for LWR safety, Nucl. Eng. Des. 221, 205-223.

294. Yan, B.H., Yu, L., Li, Y.Q., **2009**. Research on operational characteristics of passive residual heat removal system under rolling motion. Nucl. Eng. Des. 239,2302-2310.

295. Yan, B.H., Yu, L., Gu, H.Y., Yang, Y.H., **2011**. LES and URANS simulations of turbulent flow in 4 rod bundles in ocean environment. Progress in Nuclear Energy, 53, 330-335.

296. Yan, B.H., Gu. H.Y., Yu, L., **2012**. Numerical simulation of the coherent structure and turbulent mixing in tight lattice. Progress in Nuclear Energy, 54(2012)81-95.

297. Yoo, Y.J., Dae Hyun Hwang, Dong Seong Sohn., **1999**. Development of a Subchannel Analysis Code MATRA Applicable to PWRs and ALWRs, Journal of the Korean Nuclear Society, vol. 31, No 3, pp. 314-327

298. Yoshikawa, N., Ishimaru, J., Tamura, S., Ninokata, H., Hirata, N., **1981**.ASFRE: A Computer code for single-phase subchannel thermal hydraulic analysis of LMFBR single subassembly, PNC Report, PNC-N941 81-74 (April 1981).

299. Yue, F.S., Zi, D.C., Qing, G.L., **1991**. An investigation of cross flow mixing effect caused by grid spacer with mixing blades in a rod bundle. Nucl. Eng. Des. 125, 111–119.

300. Zaiyong Ma, Yingwei Wu, Zicheng Qiu, Wenxi Tian, Guanghui Su, Suizheng Qiu., **2012**. An innovative method for prediction of liquid metal heat transfer rate for rod bundles based on annuli., ANE-47-91-97.

301. Zhi Shang., **2009**. CFD investigation of vertical rod bundles of supercritical water-cooled nuclear reactor. Nucl. Eng. Des. 239, 2562-2572.

302. Zhi Shang, Simon Lo, **2010**. Numerical investigation of supercritical water-cooled nuclear reactor in horizontal rod bundles. Nucl. Eng. Des. 240, 776-782.

DOCTORAL COMMITTEE

Chairman	:	Dr. K. Velusamy Senior professor, Outstanding Scientist, Homi Bhabha National Institute, Indira Gandhi Centre for Atomic Research, Kalpakkam, 603102, Tamil Nadu, India.
Guide	:	Dr. Anil Kumar Sharma Assistant professor, Scientific Officer, Homi Bhabha National Institute, Indira Gandhi Centre for Atomic Research, Kalpakkam, 603102, Tamil Nadu, India.
Members	:	Dr. S. Murugan professor, Outstanding Scientist, Homi Bhabha National Institute, Indira Gandhi Centre for Atomic Research, Kalpakkam, 603102, Tamil Nadu, India.
	:	Dr. Anish Kumar Associate professor, Head, UIMS, Homi Bhabha National Institute, Indira Gandhi Centre for Atomic Research, Kalpakkam, 603102, Tamil Nadu, India.